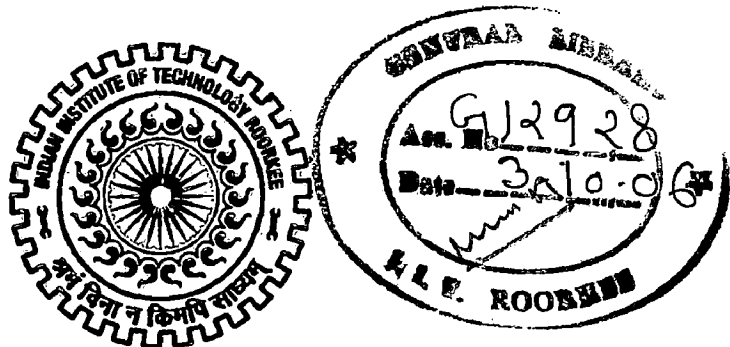# FEM STUDY TO EVALUATE PERFORMANCE OF DJATILUHUR INCLINED CORE ROCKFILL DAM IN INDONESIA

A DISSERTATION

Submitted in partial fulfillment of the
requirements for the award of the degree
of

MASTER OF TECHNOLOGY

in

WATER RESOURCES DEVELOPMENT

By

ANTON MARDIYONO

DEPARTMENT OF WATER RESOURCES DEVELOPMENT AND MANAGEMENT
INDIAN INSTITUTE OF TECHNOLOGY ROORKEE
ROORKEE -247 667 (INDIA)
JUNE, 2006

CANDIDATE'S DECLARATION

I hereby certify that the work which is being presented in the dissertation entitled, **"FEM STUDY TO EVALUATE PERFORMANCE OF *DJATILUHUR* INCLINED CORE ROCKFILL DAM IN INDONESIA"** in partial fulfillment of the requirement for the award of degree of MASTER OF TECHNOLOGY in WATER RESOURCES DEVELOPMENT and submitted in the Department of Water Resources Development and Management of Indian Institute of Technology Roorkee is a record of my own work carried out during a period from July 2005 up to June 2006 under the supervision of **Dr. R.P. Singh**, Professor and **Dr. B.N. Asthana**, Visiting Professor, Water Resources Development and Management Department, Indian Institute of Technology Roorkee, Roorkee India .

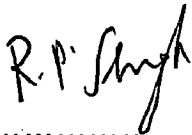The matter embodied in this dissertation has not been submitted by me for the award of any other degree.

Dated : June 23, 2006

Place   : IITR, Roorkee

(ANTON MARDIYONO)

This is to certify that the above statement made by the candidate is correct to the best of our knowledge.
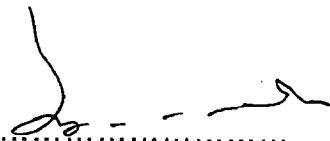
(Dr. R.P. Singh)

Professor, WRD&MD.

Indian Institute of Technology Roorkee,

Roorkee, INDIA

(Dr. B.N. Asthana)

Ex -Visiting Professor, WRD&MD.

Indian Institute of Technology Roorkee,

Roorkee, INDIA

ACKNOWLEDGEMENT

CONTENTS

LIST OF FIGURES

LIST OF FIGURES

No.	Title	Page No.

LIST OF TABLES

SYNOPSIS

Many earth and rockfill dams have been observed to have undergone large settlements and horizontal movements. The dam has experienced wide variety of movements, both in the upstream and the downstream direction. Correct assessment of movements in dam are called for better understanding the behaviour of the dam and to safe guard against cracks, hydraulic fracturing, etc. related failure at design state itself.

105 m height Djatiluhur dam as an inclined core rockfill dam in Indonesia is identified performing with significant deformation, started during construction period till the present reservoir operation period. Therefore, it is of interest to evaluate its behaviour.

This study is limited to analyze and compare the computed and the observed values of deformations Djatiluhur rockfill dam, to validate the model and thereafter to evaluate the dam performance. Central section of Djatiluhur Dam (100L-section) has been selected to be analyzed, which is in maximum height and is known to have occurrences of maximum observed deformations stated. 3D FEM incremental non-linear analyses under static condition were performed by using models of material properties based on hyperbolic elastic stress-strain relationship. Since the material properties were not available for the analysis, 3D FEM analysis was done with 3 sets of values. Model-1 has been selected by comparing observed slopes settlements with the computed values. Subsequently, discussions on those results are figured out in order to predict behaviours and performance of the dam.

The dam has been discretised into 432 numbers of 8 nodded brick elements, which consists of 637 nodes including considered layer of foundation. The finite element bases package "PENTAGON3D" is used to analysis the deformations, stresses and other related behaviours of the dam.

The interpretation of observations and results of analysis with Model-1 values reveals in the following paragraphs.

• **Performance of the dam during construction period.**

Presence of tensile zone in the top zone, susceptibility on the quality control during construction period, and the availability of high-plasticity clay predictably and potentially initiated unstable behaviours of the dam. Large value of the observed downstream horizontal deformation values may be due to elasto-plastic behaviour of the soil at observed location, where is not modeled in the analysis.

The principal stresses in the core are lower as compared to the shell material at all the levels except near crest of the dam and in upstream toe of the core. The maximum stresses are observed at the base of the dam in upstream toe of core enlargement portion.

The load transfer ratio indicates load transferred from core to shell for about 70 m height along the core height, except near crest of the dam.

• **Performance of the dam during first reservoir filling.**

The second consolidation that could not be modeled by numerical analysis probably initiated occurrence of the cracks, which presence of differential settlements and tensile zone are not confirmed by the analytical results.

Presence of tensile zone in the top zone and susceptibility of cracks along vertical plane due to hydraulic fracturing potentially initiated the occurrence of unseen-internal cracks and gradually initiated settlements on the dam crest.

Unsatisfactory agreement is found in comparison between calculated and the observed values of upstream-downstream slope settlements and horizontal deformations. These large movements may be due to effects of softening caused excessive strength loss in submerged shell and core and gradually, it initiate plastification of the materials. Susceptibility on the quality control during construction period and the availability of high-plasticity clay simultaneously cause these large movements of the dam.

The principal stresses in the upstream shell zone are lower than those in core and downstream shell zones. The maximum major and minor principal stress continuously observed at the base of the dam in upstream toe of core enlargement portion.

The core zone is generally safe against occurrence of the horizontal cracks due to hydraulic fracturing and there is no tensile zone within the dam at end of filling.

INTRODUCTION

1.1. GENERAL

In its simple and oldest form the embankment dam was constructed with low permeability soils to a normally homogeneous profile. Principally recognized that larger embankment dams required two components, a water-barrier or core of very low permeability soil and supporting shoulders of coarser earthfill or rockfill, to provide structural stability. Given the advancements in technique of design and soil testing, the possibility of sliding failure can be almost completely eliminated. Adequate knowledge and experience is now available to enable the designer to devise effective measures to protect the dam, provided these are correctly implemented and maintained.

In case of the rockfill dam type, the location of the core on the zoned rockfill dam is going to affect its performance. The factors that affect the design of the core are the core material, core thickness and the core position within the dam section. Design analysis based on the stress and strain relationship of the material used and core location should be taken to ensure its performance effectiveness.

With the construction of the embankments, as well as rockfill dams, stresses are induced in the foundation and in embankment accompanied by the displacement. The stresses and displacement play vital role in the stability of the embankment. Furthermore, the effectiveness of any embankment design depends not only on the stability of the slopes, but

on prediction of displacement also so that these can be restricted within acceptable limits. This has led to the development of analytical method, based on the stress and strain relationship of the material used.

Many earth and rockfill dams have been observed to undergo large settlements and horizontal movements. The dam has experienced wide variety of movements, both in the upstream and the downstream direction. These complex movements need to be studied under the combined effects of two counteracting effects of reservoir filling namely (1) the water loads on the dam and (2) the softening and weakening of the dam fill material due to wetting (Nobari and Duncan, 1972). Correct assessments of movements in dam are called for better understanding the behaviour of the dam and to safeguard against cracks, hydraulic fracturing, etc. related failure at design stage itself.

Three-Dimensional Finite Element Method can be applied in such analysis. The method can be systematically programmed into software to accommodate such complex and difficult problems as non-homogeneous materials, nonlinear stress-strain behavior and complicated boundary conditions.

Theories of elasticity and plasticity have been widely used in geotechnical engineering for problems involving small and large strain to which neither the theory of elasticity and plasticity are directly applicable. Furthermore, actual boundary conditions are often difficult to incorporate into the critical solutions. Recent developments of numerical methods, particularly in the Finite Element Method, have provided new computational capabilities making it possible to handle many complex boundary condition and material nonlinearity. The accuracy of the Finite Element Method depends on the proper

incorporation of nonlinear constitutive equations of the soil.

1.2. IMPORTANCE OF DEFORMATION CONSIDERATION

The stability of a rockfill dam during construction or normal operation is conventionally examined using equilibrium methods of stability analysis. These procedures indicate the factor of safety of the dam with respect to instability, but they provide no information regarding the deformation of the dam. In recent years, there has been a growing realization of the need to determine the deformation of a dam during construction or operation. These deformations may be of interest for a number of reasons:

1. Excessive settlements can lead to loss of freeboard and danger of overtopping.

2. Excessive spreading of an embankment may lead to the formation of longitudinal cracks, which adversely affect its stability. Such cracks have been observed in many embankment built on clay foundations.

3. Differential settlements between sections along the axis of a dam may lead to development of transverse cracks through the embankment, which could allow passage of water and progressive failure by erosion and piping.

4. Differential settlements between the core and the shell of a zoned embankment can lead to reduction in the stresses in the core, and may result in hydraulic fracturing if the stresses at any elevation are reduced to values less than the pressure of the water at the same elevation (Seed, Duncan and Idriss, 1975).

5. Deformation pattern of the upstream face particularly under the water load of the reservoir is necessary for the proper design of the concrete facing of a concrete faced rockfill dam. A crack on the concrete face may lead to seeping of water through it thereby softening of fill material and an unexpected deformation of the fill material may lead to further failure of concrete face.

6. Conduits through or under embankment suffer from stretching to one portion and compression to other portion due to deformation of the dam. It may lead to cracking and concentration of tension in the conduit and hence the deformations of the embankment need to be known as well as the magnitude of such deformation for the safe design of underlying conduits.

7. On wide rivers concrete gravity spillways are often built in the main river channel with earth dam embankment on each end. The connections are usually made simply by extending the concrete dam into the earth dam, and wrapping the embankment slopes around the end of the concrete dam on both sides. The embankment dam is generally compacted directly against the concrete dam with heavy rollers; therefore high embankment settlement would not be anticipated. In some cases the dams are fairly high at the junctions, creating a situation with potential for differential settlement cracking *(Sherard, 1973)*.

1.3. PURPOSES AND SCOPE OF THE STUDY

This study is limited to analyze and compare the computed and the observed values of deformations of 105 m height Djatiluhur rockfill dam with inclined core constructed in 1967 in Indonesia, to validate the model and

thereafter to evaluate the dam performance.

Central section of Djatiluhur Dam (100L-section) has been selected to be analyzed, which is in maximum height and is known to have occurrences of maximum observed deformations. Three-dimensional incremental non-linear analyses under static condition were performed by using three models of material properties (Para.4.4.4) in absence of correct data. Subsequently, the best-fit model has been selected and used for further analysis in order to predict behaviour and performance of the dam.

Two different periods under different stages are included in the analysis. These are detailed as below:

1. **Construction period.**

    The dam was modeled to be constructed in multi stages by simulating sequence of the construction to study effects of incremental construction of the dam. Static condition and embankment gravity loads were applied in the mathematical model of the dam.

2. **Reservoir filling period.**

    Softening and water-loading condition are incorporated in the model to study effects of the reservoir filling and reservoir is assumed to be filled in multi stages.

While studying both mentioned conditions, the following factors are studied:

1. Vertical and horizontal deformations.

    Predicted contours of deformations within the section will be discussed. Maximum magnitude, direction and its variations will be explained in detail. Subsequently, at the same locations the predicted magnitudes are being compared with observed ones.

2. Major and minor principal stresses.

Predicted contours of stresses within the section will be discussed. Maximum magnitude, direction and its variations will be explained in detail.

3. Load transfer between core and shell.

This load transfer can be evaluated by comparing the computed values of the major principle stress in the core and the core overburden pressure at any given depth below the crest. The ratio less than one indicate load transfer from core to shell, while the ratios greater than 1.0 indicate load transfer from the shell on the core.

4. Hydraulic fracturing susceptibility.

In this matter, predicted contour of total vertical stresses within the core zone will be studied to predict occurrence of hydraulic fracturing. Hydraulic fracturing or the formation of hydraulically induced cracks in the core can occur when the water pressure at a given depth ($\sigma1$) exceed the total vertical stress at the same depth (*Kulhawy et al., 1976*).

5. Potential cracks susceptibility.

Predicted 3-dimensional contours of deformations within the section will be discussed. Significant differences of deformations within adjacent zones either in longitudinal or transversal directions should be identified to predict occurrence of embankment cracks. Moreover, evidence of longitudinal cracks appearing at the dam crest may probably partially be attributed to the tensile stress obtained in the analysis (*Sherard, 1963*).

6. Potential plastifiction zone identification.

   Study on comparison between predicted and observed deformations is performed to identify potential material plastification developed within core zone. When observed settlement increments exceed beyond the normal, it could be an indication of plastification of the materials in the zone indicated which. A deformation of horizontal extension in a direction parallel to the river causes a reduction in the horizontal confining stress, to a degree that the material plastifies (*Albero et.al, 1982, at Chicoasen dam*).

7. Secondary consolidation due to several factors such as dissipation of pore water pressure under a constant embankment load, settlement due to infiltration during reservoir filling and creep (*Inoue et.al, 2000, at Tahamara dam*).

1.4. THE ORGANISATION OF DISSERTATION

The study is presented in seven chapters. The contents of each chapter are briefly indicated below.

Chapter 1   : Introduction of the problem, scope and objective of study are given.

Chapter 2   : Review of literature has been given in this chapter.

Chapter 3   : The finite element method and theoretical background have been discussed in this chapter.

Chapter 4   : Brief description of the Djatiluhur Dam and PENTAGON3D program software has been given in this chapter, including the presentation

of the mathematical models used and the analysis performed.

Chapter 5   : Gives the results and the discussion of results.

Chapter 6   : Gives the conclusions and suggestions for further study.

REVIEW OF LITERATURE

2.1. GENERAL

Many earth and rockfill dams have been observed to undergo large settlements and horizontal movements. The dams have experienced wide variety of movements, both in the upstream direction and the downstream direction. Measurements made in many earth and rockfill dams have shown that large settlements, horizontal movements and cracking are frequently caused by reservoir filling. The movement of embankment due to first filling of reservoir is most significant as measured and observed in a number of dams. The magnitude, rate and direction of displacement at a specific point within a dam may change during different phases of construction of the dam and operation of the reservoir.

The studies about performance of dams with reservoir filling and the use of three-dimensional analysis of finite element method for a few dams for this load condition available in literature are described below.

2.2. LAYERED ANALSYSIS OF EMBANKMENT DAM

Embankments are built up in relatively thin horizontal layers. Consequently, there will be a large number of layers during the construction of a large dam. The limitations of computer modeling require relatively thick layers to be used in the idealization. In the past, to provide an insight into the errors involved, the closed form solution of the incremental analysis was usually compared to the finite

element 'layered' analysis using a one-dimensional model, which represents either a soil column or a fill of large lateral extent. In the next approach of the conventional stress deformation, the structure is assumed to be completed in single stage and the gravity load is applied instantaneously as an external load to the complete structure. This conventional solution treats the gravity effects as an external load applied to the finished structure and valid if the state of the stresses in the structure is statically determinate at all stage of construction process, but in actual condition most embankments are constructed in layers by incremental process and the load is accumulated gradually during construction. This invalidates the assumption of one stage layer analysis.

Goodman and Brown (at Prasetyadhi, 2004) considered the difference between incremental construction and instantaneous loading in stress analysis of embankments. They focused on the stresses and displacement in structures, which is caused by the dead weight applied on the placing of material in layer. As an example, the case of an embankment built up in horizontal layers is considered and the stress results lead to a rational description of the rotational instability of slopes. The elastic analysis developed indicates the dependence on the construction sequence of the stress distribution in statically indeterminate structures. It predicts the curved failure surfaces observed in embankments and provides an explanation for the appearance of cracks on the top surface of steeps cuts.

Later Clough and Woodward (1967) applied this concept of incremental construction to the analysis of earth dam by finite element method. They evaluated the effect of incremental construction which the standard embankment was

first analyzed considering it to be constructed in single lift, and was then reanalyzed with the incremental construction process using 10 lifts. The stress distribution determined in the two cases indicated similar pattern. The displacements were, in contrast, found to be considerably affected by construction process. The horizontal displacements were seen to be quite similar in both cases but the vertical displacement for single lift case was seen to be the largest at the top due the fact that they are merely the integrated strains developed over the full height. The incremental analysis, however, shows zero vertical displacement at the top, because after the top layers were placed, no further strains were developed. The maximum vertical displacement in this case occurs near mid height as the region is affected by all the strains occurring below this level, as shown in Fig.2.1.
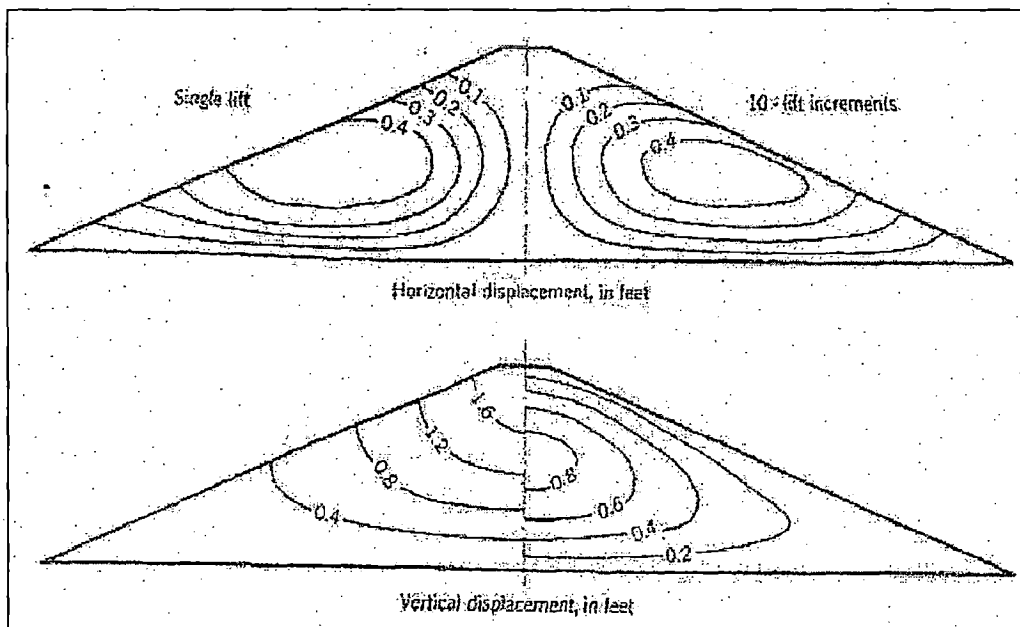
Fig.2.1. Displacements due to dead weight in standard dam

The important question remains, however, as to the number of lifts required in order to obtain good accuracy in the solution. For comparison purposes, an analysis was made of the standard embankment considering 7 lifts and 14 lifts. Vertical displacements computed at the 15 ft level and at 60 ft level are plotted in Fig.2.2 for both cases. Both sets of data points fall on the same curve for both elevations. Thus it is clear that seven lift analyses provide an adequate representation of the construction procedure.
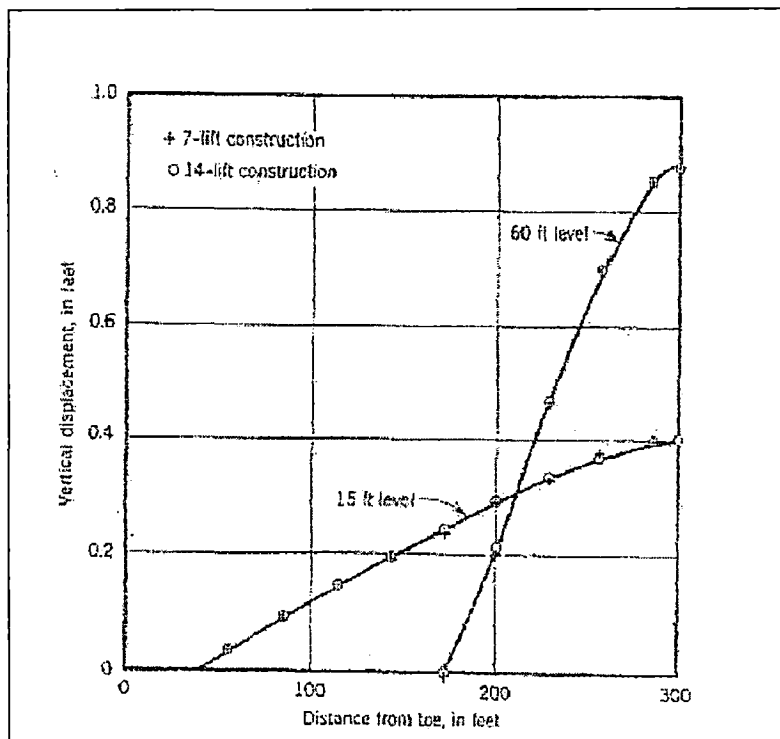
Fig 2.2. Displacements in standard dam: 7 & 14 lifts construction.

Naylor and Mattar (1988) studied about the effect of stiffness reduction factor (f) as one of main parameter in material properties model used, to reduce the layer analysis. They made a comparison in two cases, first case with linear elastic model (f=4) and K-G model (f=3). The difference was insignificant and the second case described the effect of varying f and the number of layers being kept constant at six, shown in Fig. 2.3 (a-b). The modeling of the construction of Beliche dam, Brazil, was investigated with this effect. K-G model, f equal to 3 with 2, 3 and 6 layers was used in the modeling. The very small difference

of displacement from the result was observed. Even with only two layers the central displacement only differs slightly from that in the six-layer analysis. The study concluded that the value of stiffness reduction factor from 3 to 5 with non-linear analysis could reduce the layered analysis up to 4 to 6 layers; it will normally be sufficient in any embankment dam analysis.
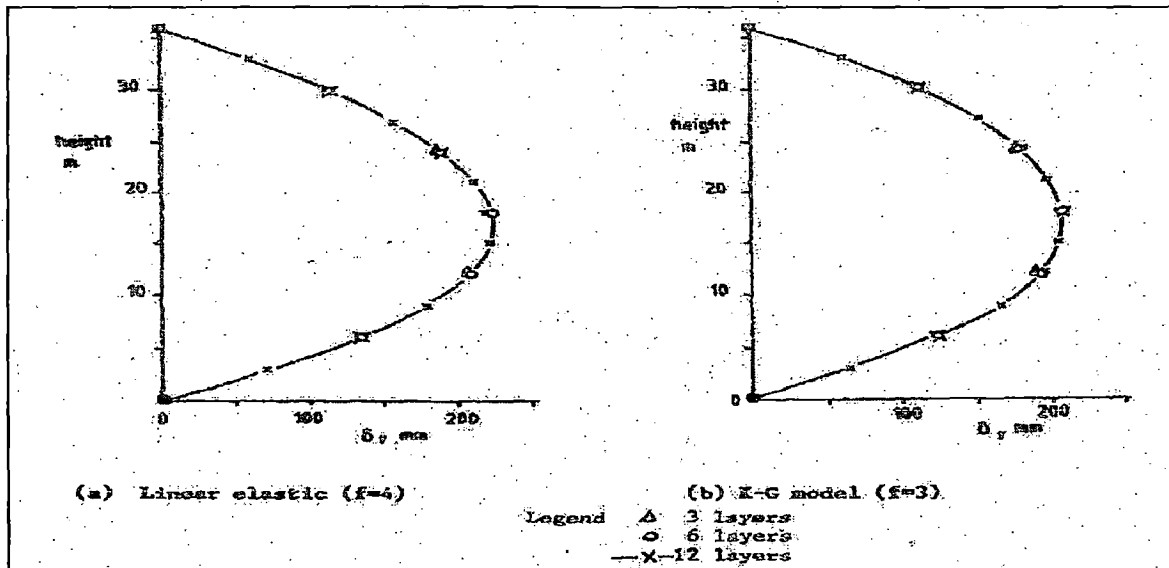
Fig.2.3(a). Rigid shoulder study-effect of number of layer on settlement
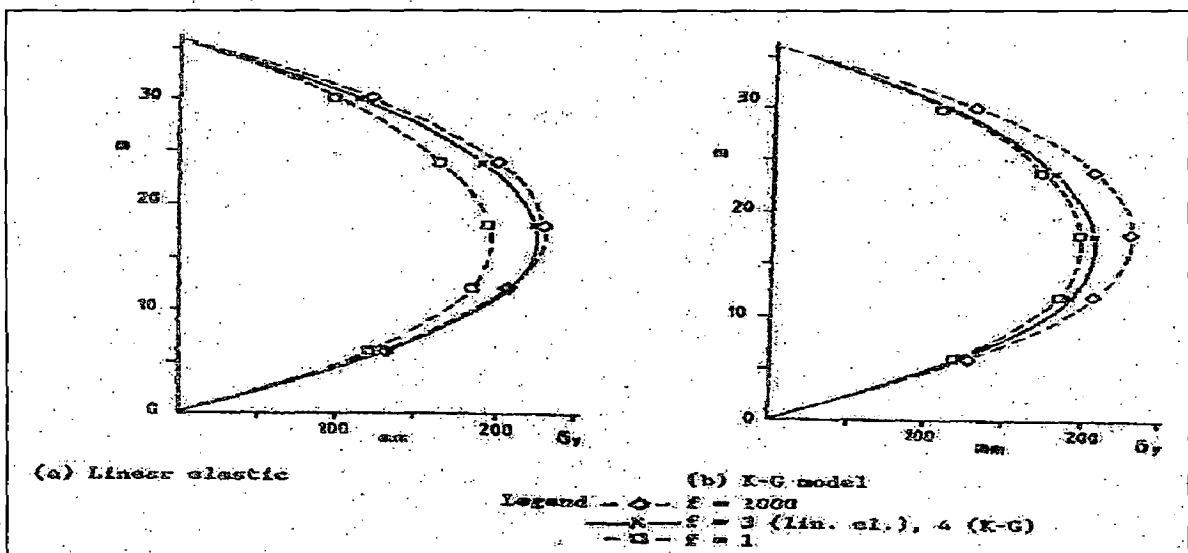
Fig.2.3(b). Rigid shoulder study-effect of 6 layers analysis
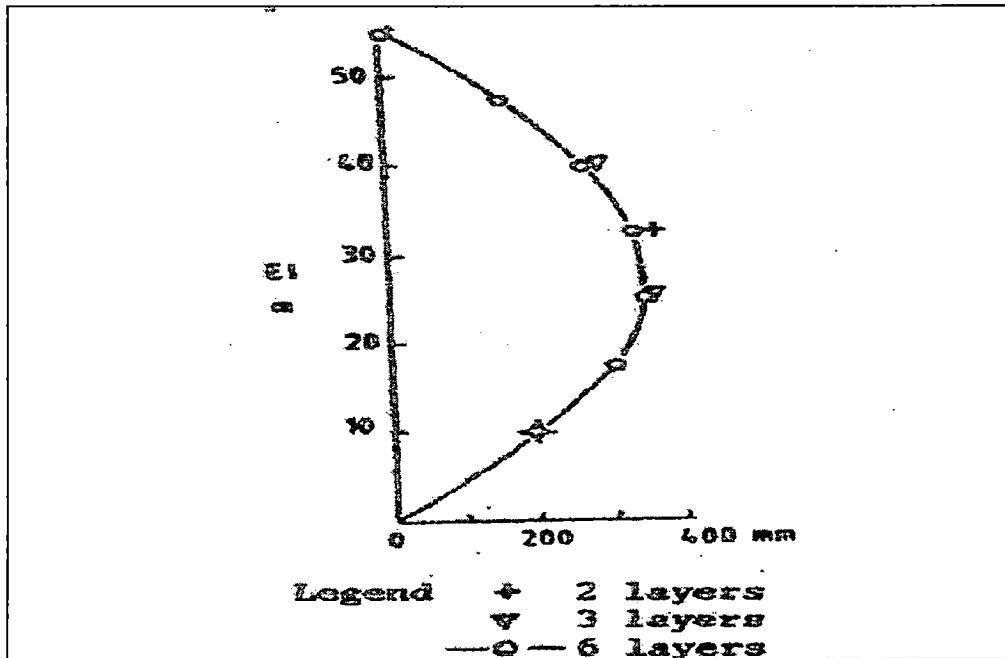
Fig.2.3(c). Settlement on Baliche dam centre·line.

2.3. ANALYSIS OF MAJOR DAMS

2.3.1. Analysis of Oroville Dam

Nobari and Duncan (1972) used finite element method to describe the movement of the dam due to reservoir filling. The stresses in the part of the dam wetted by the reservoir are changed very significantly by effect of buoyancy and water loading. The movements in Oroville dam were calculated using the finite element procedure and were compared with those measured during reservoir filling. The Oroville dam is 235 m high with a moderately inclined central·core and thick shells of rockfill compacted to 100% relative density on either side of core.

The effect of reservoir filling on zoned dam is illustrated in Fig.2.4. These effects that result directly from the water loading are in following:

1. The water load on the core causes downstream and downward

movements.

2. The water load on the upstream foundation causes upstream and downward movements.

3. The buoyant uplift forces in the upstream shell cause upward movements within this zone.

4. The effect due to softening and weakening caused by wetting of the upstream shell material.

1. Water load on core

2. Water load on foundation

3. Buoyant uplift on upstream shell

4. Softening due to wetting upstream shell material

Settlement due to wetting
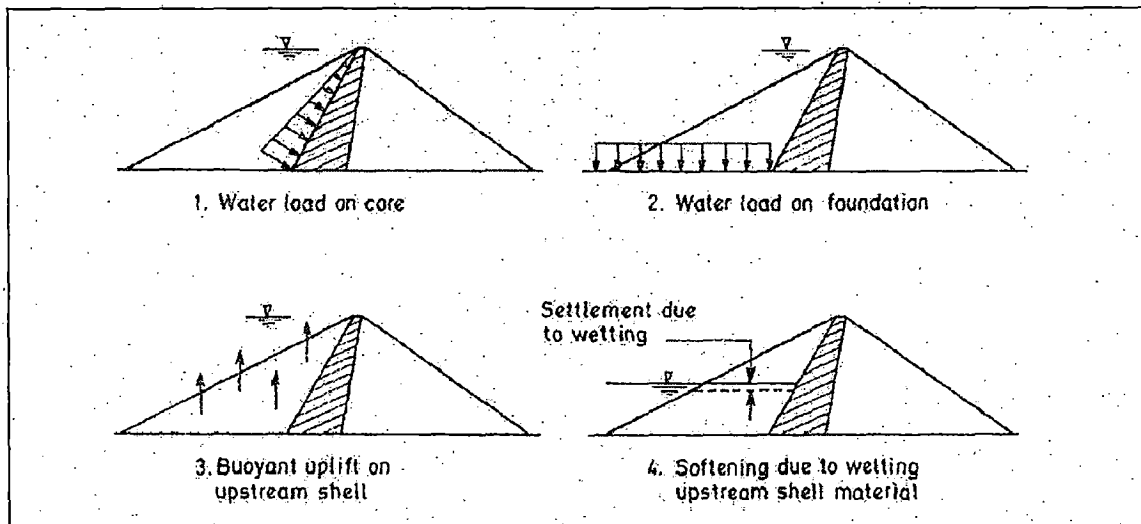
Fig.2.4. Effects of reservoir filling on the zoned dam.

The study of the movements of the Oroville dam was described as below. The movements first in the upstream direction and later in the downstream direction during continuous rise of the reservoir can be explained in terms of the counteracting effects of softening of the upstream shell and the water load on the core. The upstream movements caused by softening are greatest during the first stage of reservoir filling because the amount of compression due to wetting is greatest when overburden pressure is large. The downstream movements caused by water loads, on the other hand, are greatest during the later stages of reservoir filling, because the water load on the core increases as the

square of the depth of the impounded water. Therefore, movements resulting from softening due to wetting dominate during the early stages of reservoir filling and movements resulting from the water load dominate during the later stages, with the result that the dam moves first upstream and then downstream.

Nobari and Duncan developed the finite element procedure which may be used to calculate movements and stress changes in dams during reservoir filling, taking into account the effects of softening of the shell material due to wetting, as well as the effect of water loads. Contours of the calculated horizontal movements are shown in Fig.2.5. The movements are in the downstream direction throughout most of the dam, with exception of the toe of the upstream slope.

Displacement contours are in feet, downstream → is positive
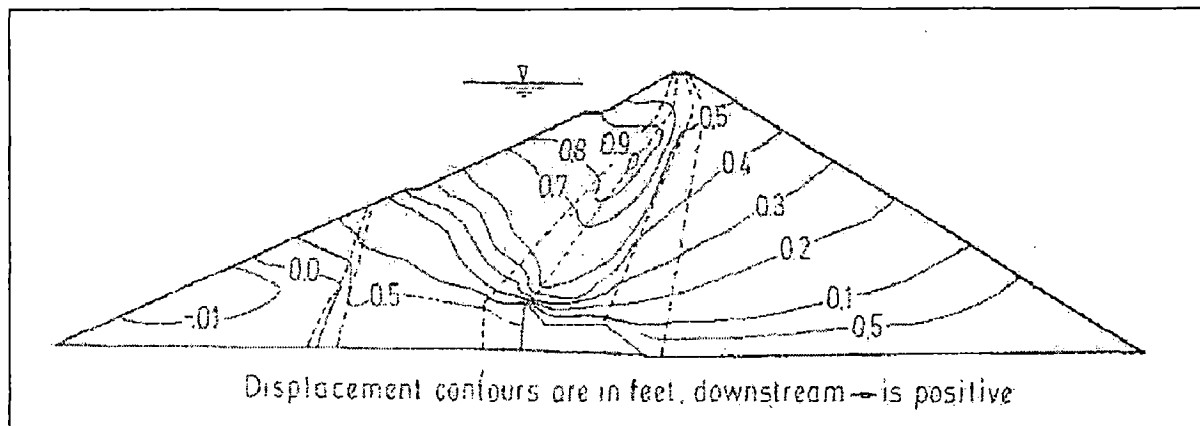
Fig. 2.5. Horizontal displacement due to reservoir filling

Contours of the calculated vertical settlements are shown in Fig. 2.6. Throughout most of the embankment the calculated settlements due to reservoir filling were between zero and 0.5 ft. At the upstream toe of the dam and at the downstream edge of the crest, the calculations indicated a small amount of heave. Within the upstream shell the settlements are dominated by compression of shell material

due to wetting and the tendency for expansion of shell as the effective stresses are reduced by submergence. These two counteracting effects result in settlement that is largest near mid-height of the dam. In addition, it may be noted that the downward movement of material within most of the upstream shell results in a displacement of material in the upstream direction and a small amount of heave near the upstream toe.

Settlement contours are in feet, settlement is positive
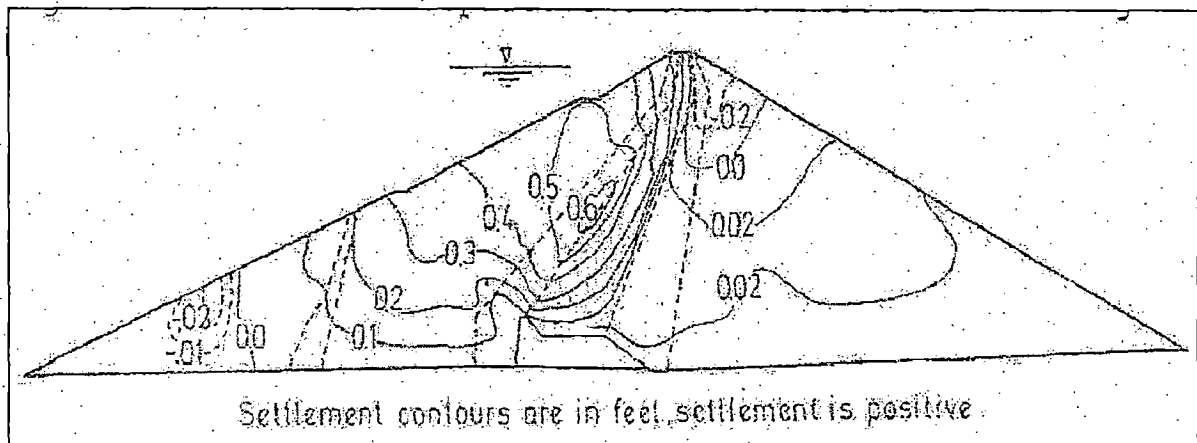
Fig.2.6. Vertical displacement due to reservoir filling

The movements of the core calculated in this procedure are shown in Fig. 2.7.
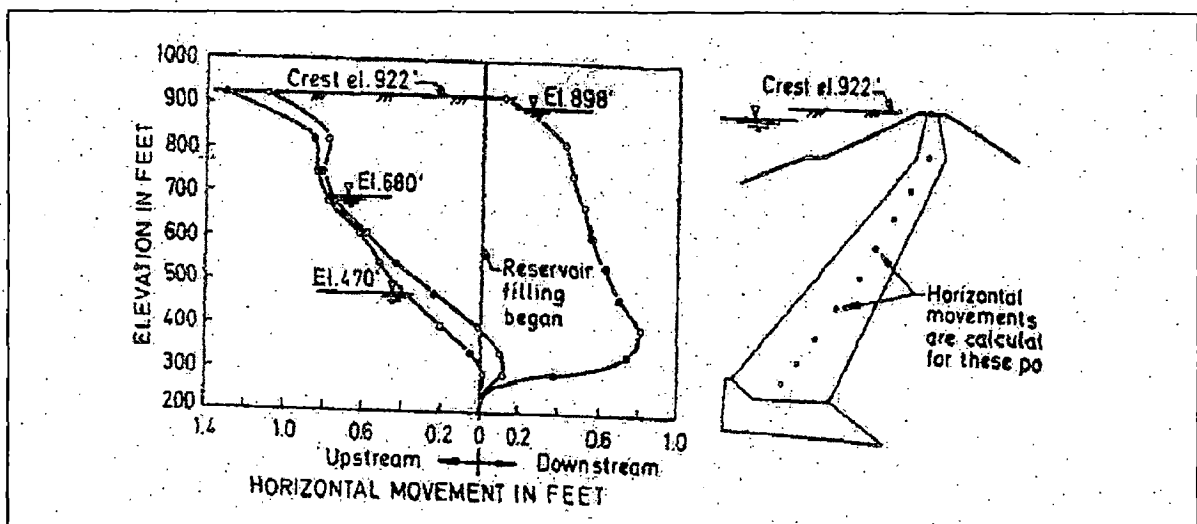
Fig.2.7. Calculated horizontal movements at 3 stages of reservoir filling, Oroville dam

The undeflected position of the core before reservoir filling is represented by vertical line and subsequent horizontal movements are indicated to the left and right.

2.3.2. Analysis of Duncan Dam

Eisenstein, Krishnayya and Morgenstern (1972) analyzed the history of cracking sequence at Duncan dam in Canada with finite element procedure which taking into account of incremental loading, non linear stress-strain relations and three dimensionality. Duncan dam, built in 1964-1967 on the Duncan River in British Columbia, Canada, is an earthfill dam of about 36 m height and 762 m length with an upstream sloping core. The dam has been built across a valley underlain by buried canyon about 378 m deep that is filled with sediment. The stratigraphy of the foundation is rather irregular with the upper layer possessing considerable compressibility. A typical cross section of the dam and longitudinal section are shown in Fig.2.8.
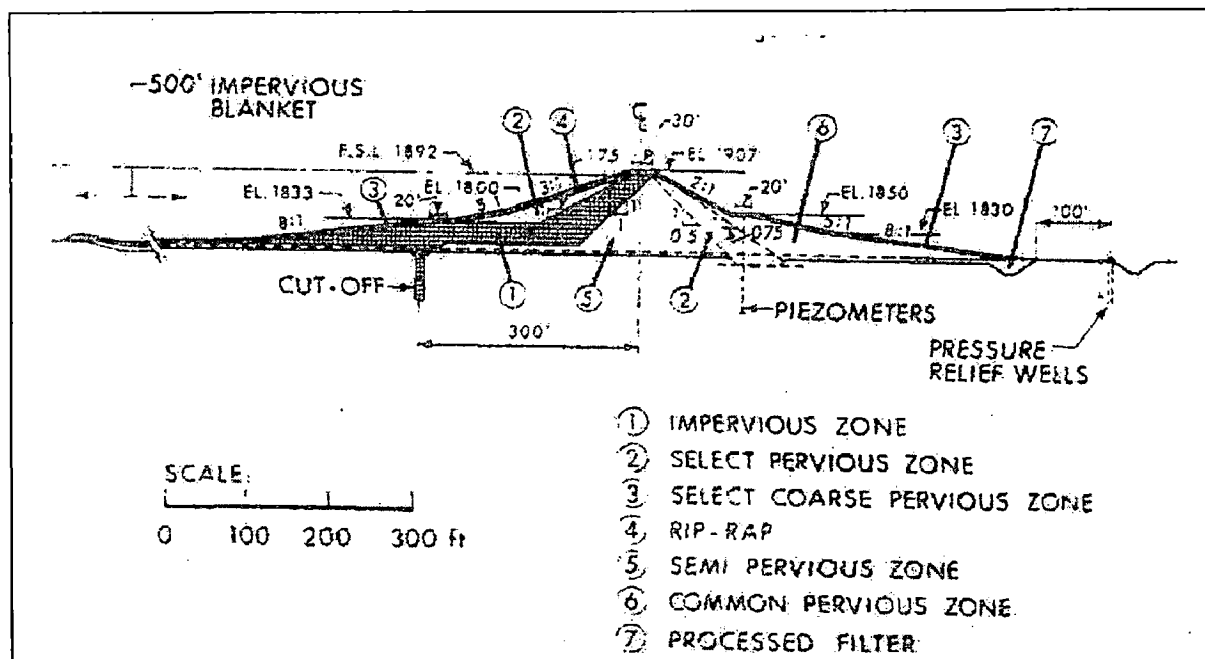
Fig.2.8(a). Typical Cross Section of Duncan Dam
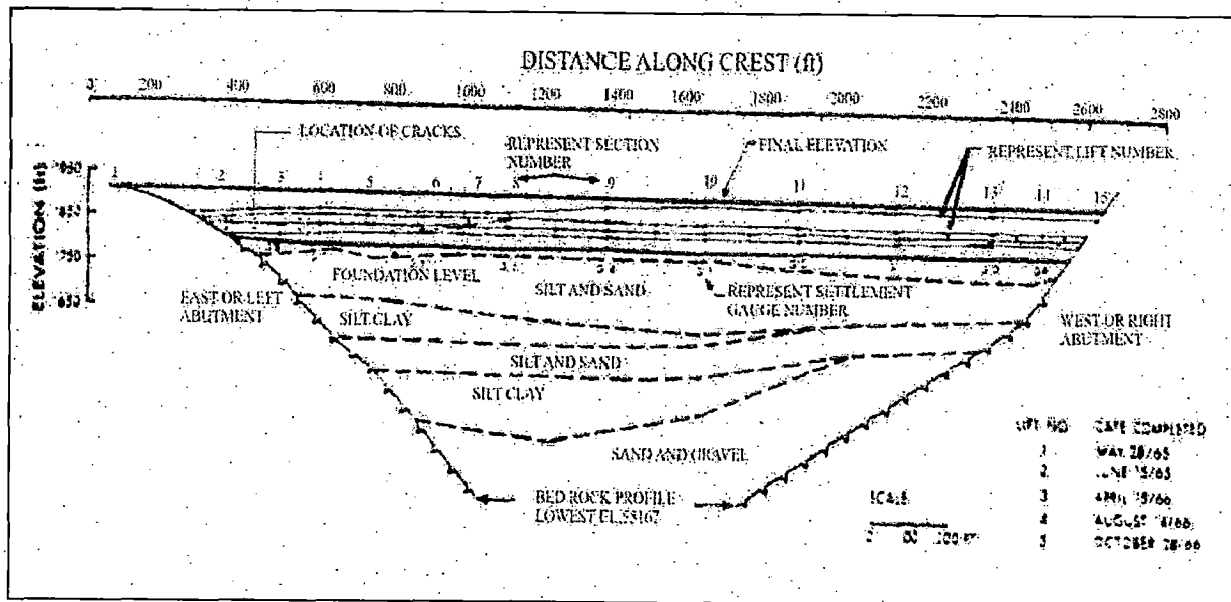
Fig.2.8(b). Longitudinal section of Duncan Dam and foundation showing construction sequence and location of crack

The designers of the dam anticipated large amount of settlement and designed the dam to accommodate these. While the predicted and observed settlements agreed in their magnitudes the observed distribution pattern differed from the predicted one. The maximum settlement that was expected beneath the middle of the dam finally appeared to be close to the left abutment. This non-uniformity exaggerated the differential movements and as a result transverse cracks appeared in an area located at the upstream side of the dam close to the left abutment. All the cracks did not appear simultaneously and at the same level of filling, illustrated in Fig.2.9.

The dam has been analyzed by a 3-D finite element program using hexahedral isoparametric elements with 8 nodes. The analysis has been performed incrementally and follows the actual sequence of filling. The elastic parameters have been derived from stress-strain relationship obtained from tri-axial compression tests on the core and

shell materials. The curves were introduced directly into the computer point by point and the tangent material stiffness parameters were interpolated from them according to the particular level of deviator and minor principal stresses. The volumetric strain data were truncated to preclude any dilatancy. The results of the area computed to be in tension agreed well with the position of the cracks observed on the dam.
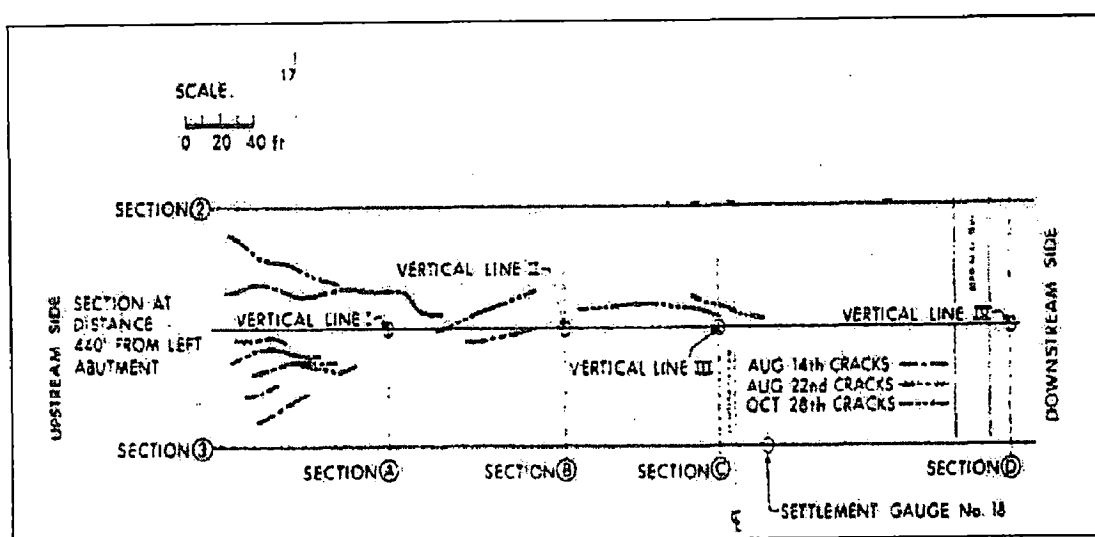
Fig.2.9.   The Cracking Sequence

The results from incremental analysis were consistent with both location of the cracks and their propagation during construction. Hence it can be inferred that finite element analysis can provide substantial information about stress and deformation and regarding the location and extent of cracks in earth dams.

2.3.3. Analysis of Mica Dam

Eisenstein and Simmons (1975) investigated the construction settlements and stresses of Mica dam in British Columbia, Canada by three dimensional finite element

analyses. The 243 m high earthfill structure in a skewed and steep valley has been extensively instrumented and observations are taken regularly. With the crest length 792 m, the dam has L/H ratio 3.26 accordingly. The main section of the dam is figured below.
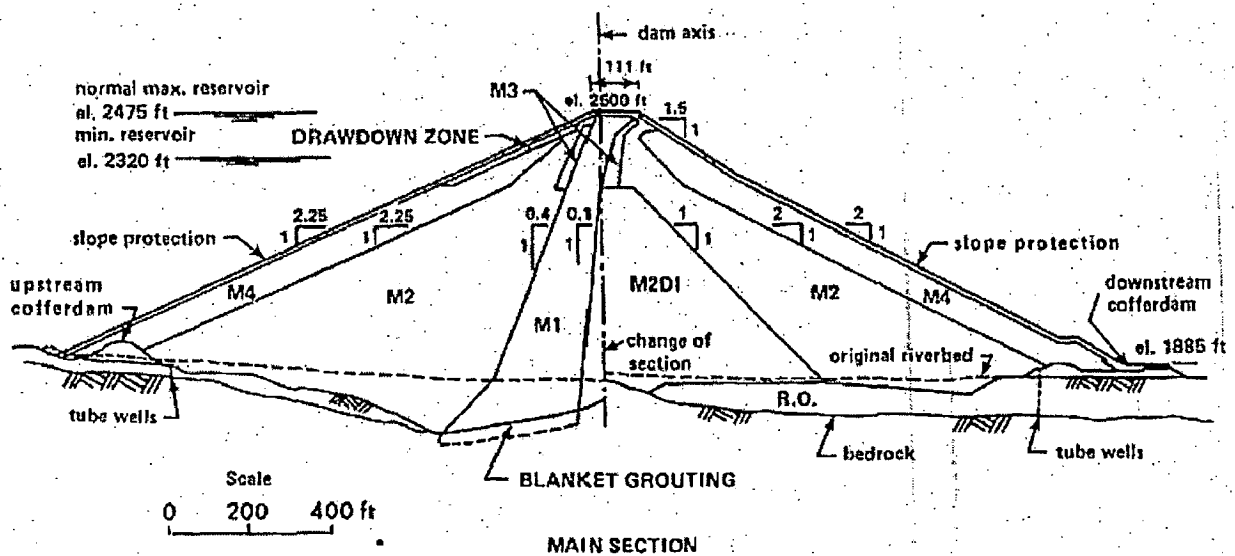
ZONE	DESCRIPTION
M1	Core, glacial till in 25 cm (10") layers
M2	Main shell, sand and gravel in 30 cm (12") layers, changed during construction to 45 cm (18") layers
M2DI	Inner zone of poorer M2 materials
M3	Core support zone, sand and gravel or rock in 15 cm (6") layers
M4	Outer shell, sand and gravel or rock in 60 cm (24") layers
Drawdown Zone	Gravel, cobbles and boulders or rock in 60 cm (24") layers
R.O.	Original River Overburden

Figure 2.10. Main Transverse Section of Mica Dam

The dam's axis is slightly curved upstream to add arching action as a measure against cracking. A 3-D finite element program FENA3D was used in this study using eight nodded isoparametric hexahedral elements and has options for linear as well as non linear stress-strain relationship for

incremental analysis. The mesh consisted of 254 elements and 276 nodes and the number of lifts taken were five with the first lift modeling the river overburden excavation and the remaining four lifts representing each of the four construction seasons (1969-1972). As the study was comparative in nature, following types of analyses were performed:

1. Two-dimensional Linear Analysis

The mesh between Sta. 22+50 and 25+50 was isolated in plane strain by fixing all nodes on or between these sections against cross-valley movement. Five lifts were used to simulate filling and linear elastic parameters represented the seven different materials in the embankment.

2. Three-dimensional Linear Analysis

The full mesh was used, assuming rigid boundaries and embankment filling in five lifts, with the same linear elastic parameter as in 2-D analysis.

3. Three-dimensional Linear Analysis with Bedrock Movements.

Excavation of river overburden material for the core trench caused bedrock to heave upward a maximum of about 15 m. The heaved zone when subsequently loaded by the fill experienced settlements larger than elsewhere. The measured vertical movements (heave or settlement) were used as known displacements at appropriate boundary nodes. Since the bedrock movements were related to the weight of fill, the boundary displacements were applied incrementally with corresponding lifts of the dam.

4. Three-dimensional Multi-linear Analysis

Using the non-linear approach, the deformation moduli of individual elements were allowed to change with the stress

level reached after each lift. This analysis also included the bedrock movements. The computed displacements of Mica dam showed good agreement with field measurement. The plane strain settlements were for most points somewhat larger than the corresponding 3-D results, the maximum difference amounting to less than 20%. However, since the difference was not uniform within the profile investigated it could be due to the coarse mesh. Horizontal movements were very small and no meaningful comparison could be made with the computed values. Of a considerable importance were the horizontal displacements computed by the 3-D analysis for the main transverse section 22+50 which was also the plane strain section used in 2-D analysis. The results, shown in Fig.2.11, indicate that the maximum longitudinal displacement was 4 cm as opposed to a maximum vertical displacement (within the same section) of 82 cm. The 3-D and 2-D plane strain stresses for the main transverse section in the zoned dam were very similar indicating that cross valley arching did not play an important role in the stress transfer.
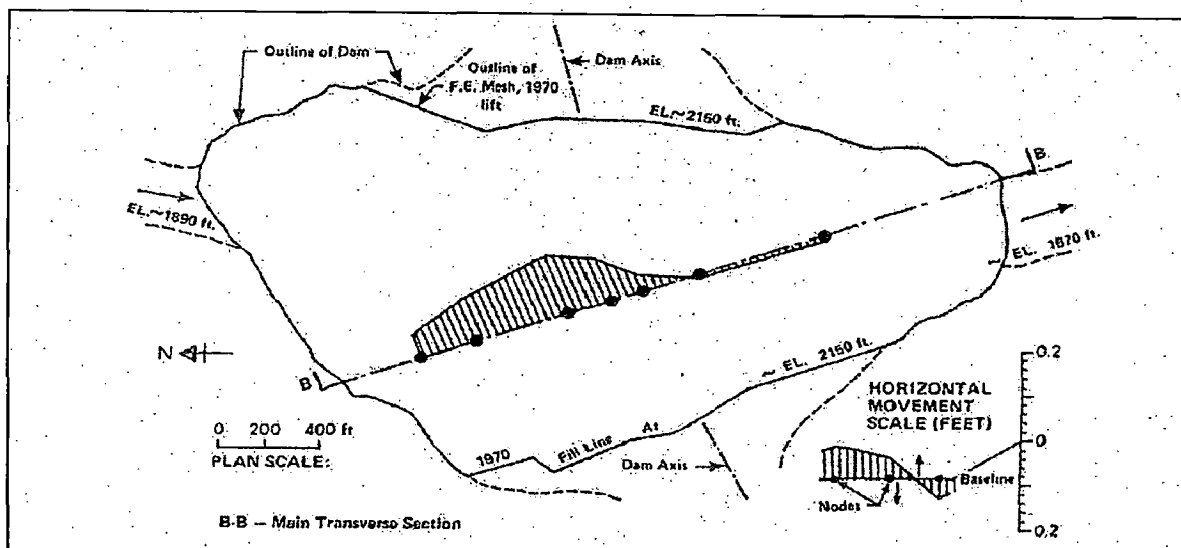
Fig.2.11. Horizontal displacements along the main transverse section at elevation 2150 due to further fill placement (linear analysis)

In order to separate the effects of non-homogeneity of the zoned profile and of the arching across the narrow valley, a 3-D analysis of an equivalent homogeneous embankment was performed. For this type of analysis a modulus value was sought which would yield overall displacement results matching approximately the overall field behaviour. The major principal stress along a vertical in the core is shown in Fig.2.12 for different analyses. It is seen that for the homogeneous dam, there is a stress transfer of about 30% from the core portion to the shell portion, while for the zoned dam the stress transfer is of the order of about 70% near the base. At higher elevations where the geometric effects would be minimal, the stress transfer was constant at about 10% and 40% respectively for the homogeneous and zoned embankment.
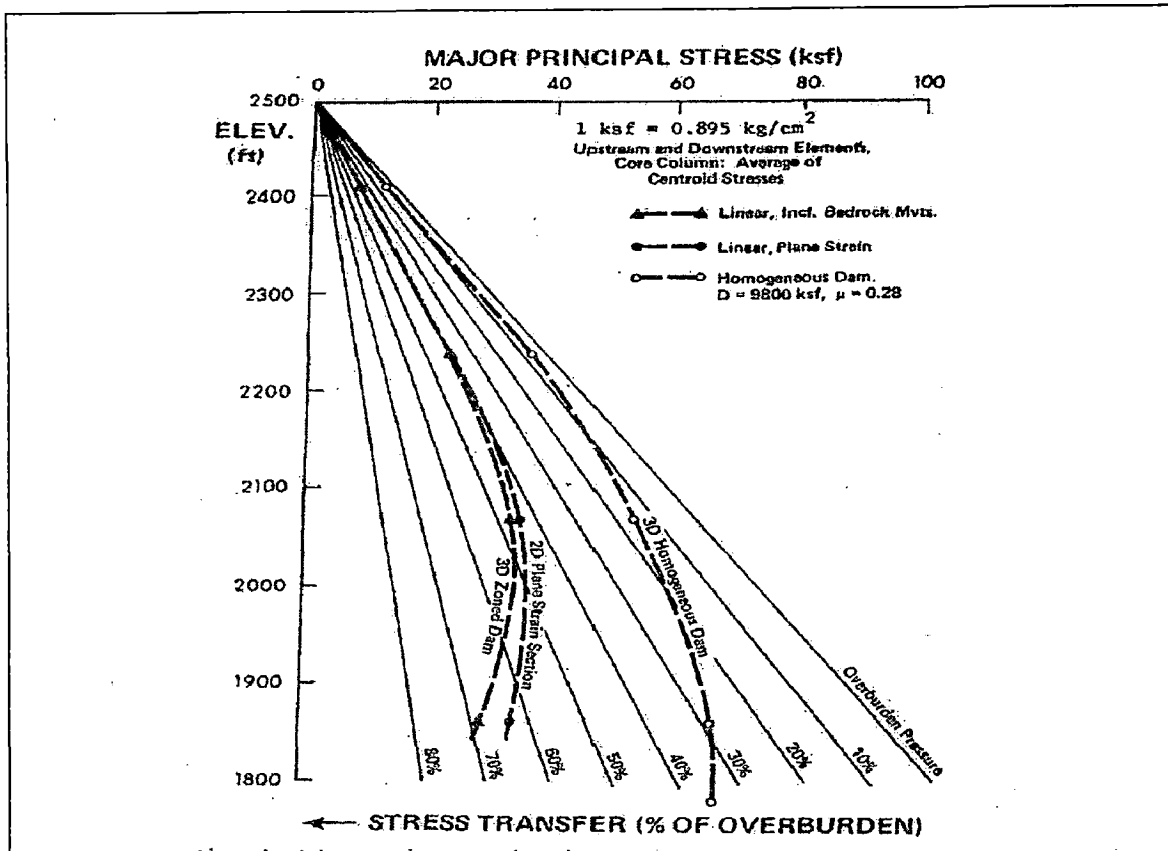
Fig.2.12. Major principle stresses along vertical column of core

According to 3.26 of L/H ratio of the dam, the study concluded that the 3-D finite element analysis despite the coarseness of the mesh has successfully reproduced aspects of the field behaviour of Mica dam. Comparison of 3-D and 2-D analysis indicated that even with a structure so markedly 3-D as Mica dam the main transverse section can be studied using the plane strain model without a significant loss of accuracy. Thus, increased detail and the complexity of stress-strain response that can be incorporated into 2-D analyses appear to be more rewarding than efforts spent on 3-D modeling. Also, the need for 3-D analysis remains when studying the cracking potential of a dam. Such potential usually is highest near abutments where a 2-D analysis can shed no light at all. Considerable but thoughtful simplification of material behaviour can be made and still produce adequate information for design and monitoring purposes.

2.3.4. Analysis of Chicoasen Dam

Marsal and Moreno (1979) reported of the changing of the dam design due to analyses of the stress-strain computation with finite element method at Chicoasen dam, Mexico. Chicoasen dam is an earth and rockfill embankment, 210 m high over riverbed with maximum height over the bedrock of 264 m. The first stress-deformation studies were made for the original design of the dam, which had an central impervious core (case I), as shown on Fig.2.13.

The finite element method was used and non-linear elastic analyses were confined to the case of plane strain. Therefore, two main cross sections were considered, (1) the maximum cross section of the dam, in a plane parallel to the

river and (2) the transverse cross section along the dam axis.
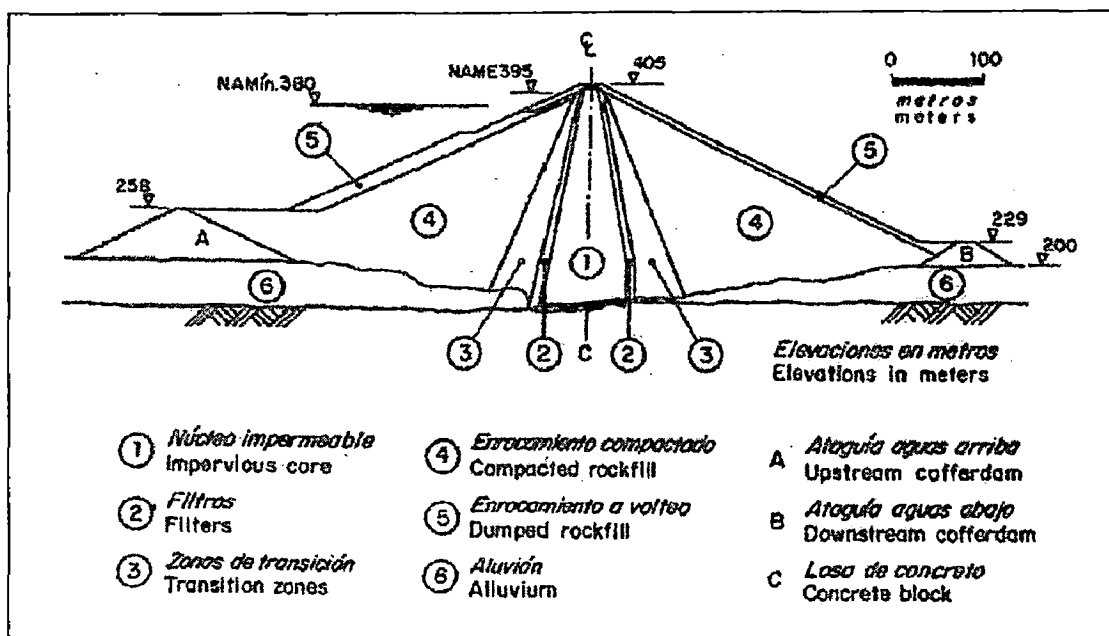
Fig.2.13. First modification of Chicoasen Dam, vertical and central impervious core

Results disclosed a strong arching induced by the walls of the canyon and also significant interaction between the compacted zones of the shells and the core. The consequence of both effects was a substantial reduction in the vertical stresses. At this stage of the studies, the lower gorge of the canyon was not included in the analysis. Furthermore, these studies suggested 3-D analyses, to take into account the influence of the canyon walls and the acceptable alluvial materials left in the river, on the distribution of the stresses inside the embankment.

The 3-D finite element analysis was undertaken assuming linear elastic behaviour of the embankment materials. The mechanical characteristic and zoning of the cross section were developed in five layers (case 2), shown on Fig.2.14.

The analysis showed that the vertical stresses within the core are greater than the adjacent pervious zones, particularly in the lower third of the embankment, and they substantially decrease towards the abutments. The maximum values of σ_z are about 25 kg/cm^2, which are of the same order of magnitude as the hydraulic head.
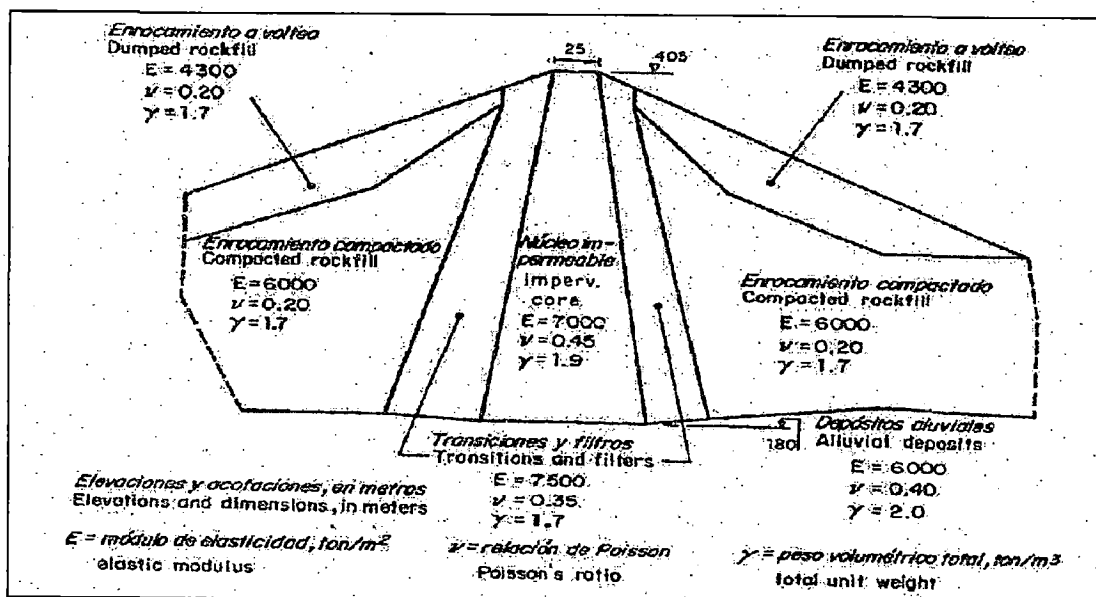
Fig.2.14. Zoning of Materials and properties, case 2

Based on those results, it was proposed to change the zoning materials within the embankments as illustrated by Fig.2.15 (case 3). Two zones of dumped rockfill adjacent to the transition materials were included and, in addition, a strip 4 m wide of soft clayey soil was provided along the abutments. Results for case 3 similar to those previously commented (case 2). Total vertical stresses, σ_z reached to values up to 30 kg/cm2 near the bottom of the canyon, or about 1.5 times the hydraulic head at that elevation. However, σ_z values close to the banks are smaller than the corresponding water pressure, thus disclosing zones of

potential fracturing; this is particularly critical on the left abutment and also a principal stress ratio in the upper central zone of core was equal to 3 or greater, which implies that the clayey material may be subject to large deformations.
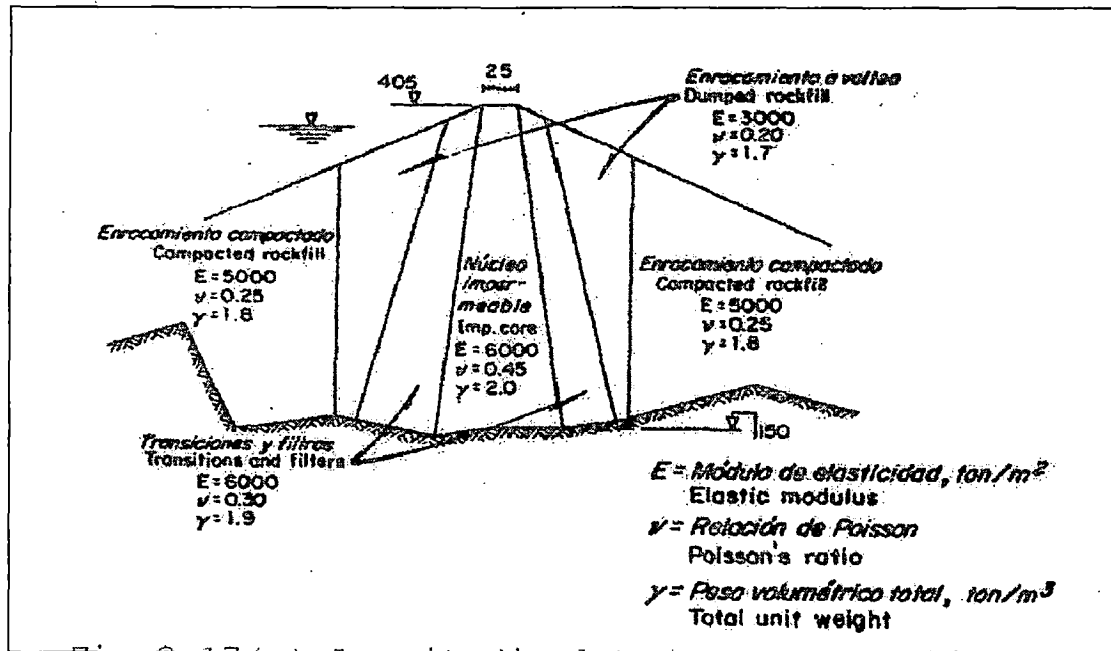
Fig.2.15. Longitudinal maximum cross section, case 3

Additional computations were made for a curved embankment (radius of crest equal to 800 m). Comparison of the stress states developed in this case with those of the straight crest structure did not reveal any significant influence of the curvature, except on the upper 30 to 40 m of the dam. The analysis was repeated considering a non-linear elastic behaviour of the embankment materials. The distribution of total stresses within the dam was similar to that given by linear elastic analysis. Important differences, however, were detected in the magnitude of the deformations calculated with the two above-mentioned assumptions (linearity and non linearity). On the basis of the stress-strain analyses briefly described, it was decided

to build adjacent to the transition, two strips 10 m wide, made of uniform rockfill with nominal grain sizes comprised between 15 and 25 mm. The final modified cross section is shown in Fig.2.16.

A.	Upstream cofferdam	8.	Limestone (U-3)
B.	Downstream cofferdam	9.	Scale in m
C.	Concrete block	B.	D/S Cooferdam
1.	Impervious core	1T.	Tajeria Material
2.	Filter	1W.	LaCostila Material (Wet Optimum)
3.	Transition zone	C.	Concrete
4.	Compacted rockfill	1C.	LaCostila Material
5.	Dumped rockfill		
6.	Selected rockfill		
7.	Alluvium		
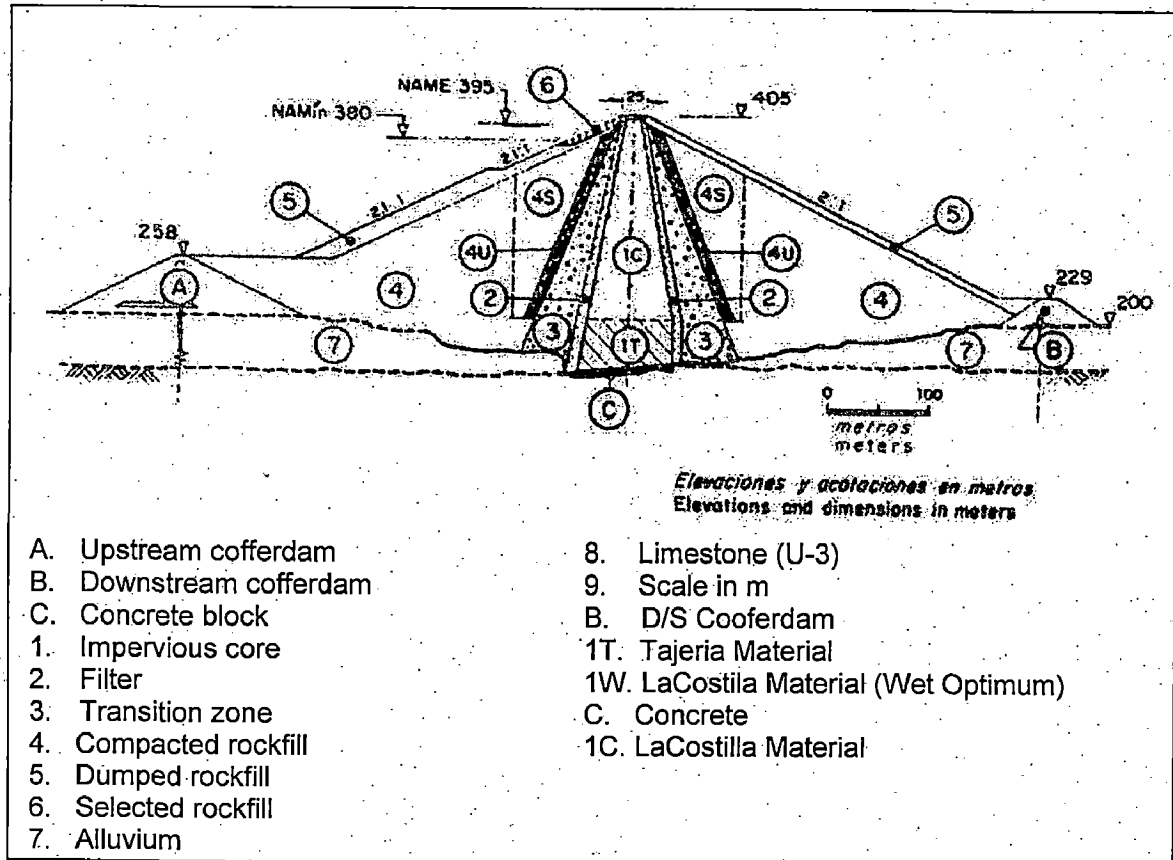
Fig.2.16. Modified Max.cross section of the Chicoasen Dam

In the same dam, Moreno and Albero (1982) analyzed the magnitude of displacements and stresses induced in the structure based upon the observations recorded during construction and the first filling. The recorded magnitudes were obtained from installed instruments such as benchmarks, inclinometers, hydraulic leveling devices, extensometers, piezometers, pressure cells, crossarms and collector drains.

At the end of construction, the instruments showed a symmetrical displacement filed without sharp changes of direction or magnitude. Maximum settlement within the core

was 2m, at El.280 and differential settlement at this between the core, filter and transition was less than 30 cm. Stress paths obtained from the pressure cells suggested that the presence of a plastified zone in the central part of the core and of the filters and transitions, and also confirmed by the data from the inclinometers and crossarms. Just as occurred in the Infiernillo dam, a notable increment in settlements along the upper boundary of the zone of plastification is to be expected in the long term after the first filling, as is the extension of this zone towards the upstream shell. To clarify this point, long-term observation will be required.

At the first of reservoir filling, the instruments showed the pronounced settlements in the zone of the upstream rockfill, transition and filter between El.270 and 320 (upper boundary of zone of plastification). This marked increase in settlements is due to the plastification of the materials in the zone indicated which. A deformation of horizontal extension in a direction parallel to the river causes a reduction in the horizontal confining stress, to a degree that the material plastifies. The maximum settlement stated in the centre of the core is of the order of 2.30 m.

2.3.5. Analysis of Dartmouth Dam

Adikari, Donald and Parkin (1982) had studied about Dartmouth dam, a 180 m high rockfill with a central clay core and well instrumented, located in North-Eastern Victoria, Australia. A non-linear finite element analysis simulating its construction behaviour was carried out, taking into account the water load prevailing at the end of construction. The finite element mesh to represent the maximum cross section of the dam was formed of four-node

linear isoparametric quadrilateral. The mesh has been built up in 10 equal layers, to simulate construction in 10 lifts, and the nodal points have been chosen to coincide with instrument location as far as practicable. The mesh has not been continued into foundation as it was assumed to be effectively rigid and having no significance to deformation within the dam.
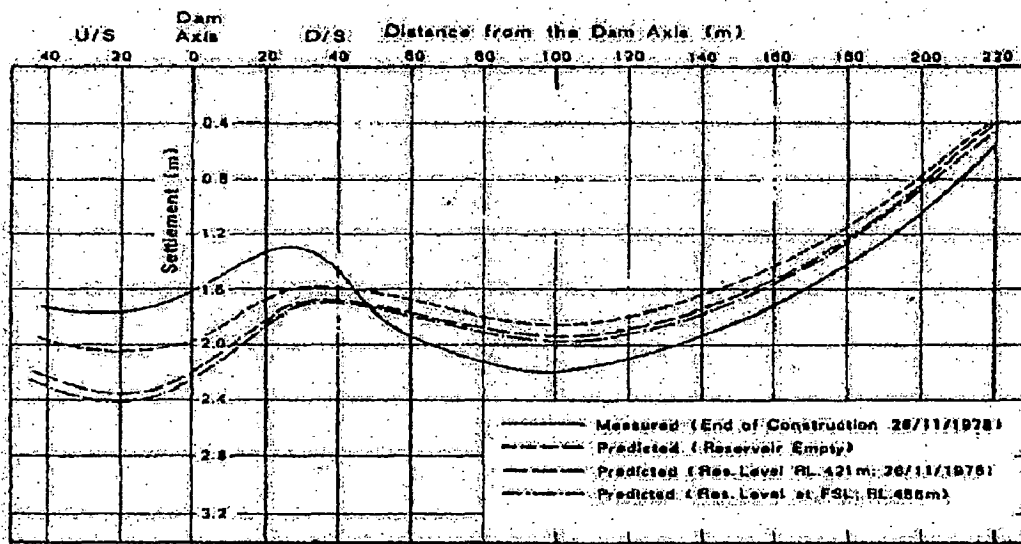
Fig.2.17(a). Settlement Profile at Elev.370
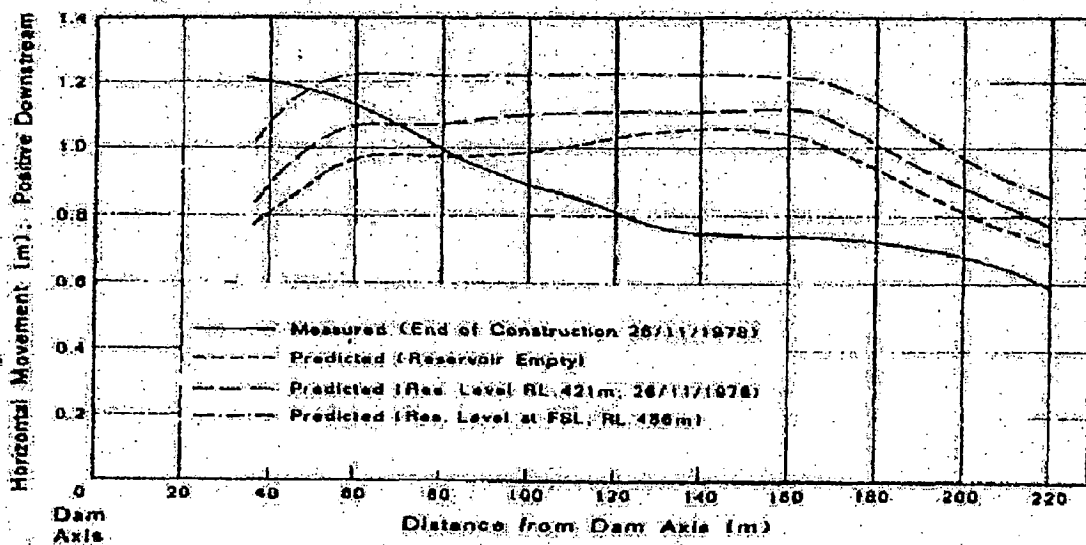
Fig.2.17(b). Horizontal Movement Profile at Elev.370

At the end of construction the reservoir water was 60% full and therefore it was necessary to incorporate 6 steps of incremental reservoir filling into analysis. The water load acts on the upstream face of the core and filling is assumed to be rapid. Agreements of the result of predicted and measured values of displacement are generally satisfactory, as shown In Fig.2.19. The highest stress occurs in the filter zone but the core stresses are lower, the maximum being about 50% of the maximum stress in the filter zone. The stiffer filter zones have resulted in significant interaction effects and a reduction in vertical stresses in the core at all elevations. The prediction of construction pore pressure in core has taken into account the difference in laboratory pore pressure response of material placed (between elev. +400 and +430) from that of the rest of the core material. Negative pore pressure were recorded at that location since November 1977 until positive reading were obtained in March 1979, and have remained positive but only a few meters head.

The behaviour of the material at this location indicates that the load transfer could have been a significant contributory cause for negative pressures.

Some difference between measured and predicted behaviour would appear to be unavoidable. Possible sources of error may be found in the approximations in forming the constitutive law, the use of tri-axial data in a plane strain problem and in the inadequate representation of real variations in material properties, including anisotropy due to rolling and variations in placement moisture content.

2.3.6. Analysis of Tehri Dam

Singh, Gupta and Saini (1985) have presented a 3-D finite element analysis of the Tehri dam to study the effect of providing curvature to the axis under different loading condition, viz. end of construction stage and reservoir full condition stage. Tehri dam is 260.5 m high earth and rockfill dam with a central moderately inclined core with upstream and downstream transition zones. The gorge at the dam site is narrow with slopes at 1.1H:1V.

(a): 2D dam section at B-11 with maximum core height (Sec.1)

(b): 2D dam section at B-15 with maximum d/s slope (Sec. 2)
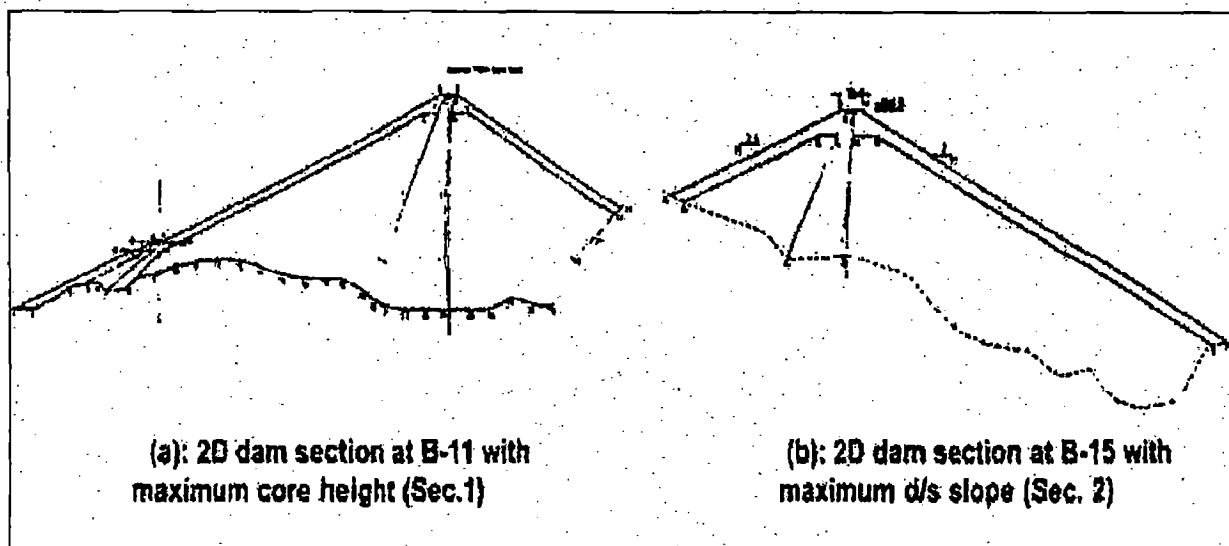
Figure 2.18. Cross Section of Tehri Dam

In the study, the construction in single lift was assumed and full reservoir load was also applied in one stage. The valley shape was assumed to be V-shaped and the linear material behaviour was used for the analysis with the straight and curved axis (radius equal to 800 m). The computer program used 20 nodded isoparametric brick element. The water load has been accounted for as below:

a. Water load on core

b. Buoyancy effect in the shell

c. Additional weight of core zone due to saturation

The results show that there is no significant change in the stresses and displacements in the dam with straight and curved axis for both loading combinations. It is observed that at the vertical normal compressive stresses got reduced in most part of upstream shell and increased in downstream shell for reservoir full condition. The horizontal stresses at end of construction get reduced allover the section with the filling of reservoir. The cross-valley horizontal stresses in the reservoir filling condition are reduced in the upstream shell but in the core the stresses are increased. Allover the upstream faces of the core, the stresses are less than the reservoir water pressure indicating potential for hydraulic fracturing. The minor principal stress for the reservoir full over the central section and longitudinal section across the valley have shown that even though the cross section of the dam does not appear under any appreciable tension, there is a large tensile zone in the shell extending from one abutment to another. To predict cracking, therefore, a 3-D analysis is necessary, as crack cannot be predicted by 2-D analysis and also to study the indication of the occurrence of hydraulic fracturing in the dam.

2.3.7. Analysis of Dabaklamm Dam

Schober and Hupfauf (1991) have studied, using 3D FEM, the behaviour of embankment dams in narrow valley with Dabaklamm dam in Austria as a study case. The Dabaklamm dam is a central core dam with 220 m height, as shown in Fig.2.19. The foundation of shell zone on the upstream side rests on the compressible overburden of fluvial sediments.

The 1.5 ratio of crest length to dam height indicates a narrow valley situation. The behavior in narrow valley is dependent on several influential factors, whereby valley shape stands in the foreground. Furthermore, the deformability and shear resistance of the fill material, the zoning of the dam section, the roughness of the valley flanks and the bearing behaviour of the foundation are of considerable significance.

Fig.2.22. Dabaklamm Dam
1. Earth Core   2. Shell Zones
3. Overburden   4. Bedrock
a. Arching effect
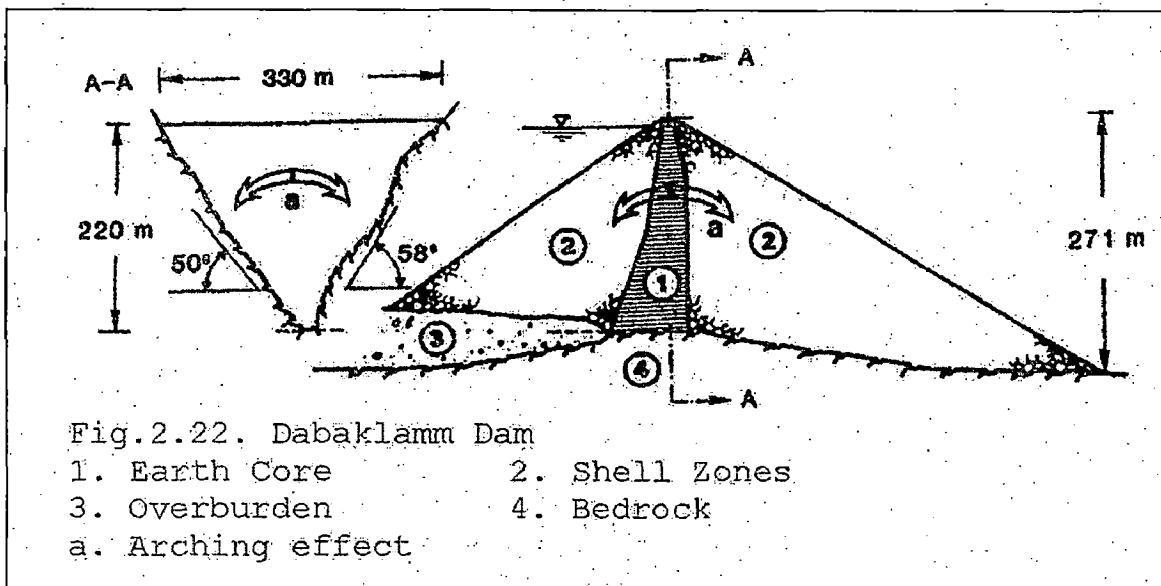
Fig.2.19. Cross section of Dabaklamm Dam

Both deformation and stress conditions were measured during and after filling. Fig. 2.20 shows several results for a flank friction angle of $37°$. The points at which stresses were measured are also marked on the FE-net on Fig.2.20 (a).

a. FEM net, M points msrmnt.   b. σy Isolines
c. Main Stress Axis
d. Isolines of Material Utilization Factor
e. Settlement Isolines   g. Vectors of Deformation
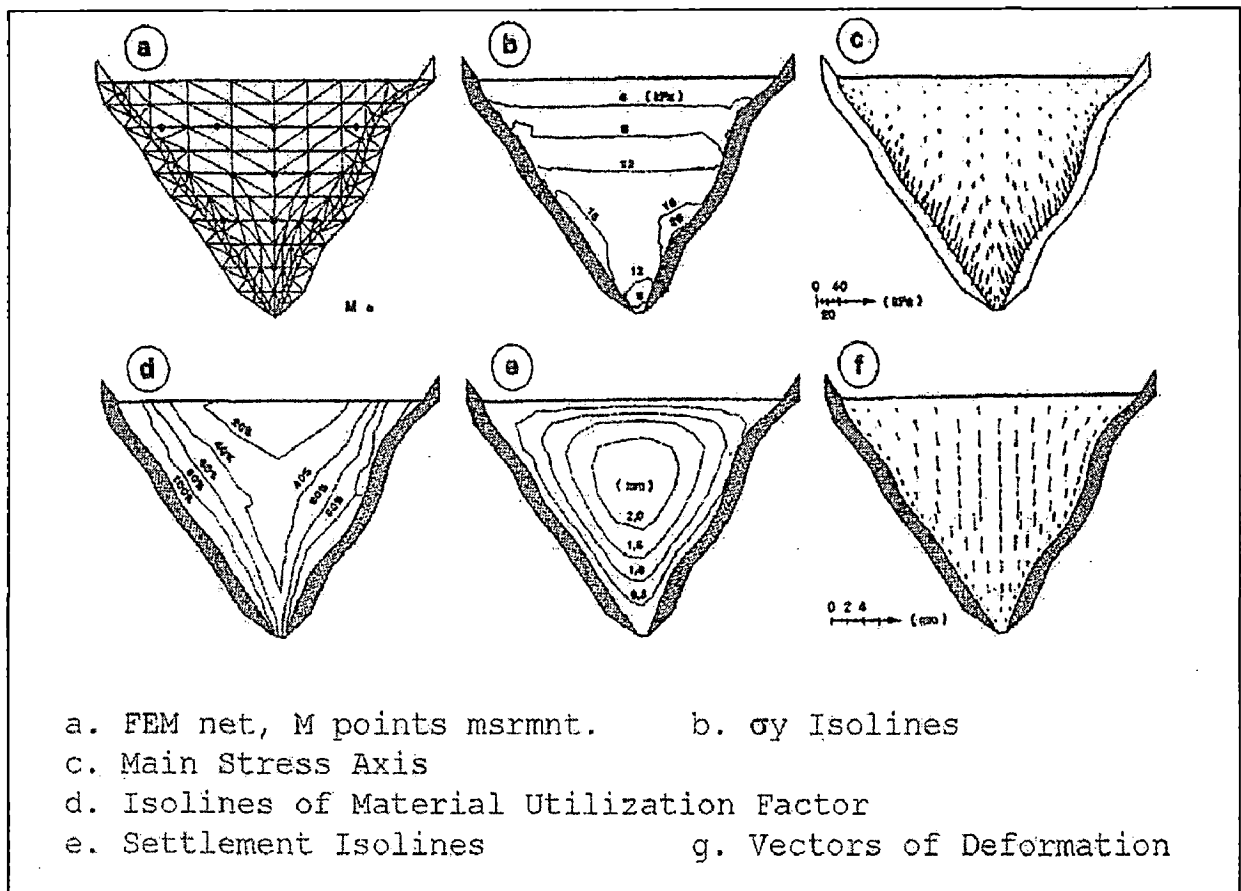
Figure 2.20. FEM Calculation Results of Dabaklamm Dam Model

Fig.2.21 (a) shows a comparison of the vertical and horizontal stresses measured in the model with calculated values for varies of the flanks. Fig.2.21(b) shows the amount of settlement which was measured at 4 different levels as compared to the calculated values. The investigation of the main cross section of the dam was shown in Fig.2.22.
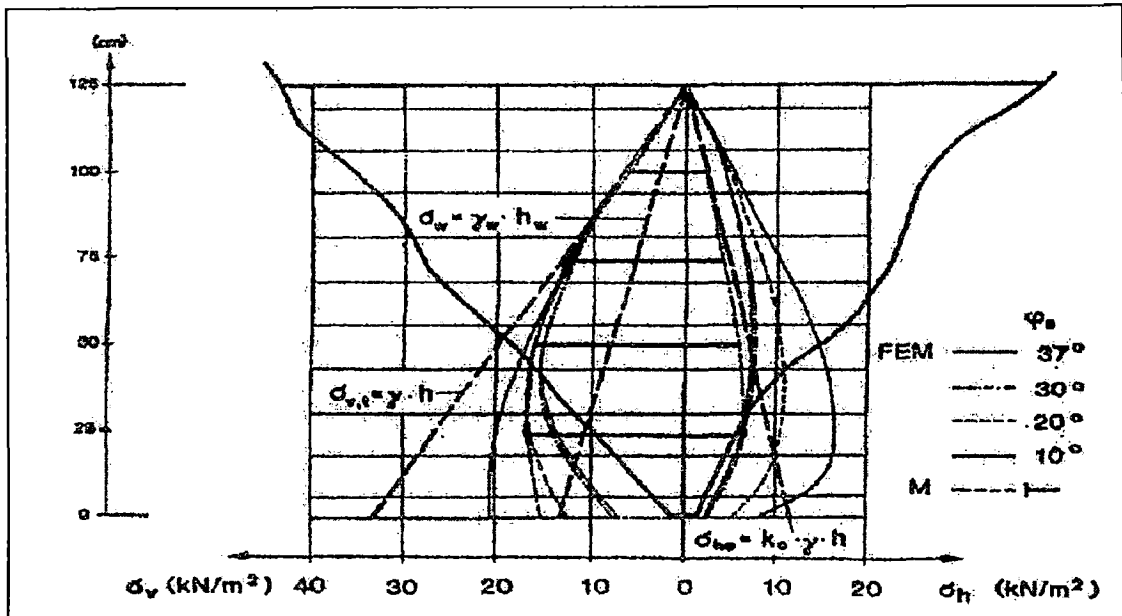
Fig.2.21 (a). Comparison of Horizontal and Vertical Stress
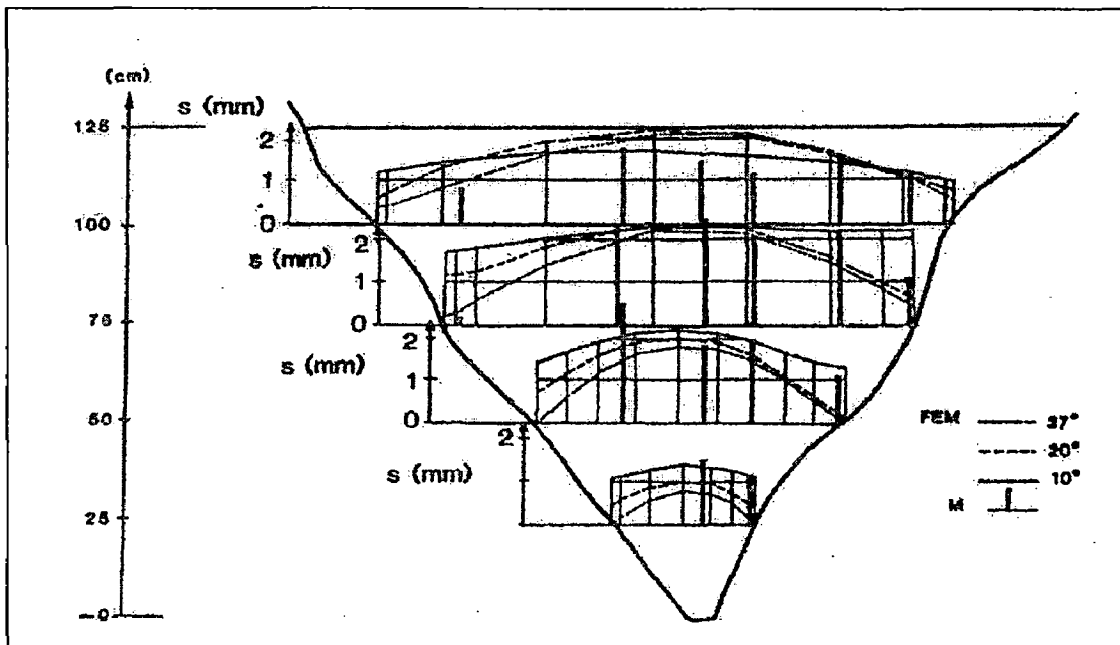
Fig.2.21 (b). Comparison of Settlement

As expected, the compressibility of the overburden has great influence in dead weight load case. Movements toward the upstream side occur which also extend to the downstream side through the upper third core (Fig.2. 22 (c)).

Particularly in the core, this led to zones of greater material utilization (Fig.2.22 (b)). Another result which deserves particular mention is that the compressible overburden affects the rise in vertical stresses in the upstream half of the core as a result of saddling (Fig.2.22(d)).

a. σy Isolines   b. Material Utilization Fac. Isolines
c. Horz. Displ. Isolines   d. Vector of Deformation
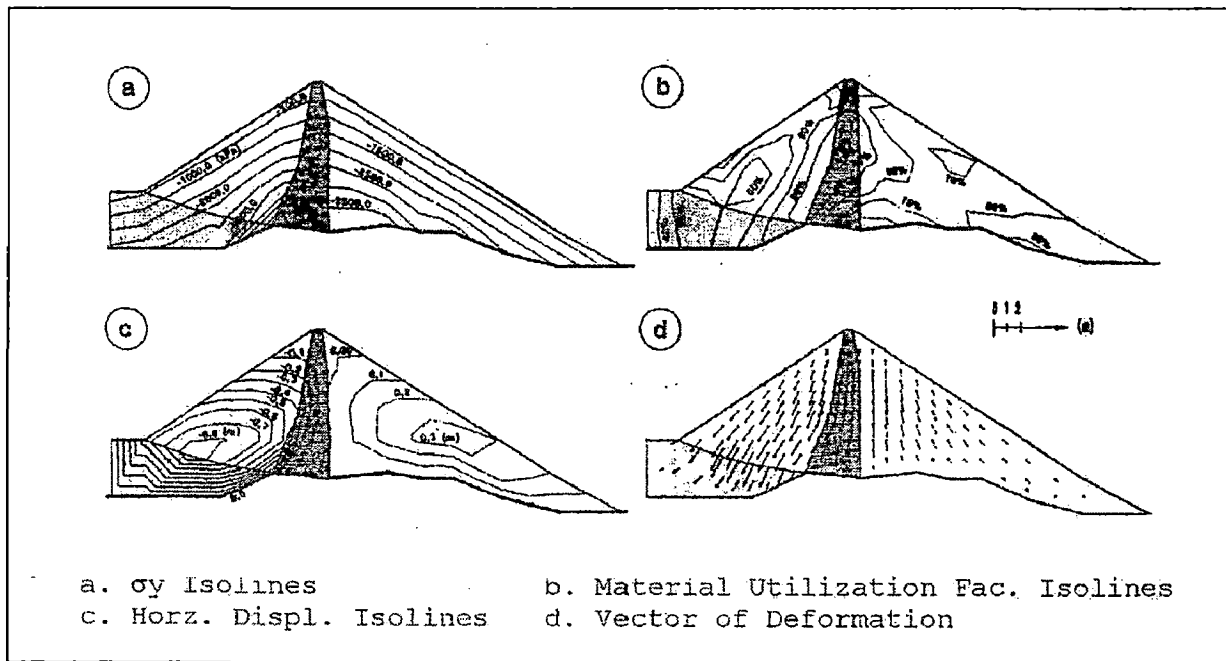
Fig.2.22. Calculation results of dead weight

In summary, the following conclusions can be drawn on the basis of the test result:

• The parametric studies on varies of flank angle, which were carried out, showed that even extreme assumptions have only minor influence on the bearing behavior in the 3D case. This stable behavior is a result of the dominant influence of the geometrical marginal conditions such as valley shape and type of dam, as well as the unchanged parameters such as water pressure, unit weights and shear resistance.

- The contact areas between the earth core and the valley flanks should be as rough as possible. This would mean that disadvantageous displacement along the valley flanks could largely be avoided and that the core would not be isolated in its behavior from these of flanking dam shells.

- To increase the level of stress in the lower half of the dam, the flanks should have as concave a shape as possible.

- The compressible overburden affects the rise in vertical stresses and settlements in the upstream shell of the dam with maximum settlement 0.8 m occurred few meters above the overburden zone.

- With 1.5 of the L/H ratio, the 3D analysis has performed well to study the influences of valley shape and vary flanks on the bearing behaviour of the dam.

2.3.8. Analysis of Yeguas Dam

Justo, et.al.,(2000) observed the settlement of Yeguas dam in France for during and after construction with 3D finite element in FORTRAN language. Yeguas dam has a height of 87 m and a central earth core, the main cross section of the dam is shown In Fig.2.23 with five main zones.

The mesh of the dam was dividing by 10 zones of homogeneous material with hexahedron elements, shown In Fig.2.24.
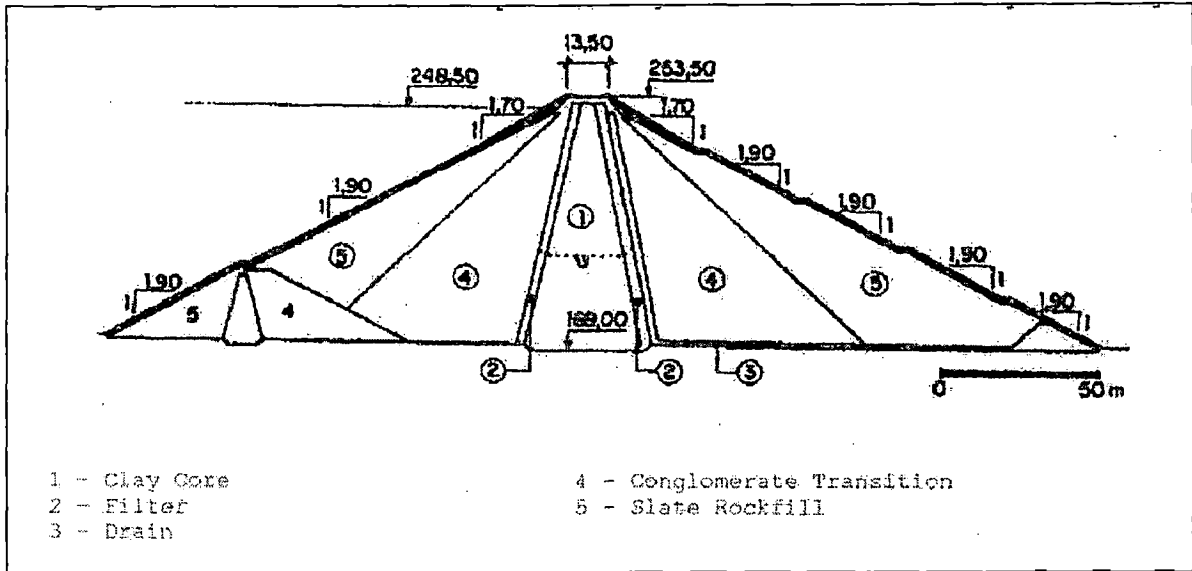
Fig.2.23. Main Cross-Section of Yequas dam

1 - Clay Core   4 - Conglomerate Transition
2 - Filter   5 - Slate Rockfill
3 - Drain

(a). Cross Section Showing the 10 Zones of Homogeneous Properties
(b). Left Half Section of Symmetrical Longitudinal Section
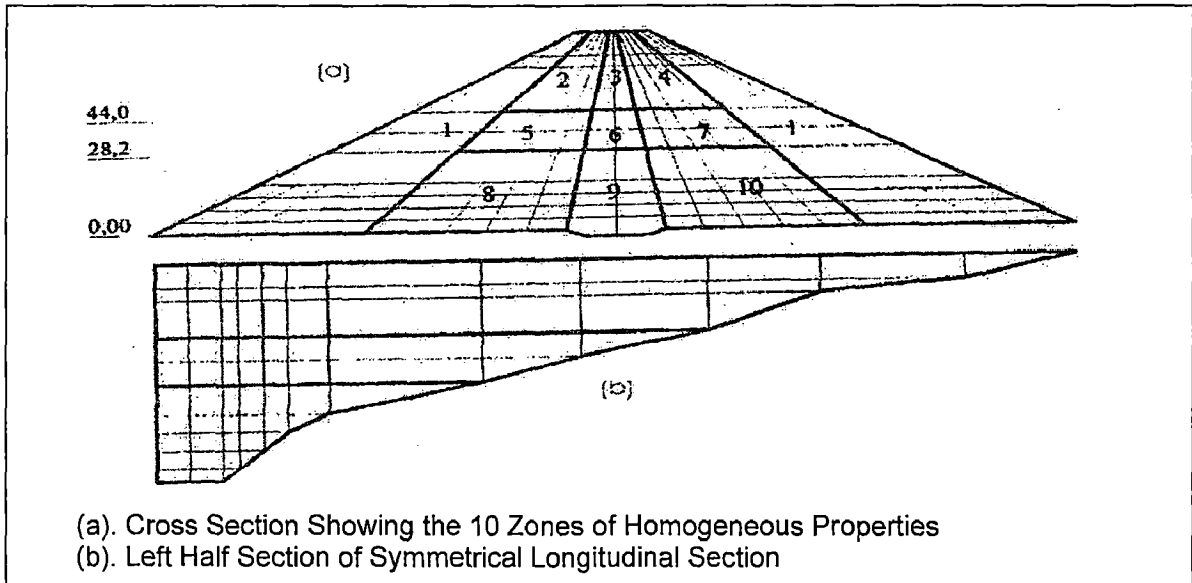
Fig.2.24. FE Mesh

The result of calculation is shown in Fig.2.25 for end of construction. And for the reservoir filling, they used Nobari and Duncan (1972) principles to accommodate the algorithm in the model, laws for the decrease of the modulus with time have been established. The result of calculation was shown in Fig.2.26. It is note that the observed settlements are in good agreement with the computed one.
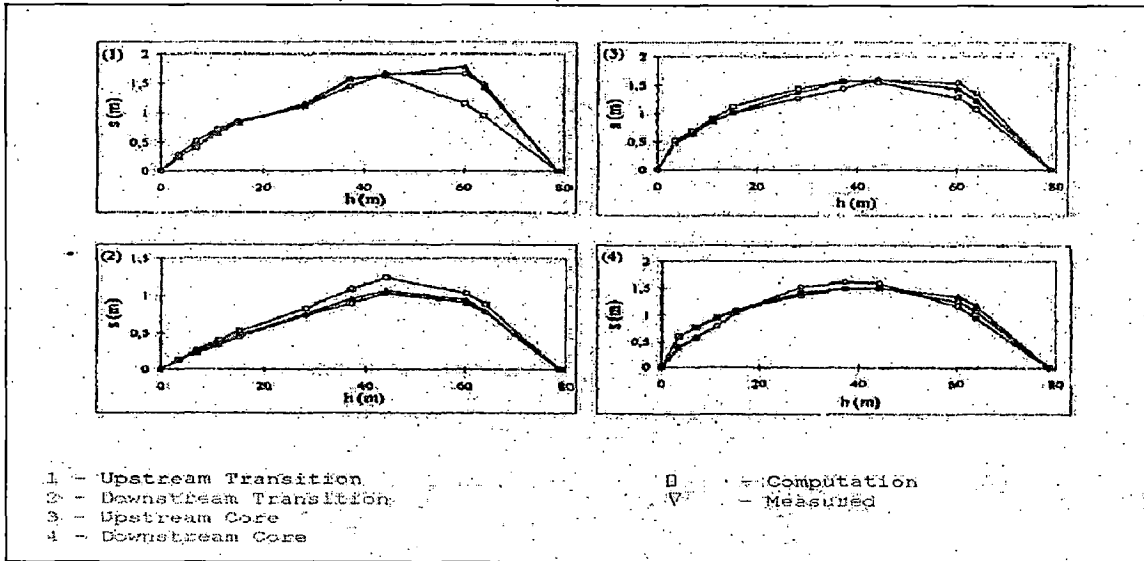
Fig.2.25. Comparison of settlement at end of construction
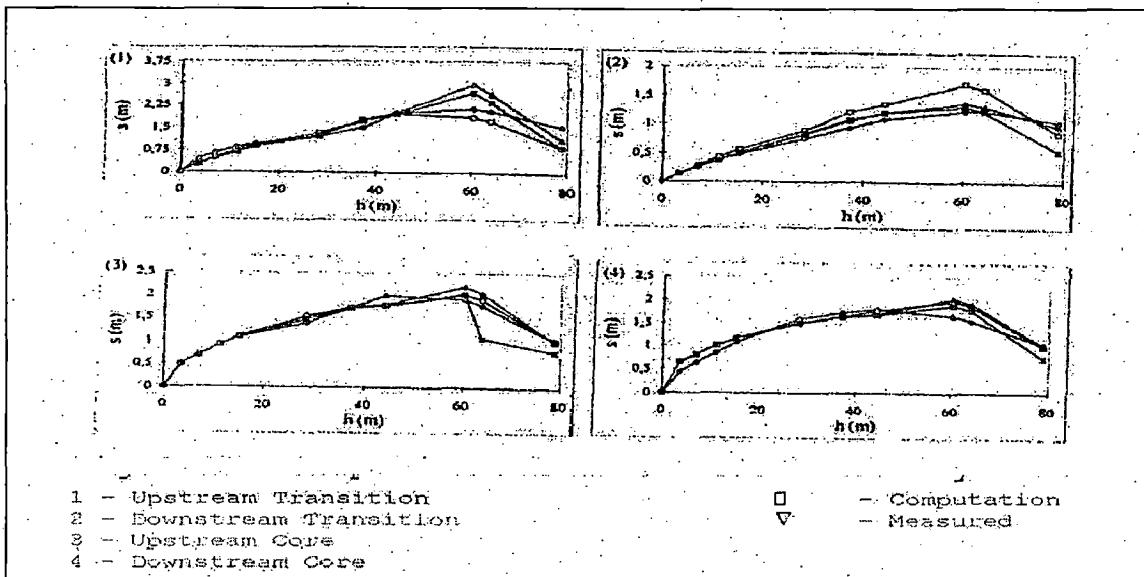
Fig.2.26. Comparison of settlement at 136 days after end construction

2.3.9. Analysis of Tahamara Dam

Inoue, et.al, (2000) studied the mechanism of long-term settlement of rockfill dam after reservoir filling with the Tahamara dam in Japan as a sample case. Tahamara dam is a zoned rockfill dam with a central earth core with height of 116 m and a crest length of 570 m, shown in Figure below.
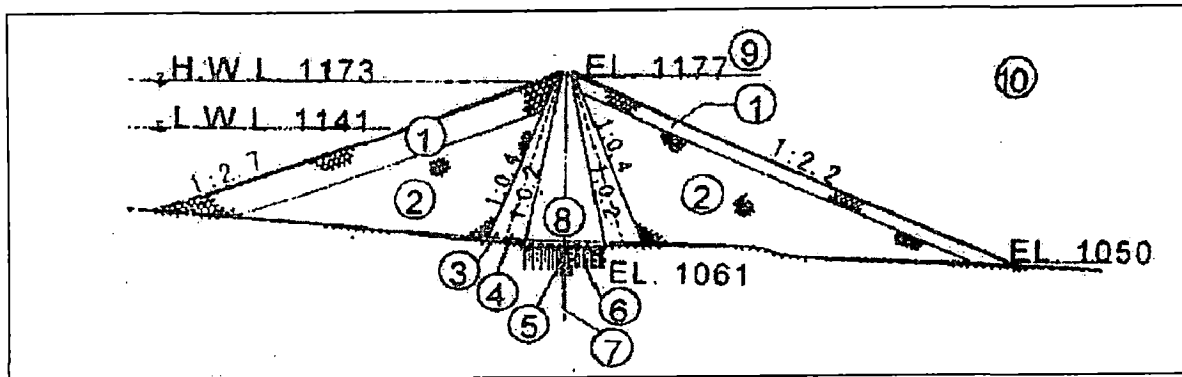
Fig.2.27. Typical Cross Section of Tahamara Dam

· The following five causes were assumed for post construction long-term settlement of the dam:

1. Settlement due to consolidation during the period between completion of embankment and start of reservoir filling. In the period between the completion and the start of reservoir filling, no additional loads are applied and only the dissipation of pore water pressure developed in the core during embankment construction continues.

2. Settlement due to secondary consolidation. Even after the dissipation of pore water pressure, long-term secondary consolidation occurs under a constant embankment load.

3. Settlement due to reservoir loading. Reservoir load acts on the dam body after reservoir filling. They are applied on the upstream face of the core zone during initial filling.

4. Settlement due to infiltration during reservoir filling. Saturation of unsaturated soil generally leads to the loss of surface tension at contacts between soil particles due to water entry into pores and to the movement of soil particles due to decrease of shear

resistance between particle contacts.

5. Settlement due to substantial drawdown of reservoir level. Each time reservoir level is lowered substantially, the settlement is increased. In other words, substantial drawdown of reservoir level causes unrecoverable settlement in an area in the core zone where the water level lowers.

Of the above five causes above, 1 through 3 were modeled by numerical analysis. For 4, infiltration settlement of the actual dam body was calculated based on the results of existing laboratory infiltration tests. For 5, quantification was carried out from the results of cyclic drained shear tests of core materials based on the mechanism assumed from analysis of measured behavior.

1. Outer Shell   4. Fine Filter
2. Inner Shell   5. Coarse Filter
3. Core   6. Foundation Rock
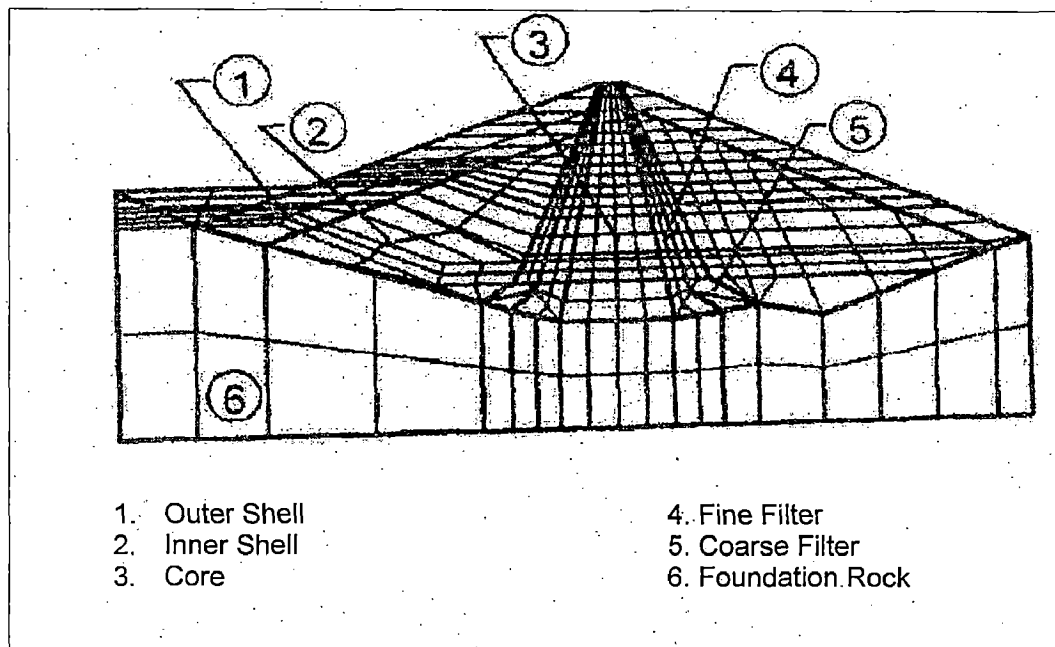
Figure 2.28. Dam Body Model Used for Analysis

Numerical analysis of causes 1 through 3 was made using plane strain finite element method. As a constitutive rule

of embankment material, an elasto-viscoplastic model was
adopted. The model used for the analysis is shown in
Fig.2.28; at each step of construction an additional element
was incorporated. During reservoir filling, water pressure
was applied to the upstream face of the core zone, as a
distributed load.

Figure 2.29.

Distributions of differential compression and cumulative settlement due to
consolidation from completion of embankment to start of reservoir filling

1	Elevation (m)	1	Cote (m)	
2	Actual measurement	2	Valeur mesurée	
3	Caculated value	3	Valeur calculée	
4	— Differential compression (calculated value)	4	— Compression différentielle (valeur calculée)	
	— Cumulative settlement (calculated value)		— Tassement cumulé (valeur calculée)	
	■ Differential compression (actual measurement)		● Compression différentielle (valeur mesurée)	
	o Cumulative settlement (actual measurement)		o Tassement cumulé (valeur mesurée)	
5	Differential compression / Cumulative settlement (mm)	5	Compression différentielle / Tassement cumulé (mm)	

Shown in Fig.2.29 are the results of calculation by
elasto-viscoplastic coupled analysis of settlement in the
core during the period between the completion of embankment

and the start of reservoir filling and demonstrating fair agreement to the actual measurement.

Fig.2.30 shows the result of calculation of the settlement due to consolidation (and secondary consolidation) in the period between the start of reservoir filling and December 1995.

Figure 2.30.
Calculation of settlement due to secondary consolidation from start of reservoir filling to December 1995.

1	Elevation (m)	1	Cote (m)	
2	Lower limit	2	Limite inférieure	
3	Mean value	3	Valeur moyenne	
4	Upper limit	4	Limite supérieure	
5	Differential compression	5	Compression différentielle	
	Cumulative settlement		Tassement cumulé	
6	Differential compression /	5	Compression différentielle /	
	Cumulative settlement (mm)		Tassement cumulé (mm)	

Fig. 2.31 shows a distribution of vertical displacement in the core when a distributed load equivalent to such water pressure was applied on the upstream of the core. Since reservoir loading acts mainly downstream, displacement of the core is predominantly in the horizontal direction. Fig. 2.32 shows the settlement due to infiltration. Infiltration

compression concentrated at high levels in the core zone. This was because the effect of post embankment consolidation is reduced by the decrease of the density due to compaction at this level and also with the reduction of loading.
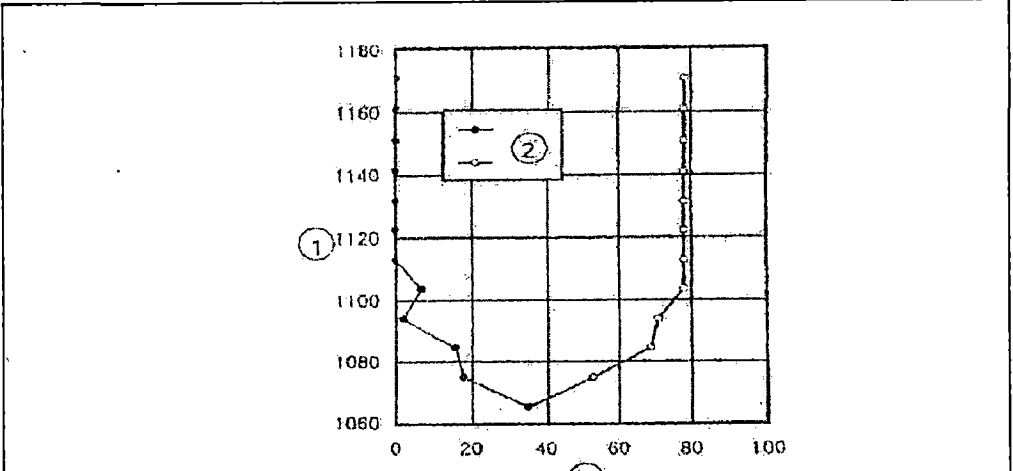
Figure. 2.31.

Calculation of settlement due to reservoir loading

1	Elevation (m)	1	Cote (m)
2	—•— Differential compression	2	—•— Compression différentielle
	—◦— Cumulative settlement		—◦— Tassement cumulé
3	Differential compression /	3	Compression différentielle /
	Cumulative settlement (mm)		Tassement cumulé (mm)

Figure. 2.32.

Calculation of settlement due to infiltration

1	Elevation (m)	1	Cote (m)
2	Differential compression	2	Compression différentielle
3	Cumulative settlement	3	Tassement cumulé
4	Differential compression /	4	Compression différentielle /
	Cumulative settlement (mm)		Tassement cumulé (mm)

Fig.2.33 shows the result of settlement due to change in reservoir level. They are based only on the settlements obtained by analysis of several elements in the surrounding area of a Crossarm. Since the volumetric strain was in proportional to the exponent of shear stress ratio, settlement concentrated at high levels in the core.

1 - Elevation (m)
2 - Cumulative drawdown in 1st to 10th phases
3 - Actual measurement
4 - Range of calculated value
5 - Incremental compression due to reservoir level drawdown
6 - Minimum calculated value
7 - Maximum calculated value
8 - Incremental diff. compression
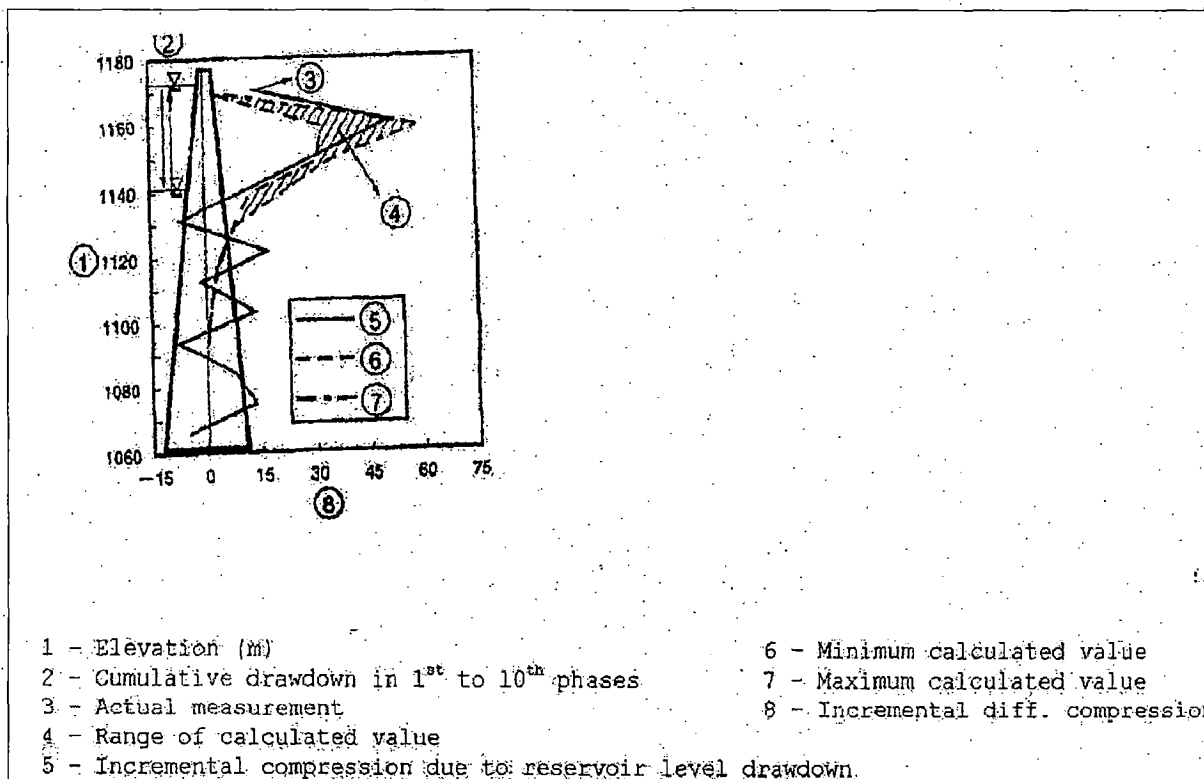
Figure 2.33. Results of calculation of settlements due to change in reservoir filling

Fig.2.34 compares a combined total of differential settlement obtained for different causes from 1 to 5 and actual measurement. As a result of calculation, differential compression was largest at top, medium and bottom levels in the core, agreeing to the actual measurement.

1 - Elevation (m)   5 - Mean value
2 - From Oct,1981 to Dec,1995   6 - Upper limit
3 - Measurement   7 - Lower limit
4 - Calculation   8 - Differential compression (mm)
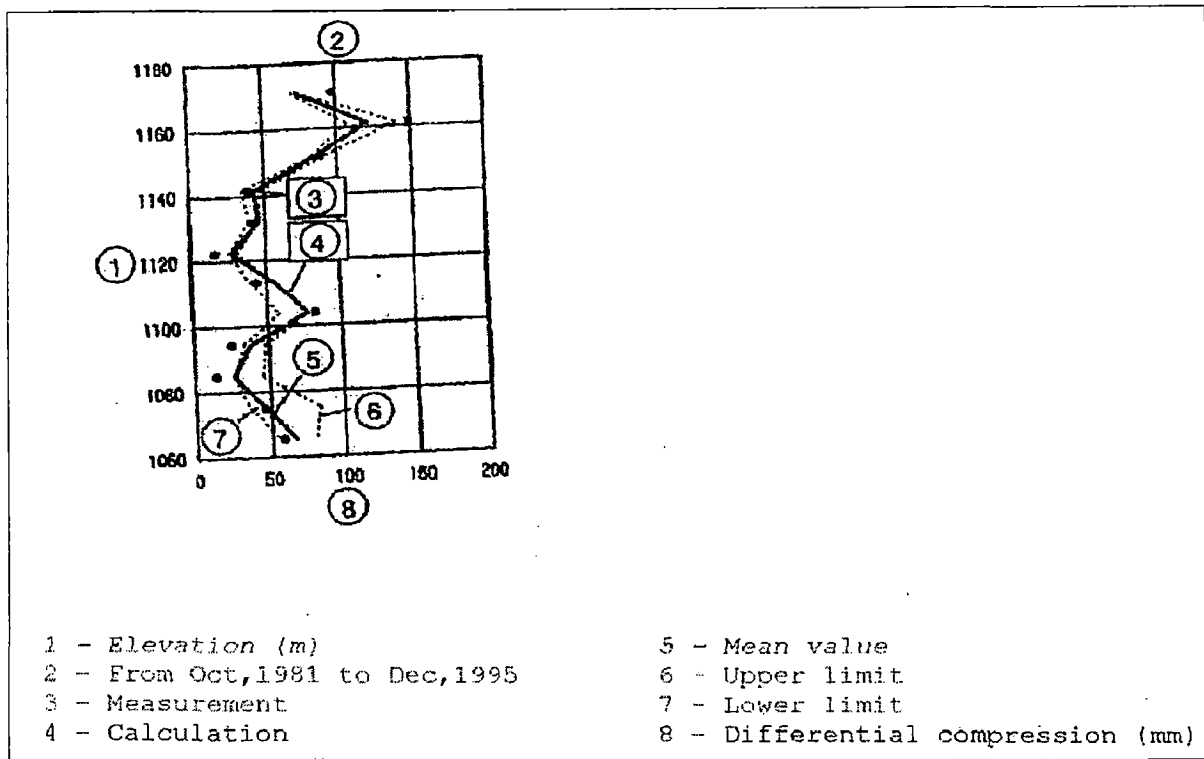
Figure 2.34. Comparison between calculated and measured differential settlements

Fig. 2.35 provides a comparison between the measured settlement and analytical cumulative settlement, the combined total of differential settlement. The curve of distribution of cumulative settlement has several inflection points. It was suggested that the mechanism of long term settlement after the start of reservoir filling is not simple and that settlement is a product of complex combination of factors including material properties, construction condition and post construction loading condition.
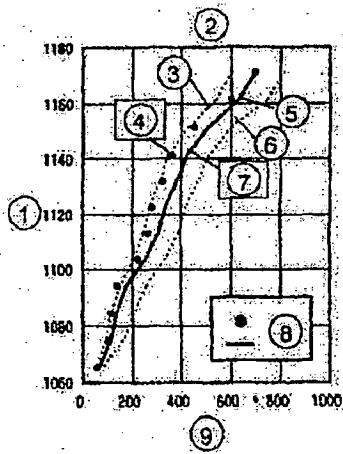
Figure. 2.35. Comparison between calculated and measured cumulative settlement

1 - Elevation (m)
2 - From Oct, 1981 to Dec, 1995
3 - Lower limit
4 - Measurement
5 - Mean value

6 - Upper limit
7 - Calculation
8 - Cumulative settlement: ■ actual measurement
                                        □ calculated value
9 - Cumulative settlement (mm)

Fig. 2.36 shows percentages of causes of crest level settlement. For the Tahamara dam, the causes are ranked in the descending order from dissipation of pore water pressure to secondary consolidation, infiltration settlement, drawdown of reservoir level and reservoir filling loading.
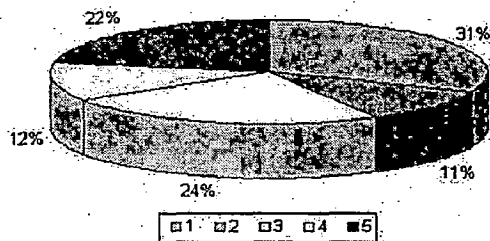
Figure 2.36. Percentage of causes of crest level settlement
1 - Consolidation settlement
2 - Reservoir Loading
3 - Secondary consolidation
4 - Drawdown of reservoir level
5 - Infiltration settlement

2.4. REVIEW OF CASE STUDIES FOR INFLUENCE OF CORE POSITION

Clough et al. (1958) performed dynamic test on scale models (1:150) of central and inclined core dams and found that the central core dam, vertical core breaks the continuity between upstream and downstream segments of the rockfill dams and constitute a zone of weakness. Whereas, the entire structure of sloping core dams acts as a single unit. Also, because of its greater rigidity, sloping core dams showed less settlement that accompanied the shearing distortion.

Sherad et al. (1963) expressed that they did not have any clear evidence and opinion to indicate that sloping core were preferable over the vertical core owing to the less weakness to cracking. However, they believed that the sloping cores could be safer than vertical cores under the earthquake shocks because of the larger body of stable rock exists downstream of the core.

Arya et al. (1978) tested models of central and inclined core dam sections (scale ratio 1:150) to compare their relative performance under reservoir full and empty conditions. Model test demonstrated that slumping of the crest was large in case of the inclined core, though the tendency of the separation of the shell from the core was more in case of central core dams.

According to Krishna (1962), a dam with vertical core vibrates transversely, there is a tendency of masses i.e., upstream shell, core and downstream shell to vibrate out of phase, because of different elastic properties. The three masses possibly tend to separate out resulting in cracks along the junction. This separation could encourage the slipping to occur on either of two slopes. The sloping core

by advantage of one mass resting on the other prevents the tendency of the separation. Therefore, sloping core was suggested as the better option under the dynamic loading.

Saini et al. (1968) studied static as well as dynamic behaviour of three dams; homogeneous dam, dam with the central core, dam with sloping core, with the help of Finite Element Method approach considering the linear elastic properties of the soil and concluded that:

a. The effect of core was to decrease the natural frequency of vibration as compared to homogeneous dams. The effect of the inclination of the core over the central core was to increase the stiffness in certain modes of vibration, but decrease in certain other modes.

b. The effect of core was to increase the static stresses. The sloping core gave rise to an increase in stresses over central core and tensile stresses were developed in a small region near the top.

c. The dynamic stresses for a dam with impervious core were generally lower than those for homogeneous dams with increased stresses near the top portion. For slopping core dynamic stresses were generally higher than those for a central portion. Thus, for slopping core dams the total stress distribution was less favourable giving rise to high tensile stresses near the top region of the dam.

d. Due to the presence of the core, horizontal displacements were decreased, and vertical displacements were increased. The sloping core resulted in increase of the vertical displacements than those for central core dams, though the effects of horizontal displacements were small.

Nayak et al. (1978) analyzed a 260 m. high rockfill dam with vertical and inclined core under two dimensional plane strain condition with linear, mix graded linear and parabolic isoparametric elements. They incorporated sequential construction and non-linear material properties. From the study, it evolved that:

a. Linear elements would be used for rockfill potion and parabolic elements for the core and transitions, where higher accuracy was required due to stress transfer.

b. In case of inclined core, vertical stress concentration in downstream transition was greater than that of vertical core. Also, higher vertical stresses were observed in downstream shell in case of inclined core.

Based on the review above, some conclusions could be resumed into several points below:

1. The separation of the shell from the core is more in case of central core dams.

2. Sloping core is suggested as the better option under the dynamic loading.

3. The sloping core gives rise to an increase in stresses over central core and tensile stresses developed in a small region near the top.

4. In case of inclined core, vertical stress in downstream transition and downstream shell are greater than that of vertical core.

5. The sloping core results in increase of the vertical displacements than those for central core dams, though the effects of horizontal displacements are small.

2.5. REVIEW OF CASE STUDIES FOR 3-DIMENTIONAL FEM

Eisenstein and Simmons (1975) investigated the construction settlements and stresses of Mica dam with L/H ratio 3.26 in British Columbia, Canada by three dimensional finite element analyses. The 3-D and 2-D plane strain stresses for the main transverse section in the zoned dam were very similar indicating that cross valley arching did not play an important role in the stress transfer. In order to separate the effects of non-homogeneity of the zoned profile and of the arching across the narrow valley, a 3-D analysis of an equivalent homogeneous embankment was performed. Comparison of 3-D and 2-D analysis indicated that even with a structure so markedly 3-D as Mica dam the main transverse section can be studied using the plane strain model without a significant loss of accuracy. Thus increased detail and the complexity of stress-strain response that can be incorporated into 2-D analyses appear to be more rewarding than efforts spent on 3-D modeling.

Marsal and Moreno (1979) reported of the stress-strain computation with finite element method at Chicoasen dam, Mexico that these studies suggested 3-D analyses, to take into account the influence of the canyon walls and the acceptable alluvial materials left in the river, on the distribution of the stresses inside the embankment.

Singh, Gupta and Saini (1985) have presented a 3-D finite element analysis of the Tehri dam with 2.2 L/H ratio and said that to predict cracking, a 3-D analysis is necessary as crack can not be predicted by 2-D analysis and to study the indication of the occurrence of hydraulic fracturing in the dam. Such potential usually is highest near abutments where a 2-D analysis can shed no light at all.

Schober and Hupfauf (1991) have studied, using 3D FEM, the behaviour of embankment dams in narrow valley with Dabaklamm dam in Austria. They concluded that the 3D analysis with 1.5 of the L/H ratio has performed well to study the influences of valley shape and vary flanks on the bearing behaviour of the dam.

Based on the review above, some conclusions could be resumed into several points below:

1. 2D analysis provides an accurate representation of condition in centrally located transverse sections of long dams of uniform cross sections and large L/H ratio (>2).

2. In 3-D analysis of dams with small value of L/H ratio, the effect of inclined core, cross valley stress transfer as restraining effects of the canyon walls, and the effect of material properties on the dam situated in narrow valley could take into account to evaluate the dam's behaviour.

2.6. REVIEW OF CASE STUDIES FOR POST-CONSTRUCTION LONG TERM DEFORMATION

Inoue, et.al, (2000) studied the mechanism of long term settlement of rockfill dam after reservoir filling with the Tahamara dam in Japan as a sample case. The following five causes were assumed for post construction long-term settlement of the dam:

1. Settlement due to consolidation during the period between completion of embankment and start of reservoir filling. In the period between the completion and the start of reservoir filling, no additional loads are applied and only the dissipation of pore water pressure developed in the core during embankment construction

continues.

2. Settlement due to secondary consolidation. Even after the dissipation of pore water pressure, long-term secondary consolidation occurs under a constant embankment load.

3. Settlement due to reservoir loading. Reservoir load acts on the dam body after reservoir filling. They are applied on the upstream face of the core zone during initial filling.

4. Settlement due to infiltration during reservoir filling. Saturation of unsaturated soil generally leads to the loss of surface tension at contacts between soil particles due to water entry into pores and to the movement of soil particles due to decrease of shear resistance between particle contacts.

5. Settlement due to substantial drawdown of reservoir level. Each time reservoir level is lowered substantially, the settlement is increased. In other words, substantial drawdown of reservoir level causes unrecoverable settlement in an area in the core zone where the water level lowers.

Of the above five causes above, 1 through 3 could be modeled by numerical analysis. For 4, infiltration settlement of the actual dam body is calculated based on the results of existing laboratory infiltration tests. For 5, quantification is carried out from the results of cyclic drained shear tests of core materials based on the mechanism assumed from analysis of measured behavior.
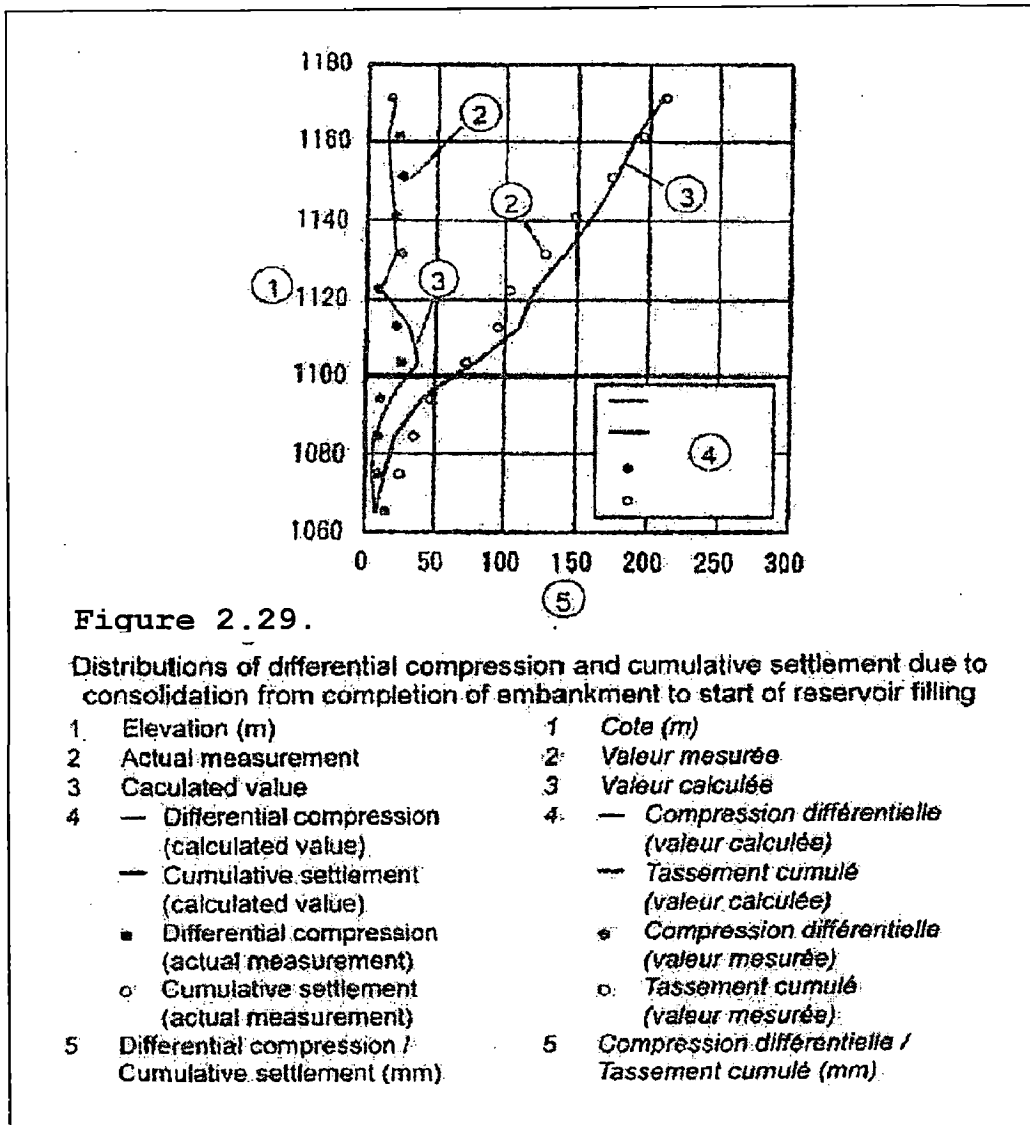
Infiltration compression concentrated at high levels in the core zone. This was because the effect of post embankment consolidation is reduced by the decrease of the

density due to compaction at this level and also with the reduction of loading.

At Chicoasen dam, Mexico, Moreno and Albero (1982) analyzed the magnitude of displacements and stresses induced in the structure based upon the observations recorded during construction and the first filling. Stress paths obtained from the pressure cells suggested that the presence of a plastified zone in the central part of the core and of the filters and transitions, and also confirmed by the data from the inclinometers and cross arms. At the first of reservoir filling, the instruments showed the pronounced settlements in the zone of the upstream rockfill, transition and filter between El.270 and 320 (upper boundary of zone of plastification). This marked increase in settlements is due to the plastification of the materials in the zone indicated which. A deformation of horizontal extension in a direction parallel to the river causes a reduction in the horizontal confining stress, to a degree that the material plastifies. Just as occurred in the Infiernillo dam, a notable increment in settlements along the upper boundary of the zone of plastification is to be expected in the long term after the first filling, as is the extension of this zone towards the upstream shell.

Dibiago et.al (1982) studied the post-construction & reservoir filling performance of Svartevann Dam, Norwegia. It is an earth-rockfill dam with maximum height of 127 m, crest length of 400 m and total volume of 4.7 hm^3. Several considerable remarks related with the dam performance as follows:

• The magnitude of construction pore pressures was found to be acceptable as they were so small they had no significant effect on the overall stability of the dam.

However, the pore pressure was rising significantly according to the raising of the reservoir water level. For each cycle of reservoir filling the pore pressure are somewhat smaller particularly in downstream shell of the dam.

- The calculated and measured seepage values agree well showing the fluctuation patterns of both values were similar for first cycle and appeared differ for subsequent cycles.

- Observed downstream shell surface settlements showed that rate of the increment of the settlements was decreased after construction period and attended to be stable during reservoir cycling. It was notable that the settlements developed very large (more than 1% of the dam height). Similar type of the observed internal displacement results also showed by the instruments installed inside the d/s shell. It was believed that process of creep affected such settlement increments.

Sherard in "Earth and Earth-Rock Dams", 1963, resumed a noticeable point regarding the post-construction movements of embankment dam that in shell rock zone, the post construction settlements results from a gradual readjustments of the rock structure, and it occurs when the rock crush at the point of contact or slip with respect to each other, throwing their loads to adjacent rocks and points of contact.

Based on the review above, some conclusions could be resumed into several points below:

1. The following causes were assumed for post construction long term settlement of the dam; 1) secondary consolidation caused by dissipation of pore water

pressure, 2) reservoir loading acts on the dam body after reservoir filling, 3) infiltration during reservoir filling, 4) substantial drawdown of reservoir level, 5) process of creep, and 6) gradual readjustments of the rock structure.

2. The presence of a plastified zone in a part of the core and of the filters and transitions potentially initiate the large deformations of the dam.

2.7. REVIEW OF CASE STUDIES FOR DEFORMATION DUE TO RESERVOIR FILLING

Measurements made in many embankments dams have shown that large settlements, horizontal movements, and cracking are frequently caused by the reservoir filling. This is known that during reservoir filling, the presence of water create 1) water load on the core and foundation, 2) softening and weakening of the shell material on wetting, and 3) buoyant uplift forces in the upstream shell.

Stresses at wetted portion of dam shell are significantly changes due to buoyancy and presence water load. Meanwhile, softening of shell materials due to wetting cause strength loss and compression at shell material and finally followed by additional settlements for the upstream shell of the dam body. These behaviors are known as secondary compression and consolidations, which tend to increase vertical settlements and decrease horizontal movements. Approximately, the stress-strain parameters reduced 10-20% due to softening, and can be obtained from tri-axial test for dry and wet specimens (Nobari and Duncan, 1971, and Dibiagio et al., 1982).
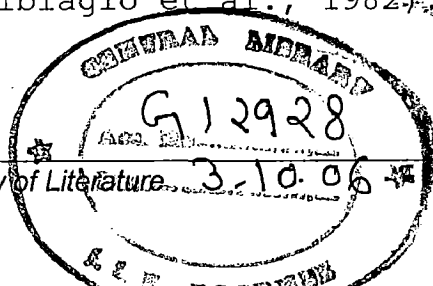
Regarding to the effects of reservoir filling mentioned above, the sequences of the deformation behaviors are found as follows:

1. Deformation due to softening and weakening of the shell material on wetting is occurred during the initial stages of reservoir filling, causes upstream and downward movements.

2. The water load on the upstream foundation causes upstream and downward movements.

3. The buoyant uplift forces in the upstream shell cause upward movements within this zone.

4. The water load on the core causes downstream and downward movements.

The movements are in the downstream direction throughout most of the dam, with exception of the toe of the upstream slope. Within the upstream shell the settlements are dominated by compression of shell material due to wetting and the tendency for expansion of shell as the effective stresses are reduced by submergence. These two counteracting effects result in settlement, which is largest near midheight of the dam. The downward movement of material within most of the upstream shell results in a displacement of material in the upstream direction and a small amount of heave near the upstream toe.

Singh, Gupta and Saini (1985) have presented a 3-D finite element analysis of the Tehri dam under different loading condition, viz. end of construction stage and reservoir full condition stage. It is observed that at the vertical normal compressive stresses got reduced in most part of upstream shell and increased in downstream shell for reservoir full condition. The horizontal stresses at end of construction get reduced allover the section with the

filling of reservoir. The cross-valley horizontal stresses in the reservoir filling condition are reduced in the upstream shell but in the core the stresses are increased.

Yasanuka, Tanaka and Nakano (1985) examined behaviour of Fukuda Earthfill Dam during its construction and first reservoir filling and concluded that the movements of the dam itself due to impounding showed a tendency to lean to upstream side until the reservoir level reached about 80% of the full water and the to move toward downstream as the reservoir level approached the full water level.

Sherard in "Earth and Earth-Rock Dams", 1963, resumed that during reservoir filling, the crest of the dams with sloping upstream cores and large downstream zoned of dumped quarried rock have moved downstream an amount commonly between of 50-75% of the vertical settlements of the crest. For these there is no measurable rebound of the crest when the reservoir is lowered.

Based on the review above, the following conclusions could be drawn:

1. The movements observed during reservoir filling were first in upstream direction and later in downstream direction.

2. The vertical normal compressive stresses got reduced in most part of upstream shell and increased in downstream shell for reservoir full condition.

3. The horizontal stresses at end of construction get reduced allover the section with the filling of reservoir.

4. Approximately, the stress-strain parameters reduced 10-20% due to softening.

2.8. REVIEW OF CASE STUDIES FOR HYDRAULIC FRACTURING

Hydraulic fracturing or the formation of hydraulically induced cracks in the core can occur when the water pressure at a given depth (σ_3) exceed the total stress at the same depth (Kulhawy et al., 1976). If the crack is horizontal, the water pressure would have to exceed the major vertical stress, σy. However, it is also possible that the crack would initiate cracks in the vertical plane, in which case the water pressure would have to exceed the minor principal stress or σp, the stress in the core which is parallel to the face of the core. Earlier studies indicate that the major principal stress in the core is parallel to the upstream face of the core and therefore to σp. Further it is confirmed also that the values of the σl, σp and σy differ by no more than about 5%. So any of theses values can be used regardless of the precise mode of crack initiation.

The hydraulic fracturing mould be most critical when the reservoir rose to maximum pool level quickly and the core did not have sufficient time to consolidate. So, in the present study the total stresses at the end of construction are compared to the hydraulic water pressure, which would occur under full reservoir condition.

Schober and Hupfauf (1991) have studied about the behaviour of embankment dams in narrow valley with Dabaklamm dam In Austria where concluded that, to increase the level of vertical stress in the lower half of the dam in objective to avoid hydraulic fracturing, the flanks should have as concave a shape as possible.

Differential settlement along the axis of the dam may lead to transverse cracking, which could allow passage of water. Differential settlement between the core an the shell can

lead to stress reduction in the core and may results lower material pressure than the hydraulic water pressure, hence hydraulic fracture could be created.

Inoue, et.al, (2000) studied about core fracturing due to saturation condition with Tahamara Dam. The saturation of unsaturated soil generally leads to the loss of surface tension at contact between soil particles due to water entry into cores. The stiffer filter zones have resulted in significant interaction effects to distribute the stresses thus eliminate the zones of potential fracturing.

Based on the review above, some conclusions could be resumed into several points below:

1. Hydraulic fracturing can occur when the water pressure at a given depth (σ_3) exceed the total stress at the same depth.

2. If the crack is horizontal, the water pressure would have to exceed the major vertical stress.

3. If the initiated crack is the vertical plane, the water pressure would have to exceed the minor principal stress or the stress in the core which is parallel to the face of the core.

2.9. REVIEW OF CASE STUDIES FOR LOAD TRANSFER

The possible development of cracks in the cores of zoned dams is one of the major problems confronting the dam designer. Numbers of field observations and studies have indicated that differential settlement leading to load transfer between the adjacent zones is the main causes of cracking. The phenomenon of load transfer (Kulhawy et al.,

1976) occurs in zoned dams because of the stiffnesses of the adjacent zones.

In the construction of the zoned dam with a soft core (low modulus) and a stiff shell (high modulus), the core will settle with the respect to the shell and, if no separation occurs along the zone boundaries, the core will tend to "hang" on the shell. The placements of successive layers of fill accentuates this process of the core settling more than the shell and "hanging" on the shell, with the results that the stresses in the core are less than would be expected before from gravity alone.

For equilibrium on a horizontal plane, the reduction in core stresses must lead to the increase in the stresses of adjacent shell. Therefore, if the core is softer than the shell, load transfer occurs from core to shell leading to hydraulic fracturing or formation of cracks by high water pressure. If the core is stiffer than the shell, then the load transfer may take place from shell to core, which may cause local over stresses in the core.

This load transfer can be evaluated by comparing the computed values of the major principle stress in the core and the core overburden pressure at any given depth below the crest. The ratio less than one indicates load transfer from core to shell, while the ratio greater than 1.0 indicate load transfer from the shell on the core.

Eisenstein and Simmons (1975) investigated the construction settlements and stresses of Mica dam in British Columbia, it is concluded that for the homogeneous dam, there is a stress transfer of about 30% from the core portion to the shell portion, while for the zoned dam the stress transfer is of the order of about 70% near the base. At higher elevations where the geometric effects would be

minimal, the stress transfer was constant at about 10% and 40% respectively for the homogeneous and zoned embankment.

Adikari, Donald and Parkin (1982) had studied about Dartmouth dam. The prediction of construction pore pressure in core has taken into account the difference in laboratory pore pressure response of material placed (between elev. +400 and +430) from that of the rest of the core material. Negative pore pressure were recorded at that location since November 1977 until positive reading were obtained in March 1979, and have remained positive but only a few meters head. The behaviour of the material at this location indicates that the load transfer could have been a significant contributory cause for negative pressures.

Based on the review above, some conclusions could be resumed into several points below:

1. If the core is softer than the shell, load transfer occurs from core to shell leading to hydraulic fracturing or formation of cracks by high water pressure.

2. If the core is stiffer than the shell, then the load transfer may take place from shell to core, which may cause local over stresses in the core.

2.10. REVIEW OF CASE STUDIES FOR COMPARISON BETWEEN CALCULATED AND OBSERVED BEHAVIOUR OF EMBANKMENT DAM

Eisenstein, Krishnayya and Morgenstern (1972) analyzed the history of cracking sequence at Duncan dam in Canada. While the predicted and observed settlements agreed in their magnitudes the observed distribution pattern differed from the predicted one. The maximum settlement that was expected below the middle of the dam finally appeared to be close to

the left abutment. This non-uniformity exaggerated the differential movements and as a result transverse cracks appeared in an area located at the upstream side of the dam close to the left abutment.

Adikari, Donald and Parkin (Dartmouth dam, 1982) had found that agreements of the result of predicted and measured values of displacement are generally satisfactory. The highest stress occurs in the filter zone but the core stresses are lower, the maximum being about 50% of the maximum stress in the filter zone. The stiffer filter zones have resulted in significant interaction effects and a reduction in vertical stresses in the core at all elevations. Some difference between measured and predicted behaviour would appear to be unavoidable. Possible sources of error may be found in the approximations in forming the constitutive law, the use of tri-axial data in a plane strain problem and in the inadequate representation of real variations in material properties, including anisotropy due to rolling and variations in placement moisture content.

Botta et.al (1985) have studied about Alicura earthfill dam, Argentina. The main topic of the study is the discussion of the use of instrument data from the construction period in order to calibrate the models, and from the impounding period as to compare measured and calculated responses in the dam. Numerical model of the dam and its foundation were developed in order to analyze stress-strain relationships. Measured data were used to test the model and revise material parameters, which used for predicting the dam behaviour during the impounding as part of the parametric study. 194 four-sided with two-dimensional model was developed representing the highest dam section and the bedrock was introduced as a rigid base in the model. The

stresses and deformations were computed for different reservoir level by introducing submerged density value in the upstream shell to the corresponding levels. The seepage force in the core is applied instead of the water load on core.

The measured settlements showed that the rates of settlements are dependant upon the rate of construction progress and elevation, always increasing and reducing slightly during impounding period. The measured (dotted) and calculated (lined) settlements in the core and downstream shell are plotted versus elevation in figure 2.37 below. These set of curve were used to calibrate the model and it can be seen for the core that a very good correlation between measured and calculated could be achieved (fig.2.37.A).
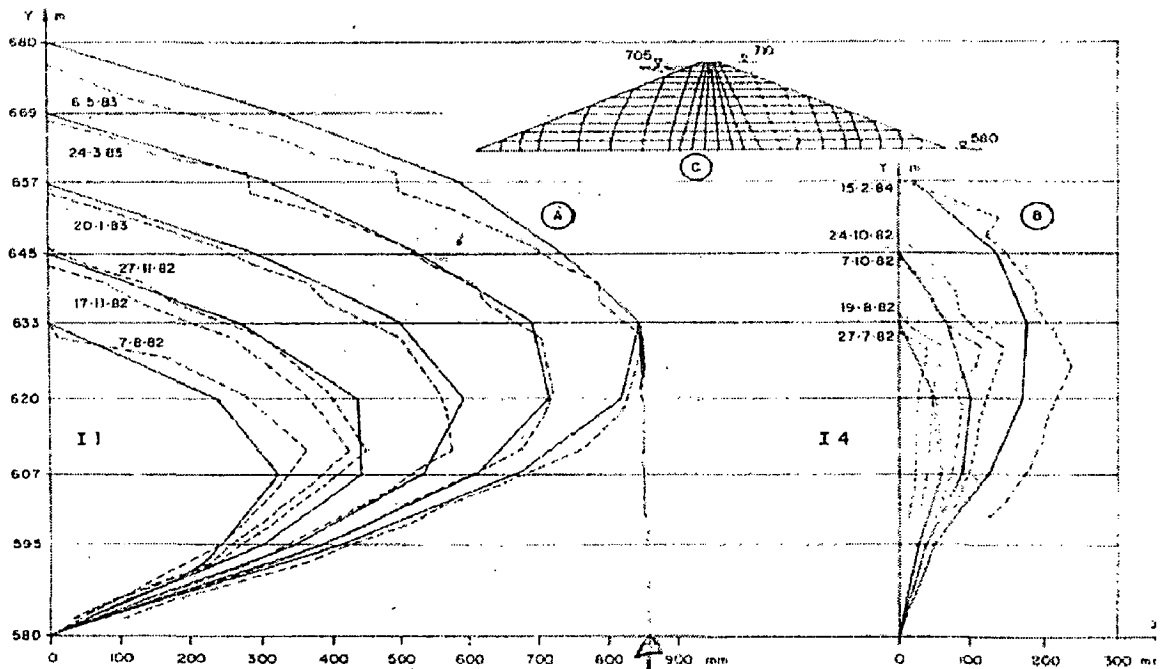
Fig.2.37. Measured and calculated settlements

It was impossible to obtain as good correlation as for the core at downstream portion (fig.2.37.B), because of the effects produced by the nearness to the core-trench slope in the natural alluvium and the inclinometer top in the middle of the downstream shell slope. On the other hand, the shell construction sequences were not reproduced in the model properly. Thought the shell and the foundation can be considered equally dense, the aging effect inherent to the foundation material can be expected to render this material somewhat less deformable than the recently compacted shell fill.

In Fig.2.38.A the isobars for the calculated effective stresses, in this case equal to the total stresses, at the end of the construction are drawn. For the calculated ones due to reservoir filling are indicated in Fig 2.38.B
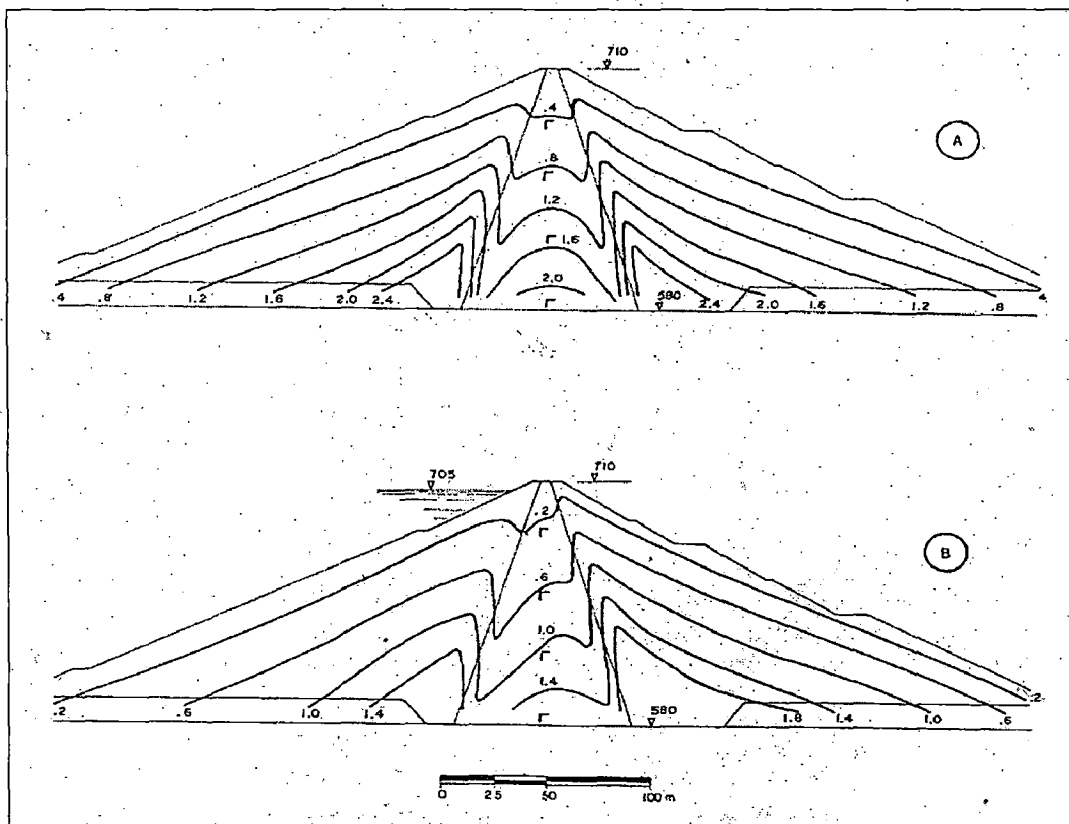
Fig.2.38. Computed distributed vertical stresses (MPa)

It is not possible to confirm the degree of the load transfer in the prototype as unfortunately no total pressure cells were installed outside the core. The total pressures registered during construction and impounding in the center of the core at different levels are plotted versus time in figure 2.39. Curves B & C are calculated stresses for CE1 and CE7 respectively. Curve A illustrates the construction of the core and the curve D for the impounding period.
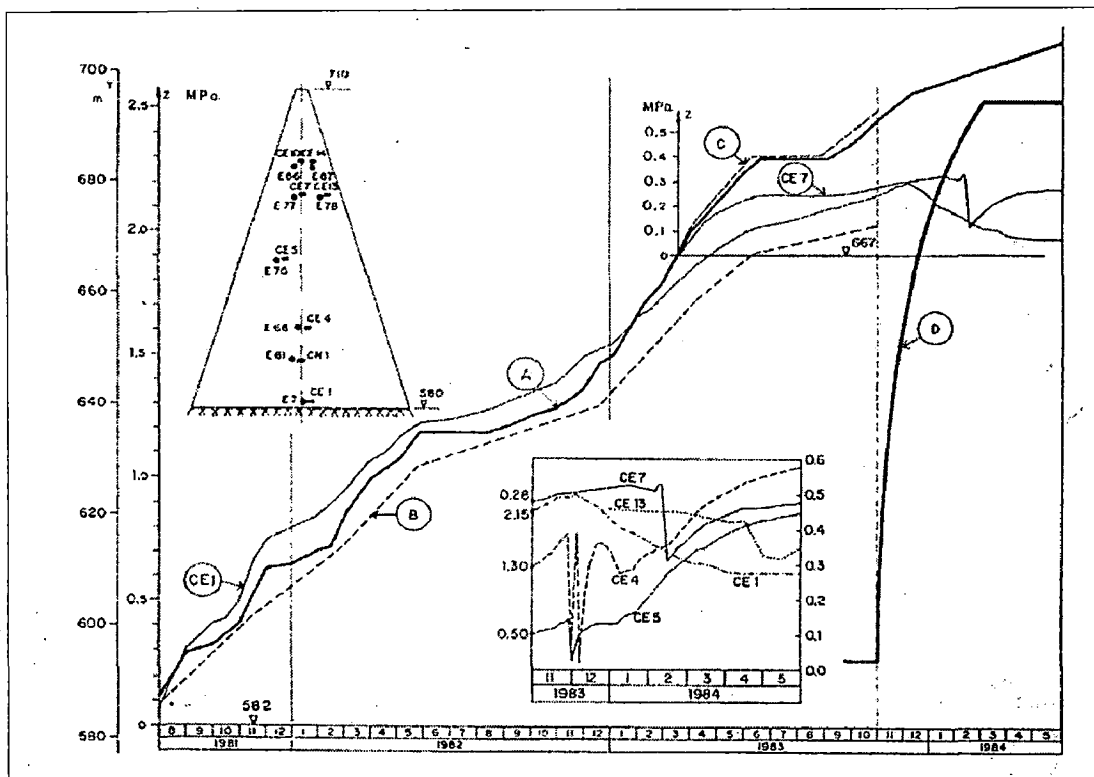
Fig.2.39. Measured and calculated core vertical stresses

It can be seen that the reading of pressure cell CE1 correlate very well with the calculated one. Otherwise, the readings of CE7 show only 60% of the calculated values. This effect is attributed to a certain arching in the core, which has been possible to account in the model. The sudden pressures drops registered in all cells but CE1. These pressure drops coincided in time with the free water surface reaching each cell. The response of cell CE1 is completely

different as this cell was the only cell located in a saturated part of the core already before the start of impounding. Total pressure cells located in the other two instrumented section all presented pressure drops as they were located in unsaturated material. These sudden pressure drops are due to a local material collapse around the cell when the hand-tamped materials around the cell become fully saturated. It is very probable that the fine-grained soils were placed too dry to facilitate the compaction. After the local collapse, the surrounding core material needs some time to settle and overcome a local arching as to newly load cell with the pressure typical for the position.

The calculated deformations for the reservoir at El.695 are indicated at Fig.2.40.A and the measured ones are indicated at Fig.2.40.B below.
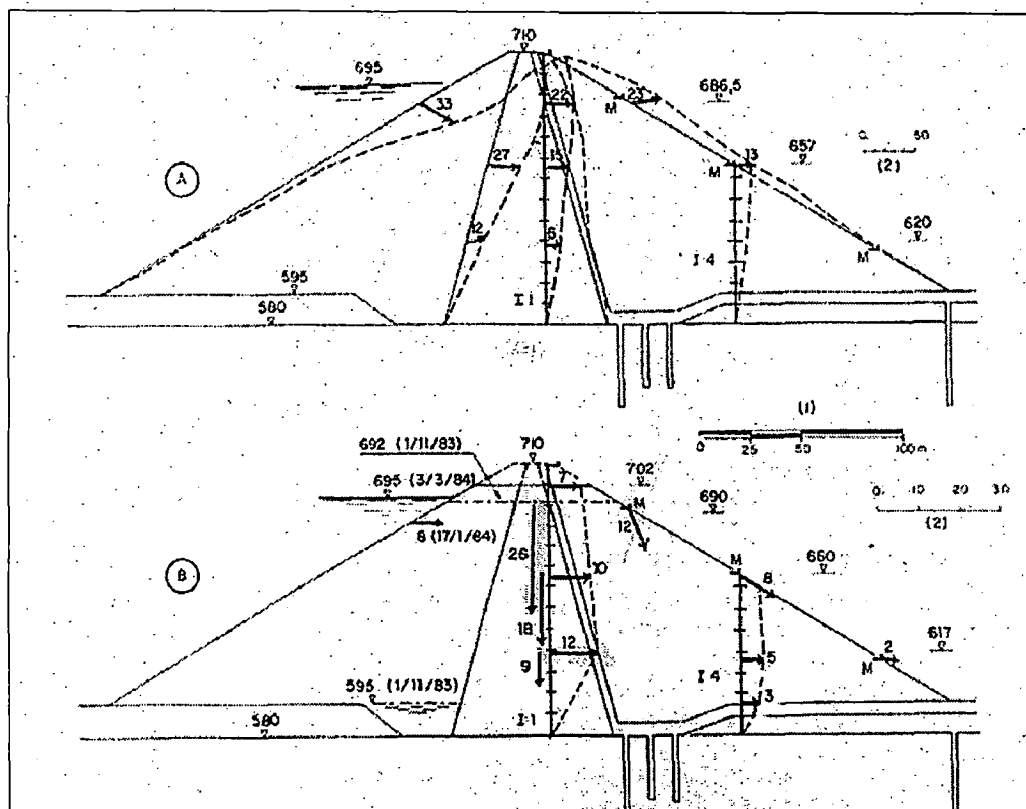
Fig.2.40. Deformation due to reservoir water level

The main difference between the model and prototype behaviour is the direction of the displacements. Part of the explanation for these differences in horizontal displacements may be that the seepage forces in the given situation were acting more inside the core in the lower than in the upper portion where the free water line was less advanced.

Hosseini and Tarkeshdooz (2000) studied the deformations of Karkheh Embankment Dam, Iran. The dam construction has been simulated by application of 14 layers and impounding has been derived into 7 stages. The material parameters are taken from parabolic Duncan & Chang and hyperbolic approximation of the stress-strain curves of tri-axial test. The total and effective stresses, displacements and the pore pressure build up in the different stages and directions were estimated. The deformations of the dam based on the analytical approaches and field measurements (at 50% of its construction process) are compared which concluded that the actual behaviour of the dam is more satisfactory than the predicted ones. Then from the compared results, some conclusions are derived in connection with the verification of the design assumptions, and also the successful remedial measure (using mixed material instead of pure clay core) to limit the settlement (from 3-4% to bel 1%) and pore pressure during construction. It may concluded that; the design remedial measure adopted mixed material; 60% clay and 40% sand and grav appropriate and fulfilled the objectives. And design assumption is verified and the dam will behave in the satisfactory range.

Dibiago et.al (1982) studied the post reservoir filling performance of Svartevar

It is an earth-rockfill dam with maximum height of 127 m, crest length of 400 m and total volume of 4.7 hm^3. Comparison of the measured and calculated internal deformations showed that the magnitude of computed to measured values was quite different for the two type displacements. Maximum measured settlements occurred at mid height of the dam when the calculated showed under estimated results, meanwhile maximum measured horizontal deformation occurred at 2/3 height of the dam when the calculated showed over-estimated results. It was believed that process of creep very well might explain the analytical under-prediction experienced for the settlements, which was not included in the analysis model. From the time histories for internal settlements observation, it was showed that creep effects performed particularly during the construction period.

Yasanuka, Tanaka and Nakano (1985) examined behaviour of Fukuda Earthfill Dam during its construction and first reservoir filling. Non-linear built up analyses based on the constructions stage were performed and the calculated values are checked with the observed values. The conclusion obtained from the observations and the analyses are summarized as follows:

- It was proved by the observations that the foundation of the dam settled due to weight of the embankment and abutment moved toward downstream due to impounding.

- The movements of the dam itself due to impounding showed a tendency to lean to upstream side until the reservoir level reached about 80% of the full water and the to move toward downstream as the reservoir level approached the full water level.

- The pore pressure in the dam responded sensitively to the variation of the reservoir water level without time lag.

- The largest settlement is at the central portion of the dam, and has been found that the non-linear FEM analysis of the dam, in which the parameters obtained by the tri-axial CD test are used, is effective to make prediction on the magnitude of final settlements expected.

- It is important to add "the engineering judgments backed up by analysis" to the results of combined observation, resulting in further contribution to maintain the safety of a dam.

Based on the review, it can be concluded that some unavoidable difference between observed and predicted behaviour would appear probably caused by:

1. Possible sources of error may be found in the approximations in forming the constitutive law

2. The use of tri-axial data in a plane strain problem and in the inadequate representation of real variations in material properties.

3. The construction sequences were not reproduced in the model properly.

4. Process of creep very well might explain the analytical under-prediction experienced for the settlements, which was not included in the analysis model.

2.11. SUMMARY OF THE LITERATURE REVIEWS

The following summary can be drawn from the review of major dams analysis described above:

1. For problem involving complex material properties and boundary conditions, the engineer resorts to numerical methods that provide approximate, but acceptable, solutions. Finite element method was one of the best tools in this area which is the approach shares many of features common to the previous numerical approximations and it possess certain characteristic that take advantage of the special facilities offered by the high speed computers.

2. The literatures show that finite element method could be used to evaluate the effect of incremental construction as compared with single step loading on the stresses and deformations developed in embankments. Seven stages of construction could be sufficient to analyze the incremental embankment construction. The horizontal displacement were seen to be quit similar in both cases but the vertical displacement in single lift was seen to be largest at the top while in seven lifts was seen at the mid height of the dam.

3. Non-linear hyperbolic stress strain model by Kondner and developed later by Kulhawy, Duncan and Chang was widely used to be a constitutive model in analyzing the stresses and deformations in dams. This model was adopted in some major dam analyses such as Oroville, El-Infiernillo, Alicura, Svartevann and Karkheh Dam, etc.

4. The literatures shows that the maximum settlement occurred in major dams have range values between 0.2%

up to 3.4% of the dam height. Below 1% is mostly recorded and 1.01% is the mean percentage. It mostly occurred in the core zone of the dam.

5. The movements observed during reservoir filling were first in upstream direction and later in downstream direction. These complex movements may be understood as the combined effect of two counteracting effects of reservoir filling; (1) the water loads on the dam and (2) the softening and weakening of the fill material due to wetting.

6. 2-D analysis provides an accurate representation of condition in centrally located transverse sections of long dams of uniform cross sections. In case of major dams with large L/H ratio (*Mica dam, 3.26 ratio and Tehri dam, 2.2 ratio*), restraining effects of the canyon walls did not play important roles in the stress transfer.

7. 2-D analysis may not provide a suitable representation of the transverse section for dam in steep valleys (small L/H ratio), because of cross valley stress transfer as restraining effects of the canyon walls. Thus, 3D analysis could be needed to evaluate stresses and deformation in steep valley.

8. In 3-D analysis of dams with small value of L/H ratio (*Dabaklamm Dam, L/H = 1.5*), the effect of inclined core, the arching of the dam and the effect of material properties on the dam situated in narrow valley could take into account to evaluate the dam's behaviour.

9. 200-250 numbers of 4-nodded elements were widely adopted in discretization of 2-D analysis. And at least 350 numbers of 8-nodded bricks elements were adopted in

3-D analysis.

10. The following causes were assumed for post construction long term settlement of the dam; 1) secondary consolidation caused by dissipation of pore water pressure, 2) reservoir loading acts on the dam body after reservoir filling, 3) infiltration during reservoir filling, 4) substantial drawdown of reservoir level, 5) Process of creep, and 6) gradual readjustments of the rock structure, and it occurs when the rock crush at the point of contact or slip with respect to each other.

11. The presence of a plastified zone in the part of the core and of the filters and transitions potentially initiate the large deformations of the dam.

12. The vertical normal compressive stresses got reduced in most part of upstream shell and increased in downstream shell for reservoir full condition.

13. The horizontal stresses at end of construction get reduced allover the section with the filling of reservoir.

14. Approximately, the stress-strain parameters reduced 10-20% due to softening, and can be obtained from tri-axial test for dry and wet specimens.

15. Hydraulic fracturing or the formation of hydraulically induced cracks in the core can occur when the water pressure at a given depth (σ_3) exceed the total stress at the same depth.

16. In reservoir filling, the stiffer filter zones have resulted in significant interaction effects to distribute the stresses thus eliminate the zones of potential fracturing.

17. There is no significant change in the stresses and displacements in the dam with straight and curved axis under both construction and reservoir full conditions.

18. Reduction in core stresses must lead to the increase in the stresses of adjacent shell. Therefore, if the core is softer than the shell, load transfer occurs from core to shell leading to hydraulic fracturing or formation of cracks by high water pressure.

19. If the core is stiffer than the shell, then the load transfer may take place from shell to core, which may cause local over stressing in the core.

20. Some unavoidable difference between observed and predicted behaviour would appear probably caused by:

    ✓ Unsatisfactory performance of the instruments used

    ✓ Possible sources of error may be found in the approximations in forming the constitutive law

    ✓ The use of tri-axial data in a plane strain problem and in the inadequate representation of real variations in material properties.

    ✓ The construction sequences were not reproduced in the model properly.

    ✓ Process of creep and infiltration during reservoir filling very well might explain the analytical under-prediction experienced for the settlements, which was not included in the analysis model.

    ✓ Undesired method of constructions and quality control applied resulting in decrement of strength properties of used materials.

FINITE ELEMENT METHOD ANALYSIS

3.1. INTRODUCTION

Numerical method allied to powerful digital computers give today the possibility of solving almost all well defined physical problems within any accuracy desirable. The Finite Element Method process of discretising and approximating continuum problems has proved itself to be most general and useful procedures. It is, therefore, natural for the engineer concerned with such important structures as dams to turn to this numerical process for the answer to the question posed at the analysis and design stages.

The Finite Element Method was introduced to the geotechnical engineering profession in 1966, when Clough and Woodward (1967) demonstrated its usefulness for analysis of stresses and movements in earth dams. Geotechnical engineering had long been aware of the limited usefulness of linear elastic analysis of soil and rock masses. The method has other unique capabilities as well; these include the fact that it can be used for problems involving non homogeneous materials complex boundary conditions, sequential loading and so on. And it was immediately obvious that the ability to analyze nonlinear behavior gave the Finite Element Method great potential to use in geotechnical engineering problems.

The analysis of the structures by the Finite Element Method comprises of an idealization of an

actual continuum as an assemblage of discrete element interconnected at their nodal points (Singh, 1991).

The various steps followed in a Finite Element analysis are:

1. Sub division of the continuum into finite element of suitable configuration.

2. Evaluation of element properties.

3. Assembly of element properties to obtain the global stiffness matrix and load vector.

4. Solution of resulting linear simultaneous equation for the primary unknowns after introducing the boundary conditions.

5. Determination of secondary unknown quantities such as stresses and train.

3.2. FINITE ELEMENT FORMULATION

Most applications of finite element method in soil and rock mechanics have been made by adopting or suitably modifying formulation and programs developed for structural and continuum mechanics. Three basic variation principles for stress analysis employed in structural mechanics are:

1. The principle of minimum potential energy

2. The principle of minimum complementary energy and

3. The Hellinger-Reissner mixed principle

Displacements are adopted as primary unknown in the first case, stresses are adopted as unknowns in the second case, and both displacements and stresses become primary unknown in the Hellinger-Reissner principle. Procedures based on the first and second and third principles are

called the displacement, the equilibrium and the mixed methods, respectively. Often hybrid procedures have been developed in which some displacements or stresses within an element and some stresses or displacements on the boundary of the elements are adapted as primary unknown. The displacements procedure is most commonly employed in Geotechnical Engineering.

The displacements method offers a number of advantages over other methods. It is often more difficult to construct an approximate stress model that satisfies stress equilibrium than to construct a compatible displacement model. On the other hand, in the displacement method, the stresses are derived from computed (primary) displacement; hence the stress may not be as accurate and are often discontinuous across element boundaries. A majority of non-linear formulation by finite element method has been written in terms of the displacements.

3.3. DISPLACEMENT FUNCTION

An 8 noded isoparametric finite element is shown in fig.3.1. For typical finite element 'e', defined by nodes i,j,m etc, the displacement {f} within the element are expressed as:

$$\{f\} = [N] \{\delta\}^e \qquad \qquad \text{.............(3.1)}$$

where $[N] = [Ni, Nj, Nm ...]$

and $\{\delta\}^e = \{ \delta i, \delta j, \delta m ...\}^T$ ....(3.2)

The component of [N] are general functions of position and $\{\delta\}^e$ represent a listing of nodal displacements for a particular element.

For the three dimensional element

$$\{f\} = \begin{Bmatrix} u \\ v \\ w \end{Bmatrix}$$ ....(3.3)

represent the displacement in x, y, z direction at a point within the element and

$$\{\delta_i\} = \begin{Bmatrix} u_i \\ v_i \\ w_i \end{Bmatrix}$$ ....(3.4)

are the corresponding displacement of node i.

[Ni] is equal to the [INi'] where Ni' is the shape function of node i and I is the identity matrix.

3.4. SHAPE FUNCTION

The shape functions for an 8 noded hexahedral element used in this essay are given by the following. At the corner nodes (nodes no.1,2,3,4,5,6,7,8).

Fig.3.1. Shape functions for an 8 nodded hexahedral element

$$Ni = \frac{1}{8}(1+\xi_0) + (1+\eta_0) + (1+\zeta_0)$$

$$\xi_i = \pm 1$$
$$\eta_i = \pm 1 \qquad\qquad\qquad \dots\dots\dots(3.5)$$
$$\zeta_i = \pm 1$$

Where:

$$\xi_0 = \xi.\xi_i$$
$$\eta_0 = \eta.\eta_i \qquad\qquad\qquad \dots\dots\dots(3.6)$$
$$\zeta_0 = \zeta.\zeta_i$$

ξi , ηi , ζi are the local coordinates of the ith node and ξ , η , ζ are the local coordinates of the point concerned.

3.5.   STRESS-STRAIN RELATIONSHIPS

With displacements known at all points within the element, the strains at any point can be determined. Six strain components are relevant in the 3D analysis and the strain vector can be expressed as:

$$\{\varepsilon\} = \begin{Bmatrix} \varepsilon_x \\ \varepsilon_y \\ \varepsilon_z \\ \gamma_{xy} \\ \gamma_{yz} \\ \gamma_{zx} \end{Bmatrix} = \begin{Bmatrix} \dfrac{\partial u}{\partial x} \\[2mm] \dfrac{\partial v}{\partial y} \\[2mm] \dfrac{\partial w}{\partial z} \\[2mm] \dfrac{\partial u}{\partial y} + \dfrac{\partial v}{\partial x} \\[2mm] \dfrac{\partial v}{\partial z} + \dfrac{\partial w}{\partial y} \\[2mm] \dfrac{\partial w}{\partial x} + \dfrac{\partial u}{\partial z} \end{Bmatrix} \qquad \dots\dots\dots(3.7)$$

This can be further written as:

$$\{\varepsilon\} = [B]\{\delta\}^e = [B_i B_j B_m \ldots][\delta]^e \qquad \ldots\ldots\ldots\ldots(3.8)$$

[B$_i$] is given by:

$$[B_i] = \left\{ \begin{array}{ccc} \dfrac{\partial N_i'}{\partial x} & 0 & 0 \\[2mm] 0 & \dfrac{\partial N_i'}{\partial y} & 0 \\[2mm] 0 & 0 & \dfrac{\partial N_i'}{\partial z} \\[2mm] \dfrac{\partial N_i'}{\partial y} & \dfrac{\partial N_i'}{\partial x} & 0 \\[2mm] 0 & \dfrac{\partial N_i'}{\partial z} & \dfrac{\partial N_i'}{\partial y} \\[2mm] \dfrac{\partial N_i'}{\partial z} & 0 & \dfrac{\partial N_i'}{\partial x} \end{array} \right\} \qquad \ldots\ldots\ldots\ldots(3.9)$$

In which [B] is the strain displacement matrix that derived by considering natural & global coordinates, global derivatives and Jacobian Matrix, [J].

$$[J] = \left\{ \begin{array}{ccc} \dfrac{\partial x}{\partial \xi} & \dfrac{\partial y}{\partial \xi} & \dfrac{\partial z}{\partial \xi} \\[2mm] \dfrac{\partial x}{\partial \eta} & \dfrac{\partial y}{\partial \eta} & \dfrac{\partial z}{\partial \eta} \\[2mm] \dfrac{\partial x}{\partial \zeta} & \dfrac{\partial y}{\partial \zeta} & \dfrac{\partial z}{\partial \zeta} \end{array} \right\} \qquad \ldots\ldots\ldots\ldots(3.10)$$

The stresses are related to the strains as:

$$\{\sigma\} = [D](\{\varepsilon\} - \{\varepsilon_0\}) + \{\sigma_0\} \qquad \ldots\ldots\ldots\ldots(3.11)$$

where [D] is an elasticity matrix containing the appropriate material properties, $\{\varepsilon_0\}$ is the initial strain vector, $\{\sigma\}$ is the stress vector and $\{\sigma_0\}$ is the initial stress vector.

The elasticity matrix is given by:

$$[D] = \frac{E}{(1+v)(1-2v)} \begin{bmatrix} 1-v & v & v & 0 & 0 & 0 \\ & 1-v & v & 0 & 0 & 0 \\ & & 1-v & 0 & 0 & 0 \\ & & & \frac{1-2v}{2} & 0 & 0 \\ & & & & \frac{1-2v}{2} & 0 \\ & & & & & \frac{1-2v}{2} \end{bmatrix} \quad \text{............(3.12)}$$

Where E is the Young's modulus of elasticity and υ is the Poisson's ratio of the material of the element

3.6. STIFFNESS MATRIX

The stiffness matrix of the element is given by the following relation:

$$\{F\}^e = [K]^e \{\delta\}^e \qquad \text{............(3.13)}$$

where $\{F\}^e$ is the element nodal load vector, and $[K]^e$, the element stiffness matrix given by :

$$[K] = \int_V [B]^T [D] [B] dV \qquad \text{............(3.14)}$$

where V refers to the volume of the element.

The global stiffness matrix [K] is obtained by directly adding the individual stiffness coefficients in the global stiffness matrix.

The mathematical statement of the assembly procedure is given below that similarly for the global load vector.

$$[K] = \sum_{e=1}^{E} [K]^e$$

$$[F] = \sum_{e=1}^{E} \{F\}^e$$ ....(3.15)

3.7. TECHNIQUES FOR INCORPORATING MATERIAL NON-LINEARITY

The solution of non-linear problems by Finite Element Method is usually attempted by one of three basic techniques viz. (a) incremental or step wise procedure (b) iterative or Newton methods and (c) step-iterative or mixed procedure.

3.7.1. Incremental Procedure

The basic of this procedure is the subdivision of the load into many small partial loads or increments. Usually these loads increments are in general of equal magnitude, but need not be equal. The load is applied one increment at the time and during application of each element, the equation is assumed to be linear. A fixed value of [K] is thus assumed throughout each load increment but [K] take different value during different increment.

The solution for each step of loading is obtained as an increment of the displacement ($\Delta\delta$), which is added up to give the total displacement at any stage of loading, and the incremental process is repeated until the total load has been reached. Essentially, the incremental procedure approximates the non-linear problem as a series of linear problems, that is, the nonlinearity is treated as piecewise linear.

The total load {f} is given by

$$\{F\} = \{F_0\} + \sum_{i=1}^{M} \{\Delta F_i\}$$ ....(3.16)

Where $\{F_0\}$ is the initial load vector and M is the total number of increments and $\{\Delta\delta\}$ is the incremental load vector in the ith increment. Hence after the application of the ith increment, the load is given by

$$\{F_i\} = \{F_0\} + \sum_{j=1}^{i} \{\Delta F_j\}$$ ....(3.17)

Similarly after the ith iteration, the displacement is given by

$$\{\delta_i\} = \{\delta_0\} + \sum_{j=1}^{i} \{\Delta\delta_j\}$$ ....(3.18)

where $\{\delta_0\}$ represents initial displacement.

Usually $\{F_0\}$ and $\{\delta_0\}$ are null vectors because the solution is started from the undeformed state of the body. However, any initial equilibrium state of $\{F_0\}$ and $\{\delta_0\}$ can be specified.

To compute the increment of displacement, a fixed value of stiffness is used which is evaluated at the end of the previous increment. Therefore,

$$[K_{i-1}]\{\Delta\delta i\} = \{\Delta F_i\} \quad \text{for } i=1,2,3,\ldots M$$ ....(3.19)

Where the subscripts refer to the incremental stage and [K0] are the initial value of stiffness [K]. $[K_0]$ is computed from material constant deriving from the given stress-strain curve at the start of the loading.

The incremental procedure is systematically indicated in figure below. Usually, in the incremental procedure the tangent moduli (E_t) is used to formulate

[D{σ}] and to compute the stiffness [K]. The matrix [K] is often referred to as the tangent stiffness matrix.
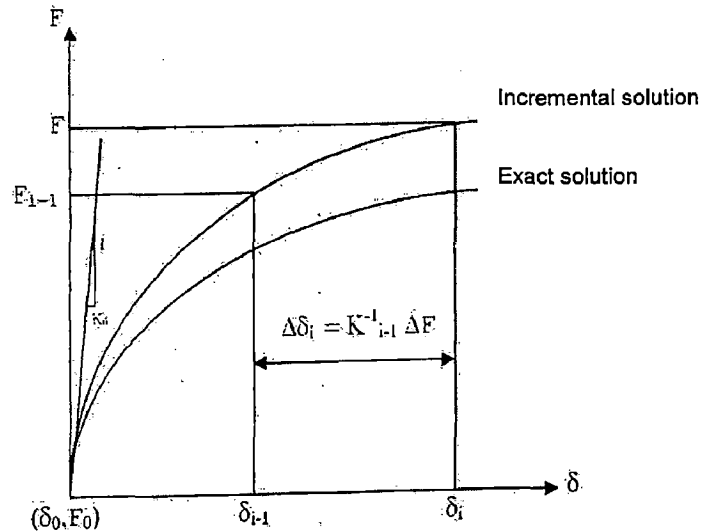
Fig. 3.2. Basic Incremental Procedures

The accuracy of the incremental procedure can be improved by taking smaller increments of the load, say by adopting half of the load increment.

3.7.2. Iterative Procedure

The iterative procedure involves a sequences of calculation in which the structure is fully loaded in each iteration. Because some approximate, constant value of stiffness is used in each step, the equilibrium is not necessary satisfied. After each iteration, the portion of the total load that is not balanced is calculated and used in next step to compute an additional increment of the displacements. The process is repeated until equilibrium is approximated to some acceptable degrees. Essentially, the iterative procedure consists of successive correction to a solution until equilibrium under the load [F] is satisfied.

For the ith cycle of iteration process, the necessary load is determined by:

$$\{F_i\} = \{F\} - \{F_{e,i-1}\} \qquad \dots\dots\dots(3.20)$$

where $\{F_{e,i-1}\}$ is the load equilibrium after the previous step.

An increment to the displacement is computed during the ith step by using the relation.

$$[K_{i-1}]\{\Delta\delta i\} = \{F_i\} \qquad \dots\dots\dots(3.21)$$

where the subscript, i, denote the cycle of iteration.

The total displacements after the ith iteration is computed by using the relationship of eq.(3.18).

Finally, $\{F_{e,i}\}$ is calculated as the load necessary to maintain the displacement $\{\delta i\}$. The procedure is repeated until the increment of displacement or the balanced forces become zero, that is, $\{\Delta\delta i\}$ or $\{Fi\}$ become null according to some preselected criterion.

Instead of computing a different stiffness for each iteration, a modified iterative technique is also employed which utilizes only the initial stiffness $[K_0]$. Obviously, the modified procedure necessitates a greater number of iterations. However, there is a substantial saving of computation because it is not necessary to invert a new stiffness at each cycle.

The iterative procedure is illustrated schematically in figure below.

(a) Tangent Stiffness Procedure   (b) Modified Procedure
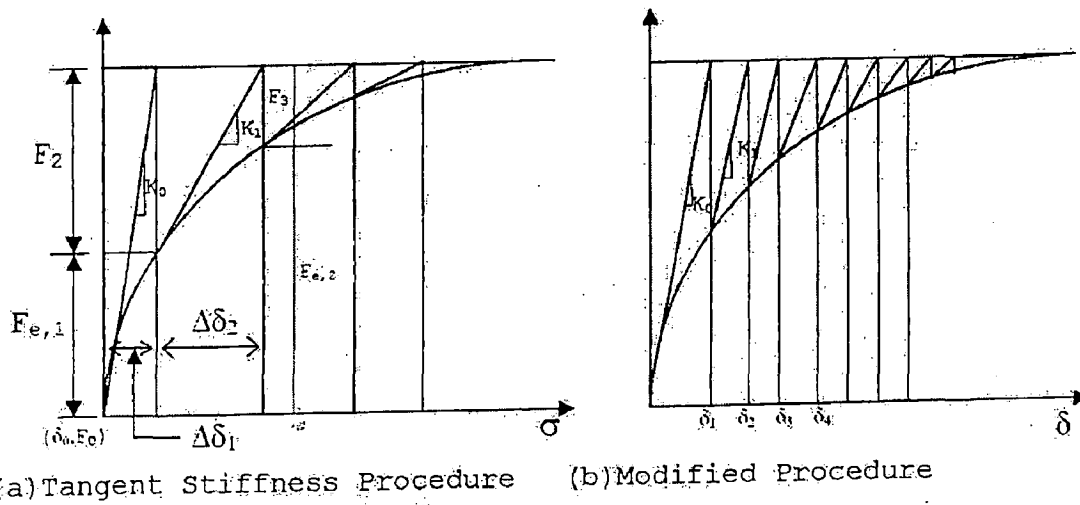
Fig. 3.3. Iterative Procedures

3.7.3. Mixed Procedure

The step iteration or mixed procedure utilizes a combination of the incremental and iterative schemes. In this method, the load is applied incrementally, but after each increment successive iterations are performed. This method yields higher accuracy at the price of more computational efforts. The schemes of procedure are illustrated in figure 3.4 below.
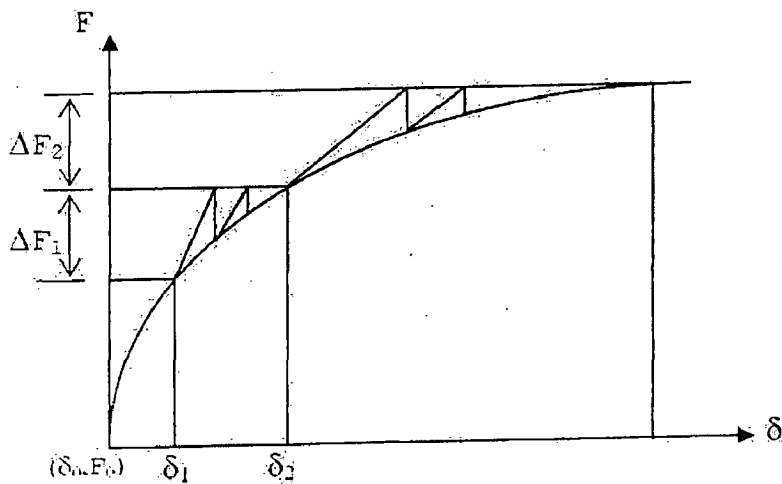
Fig. 3.4. Step Iterative Procedures

Because the mixed method combines the advantages of both the incremental and iterative procedures and tends to minimize the disadvantages of each, step iteration is being utilized increasingly. The additional computational effort is justified by the fact that the iterative part of the procedure permits one to assess the quality of the approximate equilibrium at each stage.

3.8. CONSTITUTIVE LAWS

It has been repeatedly shown that the most influential factor in the finite element analysis of embankment dams is the modeling of the stress-strain behavior of the fill by an appropriate constitutive law. However, in spite of the diversity of the stress-strain relationship being used, reasonable agreement has usually been found when the results of finite element analyses (typically movements) have been compared with field observations. This is not surprising bearing in mind the fact that most of the analyses were done after the field measurement had been made.

3.8.1. Linear Elastic Analysis

Soils are far from being either linear or elastic. Nevertheless, because of simplicity, geotechnical engineers have often characterized the behavior of real soil using idealized models of linear isotropic elasticity. Reasonable results can only be obtained for conditions far away from failure, when a significant factor of safety operates. These conditions usually prevail in rockfill dams, and thus it is not surprising that linear elastic analyses have been successful in

number cases.

Only two elastic constants are needed to characterize the stress-strain behavior of isotropic linear elastic materials. They are usually Young's modulus, E, and Poisson's ratio, e. In order to obtain reasonable values of stresses and particularly displacements, it is essential to find the most suitable values of the above elastic constants. A 'constant equivalent compressibility' method for determination of Young's modulus using data from oedometer tests was proposed by Penman and Charles (1973). They showed that the internal distribution of vertical displacement during construction of a thick, broad layer (one dimensional condition) possessing self weight, can be predicted with little error by the use of constant Young's modulus determined to give the correct final displacement of a point half-way up the complete layer.

Justo and Saura (1983) carried out a 3-D linear analysis of EI-Infiernillo dam wherein the parameters E and u used in the analysis were derived from the behavior during construction. The value of Young's Modulus E was found out from Oedometric modulus as described:

$$E = E_{oed} \frac{1 - \nu - 2\nu^2}{1 - \nu}$$ ....(3.22)

And the Poisson's ratio, u, was estimated by the method used by Simmons (at Singh, 1991).

It was recognized a long time ago that modeling of soils in terms of the bulk modulus, K, and the shear modulus, G, had some advantages over the use of Young's modulus, E, and Poisson's ratio, è.

This model was used by Domaschuk and Wade (1969) and Domaschuk and Valliappan (1975); $K_t - G_t$ models employed by Izumi, Kamemura and Sato (1976). In comparison with the hyperbolic model, this model is simpler. Only five parameters are required. For unloading an additional parameter is needed. As with the hyperbolic model discussed above, it seems that CI good fit to both oedometer and triaxial test data cannot be obtained.

3.8.2. Nonlinear Stress-Strain Behavior

Theories of elasticity and plasticity have been widely used in geotechnical engineering for problems involving small and large strain to which neither the theory of elasticity and plasticity are directly applicable. Furthermore, actual boundary conditions are often difficult to incorporate into the critical solutions.

Recent developments of numerical methods, particularly in the Finite Element Method, have provided new computational capabilities making it possible to handle many complex boundary condition and material nonlinearity. The accuracy of the Finite Element Method depends on the proper incorporation of nonlinear constitutive equations of the soil.

The relationships between stress and strain in soils are more complicated than the simple, linearly elastic ones described in previous section. The stress-strain relation being represented by a number of lines. Two general forms, which are available for this purpose, are tabular forms and functional forms.

Tabular Form:

The stress-strain results obtained from laboratory tests can be used directly in tabular form for finite element analysis as was done in case of Duncan Dam by Einstein, Krishnayya and Morgenstern (1972). For this, several points of the stress-strain curves are fed as input to the computer in the form of number pairs denoting stress and strain at these points, The material parameters E and v are interpolated for the desired level of stress or strain by a suitable interpolation method, if it is on a single curve. If instead, there is more than one curve, as will be the case for materials whose stress-strain relationship is a function of the confining pressure; interpolation is done for the different curves as well. The tabular form is cumbersome as it occupies a relatively large storage space in the computer.

Functional Form:

An obvious advantage of the use of the mathematical function is that, in contrast to the tabular form in which a number of data points are input, only a few parameters are needed to describe the curves.

The most widely used function for simulation of stress-strain curves in finite analysis was formulated by Duncan and Chang (1970) using Kondner's (1963) finding that the plots of stresses vs. strain in triaxial analysis compression test is nearly a parabola. The procedures uses Mohr Coulomb failure criterion and develops relationship for the tangent modulus and poison's ratio which may be expressed in terms of total or effective stresses.

Kondner's approximated the equations of stress-strain curves for both clays and sands by the following hyperbolic relation:

$$\sigma_1 - \sigma_3 = \frac{\varepsilon_1}{a + b\varepsilon_1}$$ ....(3.22)

where, σ_1 = major principal stress, σ_3 = minor principal stress, ε_1 = major principal strain, and a,b = constants whose values are determined by fitting experimental data
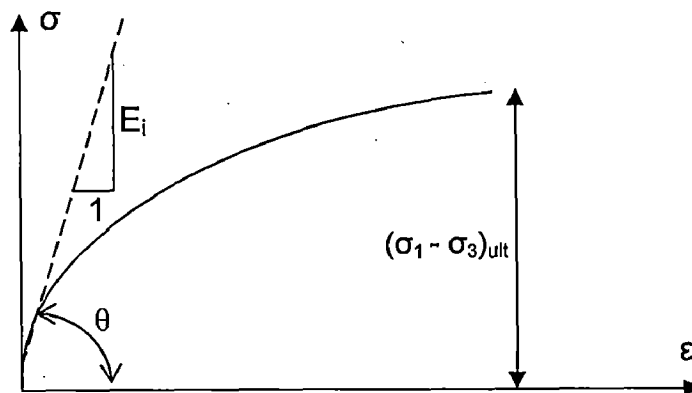
It is shown at the figure that

$$b = \frac{1}{(\sigma_1 - \sigma_3)}$$ and $$a = \frac{1}{E_1}$$ ....(3.23)

Where, E_i = initial tangent modulus, $(\sigma_1 - \sigma_3)_{ult}$ = asymptotic value of the principal stress difference at infinite strain. The tangent modulus at particular stress, E_t is given by:

$$E_t = \frac{1}{a}\left[1 - b(\sigma_1 - \sigma_3)\right]^2$$ ....(3.24)

Duncan and Chang noted that each of the constant a and b should be depend on the minor principal (confining) effective stress, σ_3. More precisely, they suggested that E_i vary in the following manner:

$$E_i = \frac{1}{a} = K.P_a \left(\frac{\sigma_3}{P_a}\right)^n$$ ....(3.25)

where:

σ_3 = the confining pressure

P_a = the atmospheric pressure expressed in the same unit as E_i

K = a dimensionless number termed the modulus number

n = dimensionless exponent which determines the rate variation of E_i and σ_3

R_f is the failure ratio defined as the ratio of the deviatoric stress at failure to the ultimate deviatoric stress given by

$$(\sigma_1 - \sigma_3)_f = R_f (\sigma_1 - \sigma_3)_{ult}$$ ....(3.26)

Based on the results of a number of loading-unloading – reloading test on sands, Duncan and Chang proposed the following relationship for the variation of the initial elastic modulus:

$$E_{ur} = K_{ur}.P_a \left(\frac{\sigma_3}{P_a}\right)^n$$ ....(3.27)

where: E_{ur} = the loading-reloading modulus

K_{ur} = the corresponding modulus number

Kulhawy and Duncan (1972) modify expression for poisson's ratio, υ, it is assumed that the soil possesses a constant bulk modulus B, the incremental value of the υ is then calculated from the expression:

$$\nu = 0.5\left(1 - \frac{E_i}{3B}\right)$$ .... (3.28)

The meaning of parameter K, K_{ur}, υ, ϕ, c, and R_f, is the same as for the other versions of the hyperbolic model. The quantities K_b and m are used to make the bulk modulus B a function of confining pressure σ_3:

$$B = K_b.P_a\left(\frac{\sigma_3}{P_a}\right)^m$$ .... (3.29)

where:

K_b = the dimensionless 'bulk modulus number'(equal to the value of B/P_a at $\sigma_3 = P_a$)

m = the dimensionless 'bulk modulus exponent'.

3.9. SEQUENTIAL CONSTRUCTION ANALYSIS

Embankments are built up in relatively thin horizontal layers. Consequently, there will be a large number of layers during the construction of a large dam. The limitations of computer modeling require relatively thick layers to be used in the idealization (Figure 3.5). In the past, to provide an insight into the errors involved, the closed form solution of the incremental analysis was usually compared to the finite element 'layered' analysis using a one-dimensional model that represents either a soil column or a fill of large lateral extent.
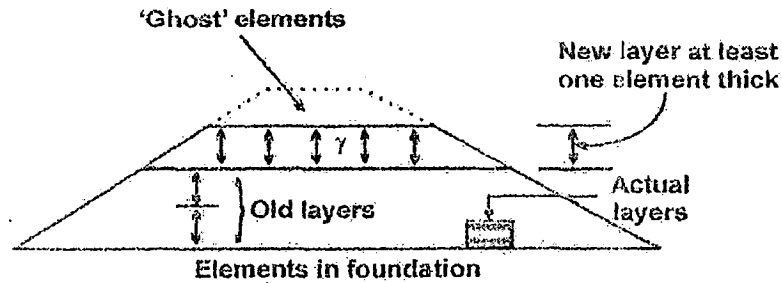
Fig.3.5. Layered idealization

In the next approach of the conventional stress deformation, the structure is assumed to be completed in single stage and the gravity load is applied instantaneously as an external load to the complete structure. This conventional solution treats the gravity effects as an external loads applied to the finished structure and valid if the state of the stresses in the structure is statically determinate at all stages of construction process, but in actual condition most embankments are constructed in layers by incremental process and the load is accumulated gradually during construction thus invalidates the assumption of one stage layer analysis.

Engineering structures are usually constructed in a definite sequence of operations. A conventional linear analysis of such structures is performed by assuming that the entire construction takes place in a single operation. The stresses and deformation are computed by considering loads on completed structures. However, for the non-linear problem typical in soil and foundation engineering, the behavior at particular stage of loading is depend upon the state of stress and stress history. Thus the stresses in the final configuration are depending upon the sequence of intermediate configurations and loading (desai and abel, 1987).

Most embankments are constructed in layers by incremental process and the load is accumulated gradually during construction that invalidates the assumption of instantaneous of the entire gravity load in on stage. For realistic analyses of both stresses and movements in complex condition, the sequence analysis provides a rational procedure of considerable engineering value.

In the sequential analysis, the structure is first divided into horizontal slices, known as lifts or layers corresponding to the construction scheme. The analysis is then carried out in succession for stresses and displacements corresponding to different stages of construction. Thus, first of all, the analysis is carried out for the first lift for its own load, i.e. the structure is supposed to comprise one lift only and the stiffness is formulated for the elements of this lift only. These stresses and deformation are stored, and the second lift is added to the structure. Now the structure is supposed to be made up of two layers and stiffness is generated for the elements of these two layers but the gravity forces considered are due to the dead weight of the second layer only, whereas the first layer is considered weightless. The stresses and deformation due to this incremental load are calculated for the whole structure and are added up to the previously stored value. This process is repeated till the analysis is complete for the whole structure.

3.10. STEPS OF THE ALGORITHM

Incremental construction analysis as proposed by Clough and Woodward (1967) has been modified to analyze the dam behavior for the construction stage by Sharma (1975) and

Singh (1985), which is used in this study. For the water loading and effect of softening the approach as adopted by Nobari and Duncan has been adopted.

The various steps in the solution algorithm are:

1. Take first layer

2. Calculate the elastic constant based on the anticipated values of stress. $\sigma_1 = \gamma$ h and $\sigma_3 = K_0 \sigma_1$, where h is the average height of the fill in the layer and a constant value of 0.50 for K_0, the coefficient of earth pressure at rest, has been adopted for all zones of the dam.

3. The gravity loads of the new layer only (ΔF^i) are calculated. These are added to the loads of the previous layer to get the total loads.

4. The stiffness matrix [K] of the structure up to the end of current layer is calculated.

5. The incremental displacement $\{\Delta\delta\}$, the incremental strains $\{\Delta\varepsilon\}$ and incremental stresses $\{\Delta\sigma\}$ are calculated.

   $\{\Delta\delta\} = [K]^{-1} \{\Delta F^i\}$

   $\{\Delta\varepsilon\} = [B] \{\Delta\delta\}$

   $\{\Delta\sigma\} = [D] \{\Delta\varepsilon\}$

   The D matrix used here is calculated according to the proposed stress-strain model at the existing stress level, prior to this iteration.

6. The stress-strain matrix is found out at the stress state obtained by adding the incremental stresses in step 5 to those at the beginning of the iteration.

7. Incremental stresses are recalculated with the new value of iteration.

8. The total stresses are found out by adding incremental stresses of step 7 to the stresses at the beginning of the iteration.

9. The equilibrium load vector is calculated by

$$\{Fe\} = \int_v [B]^T \{\sigma\} dv$$ and the residual load vector $\{\psi\}$ by :

$$\{\psi\} = \{F^i\} - \{Fe\}$$

10. $\{\Delta F_j\}$ is set equal to $\{\psi\}$, where j is the iteration number and the superscript refers to the layer number.

11. Calculate the norms of the residual load by the relation

$$\|\psi\| = \left(\{\psi\}^T \{\psi\}\right)^{\frac{1}{2}}$$ and compare it with the norm of total load applied, find convergence factor :

$$Convergence\ factor = \frac{Norm\ of\ residual\ loads}{Norm\ of\ applied\ loads}$$

12. If the ratio of norm residual to that of total applied load is within specified tolerance factor, the stresses, strains, displacements and principal stresses are stored and the next step is skipped, otherwise the next step is followed.

13. If the ratio of norm residual with the normal of applied forces is not within the specified tolerance limit, convergence ratio is calculated

$$Convergence\ ratio = \frac{Conv.\ factor\ in\ the\ current\ iteration}{Conv.\ factor\ in\ the\ prev.\ iteration}$$

If the convergence ratio less than 1.5 goes to step 4, otherwise go to step 5.

14. Take next layer, if left and proceed from step if the analysis is for construction stage. If the analysis is to be done for reservoir filling also go to next step if any stage is left. Stop if no layer / stage is left.

15. Calculate the additional gravity loads for the elements in the current layer only leaving the elements in the previous layer. The additional gravity loads will be upward in case of upstream shell and transition due to buoyancy and downward in the core due to saturation of the core material. These will be no additional gravity loads in elements downstream of core.

16. Calculate the water pressure load on the upstream face of core elements up to the end of current layer. For elements in current layer it will be calculated on the basis of the water pressure head at the nodes while the elements in the previously filled stages the water pressure head will be equal to the height of current reservoir rise.

17. Calculate the water load acting on top each layer based on the pressure head equal to the height of reservoir rise in that stage.

18. Calculate softening load for the elements upstream of core lying in the current layer only.

19. Add the loads in step 15 to 18 to get $\{F_i\}$ for further calculations.

20. The stiffness matrices is calculated for the entire load

21. Go to step 5

CASE STUDY

4.1. GENERAL

Correct assessment of movements in dam are called for better understanding the behaviour of the dam and to safe guard against cracks, hydraulic fracturing, etc., related failure at design state itself.

Djatiluhur dam, an inclined core rockfill dam in Indonesia, is identified with significant deformation, started during construction period till the present reservoir operation period. Therefore, it is of interest to evaluate its behaviour.

This study is limited to analyze and compare the computed and the observed values of deformations of Djatiluhur dam, to validate the model and thereafter to evaluate the dam performance. The details of the dam studied as a case study, and the model and software used for analysis are given in this chapter.

4.2. STUDY AREA

4.2.1. Introduction of DJATILUHUR Dam

Djatiluhur Dam is located on Citarum River in west Java, for location refers **Fig.4.1.** The main embankment dam is 105 meter high above minimum foundation level and is 1220 meters in length at crest level with an embankment volume of 9.1×10^6 m3.
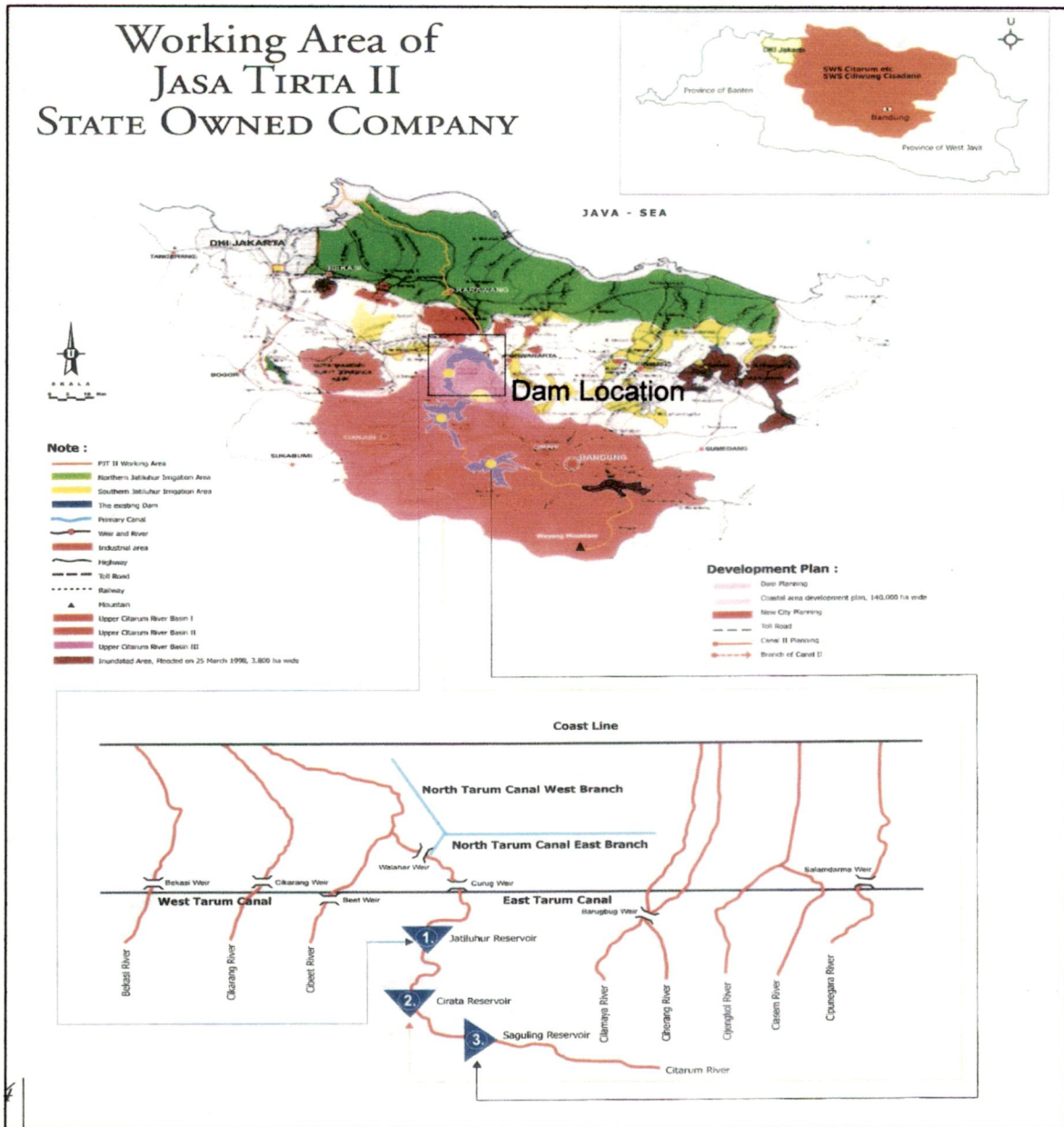
Fig.4.1. Location Map of Djatiluhur Dam

For plan, refer **Fig 4.2.** The reservoir so formed (named Ir H Juanda Reservoir in memory of late Prime Minister Ir H Juanda) has an operable storage of 2.1 billion m3 between the minimum reservoir El. 75.0 m and maximum conservation El. 107.0 m which is incidentally the sill level of the uncontrolled morning glory main spillway.
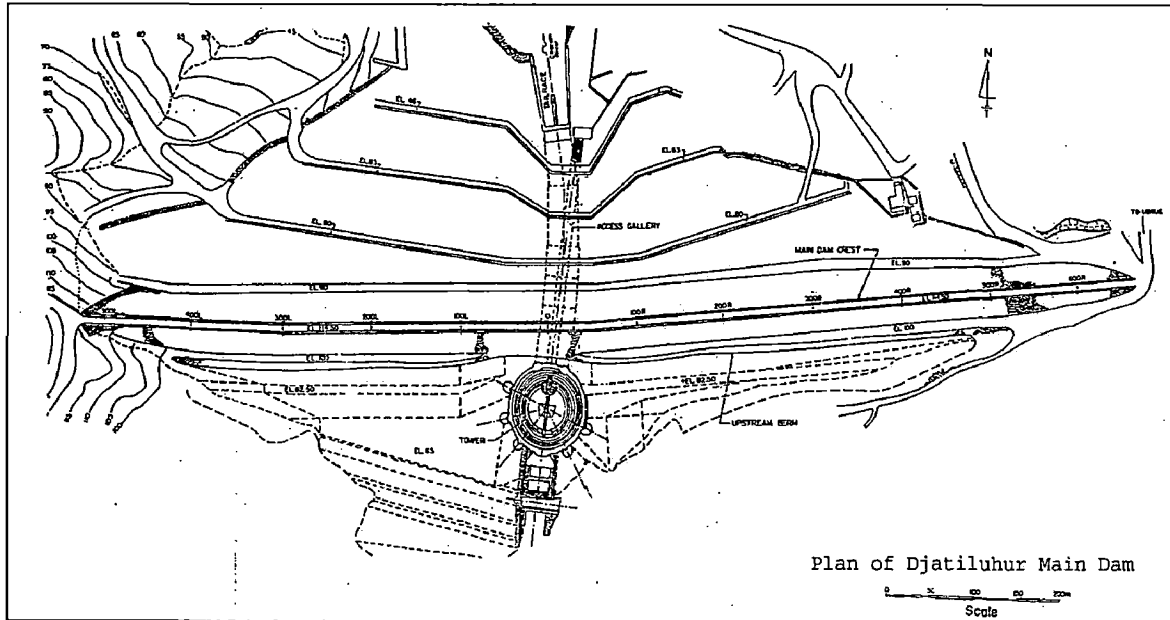
Fig.4.2. Plan of Djatiluhur Main Dam

The Djatiluhur dam is a multipurpose Project and priority of water releases is for municipal demand (water supply, flushing foul water drains) and irrigation with hydroelectric generation as a third priority. Water releases are made into the old riverbed and are diverted into two canals, namely East Tarum Canal and West Tarum Canal at Curug weir, 8 km downstream of the dam. Further downstream Walahar weir supplies water to North Tarum Canal. About 260,000 hectares of rice fields in the northern plains of West Java extending eastward from Jakarta to Indramayu have now a regulated assured supply for irrigation and it is possible to have double cropping. Incidentally the storage of inflows and control of Citarum River has protected the town of Karawang and surrounding area from heavy losses in terms of life and property in case of floods. The 4500 km² catchment at Djatiluhur receives an average annual precipitation of 2600 mm. The mean annual inflows of Citarum River at Djatiluhur are of the order of 5650 million m³, out

of which about 4500 million m^3 i.e. 80 % occur during the rainy season from November to May.
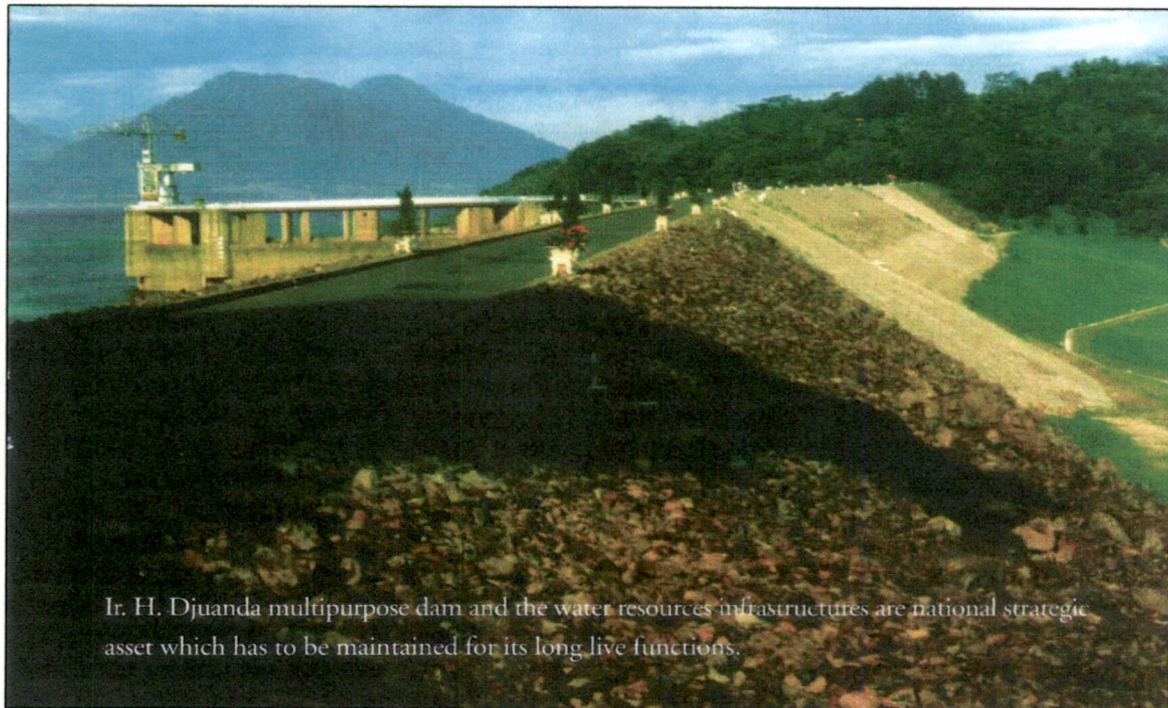
Fig.4.3. Downstream view of Djatiluhur Main Dam

The Project structures were designed and supervised during construction by COYNE et BELLIER, Paris Consultant. The hydraulic model tests were carried out in the laboratories of SORGREAH at Grenoble while the Soil mechanics testing was done by MECASOL in Paris. Civil engineering works were done by the COMPAGNIE FRANCAISE d'ENTERPRISE of Paris and associates CITRA, BATIGNOLLES, DRAGAGES, Drilling and grouting work was done by SOLETANCHE (Paris) as sub-contractor and electrical and mechanical equipment were supplied by COMPAGNIE GENERALE D'ENTERPRISES ELECTRIQUES — COGELEX (Paris), NYRPIC (Grenoble-France) and GRUPPO INDUSTRIE ELECTRO MECCANICHE PER IMPIANTI ALL'ESTERO G.I.E. of Milan Italy. The construction work was commenced in 1958 and was completed in 1967 and inaugurated by the President of Indonesia on August 26, 1967.

4.2.2. Description of the Dam Structure

The major structures of Djatiluhur Project are the Main Embankment Dam and Power station/Main Spillway Tower. In addition there are four saddle embankments with an Emergency spillway on the left abutment of Ubrug dike. Djatiluhur main embankment dam is founded on poor rock consisting of sandstone, claystone with an occasional thin stratum of limestone.

CLAY CORE

The impervious element of the dam is a thin clay core, slightly sloping upstream. The material of the core is high plasticity clay (CH), which is the weathered claystone. The other properties of the clay on the average are:

Liquid limit	65%
Plasticity index	35%
% Finer than # 200 sieve	60%
% Finer than 0.005 mm	35%
Optimum standard Proctor density	1.6 T/m^3
Optimum moisture content	22%
Shear strength	$c' = 2$ T/m^2, $\phi' = 19°$

The clay have liquid limit varying from 50 to 75 and plasticity index varying from 25 to 45 and falls in CH group on the Casagrande Classification Chart. The shear strength parameters as above were considered conservative at the time of design.
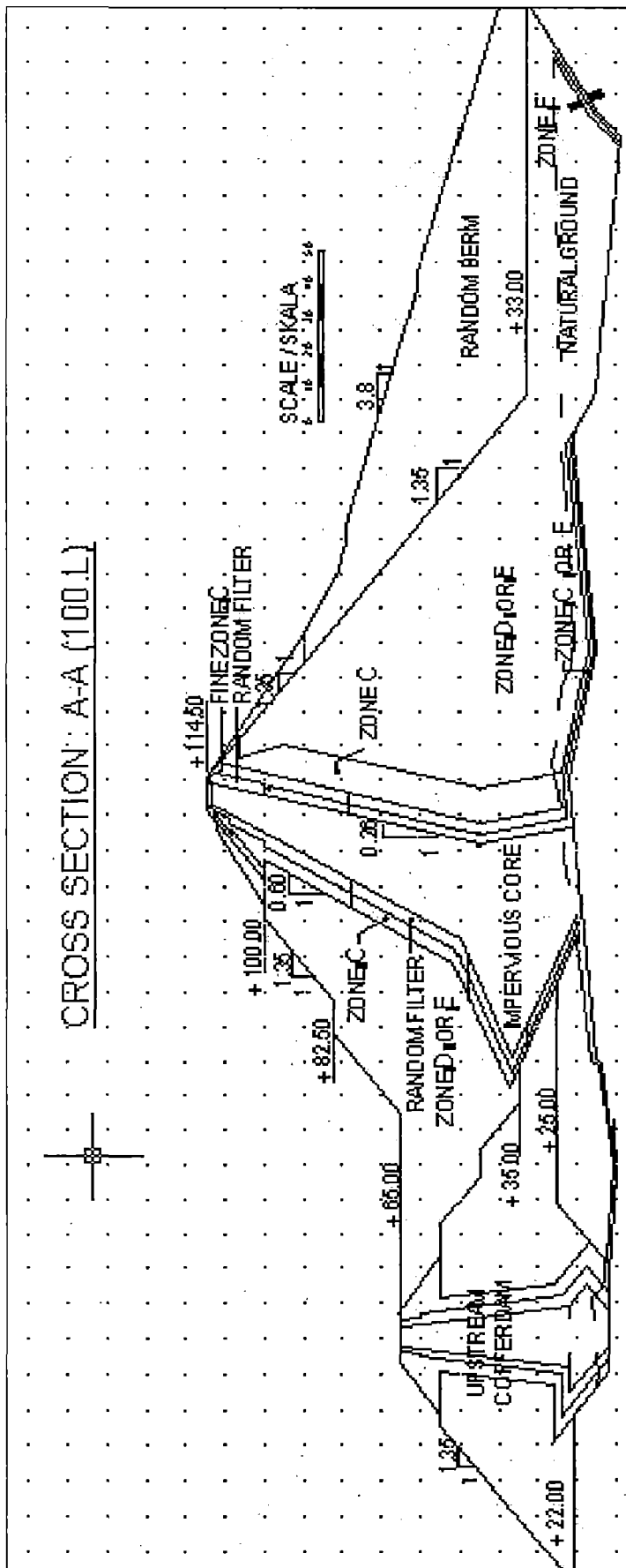
Fig.4.4.
Djatiluhur Dam
Section at 100L

Clay was processed before transporting to site by addition of water and breaking down the lumps, however water was sprinkled at site to bring it to specify moisture content of to 2% wet of Proctor optimum. Compaction was done by rolling in 0.2 meter thickness. Recently (1989-1990) while drilling for rehabilitation of Instruments investigation of the clay core was done by drilling 14 holes from the crest and testing samples. The results of laboratory tests for strength are as per figure below. The mean strength so found is lower than the designed strength as above being $c' = 0.36$ kg /cm^2 and $\phi' = 16.9°$ whereas the lowest values fit in as $c' = 0.17$ kg.cm^2 and $\phi' = 13.2°$.
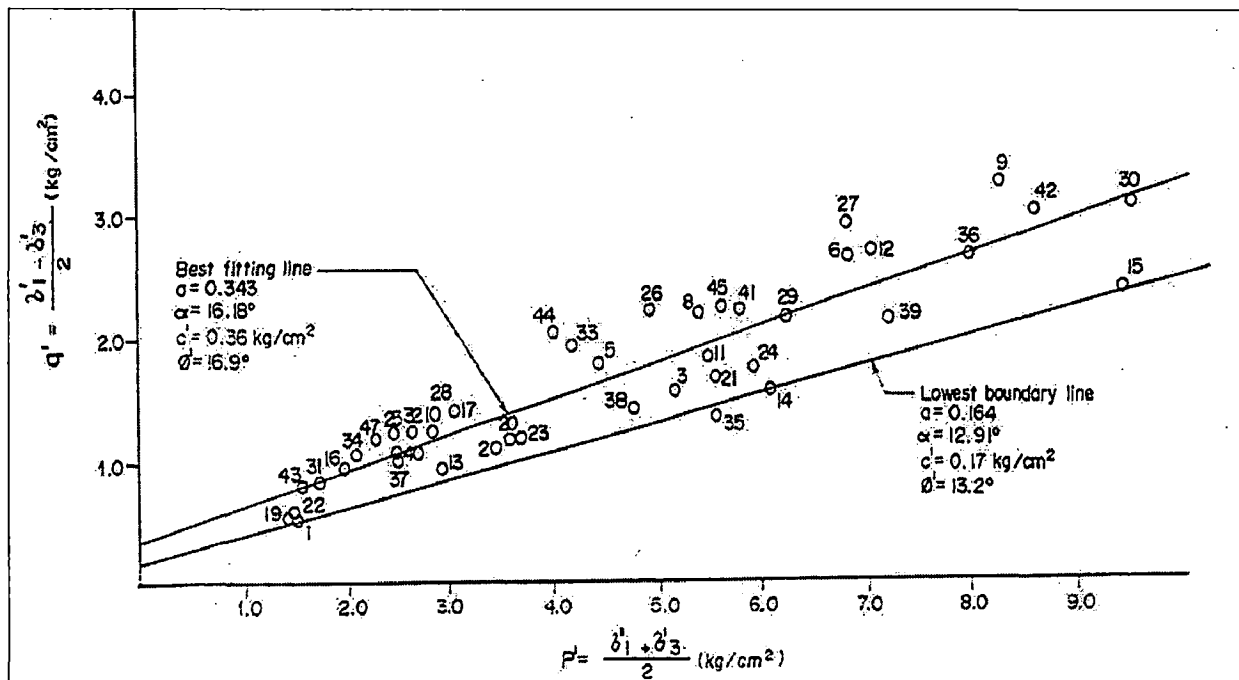
Fig.4.5. Clay Core Tri-axial Test results.

ROCKFILL

The rock fill used in the construction of main embankment dam shoulders is of several kinds as described hereafter:

– Zone D material was the main rock fill that was hauled from the quarries of andesite outcrop at Cilalawi and Pamojanan about 7 km along the haul road on the upstream of the site. There was no limit on the maximum size of the rock but material sizes less than 20 mm were not to be more than 25%. The larger size rock fill was specified for the downstream shoulder. The D zone was built in lifts of 5 to 10 meters by dumping and sluicing. Zone D or E were specified for upstream shoulder rock fill.

– Zone C rock fill is a selected rock fill to act as a transition material between coarse filter and rock fill zone D in the downstream and upstream shoulder. The maximum size in this zone was limited to 0.6 meter and material in the 20 mm size was not more than 25% as specified also for Zone D however this zone was compacted in layers of 1 meter thickness by a vibratory roller. There is also a fine zone C material which is to protect the coarse filter in the downstream chimney drain above El. 100.0 m.

– Zone E is a smaller size material placed in layers of 1 to 2 meter, also sometimes specified as an alternate to zone D. The actual placement has been detailed subsequently. As for other rockfill the maximum percentage of particles smaller than 20 mm was 25%. Zone E was also used under the downstream shoulder as a protection layer over the sand placed on the foundation as a protection/distribution layer.

– Rockfill strength was determined from tests in large shear apparatus that gave angle of friction between 42° and 45°. The rockfill as dumped on the upstream cofferdam for construction had an angle of repose of 1.3 horizontal to 1 vertical and this supported the laboratory results.

FILTERS

Three different filters were used to prevent migration of fines whether from the core upstream or downstream or to protect the foundations.

– Fine filter, specified size between 0-20 mm

– Coarse filter specified size between 2-125 mm

– Random filter specified size between 0-150 mm

Filters were compacted by vibratory roller and were placed in layers of 0.5 meter. Random filter was used as a transition material on upstream and also above El. 100 m in downstream chimney filter.

CLAY BEDROCK

Analysis of stability following the discovery of sheared zones in clay bedrock on exactions for foundations led to an extensive investigation of clay bedrock shear strength along the shear surfaces. The shear strength of the sheared zone material of the bedrocks i.e. claystone and sandy claystones was investigated thoroughly and also each bed was examined by scrap sampling and sheared zones identified.

Laboratory testing on the most plastic material gave as low a shear strength value as $\phi' = 14°$ and $C' = 19,6$ KN/m^2 i.e tan $\phi' = 0.2$ and $C = 2$ T/m^2 whereas assumed shear strength

was $\phi' = 11.3°$ and $C' = 196$ KN/m^2 on a shear surface parallel with bedding of the rock. For sheared surface not parallel with bedding, shear strength of tan = 0.5 ($\phi' = 26.5°$) and $C' = 0$ was assumed.

Table 4.1. DJATILUHUR MAIN DAM DESIGN PARAMETERS

PART OF DAM	MATERIAL/ ZONE	DENSITY (t/m3)	SHEAR STRENGTH	
			P1-II' (deg)	C' (t/m2)
EMBANKMENT	CLAY CORE	sat = 2.05 sub = 1.05	19	2
	ROCKFILL (Andesite)	Dry = 1.3 Sat = 2.13 Sub = 1.3	42	0
	CLAYSTONE BERM	Dry = 2.0 Sub = 1.0	26.5	0
	SANDSTONE	Sat = 2.6 Sub = 1.6	26.5	0
FOUNDATION	CLAYSTONE Not parallel To bedding	Sat = 2.6 Sub = 1.6	26.5	0

4.2.3. Embankment Section

The main dam embankment has an upstream slope of 1:1.35 with horizontal berms at El. 100 m and El. 82.5 m. These berms are not provided in the central portion of the main embankment dam. This was due to restriction in the section by the outlet works section BB (0).

Section AA

Section AA at 100L Fig 4.5 shows the upstream slope having the advantage of cofferdam that has been incorporated in the section. There were berms at El. 100 m and El. 82.5 m. The core has a protection of random filter and zone C as chimney filters on upstream. The upstream shoulder rockfill can be Zone D or Zone E. The downstream shoulder laid on a protection and distribution layer for almost the portion of original section (i.e. without the riseberm) has a further protection of Zone C or Zone E material over the protective layer.

Under the riseberm for most of the length, a thick layer of zone E was placed, however for the inclined contact zone of excavated slope, a double protection layer was placed. The downstream cofferdam of Zone D plus impervious blanket was incorporated in the section. The sloping ground beyond was used to put random material over Zone D material. The core has fine filter and coarse filters as chimney filters on downstream up to El. 100.0 m further strengthened by 10 m wide Zone C material specifically compacted in layers of 1.0 m by vibratory roller. Above El. 100.0 m, the filters downstream of core are the random filter and then fine filter. The riseberm starts at El. 90.0 m and has a berm at El. 80.0 m.

Section BB

Section BB at (0) Figure 4.6 differs from section AA (100L), in that the upstream slope has no berm. No specific material has been placed at the contact with the Tower; however the contact of impervious core with the Tower has a cover of random filter and zone C. The upstream cofferdam supports

the Tower on upstream. The downstream shoulder has the foundation with a complete protective layer cover plus Zone C or Zone E under the rockfill Zone D or Zone E. Even under the riseberm a layer of random filter was placed however a thick clay cover was introduced which is over the tailrace conduits under the dam in the downstream shoulder which continues to the outlet works but is reduced in thickness. The riseberm has berms at El. 46.0 m, El. 63.0 m, El. 80.0 m and goes upto El. 90.0 m as elsewhere.
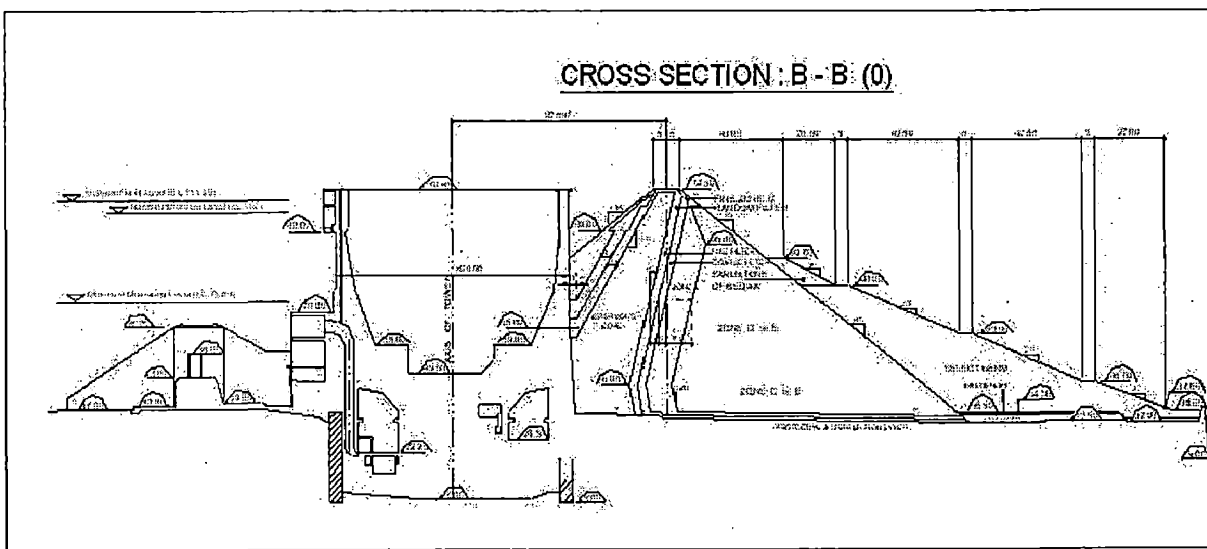
Fig.4.6. Main Dam Section BB at (0).

4.2.4. Grout Curtain

A watertight grout curtain was provided under the main dam for controlling seepage and pressure in the foundations refers Figure 4.7. The figure also shows general lithology. It is shown that the curtain is installed with 30 - 35 meter depth, which is 36% of maximum pressure head. No advantage has been taken of the dipping of the beds and the alternating layers of claystone with more permeable sandstones.
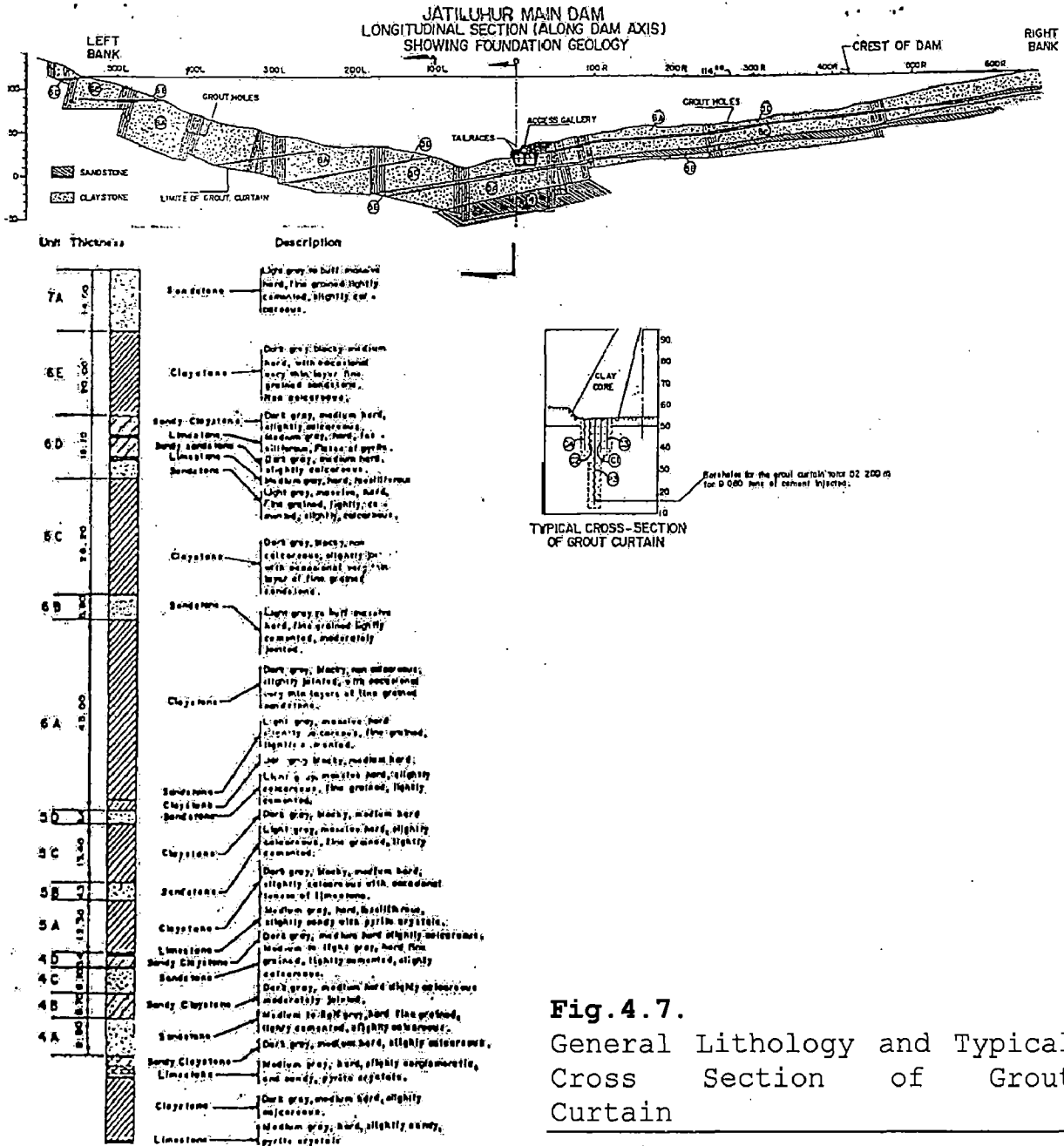
Fig.4.7.
General Lithology and Typical Cross Section of Grout Curtain

There is also no consideration to tie the grout curtain in depth with an impermeable layer or on the sides of the ravine. The curtain hardly goes beyond the fill into the abutments. Also shown in the figure above is the columnar geological section of lithology of the site-exposed strata.

The grout curtain was proposed at the design stage, as there was concern about seepage along interfaces of sandstones and claystones.

4.2.5. Embankment Behaviours and Performance Histories

The cracking at the crest, settlements and horizontal movements shown by crest markers, differential settlements between downstream and upstream shoulder markers on crest, have all dodged the Djatiluhur dam ever since its construction in 1965. Drawdown to lower reservoir levels in 1972 & 1982 accelerated these movements that only decreased when reservoir regained its height in each case.

Incidentally movements occur in central portion of the embankment dam which was modified to balance the fill quantities by reduction in the quantity of upstream rockfill in lieu of riseberm placed on downstream slope, as also modification of the core geometry, to prevent possible failure of the downstream slope along shear zones in clay bedrock of the foundation.

Regarding to the dam performance history, differential settlement is occurred during dam operation, started from its appurtenant structures completed in 1967 till at the present. Fig.4.8 and 4.9 below illustrate the measured differential settlement at the crest of the dam. More than 1800 mm magnitude of maximum settlement was occurred at downstream crest edge in 2002, and the increment is predicted being never ending.

First crack along crest of Main Dam occurred after Main Dam was completed in 1965. It was shown in fig. 4.10. The rehabilitation was limited to filling the cracks with selected material similar to the upper part crest material.
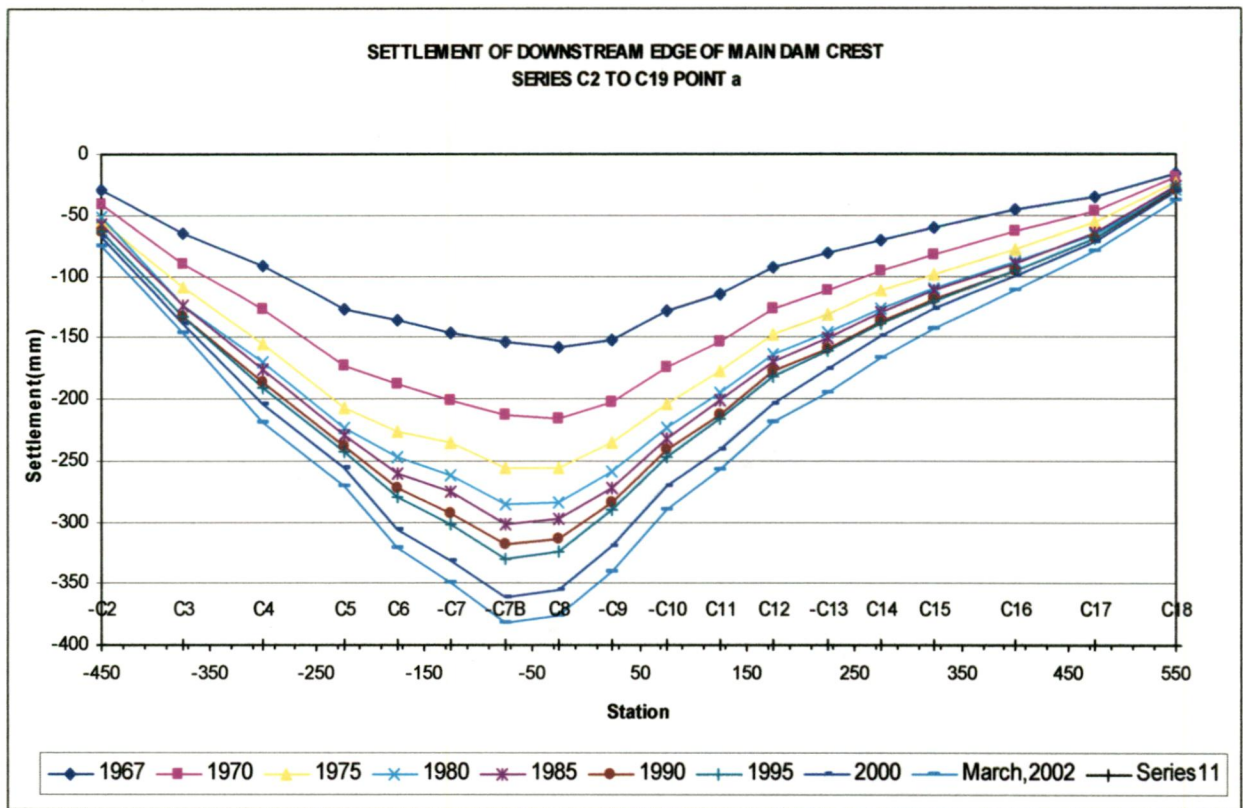
Fig.4.8. Settlement History of Downstream Edge of Crest
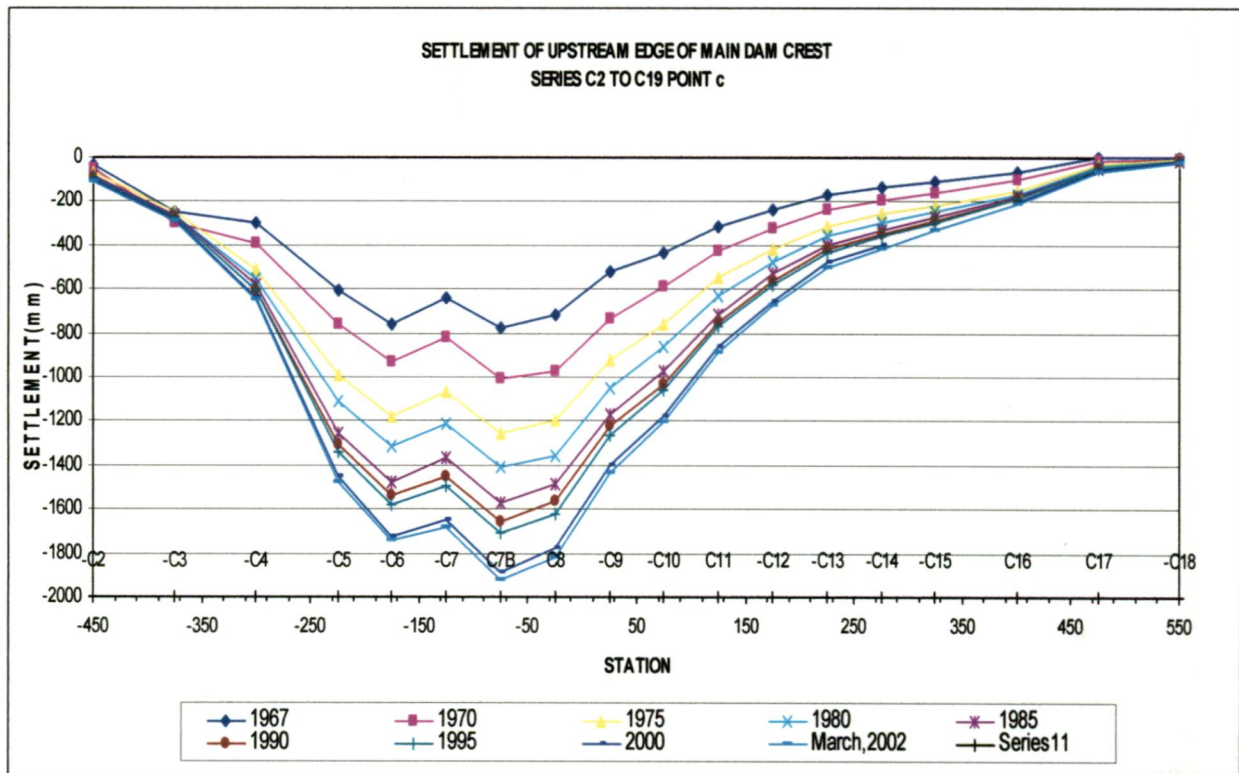
Fig.4.9. Settlement History of Upstream Edge of Crest
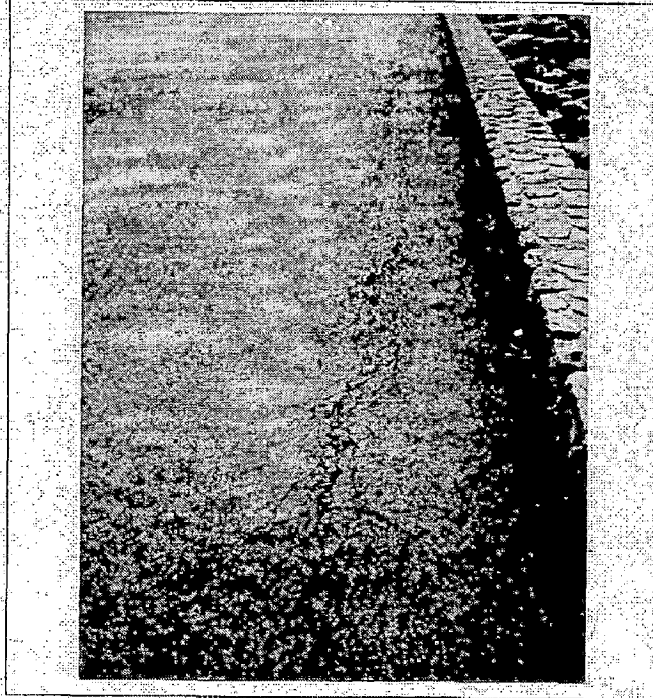
Photo no.1   Main Dam
        Longtudinal crack on crest
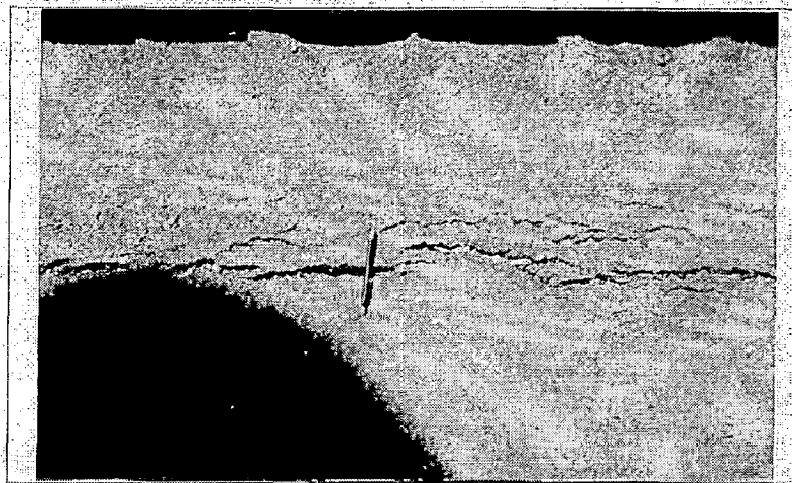
Photo No.2   Main Dam
        Longtudinal crack along crest road near d/s crest wall

Fig.4.10. Documentations of Crack Occurrences at the
        crest of the dam.

Differential settlement in 1972 at lower water level
(at + 78.50) was made-up with road materials after condition
was stable. Differential settlement in 1976 at lower water
level (at + 87.45) was made-up with road materials after

condition was already stable. Differential settlement in 1982 at lower reservoir level (at + 76.65) was made-up with road material after condition was stable. Differential settlement in 1987 at reservoir water level at El. + 87.50 m for considerable period because of impounding of Cirata Reservoir, crest repaired in 1991.

Concavity of the upper part of the upstream shell (El. + 100.00 to + 114.50), were observed in 1987 and were made-up by placing more than 500 m^3 of stone in about 90 meter stretch. Drilling was done in 1989-90 to install instruments and also to get samples of core material for testing. This also covered drilling in access gallery, drainage gallery and Ubrug dyke. Tracer tests and permeability test were also done; clearing their full depth rehabilitated also existing inclinometer.

4.3. SOFTWARE USED

4.3.1. Pentagon 3D

PENTAGON3D finite element analysis software, which is developed by Emerald Soft P.E. South Korean, enables users to perform the following tasks:
1. Build computer models of geotechnical structures
2. Apply operating loads or other design performance conditions
3. Study physical responses, such as deformation level and stress distributions

The PENTAGON3D program has a comprehensive Graphical User Interface (GUI) that gives users easy, interactive access to program functions, commands, documentation, and reference material. The users use the GUI for virtually all-interactive PENT AGON3D work. The GUI provides an

interface between users and the PENTAGON3D program, which commands drive internally. Each GUI function a series of picks resulting in an action - ultimate produces one or more PENTAGON3D commands that the program executes and records on the input history file. An intuitive menu system helps users navigate through the PENTAGON3D program. The PENTAGON3D program is organized into three basic levels:

1. PENTMESH
2. PENPRE
3. PENPOST

The PENTMESH level acts as a gateway into and out of the PENTAGON3D program. It is also used for certain global program controls such as build the model, input and clearing the database, loading or stages, and solve the FEM data with the main processor, Frontdbx. When users first enter the program, they are at the PENTMESH level. At the PENPRE level, the model including data input from PENTMESH level am verifying. The boundary condition and the sequence of construction could be easily checked to find out the errors. The PENPOST is the level to evaluate the results of a solution.

The program, which is permitted to be used for limited version only by the developer, is feasible to cope with 700 elements of 8-noded isoparametric hexahedral and 1500 nodes. The program has been executed on PC PENTIUM IV 2400 MHz.

4.3.2. Pentmesh

PENTMESH is the preprocess program of PENTAGON3D system. These provide the full graphical user interface

to complete the analysis model including the geometry, the material properties, the boundary condition, loading and the construction stages etc. The screen of PENTMESH, is categorized with two groups in the main menus. The one group in mainly used to form and to display the entities in the workspace. The entities mean the nodes and the elements. The elements are composed with the quadratic, the frame, the truss, and the spring element types.

The menus are: (1) Edit Menu (2) Model Menu (3) Mode2 Menu (4) Delete/Select Menu (5) Display Menu (6) Set Menu (7) MeshGen Menu (8) Layer Menu and (9) Misc Menu. The other menu group is mainly used to do the works except forming the entities, they are: (1) File Menu (2) View Menu (3) FEM Menu and (4) Help Menu.
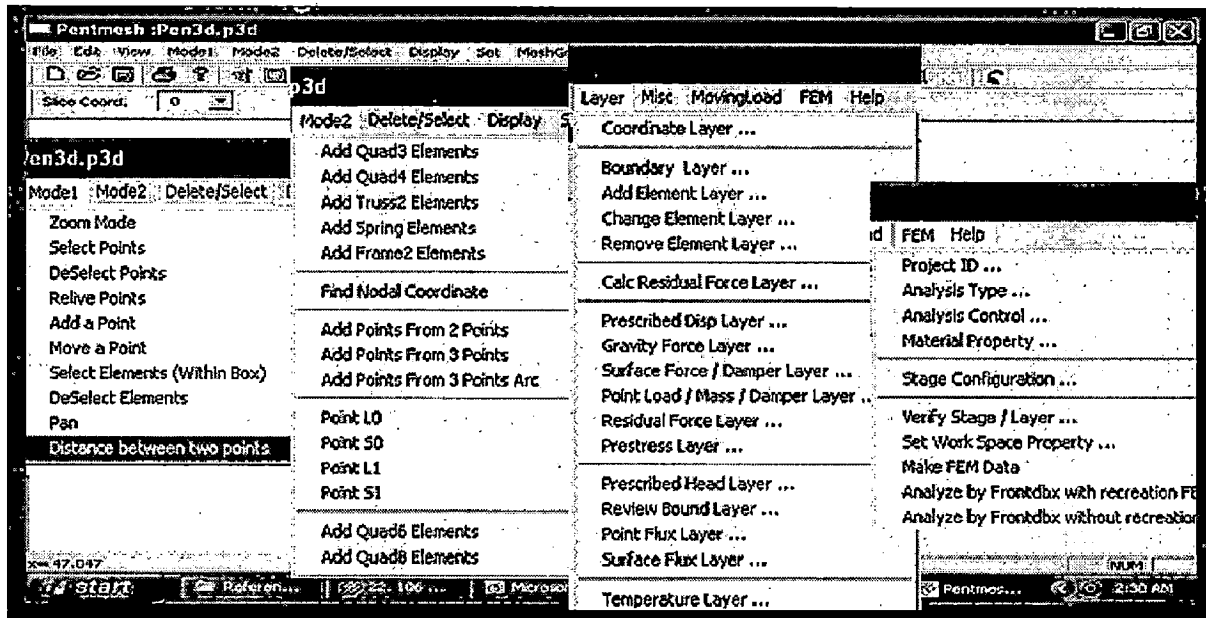
Fig.4.11. Pentmesh Screen and types of Menu

A short description about the functions of the various menus following:

1.   Edit Menu: The menu for copy and paste the points and the elements

2. Model Menu: This menu specifies the mouse mode to a certain mode (or state). Once users choose a mode, the mode is effective until another mode is selected. The menu contains: Zoom Mode, Select Points, Deselect Points, Relive Points, Add Points, Move Points, Select Elements (Within Box), . Deselect Elements, Pan and Distance between Two Points

3. Mode2 Menu: This menu specifies the elements used on the model and generate the meshing on the geometrical plane. The menu contains: Add Quad3 Elements, Add Quad4 Elements, Add Truss2 Elements, Add Spring Elements, Add Frame2 Elements, Find Nodal Coordinate, Add Point from 2 Points, Add Point from 3 Points, Add Point from 3 Points Are, Point LO – Point SO – Point L 1 – Point S1, Add Quad6 Elements, Add Quad8 Elements and Moving Line Node

4. Delete/Select Menu: The menu is used to delete the points and the elements, which are selected. The menu contains: Select All Active Points, Select All Active Elements, Deselect All Points, Deselect All Elements, Delete Selected Points and Delete Selected Elements.

5. Display Menu: The display Menu controls the screen display by the view scaling and the view translation. With the various menu lists, users can choose the preferred view by selecting the viewing items, refreshing the window, displaying entire model, displaying the Introduced model, displaying previous screen scale, and translating the model. The menu contains: Display Toggle, Redraw, Redraw All, Zoom Out, Pervious View, View Up, View Down,

View Left, and View Right.

6. Set Menu: The Set Menu specifies the various settings for the modeling environment. The menu contains: Analysis range, Coordinate Resolution, Entity Toggle, Entity Capacity, Entity Scale, Entity Color, Print Offset/Scale, Background Color, Save Time Interval, Options, Grid Size for Node Numbering, and Set Star Number of Entities for Save Process.

7. MeshGen Menu: In MeshGen Menu, there are sub-menus to create the finite element geometry. Users can generate elements and nodes, mirror the mesh, copy the mesh, and rotate the mesh and so on. The menu contains: Generate Quad4, Generate Truss2, Generate Spring, Generate Frame2, Mirror Elements, Add a Point, Add (Generate) Points, Copy Points, Move a Point, Move Points, Move Point onto a Circle, Rotate Points, Rotate Seq. No, Change Element Type, Smoothing, Generate Poil'1[s From Background, Undo, and Covert to Quad6 Quad8, and Renumber.

8. Layer Menu: in the Layer Menu, the layers are defined for the 3D mesh generation and boundary condition, the construction and loading conditions and so on. The number of input layers for each Layer Menu is limited to 300 and that of sub-layers is limited to 1500. The layer is defined for the selected nodes or elements. The sub-layer is created when some nodes or elements are selected. The menu contains: Coordinate Layer, Boundary layer, Add Element layer, Change Element layer, Remove Element layer, Calc Residual Force Layer, Prescribed Disp. Layer, Gravity Force layer, Surface Force layer, Point Load Layer,

Residual Force Layer, Prestress Layer, Prescribed Head layer, Review Bound layer, Point Flux layer, Surface Flux Layer and Temperature layer.

9.   Mise Menu: In this menu, users can change the material number, boundary type, degenerate elements or other function that used to modify the element model. The menu contains: Material No, Mechanical Boundary, Arc layer, Degenerated Hexa Layer, Node Sublayer List, Element Sublayer List, Remove Unused Sublayer List, Load Function for Time History Analysis, Ground Motion Function for Ground Motion Analysis and Current Coordinate ↔ Slice Coordinate.

10. File Menu: The menu used for clears all the database of current project from memory, open the file, save the file or others function, which is connected to, arranged the file. The menu contains: New, Open, save, save As, Import, Print, Print Preview, Print Setup, and Exit.

11. View Menu: In the View Menu, users can set the toolbar and the status bar to be displayed in the PENTMESH window, and users can view the model and the result in 3D in PENPRE and PENPOST respectively. The PENPRE and the PENPOST are executed by clicking the menu then another window will pop-up. The menu contains: Toolbar, Status Bar, 3-D Preview by PENPRE, 3D Result by PENPOST, 3-D Preview by PENPHE without recreation FEM Data, 3-D Result by PENPOST without recreation FEM Data.

12. FEM Menu: This menu used to complete the FEM data such as analysis control, material properties or stages configuration. The menu contains: Project 10,

Analysis Type, Analysis Control, Material Property, Stage Cohfiguration, Verify Stage/Layer, Set Work Space Property, save FEM Data, Analyze by Frontdbx with recreation FEM Data and Analyze by Frontdbx without recreation FEM Data.

Slice on PENTMESH

The real three-dimensional entities (elements and nodes) are created and specified in Layer Menu. The real three-dimensional entities are described and prescribed by combining the two dimensional entities with the concepts of slices. Here, the two-dimensional entities are just the ones that view on the PENTMESH workspace that represents the two-dimensional X-Y plane.

And the slice represents the remaining z axis, after creating the multiple X-Y plane along to the minus (-) z axis direction, each X-Y plane is called the Slice. The slice 0 means the first X-Y plane, the largest z coordinate, and the Slice 1 means the second X-Y plane, the next largest z coordinate, etc. The slices are created in the Layer Coordinate Layer Menu, in which the slices are created with assigning the z coordinate at each slice.

In view of the node connection, there are three element forms in PENTMESH workspace, because the element is combined by linking the nodes. They are: (1) Quad4: consist of 4 node's links, (2) Quad8: consist of 8 node's links, and (3) frame, truss, spring: consist of 2 node's link. Therefore, the elements can be created after nodes are created.

Creation of 3D Element that Use 2D Entity

Addition of three-dimensional element in PENTMESH is accomplished in 'Layer - Add Element Layer Menu'. The two-dimensional entity and three-dimensional shape for each type of added three-dimensional elements are the following. The example below is the case for adding 3D elements in one slice from 2D entity. If several slices are selected, 3D elements are added in the each selected slices. This study creates 3D 9-node solid elements using 20 Quad4 elements. Select 'Slice 3" in 'Applied Slice' column in the prior figure, then 3D 8node solid elements are created between slice 3 and 4.

Degenerate Elements

Users should specify it in 'Misc - Degenerated Hexa Layer' Menu in advance of degenerated elements, then the dialog box is pop up. Front Slice Surface No. represents surface number of divided element part. Front Slice No. represent front element slice number of where the generate elements exists. When the generated exist among Add Element Layer List, 'Degenerated' check box should be check such as in box 'Add Element layer Configuration". If the degenerated element does not exist in the 'Applied Slices' users should not check on the 'Degenerated' button, reversely, but if the generated element exist in more than one slice among the selected 'Applied Slices', users should check on the 'Degenerated' button. This time, the dialog box of 'Degenerated Hexa' pops up. In this dialog box, users should choose the applied position of added elements. Front position means the element that is surface contact to front slice. Rear position means the element that is in corner contact to front slice.

4.3.3. Penpre & Penpost

PENPRE can be used to check the input data before being analyzed by the FEA solver, Frontdbx. By using PENPRE, various input information can be displayed such as the model evolution along construction stages, the boundary conditions and the loading conditions. The graphics of PENPRE is programmed by OpenGL, the 3D graphic library; the model can be rendered with beautiful color and lights, and also can be cut, rotated, and even mirrored simply. The screen of PENPRE displays the first stage of construction. The next step for check of the sequence of construction, users can select Control – Go to the Specified Stage Menu to check the stages. Users can check the element status or material color in this level according to the stage of construction. For check of the boundary conditions, users can select Set Display Entity Menu to see the type of boundary and the direction.
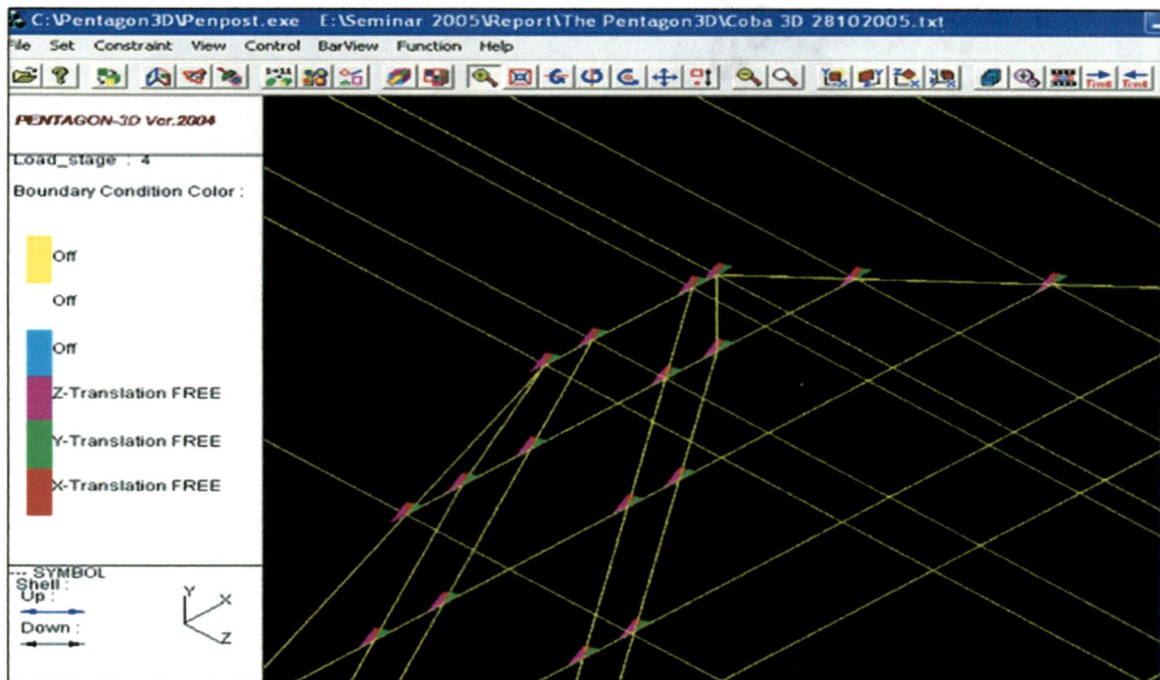
Fig.4.12. PenPre Screen displays the Boundaries

PENPOST is the level in which users could analysis the solution from the solver Frovtdbx. In PENPOST, as users open the input file name, the corresponding post-processing result file (*.pos) is opened automatically. The role of input file for PEN POST is to provide the information such as the geometry, the boundary condition, the loading condition and the save condition.

The role of result file (*.pos) is to provide PENPOST with the analysis result only. PENPOST can display the FEA result in texts, contours and vectors. Some items are displayed in global coordinate systems and other items in local coordinate system.
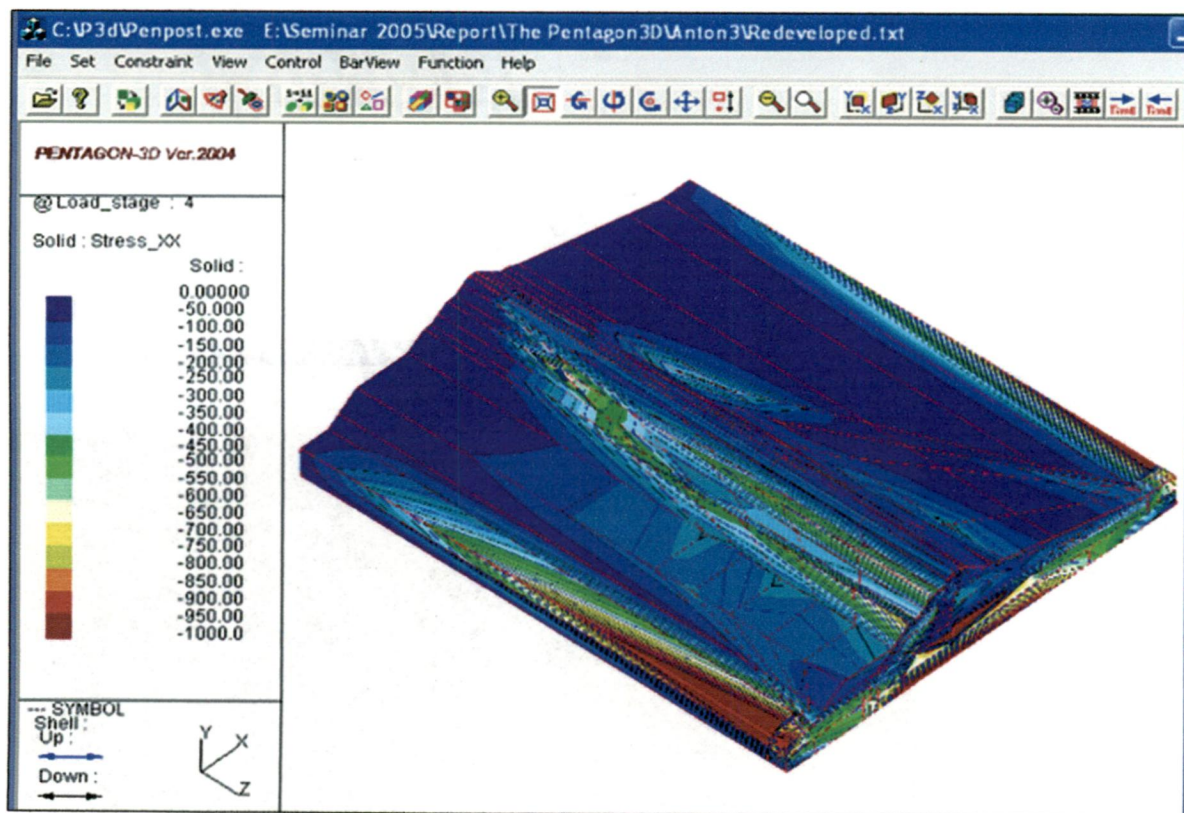
Fig.4.13. PenPost Screen displays the Results Contour

A short description about the functions of the various menus following:

1. File Menu: In this menu the FEM data could be opened and saved. The menu contains: Open, Open Environment, Save Environment, Save Environment, Save as Environment and Exit.

2. Set Menu: Users could set the entity related items and the environmental variables, such as rendering light the object, select color of element, material or boundary. The menu contains: Information, Display Entities, Element Status and Font Size.

3. Constraint Menu: This menu is used to restrict the coordinate and the entity number for specific purpose. The menu contains: Display range and Display Entity.

4. View Menu: This menu is used for adjusting the screen menu for specific object such as zooming, mirror or rotates the object. The menu contains: Select View, Set View Parameter, Redraw, Previous Zoom, Zoom In, Rotate U. V, W axis and Mirror.

5. Control Menu: Users can specify the stages that require to be checked. The menu contains: Next Stage, Pervious Stage, Go to Specified Stage, Next Time/Mode, and Previous Times/Mode. Start Animation and Stop Animation.

6. Function Menu: In this menu users can view the Eigen values; get the results in text format and save the result in the text file. The menu contains: Eigen Value, Graph, Save the Result History" and Save Image to File.

4.3.4. Steps in Making the Model

PENTAGON3D is the program that uses 20 entities with

layer to make 3D entities. The following steps are used in making the model at the PENTMESH level:

1. Set of the Coordinate Range

2. Input Nodes with Add a Point Menu

3. Generate Nodes with Add Point Menu

4. Create 2D four node quadratic elements

5. 2D node renumbering.

6. Assign the material number to the 2 elements

7. Assign the 2D boundary

8. Set of the material properties for each material numbering in Finite Element Method-Material Property Menu. In this stage the 15 material properties for each material are given in the following order: Young modulus of elasticity, Poisson's ratio, Unit weight, Cohesion, Friction Angle, K0-X, K0-Y, K0-Z, n (Ei exponent),Kb (Bulk number), m (Kb exponent), Pa (the Atmospheric pressure), Rf (Failure ratio), Ke.(the modulus number) and Kur (the Corresponding modulus number).

9. Set of the stage configuration for the construction system and the analysis in FEM - Stage Configuration Menu. The sequence of construction was detailed in this level.

10. Set of 3D coordinate from 20 nodes with Coordim1te Layer Menu. Coordinate Layer Menu used for users in making slice of a 3D model from 2D model.

11. Degenerate elements such as described at preview paragraphs.

12. Add the 3D elements from 2D elements with Add Element Layer Menu. Add Element Layer connected with the stage

configuration that is used for determines the sequence of element was built accordance to the stages.

13. Set of the 3D mechanical boundary condition from 2D nodes with Boundary Layer Menu, Boundary Layer used for establishes the boundary type in each node, users should determine for fixed, free or rotational type in x, y, z direction.

14. Add the body force with Gravity Force Layer. All elements defines in the model should be identified with the gravity force.

15. Change material properties due to wetting conditions with Change Element Layer Menu. Users should determine the wet elements due to reservoir filling and replace the material properties according to the condition.

16. Add the surface pressure with Surface Force Layer Menu. In this stage users should determine the node which is connected with the water pressure load.

17. Set of Analysis Control in FEM - Analysis Control Menu. The program solves the set of simultaneous linear equation with frontal solver method and the convergence criterion was fixed in this level.

18. Verify 30 FEM data with PENPRE level

19. Run solver process, Frontdbx.

20. Check the result at PENPOST level.

4.3.5. Validation of the Software

User understandings about the capabilities and accuracy of the software were verified by reviewing the published dam studies. Magnitudes and contour of movements and stresses

during sequential construction stages and reservoir filling period were compared between the calculated results and the published ones. Models performed by Singh (1991) and Alicura model (Botta et al, 1985) were chosen and reperformed to verify the software understanding and its capabilities. Based on the sequential multi-stages of construction and impounding periods, Nobari and Duncan (1972) models are taken to incorporate water loads, softening due to wetting and buoyant force due to reservoir filling. Parabolic function of relationships between stress and strain in soils formulated by Duncan and Chang (1970) was adopted, which was also accommodated by the software.

Three-dimensional sequential non-linear analysis of 260 meter height rockfill dam was analyzed by Singh (1991) to work out the effects of valley shapes. The canyon with valley width factor of 2.25 was chosen to redeveloped and analyzed. The three-dimensional redeveloped Finite Element idealisation model is shown in figure below.
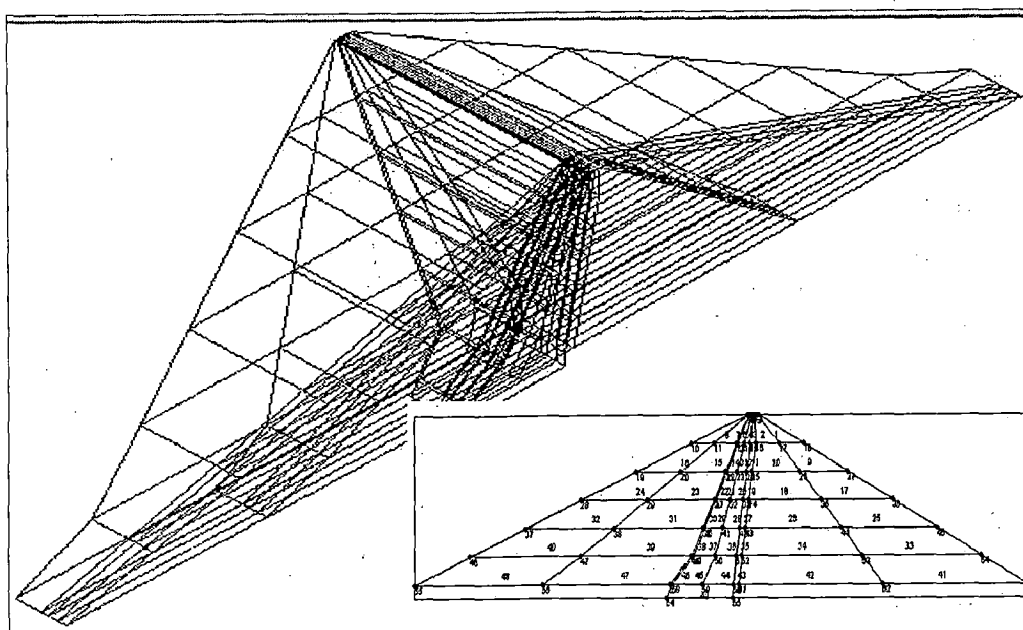
Fig.4.14. 3D Finite Element idealization of the dam

Contours of the calculated settlements at the end of construction period are shown in Figure 4.15 below. The maximum settlements in upstream shell (vertical no.1), central core (vertical no.4) and downstream shell (vertical no.7) portions are 475 mm, 907 mm and 510 mm respectively. Compared with the resource values in the same portions, the settlements are 490 mm, 875 mm and 505 mm with percentage differences 3%, 3.7% and 1% respectively. Contours of the horizontal movements are shown in Figure 4.16 below. The maximum movements in upstream shell (vertical no.1), central core (vertical no.4) and downstream shell (vertical no.7) portions are (−) 256 mm, (−) 109 mm and 289 mm respectively. Compared with the resource values in the same portions, the movements are 310 mm, 80 mm and 260 mm with percentage differences 17%, 36% and 11% respectively. Average differences between calculated and resource values were about 11% and comparison of the both contours showed good relations.
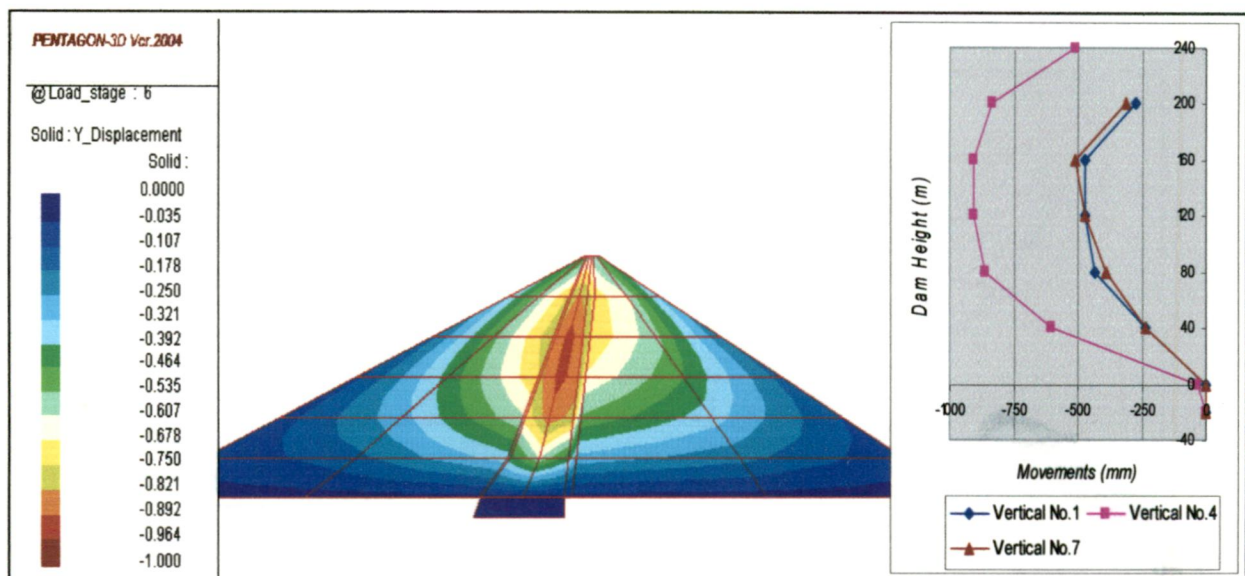
Fig.4.15. Calculated settlements contour and curve
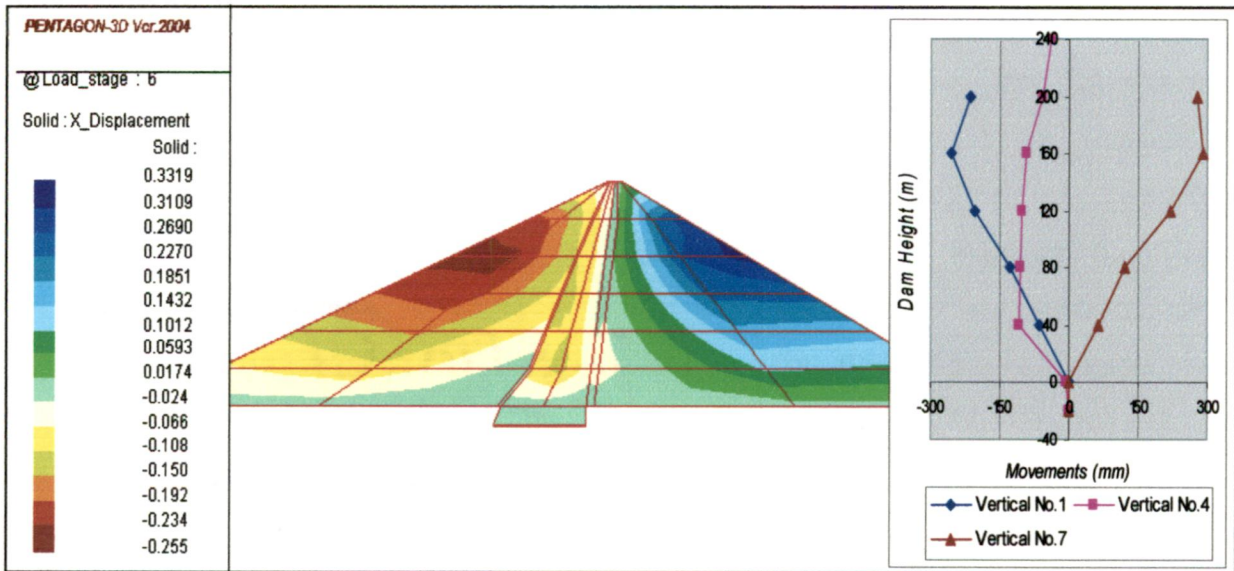
Fig.4.16. Calculated horz.movements contour and curve

Secondly, the software validation is performed by comparing the calculated behaviour parameters of Alicura dam (in Argentina) with the established values studied by Botta et al. (1985). A symmetrical central core earthfill dam with the maximum height of 130 m is studied during construction and impounding periods. By using the software, three-dimensional sequential non-linear analysis is performed on the redeveloped model as shown in Figure 4.17 below.
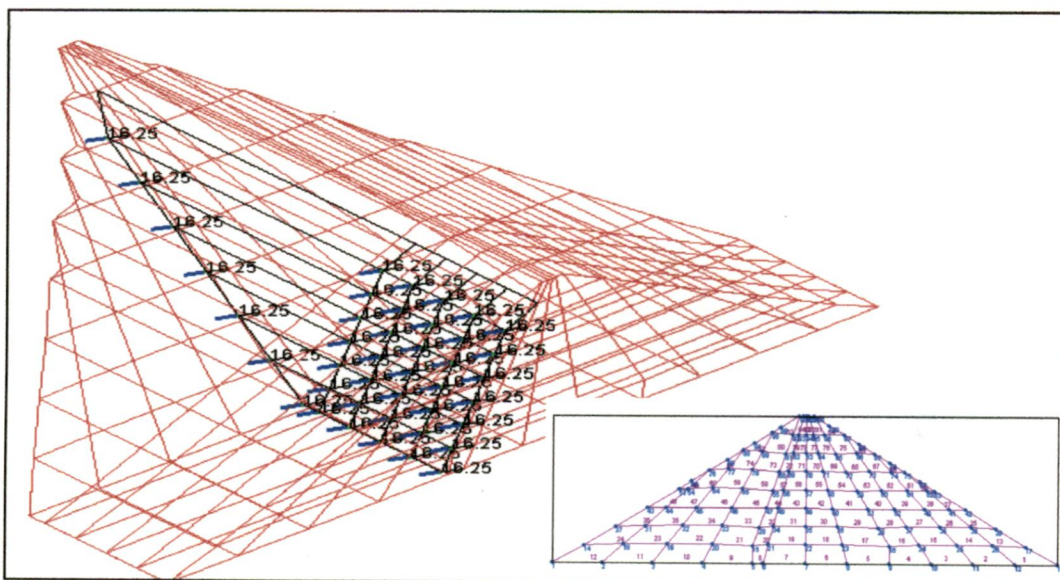
Fig.4.17. 3D Finite Element idealization of the dam

Contour of the calculated settlements at the end of construction period is shown in Figure 4.18 below. The curve illustrated maximum settlements in central core and downstream shell portions are 940 mm and 210 mm respectively. Compared with the resource values in the same portions, the settlements are 875 mm and 230 mm with percentage differences 7.4% and 8.7% respectively.
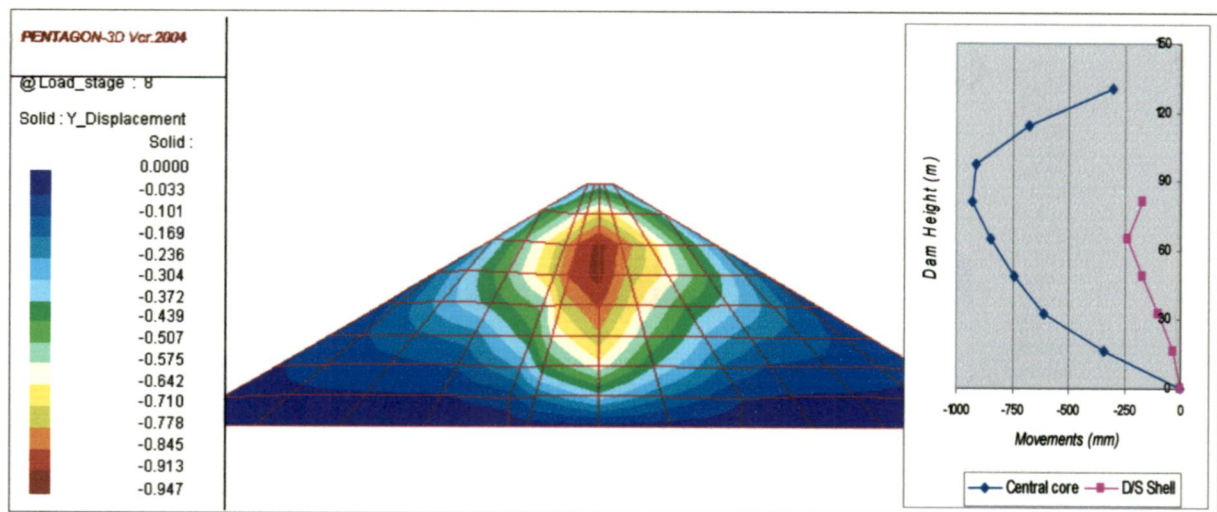
Fig.4.18. Calculated settlements contour and curve

The model accommodated water loads, softening due to wetting and buoyant force during impounding period subsequently. Contour of the calculated vertical stresses at impounding period is shown in Figure 4.19 below, which the values at somewhat above the foundation, one-fourth dam height and mid height of the dam are 145.65, 112.5 and 101.7 T/m^2 respectively. Compared with the resource values at the same portions, the stresses are 145, 115 and 85 T/m^2 with percentage differences 0.4%, 2.2% and 19% respectively. Average differences between calculated and a resource value was about 7% and comparison of the both contours showed good relations. Also in this period, the maximum calculated settlement about 629 mm occurred at mid height of upstream

core surface and the maximum horizontal movements about 547 mm at mid height of downstream shell portion. Both movements could not be compared directly with the sources results because of the lack of detail measured or calculated values registered during this period.
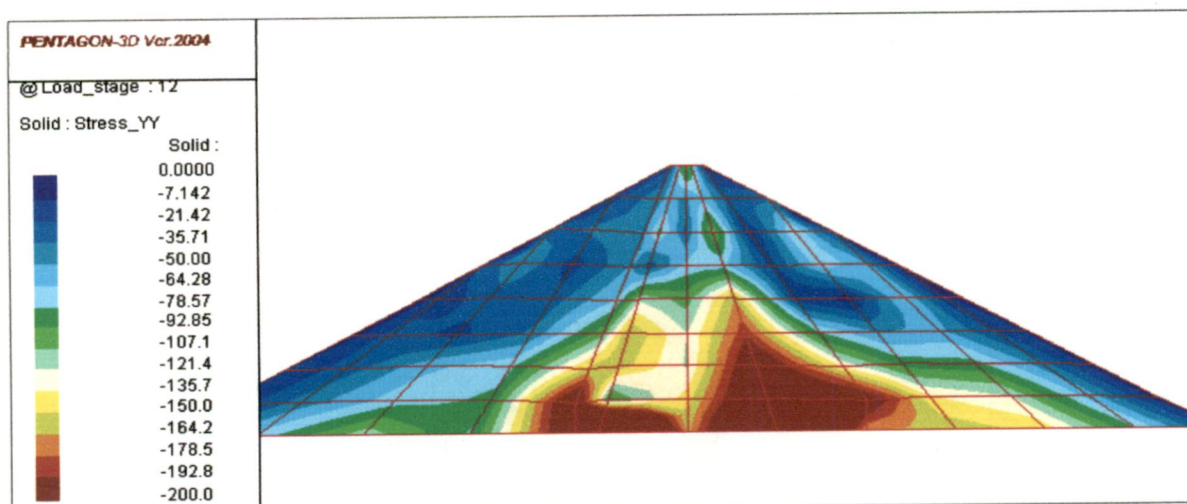
Fig.4.19. Calculated vertical stresses contour

According to both analyses, the calculated results were found to be within the permissible limit (i.e. less than 10%) of the sources values. It also indicated good agreements for the software performances.

4.4. MATHEMATICAL MODEL

4.4.1. Dam Section

Djatiluhur dam in Indonesia is 85 m high at its deepest section. It is 10 m wide and 1,200 m long at the top. Regarding to the geometrical longitudinal and cross section of the main dam in figure 4.20 and 4.21 below. The main dam embankment had an upstream slope of 1:1.35 with horizontal berms at El. 100 m and El. 82.5 m.

The mesh has been developed regarding to the transversal section of the dam at 100L section which maximum recorded dam deformation occurred. The dam foundation is not taken to be rigid and as such, the movements at base of the dam in both directions are taken to be free. Geometrical simplifying for the geometrical model also developed as follow:
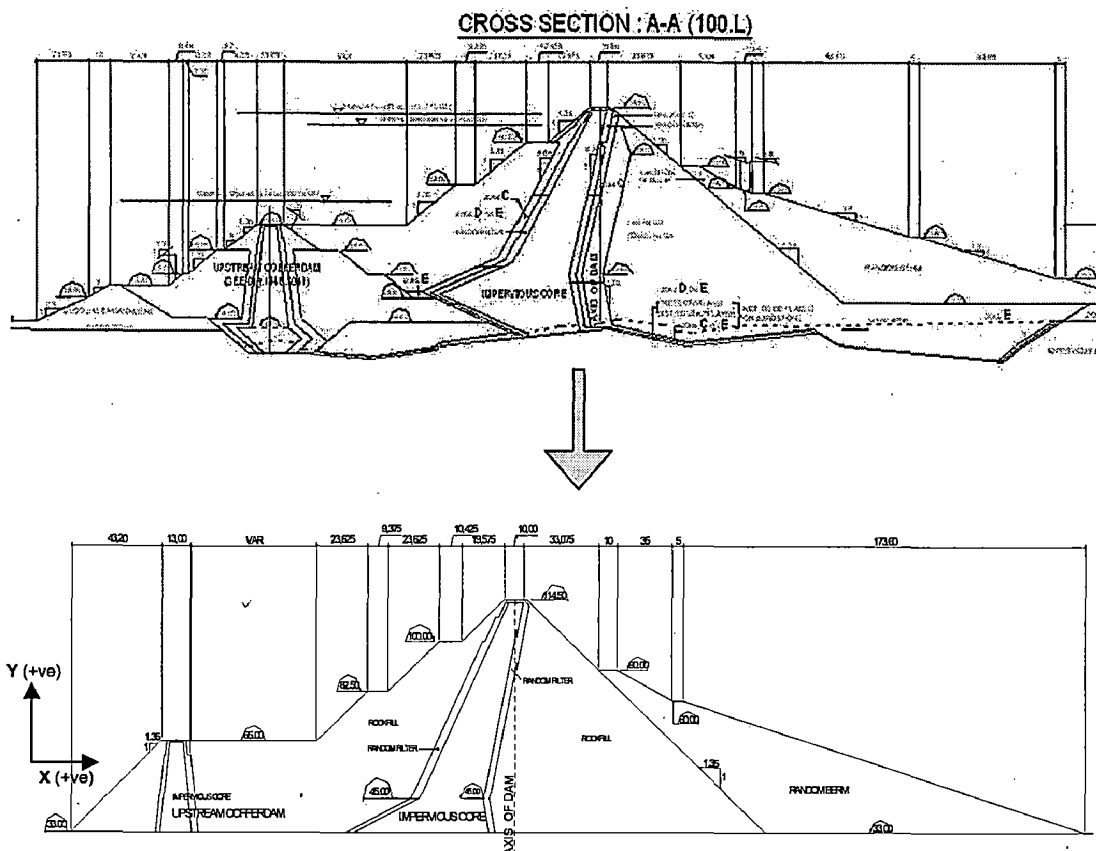
Figure 4.20. Transversal dam section modeling

In order to develop the geometrical model of longitudinal section of the dam which represents the two dimensional Z-Y plane, geometrical simplifying was developed by create straight line along the entire foundation ground surface as follow:
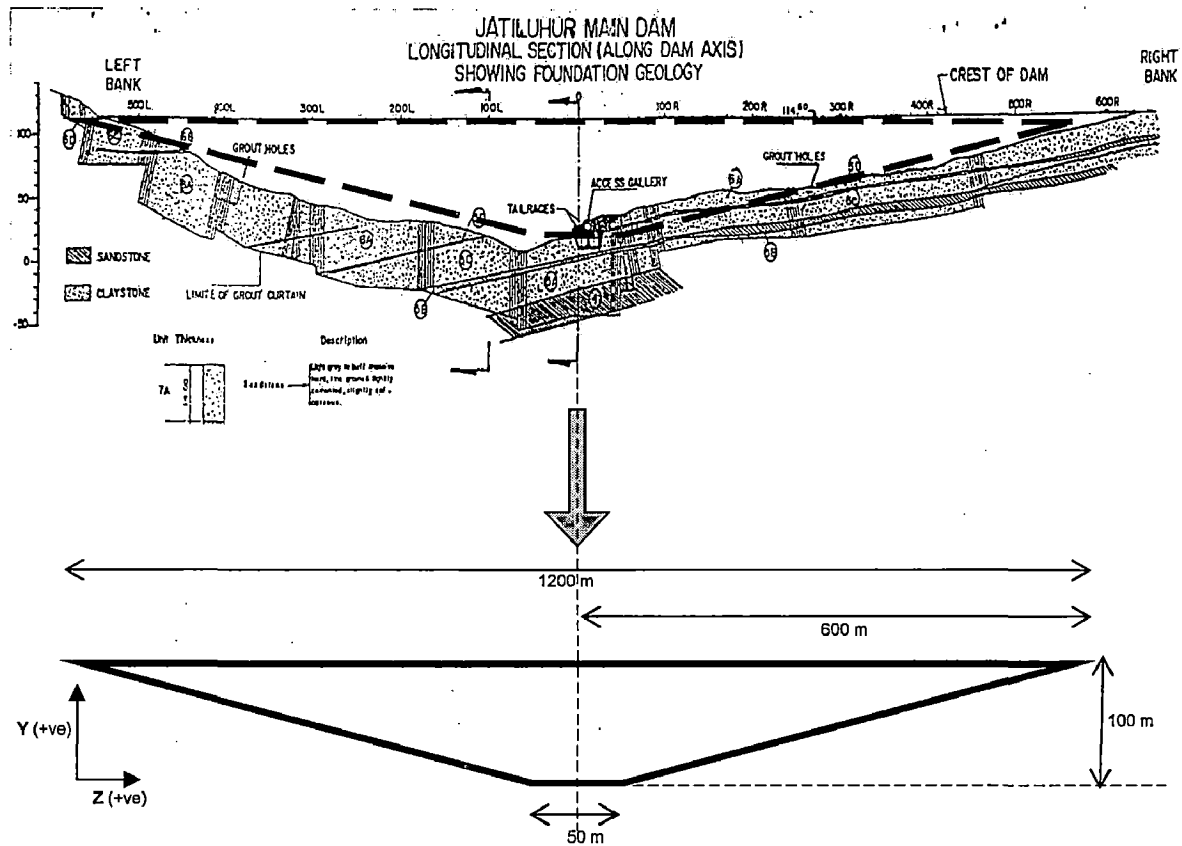
Figure 4.21. Longitudinal dam section modeling.

It can be seen that the dam has been assumed symmetrical about the centre line of the valley and, therefore, only a half of the dam has bee considered in the analysis.

4.4.2. Mathematical Idealization

Based on the geometrical models either transversal or longitudinal section which developed above, the two-dimensional entities (Mesh) which represents the two dimensional X-Y plane has been idealized on the PENTMESH work space of PENTAGON3D software as shown in Figure 4.22 below and the 3-D elements are created using that figure. The optimum number of 2-D element has been made into 72

numbers of Quad4 (consist of 4 node's links) elements, including the numbers of foundation elements that were not assumed as rigid foundation. To simulate sequential construction, the dam is assumed to be raised in 7 layers with the layer thickness as 10 m, 22 m, 17 m, 9 m, 9 m, 7 m and 7.5 m and filled in four stages with water level at 82 m, 91 m, 100m and 107 meter.
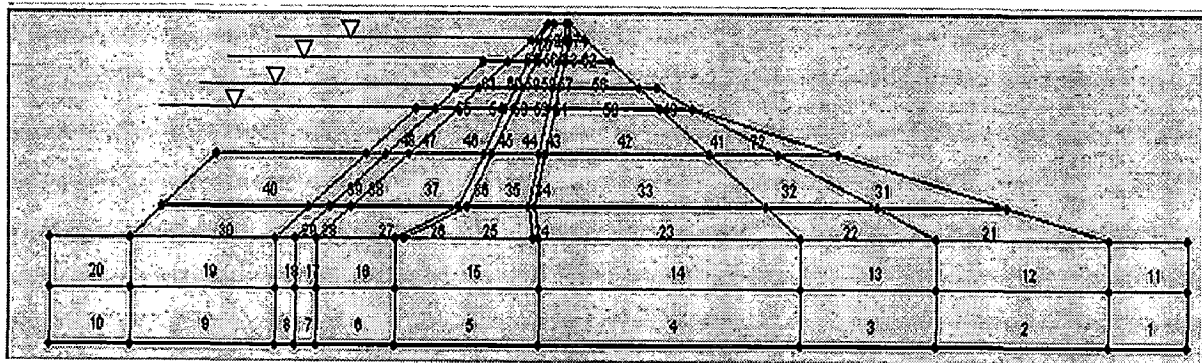
Figure 4.22. The idealized Meshing of Dam Model

The real three-dimensional entities are described and prescribed by combining the two dimensional entities with the concepts of slices. And the slice represents the remaining z axis, after creating the multiple X-Y plane along to the minus (-) z axis direction, each X-Y plane is called the slice.
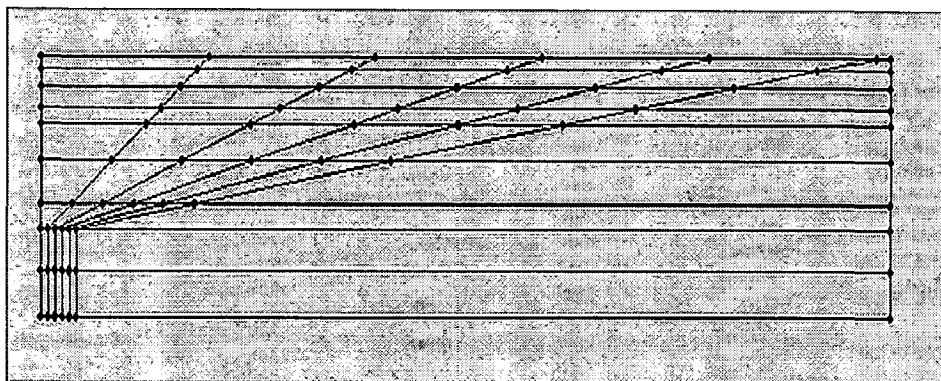
Figure 4.23. The idealized Slicing of Dam Model.

For this case, number of slices is 7 and started from 0 up to 6, as shown in figure 4.23, according to the half symmetrical portion of the Longitudinal dam section modeling. Since the valley is symmetrical in the z-direction all the nodes on the central section have been assigned zero movement in that direction. The 3-D elements of dam may not be more than 500 numbers of elements because of PENTAGON3D discretization for evaluation version. The optimum number of element has been made into 432 numbers of 8 nodded brick elements, which consists of 637 nodes including considered layer of foundation.

4.4.3. Sign Convention

The following sign convention has been followed in this study. The positive x-direction is from upstream to downstream along the river, positive y-direction is from downward to upward along the height of the dam and positive z-direction from the abutment to the central section along the dam axis.

The displacements u and y are positive in the positive x and y directions respectively. The normal stresses σ_x in the transverse direction and σ_y in the vertical direction are positive if tensile and negative if compressive.

4.4.4. Material Properties

Parabolic function of relationships between stress and strain in soils formulated by Duncan and Chang (1970) was adopted, which was also accommodated by the software.

Limitations or undesirable conditions were identified dealing with the required material properties such as:

1. Stress-strain parameters required for non-linear analysis were not available, considering that the dam was already completed in 1965 and known that non-linear technique was established in early 1970's and research on the non-linear properties of soils has not kept pace with the fast developing techniques of Finite Element Method (Domaschuck and Valliapan, 1975).

2. There were no standard laboratory tests on large diameter sample similar to oedometer test performed to derive the elastic and stress-strain parameters to be analyzed. On the other hand, the way of derivation the parameters works well for prediction of movements during construction because a typical stress path in an embankment dam during construction during construction is simulated relatively closely by oedometer testing (Kovacevic et al. at Winscar Dam, 2002).

To accommodate the undesirable conditions mentioned above and according to software validated (Para.4.3.5) which Singh's and Alicura models of material properties were used, the analysis were performed by adopting both mentioned models as model-2 and Model-3 respectively. Another alternative model also was developed, which the measurements during construction provided step-by-step new sets of properties through back-analysis from observed deformations. The best fit of this setting were used to predict the behaviours during impounding *(Botta et.al at Alicura Dam, 1985)*, and named as Model-1.

The material properties used in Model-1, Model-2 and Model-3 can be seen in the following tables:

Table.4.2. Material Properties Model-1 (Modification)

No.	Parameters	Shell	Filter	Core
1.	E (kN/m2)	80000	85000	54000
2.	γ (kN/m3)	17.7	17.7	20.5
3.	C (kN/m3)	-	-	20
4.	ϕ	42	40	19
5.	G	800	850	300
6.	n	0.2	0.2	0.22
7.	Kb	850	900	400
8.	m	0.75	0.75	0.93
9.	Rf	0.65	0.65	0.76
10.	ν	0.4	0.4	0.49

Table.4.3. Material Properties Model-2 (Singh's Model)

No.	Parameters	Shell	Filter	Core
1.	E (kN/m2)	145,000	165,000	54,000
2.	γ (kN/m3)	18	19.9	19.6
3.	C (kN/m3)	-	-	10
4.	ϕ	38	42	27
5.	G	2,500	3,000	500
6.	n	0.25	0.25	0.6
7.	Kb	3,250	4,000	650
8.	m	0.3	0.4	0.95
9.	Rf	0.76	0.76	0.9
10.	ν	0.49	0.49	0.49

Table.4.4. Material Properties Model-3 (Alicura's Model)

No.	Parameters	Shell	Filter	Core
1.	E (kN/m2)	165,000	165,000	53,000
2.	γ (kN/m3)	24.5	24.5	23
3.	C (kN/m3)	-	-	60
4.	ϕ	45	45	36
5.	G	3,500	3,500	200
6.	n	0.45	0.45	0.22
7.	Kb	4,375	4,375	300
8.	m	0.75	0.75	0.925
9.	Rf	0.55	0.55	0.76
10.	ν	0.43	0.43	0.4

Based on the sequential multi-stages of construction and impounding periods, Nobari and Duncan (1972) models are taken to incorporate water loads, softening due to wetting and buoyant force due to reservoir filling.

4.4.5. Analysis Performed

This study was limited to analyze the comparison between the predicted results and the observed values in order to evaluate the dam performance. Theoretical backgrounds (discussed in Chapter 2 and 3) have been applied to study the comparison.

Central section of Djatiluhur Dam (100L-section) has been selected to be analyzed, which is in maximum height and known that occurrences of maximum observed deformations stated. Three-dimensional incremental non-linear analyses under static condition were performed by using three models of material properties (Para.4.4.4). Subsequently,

discussions on those results were figured out, while the best-fit model was selected to be discussed in order to predict behaviours and performance of the dam.

Two different periods under different stages were accommodated in the analysis as follow:

1. **End of Construction period.**

   By simulating sequence of the construction stages to study effects of incremental constructions of the dam, when the dam was assumed to be constructed in seven lifts (described in Para.4.4.1). Static condition and embankment gravity load were applied in the mathematical model of the dam.

2. **End of Reservoir filling period.**

   Softening, buoyant uplift and water-loading conditions are incorporated in the model to study effects of the reservoir filling, when reservoir is assumed to be filled in four stages (described in Para.4.4.1). The unit weight of the upstream shell under the water is taken as submerged unit weight while saturated unit weight for the core is considered. Approximately, the stress-strain parameters reduced 10-20% due to softening, and can be obtained from tri-axial test for dry and wet specimens *(Nobari and Duncan, 1971, and Dibiagio et al., 1982)*. Free-drained materials for shell and filter zone are assumed, therefore, water pressure is assumed to act as edge load on the upstream sloping face of the core.

While studying on comparison of both mentioned conditions, the following factors are studied:

1. Vertical and horizontal deformations.

   Predicted contours of deformations within the section will be discussed. Maximum magnitude, direction and its variations will be explained in detail. Subsequently, at the same locations the predicted magnitudes being compared with observed ones.

2. Major and minor principal stresses.

   Predicted contours of stresses within the section will be discussed. Maximum magnitude, direction and its variations will be explained in detail.

3. Load transfer between core and shell.

   This load transfer can be evaluated by comparing the computed values of the major principle stress in the core and the core overburden pressure at any given depth below the crest. The ratio less than one indicate load transfer from core to shell, while the ratios greater than 1.0 indicate load transfer from the shell on the core.

4. Hydraulic fracturing susceptibility.

   In this matter, predicted contour of total vertical stresses within the core zone will be studied to predict occurrence of hydraulic fracturing. Hydraulic fracturing or the formation of hydraulically induced cracks in the core can occur when the water pressure at a given depth ($\sigma 1$) exceed the total vertical stress at the same depth (*Kulhawy et al., 1976*).

5. Potential cracks susceptibility.

   Predicted 3-dimensional contours of deformations within the section will be discussed. Significant differences of deformations within adjacent zones either in longitudinal or transversal directions should be

identified to predict occurrence of embankment cracks, moreover, evidence of longitudinal cracks appear at the dam crest probably due in part of the developed tensile stress (*Sherard, 1963*).

6. Potential plastifiction zone identification.

   Study on comparison between predicted and observed deformations is performed to identify potential material plastification developed within core zone. When observed settlement increments stated beyond the normal, it could be an indication of plastification of the materials in the zone indicated which. A deformation of horizontal extension in a direction parallel to the river causes a reduction in the horizontal confining stress, to a degree that the material plastifies (*Albero et.al, 1982, at Chicoasen dam*).

7. Secondary consolidation due to several factors such as dissipation of pore water pressure under a constant embankment load, settlement due to infiltration during reservoir filling and creep.

RESULTS
and DISCUSSION

5.1. GENERAL

Three dimensional incremental non-linear analyses under static condition have been performed on central section of Djatiluhur Dam (100L-section), by using three models of material properties and two different periods under different stages (Para.4.4.4 and 4.4.5).

Presentations and discussions on those results are figured out in this chapter. Subsequently, discussions on comparison between the results and the observed behaviours have been prepared, while the best-fit model has been selected and verified to be discussed in order to predict behaviours and performance of the dam.

5.2. PRESENTATION OF THE OBESREVED DATA

The observed behaviours data were taken from weekly monitoring and measurement of the Djatiluhur Dam. The standard benchmarking technique is used for the deformation data acquisitions. Triagonal benchmarking of main and secondary benchmarks are obtained by using standard leveling instrumentations.

During construction and impounding, only surface markers installed as measurement devices and there were no internal instruments installed in the dam body to observe the deformations till 1989. Therefore, internal behaviour

parameters within the dam (particularly on the core portion) could not be measured. Figure 5.1 and Table 5.1 below show the location of the surface markers installed on the upstream and downstream slope of 100L section of the dam.
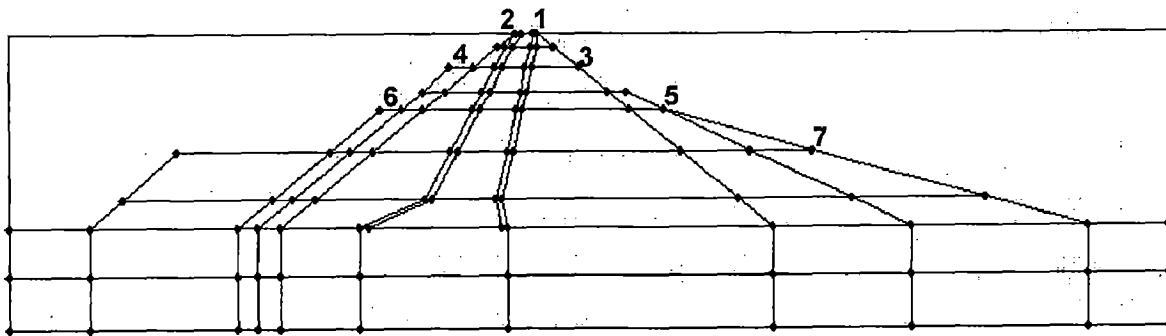
Figure 5.1. Location of surface markers

Marker No.	2	4	6	1	3	5	7
Level (m)	114.5	100	82	114.5	100	82	65
Location	Upstream			Downstream			

Table 5.1. Location and level Identifications of surface markers.

Based on the introductions of the Djatiluhur dam in Para 4.2, several considerable conditions of the dam should be noticed for the discussion on dam performance in this chapter. These are detailed as below:

1. The selected value of friction angle (ϕ = 19°) for design parameter of clay is above the best fitting line of obtained tri-axial values (ϕ = 16.9°). This assumed strength parameter is potentially resulting in over-estimated performance of the dam.

2. Compared with general slopes of the constructed rockfill dam in the world, Djatiluhur dam with 1V:1.35H slopes could be considered as a dam with steep slopes. In slope stability point of view, the failure circles

of steep slopes potentially develop through the inclined core zone, and subsequently induce the significant settlement of the mentioned zone.

3. The zone D of the dam was built in lifts of 5 to 10 meters by dumping and sluicing. This technique was known and applied in the earlier period (1940-1965) of rockfill dam construction. Based on the problem of compressibility of dumped rockfill, the different techniques were applied during modern period (post-1965) such as widespread use of well-graded, compacted rockfill and placing in layers of limited thickness in different zones. Layered placement of rockfill and clay material is recommended, followed by compaction normally done with vibratory roller (rockfill) and static roller (clay/soil). For compacted rockfill, it is usually less than 2 m, often 1 m or less. For clay/soil, it is usually in 15 cm compacted layers with sheepsfoot roller and 22.5 cm with the 50-ton rubber-tired roller. This practice suffers much smaller settlements than dumped rockfill.

4. The availability of undesired clay materials (high-plasticity clay) might be used without proper pre-constructed treatments for the materials, potentially initiated unstable behaviours of the dam. In a few dams the embankment strength has also been controlled by limiting the plasticity of the fines to predetermined maximum values. High plasticity clay from the borrow pit should be blended with well-graded materials (Pre-process) in order to minimize the danger of embankment cracking during construction and also to increase the compressive strength of the clay. Optimum moisture content (optimum water content that results optimum

densities) of compacted-impervious embankment material is controlled to be achieved in order to optimize the strength of the materials.

5. It is known from Figure 4.7 that the constructed grout curtain has not gone below the claystone. The figure also illustrates the depths of the curtain, which are only 30 - 35 meters depth below the dam base downward through the sandstone layer. According to 75 m pressure head of the dam at FRL, the curtain depths are 35% - 40% of the pressure head. Otherwise, the general curtain depth for embankment dams is greater than 70 % of the pressure head. It also potentially initiated unstable behaviours of the dam.

Such type of conditions mentioned above predictably affected performance of the dam and most of those could not be reflected in the analytical model in this study. Therefore, it could be noticed that, if the disagreements between observed and calculated behaviours are found, predictably affected by those types of conditions.

5.2.1. Dam Behaviour and Performance During Construction Period

Magnitudes of deformations recorded by the surface markers on both upstream and downstream slopes at various levels during construction are presented and discussed in the following paras.

1. In January 1965, when the embankment construction surface reached El. 103 m, about 11.5 meters below the crest, a longitudinal crack appeared along the joint between the core and the downstream fine filter. It first appeared near the midpoint of the dam axis and then extended rapidly in both directions, reaching a total length of

more than 500 meters, or half the length of the dam. A few water tests in boreholes gave no evidence of cracks in the core. The presence of cracks could be initiated by several factors such as developed differential construction movements, presence of tensile zones and presence of transition filters layers and banking on the quality and thickness of the layers (Sherard, 1963). It is also considered that in case of sloping core, tensile stresses were developed in a small region near the top (Saini et al., 1968). Most factors can be verified by observing the predicted deformations and stresses according to such levels of construction.

2. Soon after construction was completed in August 1965, a longitudinal crack approximately 300 meters long appeared on the crest in the central portion of the dam. The maximum width of the crack ranged generally from 1.0 to 1.5 inch. It can also be verified by observing the predicted deformations and stresses at the end of construction period.

3. Figure 5.2 shows settlements along the various heights of the dam recorded by upstream slope markers and the adjacent table lists the magnitudes.

Settlements at Upstream Slope Surface
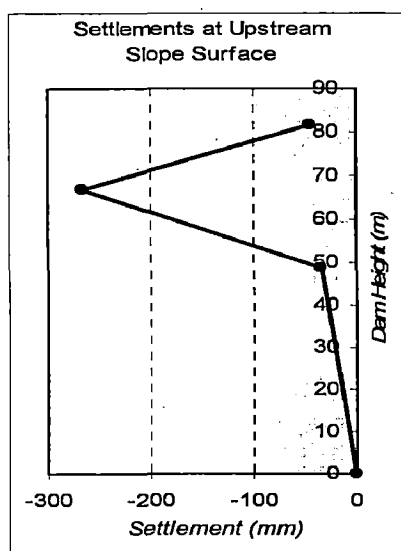
Marker No.	Level (+ m)	Height (m)	Settlements (mm)
2	114.5	81.5	-44
4	100	67	-267
6	82	49	-33.2

Figure 5.2.
Upstream slope settlements along the various heights of the dam

The figure shows that the maximum settlements on the upstream slope occurred at about three-forth of the dam height, stated by marker no.4 with the magnitude of 267 mm. The settlement of the upstream shell which rests on inclined core portion will depends on settlement of the core. And normally, the settlement within core portion is higher than outer zones due to high compressibility of the clay core. The predicted settlements will be studied to verify these observable facts.

4. Figure 5.3 shows settlements along the various heights of the dam recorded by downstream slope markers and the adjacent table lists the magnitudes.
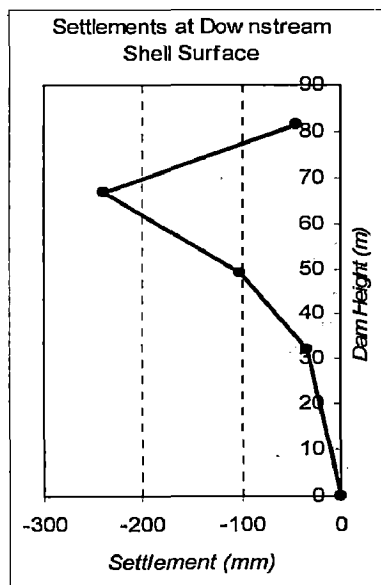
Marker No.	Level (+ m)	Height (m)	Settlements (mm)
1	114.5	81.5	-44
3	100	67	-238
5	82	49	-110
7	65	32	-33.2

Figure 5.3.
Downstream slope settlements along the various heights of the dam

The figure shows the maximum settlements on the downstream slope also occurred at about three-forth of the dam height, stated by marker no.3 with the magnitude of 238 mm. Comparing with the upstream slope settlements, it can be identified that on the same slope level, large settlements were stated whereas the upstream settlements is higher than stated downstream. The predicted settlements will also be studied.

5. Figure 5.4 shows horizontal deformations at the end of construction along the various heights of the dam recorded by downstream slope markers and the adjacent table lists the magnitudes. Extraordinary horizontal movements observed at the downstream edge of the dam were undoubtedly the matter of serious concern. 559 mm of deformation are recorded at about three-forth of the dam height, indicated by marker no.3.

Marker No.	Level (+ m)	Height (m)	Settlements (mm)
1	114.5	81.5	12
3	100	67	559
5	82	49	37
7	65	32	18

Figure 5.4.
Downstream slope horizontal deformations along the various heights of the dam

In normal cases the horizontal movement is always less than the vertical settlement but in case of Jatiluhur Dam horizontal movements are about three times larger than the settlement values. This is an indication to the structural stability problem of the dam. Horizontal movements can develop cracks in clay core and endanger its role as water barrier. On the other hand, comparing and observing the predicted contour of deformations should verify accuracy of the observed data particularly in marker no.3. Discussion of the comparison between observed and predicted behaviours is made out in Para 5.4 of this Chapter.

5.2.2. Dam Behaviour and Performance During First Reservoir Filling

Magnitudes of deformations recorded by the surface markers on both upstream and downstream slopes at various levels during first reservoir filling are presented and discussed in the following points below.

1. In February 1966 (Impounding reached level 80-82 m) numerous horizontal cracks were observed in the upper portion of the core between 0 and 10 meter depths. The presence of cracks could be initiated by several factors as follows:

   ✓ Presence of differential construction movements, tensile zones and transition filters layers and depending on the quality and thickness of the layers during construction period (Introduction of Para 5.2).

   ✓ Extraordinary horizontal movements observed at the downstream edge of the dam after end of dam construction. It could gradually initiate horizontal cracks within the core zone.

   Presence of differential movements and tensile zones can be verified by the predicted magnitudes of settlements obtained from analysis according at corresponding level of impounding.

2. Between October 1965 and June 1966 (Impounding reached level 100-103 m) the upstream edge of the crest settled about 50 cm with respect to the downstream edge thereby indicating the possibility of various phenomenon, namely:

   ✓ Unseen internal cracks might have developed in the core due to presence of differential movements and tensile zones.

   ✓ Hydraulic fracturing susceptibility. It can occur when

the water pressure at a given depth ($\sigma3$) exceed the total vertical stress at the same depth (*Kulhawy et al., 1976*). Hydraulic fracturing induced cracks in the core then resulted in settling in top zone. In this case, predicted contour from the results of analysis of total vertical stresses within the core zone will be studied to confirm the occurrence.

3. Figure 5.5 shows settlements at the end of first reservoir filling along the various heights of the dam recorded by upstream slope markers and the adjacent table lists the magnitudes.

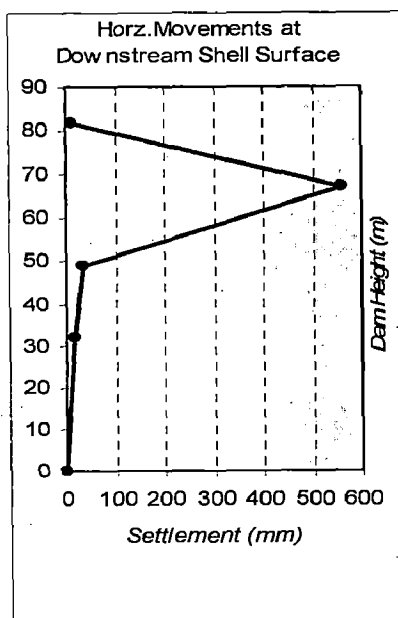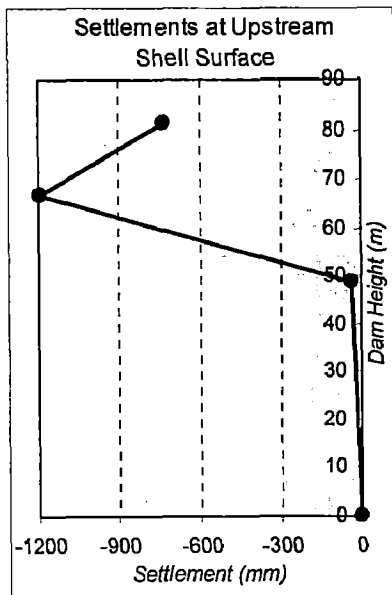| Marker No.	Level (+ m)	Height (m)	Settlements (mm)
2	114.5	81.5	--728
4	100	67	-1195
6	82	49	-33.2

Figure 5.5.
Upstream slope settlements along the various heights of the dam at the EoRF

The figure shows that maximum settlements on the upstream slope occurs at about three-forth of the dam height, initiated by marker no.4 with the magnitude being 1195 mm.

It is known that during reservoir filling, the presence of water create water load on the core and foundation, softening and weakening of the shell material on wetting, and buoyant uplift forces in the upstream shell. Stresses in wetted portion of dam shell significantly change due to buoyancy and presence of water load. Meanwhile, softening

of shell materials due to wetting results strength loss and compression of upstream shell material. This resulted in additional settlements within the upstream shell of the dam body *(Nobari and Duncan, 1971, and Dibiagio et al., 1982)*.

Good rigidity at the mid-height of upstream slope was observed at marker no.6. It could be affected by the construction of the concrete tower.

4. Figure 5.6 shows settlements along the various heights of the dam recorded by downstream slope markers and the adjacent table lists the magnitudes.
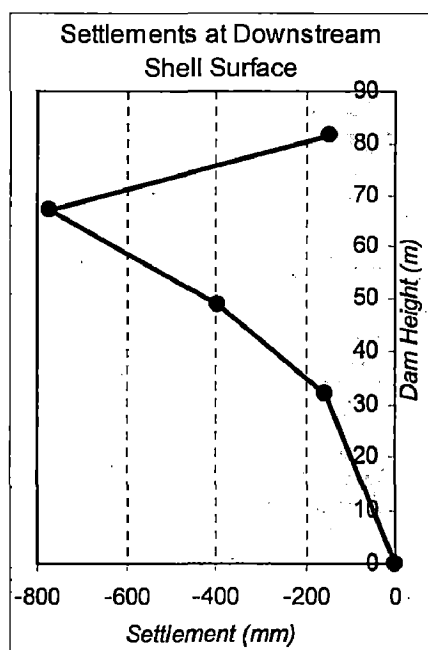
Marker No.	Level (+ m)	Height (m)	Settlements (mm)
1	114.5	81.5	-148
3	100	67	-773
5	82	49	-396
7	65	32	-154

Figure 5.6.
Downstream slope settlements along the various heights of the dam at the EoRF

The figure shows that a maximum settlement on the downstream slope also occurs at three-forth of the dam height, shown by marker no.3 with the magnitude of 773 mm. It may be noticed that the settlement increments stated on both slopes are very large. It may be attributed to the mode of construction of shells. The upstream value is higher than the downstream value due to presence of reservoir water.

It is known that when observed settlement increments are exceptionally larger then the normal, it could be an indication of plastification of the materials in the zone.

5. Figure 5.7 shows horizontal deformations at the end of reservoir filling along the various heights of the dam recorded by downstream slope markers and the adjacent table lists the magnitudes.

Horz.Movements at Downstream Shell Surface
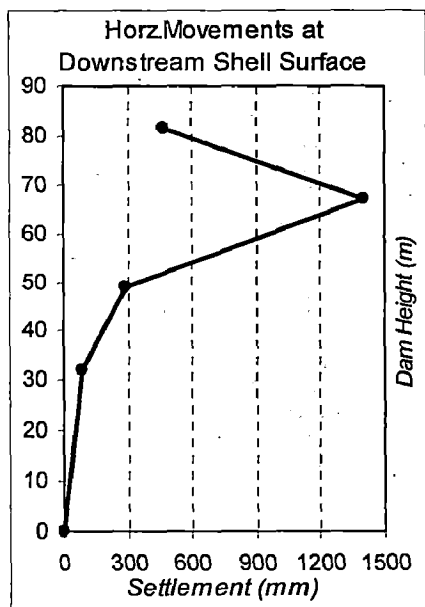
Marker No.	Level (+ m)	Height (m)	Settlements (mm)
1	114.5	81.5	468
3	100	67	1400
5	82	49	298
7	65	32	87

Figure 5.7.
Downstream slope horizontal deformations along the various heights of the dam at the EoRF

Extraordinary horizontal movements were continuously observed at the downstream edge of the dam given by marker no.3. 1400 mm of deformation towards downstream is recorded at three-forth of the dam height. This fact also shows indication of plastification of the materials in the zone indicated. A deformation of horizontal extension in a direction parallel to the river causes a reduction in the horizontal confining stress, to a degree that the material plastifies *(Albero et.al, 1982, at Chicoasen dam)*. Therefore, a comparative increments of deformations among similar dams in the world is given in Para 5.5.2 (point 7) of this chapter, in order to investigate accuracy and range of those observable facts.

5.3. PRESENTATION OF THE ANALYTICAL RESULTS

5.3.1. Material Properties Model-1

By using material properties model-1, contours and magnitudes of deformations given by the software are presented and discussed below.

1. Figure 5.8 shows the contour of the settlements at the end of construction period. It can be seen that the maximum settlements occurs at two-third of the dam height within the core zone, with the value at 501 mm. On an average, settlements within the upstream shell are little higher than the downstream shell. The contour also shows the magnitudes of the settlements on the upstream and downstream slope surface, wherein the maximum settlements occurs at the three-forth of the dam height. It should be noticed that the constructed berms on the both slope affected the contours.

Figure 5.8.   Contours of Model-1 settlements at the end of construction

2. Figure 5.9 gives the contour of the horizontal deformation at the end of construction. It can be seen that the upstream and downstream shells moved in opposite directions. Downstream shell totally moved towards

downstream with the maximum magnitude at two-third of the dam height being around 130 mm. Most of upstream shell moves towards upstream except in top portion that moves towards downstream. The maximum magnitude obtained at one-third of the dam height with the value being around 120 mm.

Figure 5.9. Contours of Model-1 horizontal deformations at the end of construction

3. Figure 5.10 shows the contour of the settlements at the end of first reservoir filling period. It can be seen that the maximum settlements appears at mid-height of the dam within the core zone with the value being 540 mm. Comparing with the contour at the end of construction, settlements at the end of reservoir filling within the upstream shell and core zone generally increased. These increments and differences are caused by effects of the presence of reservoir water such as load on core, the softening of the submerged materials and buoyant uplift forces in the upstream shell. Particularly, increments of the settlements within the upstream shell indicated that the water load and softening of material are predominant over the buoyant uplift.

Figure 5.10. Contours of Model-1 settlements at the end of reservoir filling

4. Figure 5.11 shows the contour of the horizontal deformation at the end of reservoir filling. It can be seen that the movements are in the downstream direction throughout most of the dam, with exception at the toe of the upstream slope. The maximum magnitude stated at two-third of the dam height with the deformation at 629 mm. However, the maximum incremental magnitude stated at the mid-height of the dam with the deformation being around 680 mm. Therefore, it can be concluded that the reservoir water imposed a significantly loading on inclined core resulting in deformation towards downstream.

Figure 5.11. Contours of Model-1 horizontal deformations at the end of reservoir filling

5.3.2. Material Properties Model-2

By using material properties model-2, contours and magnitudes of deformations obtained by the software are presented and discussed below.

1. Figure 5.12 shows the contour of the Model-2 settlements at the end of construction period. It can be seen that the maximum settlements appears at mid-height of the dam within the core zone with the value at 147 mm. On an average, settlements within the upstream shell are also little higher than the downstream shell and it was surely caused by the inclination of the core. Typical with Model-1, the maximum settlements on the upstream and downstream slope surface are illustrated at the three-forth of the dam height. It also confirmed that the constructed berms on the both slope affected the contours. By comparing with the Model-1, magnitudes of settlements of Model-2 are lesser than those with Model-1. It can be concluded that material properties adopted in Model-2 gives smaller settlements value.
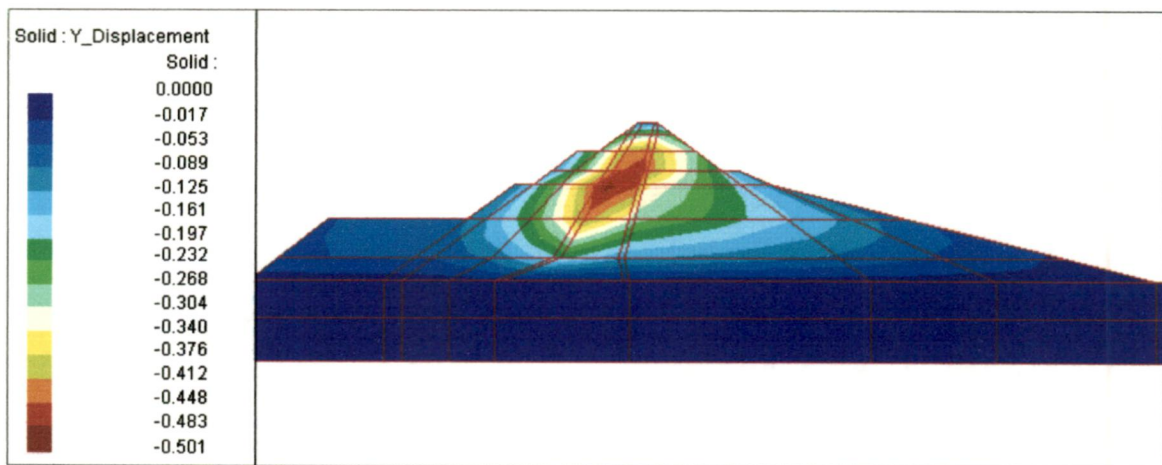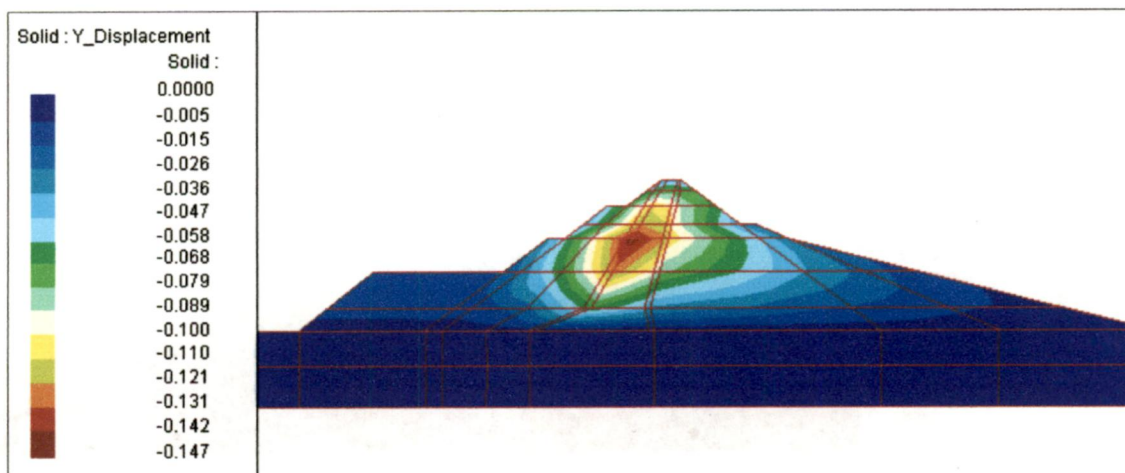

Figure 5.12. Contours of Model-2 settlements at the end of construction

2. Figure 5.13 shows the contour of the Model-2 horizontal deformation at the end of construction. It can be seen that the upstream and downstream shells moved in opposite direction. Downstream shell totally moved towards downstream and the maximum magnitude is observed at mid-height of the dam with the value around 39 mm. Most of upstream shell moved towards upstream except in top portion that slightly moved towards downstream. The maximum magnitude is observed at mid-height of the dam with the value around 42 mm. In this model as well, inclination of the core still resulted in change of deformation direction within the upstream shell. By comparing with the Model-1, magnitudes of horizontal deformations of Model-2 are also lesser than those of Model-1. It is concluded that material properties adopted in Model-2 gives lesser horizontal movements as compared with Model-1.
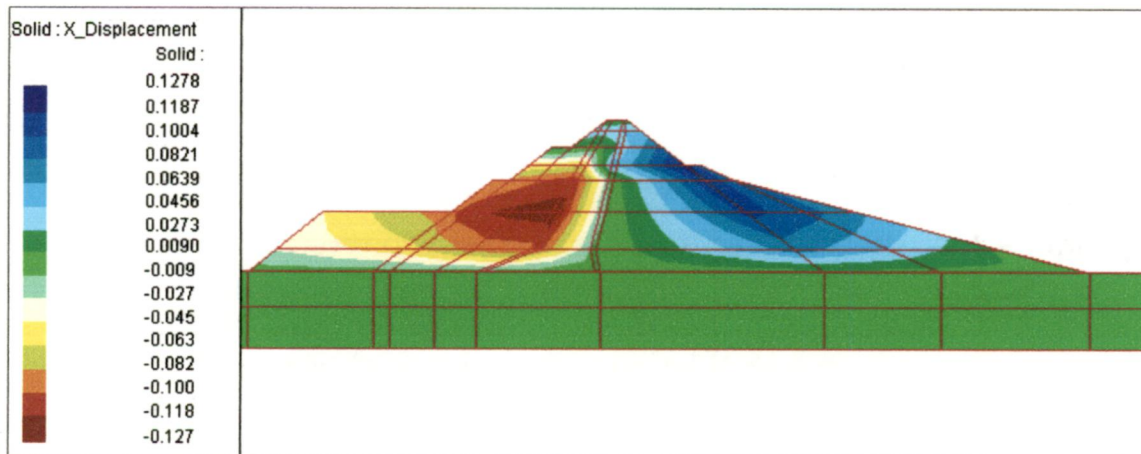

Figure 5.13. Contours of Model-2 horizontal deformations at the end of construction

---

3. Figure 5.14 shows the contour of the Model-2 settlements at the end of first reservoir filling period. It can be seen that the maximum settlement appears at one-third of the dam height within the core zone with the value at 164 mm.
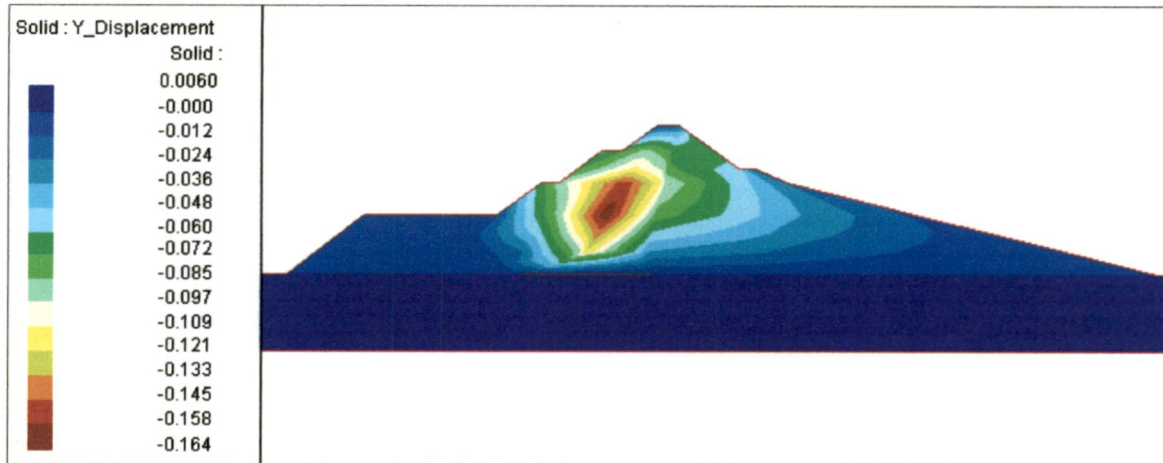
Figure 5.14. Contours of Model-2 settlements at the end of reservoir filling

Comparing with the contour at the end of construction, settlements at the end of reservoir filling within the upstream shell and core zone are generally more. These increments and differences are also caused by effects of the presence of reservoir water. Increments of the settlements within the upstream shell indicated phenomena that the water load and softened material are dominating over the buoyant uplift.
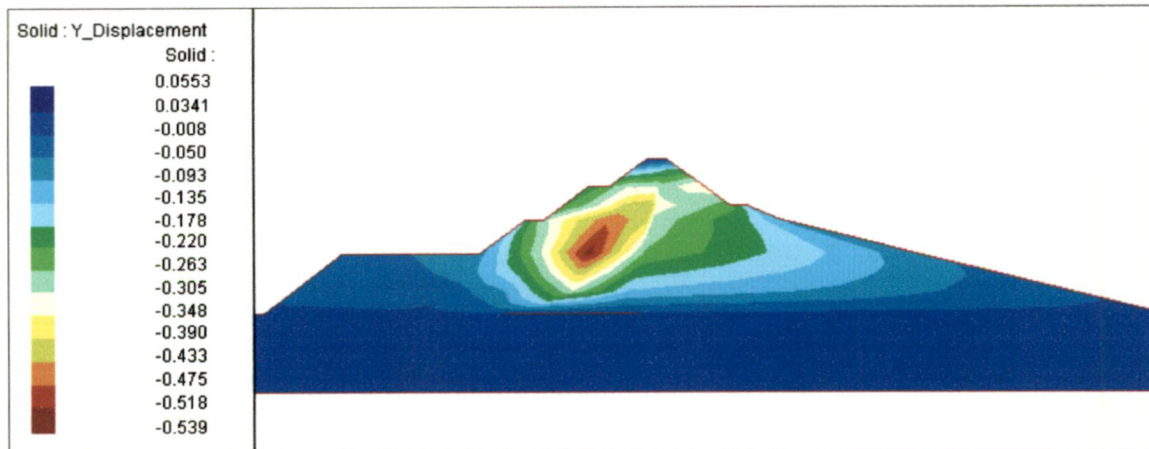
4. Figure 5.15 shows the contour of the Model-2 horizontal deformation at the end of reservoir filling. As compared with the Model-1, the trends of deformations are typical. The maximum magnitude is observed at top zone of the dam with the deformation at 164 mm. However, the maximum incremental magnitude is observed at the mid-height of the dam with the deformation around 170 mm. It still shows that material properties adopted in Model-2 gives lesser
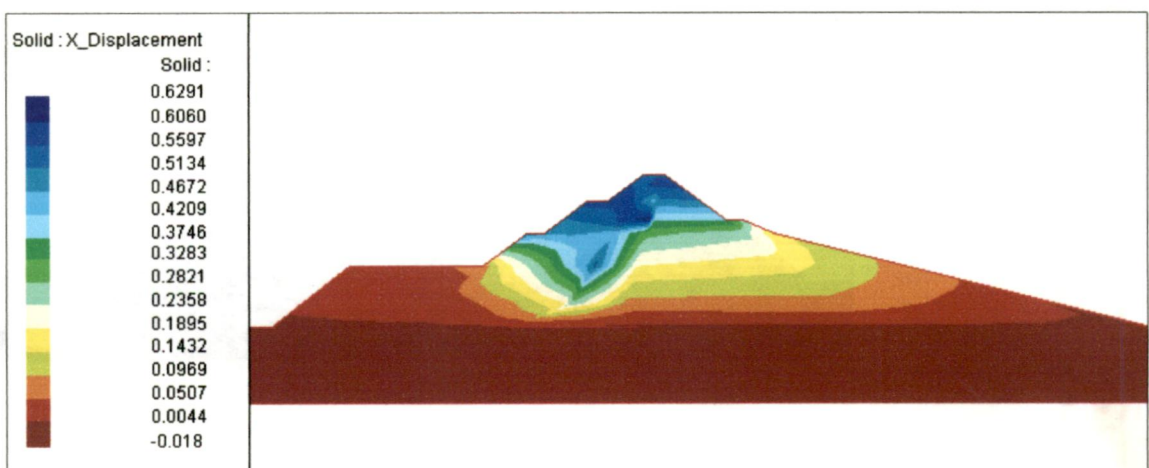
deformations as compared with the Model-1.
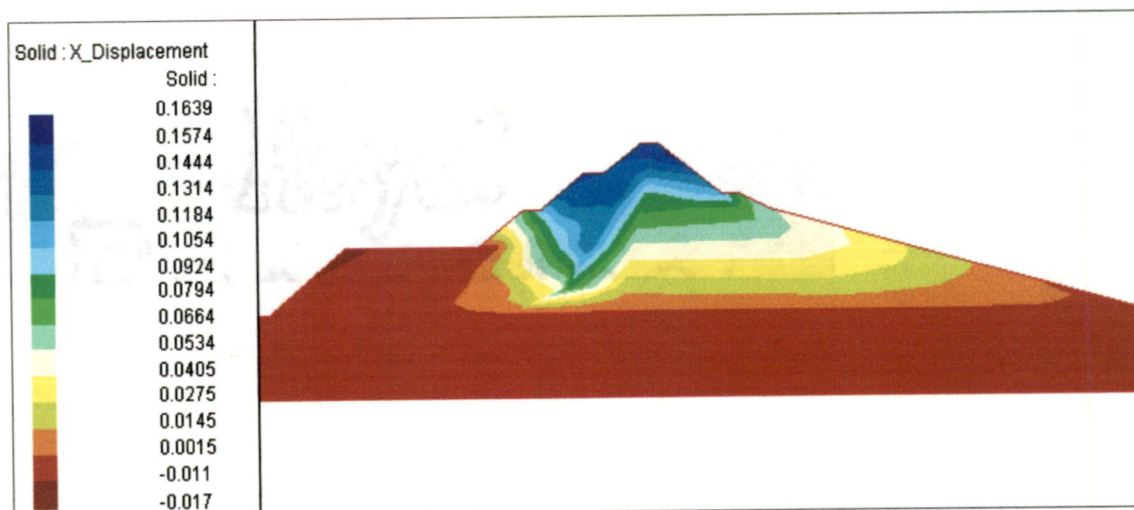
Figure 5.15. Contours of Model-2 horizontal deformations at the end of reservoir filling

5.3.3. Material Properties Model-3

By using material properties model-3, contours and magnitudes of deformations obtained by the software are presented and discussed below.

1. Figure 5.16 shows the contour of the Model-3 settlements at the end of construction period. It can be seen that the maximum settlements occurs at two-third height of the dam with the value is 627 mm. It should be noticed that the contour shows the maximum settlements occurs in the downstream filter zone, whereas generally in case of inclined core, the maximum settlements is observed within core zone as an effect of core inclination. Generally, the trends of slopes settlements typical with Model-1 and Model-2.
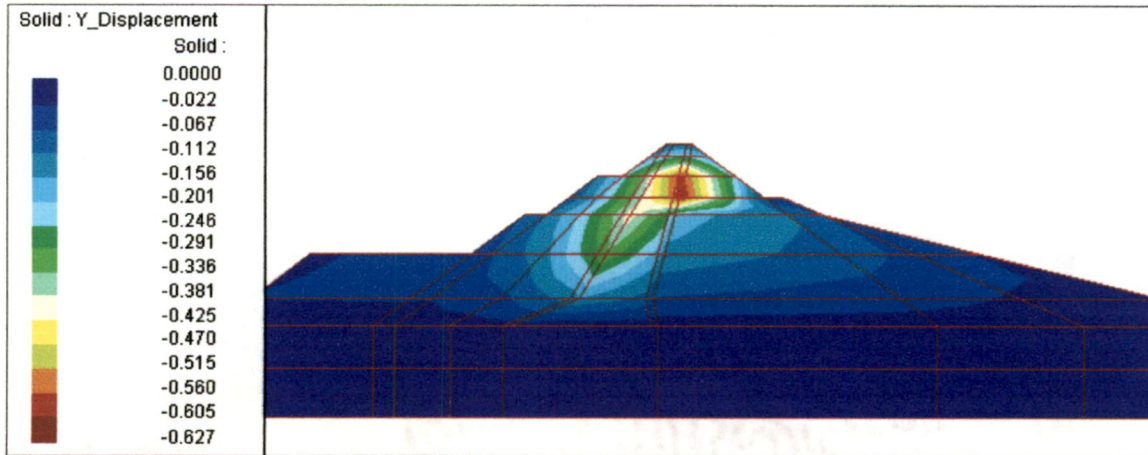
Figure 5.16. Contours of Model-3 settlements at the end of construction

By comparing with the Model-1 and Model-2, magnitude of internal settlements during construction period of Model-3 is the highest.

2. Figure 5.17 shows the contour of the Model-3 horizontal deformation at the end of construction. The trends of deformations are typical with the Model-1 and Model-2. Downstream shell moved towards downstream and the maximum magnitude is observed at two-third height of the dam with the value around 133 mm. However, the top zone below the crest slightly moved towards upstream. Most of upstream shell moved towards upstream except in top portion that slightly moved towards downstream. The maximum magnitude is observed at mid-height of the dam with the value around 111 mm. By comparing with the Model-1, magnitudes of horizontal deformations of Model-3 are almost same but higher then the Model-2.
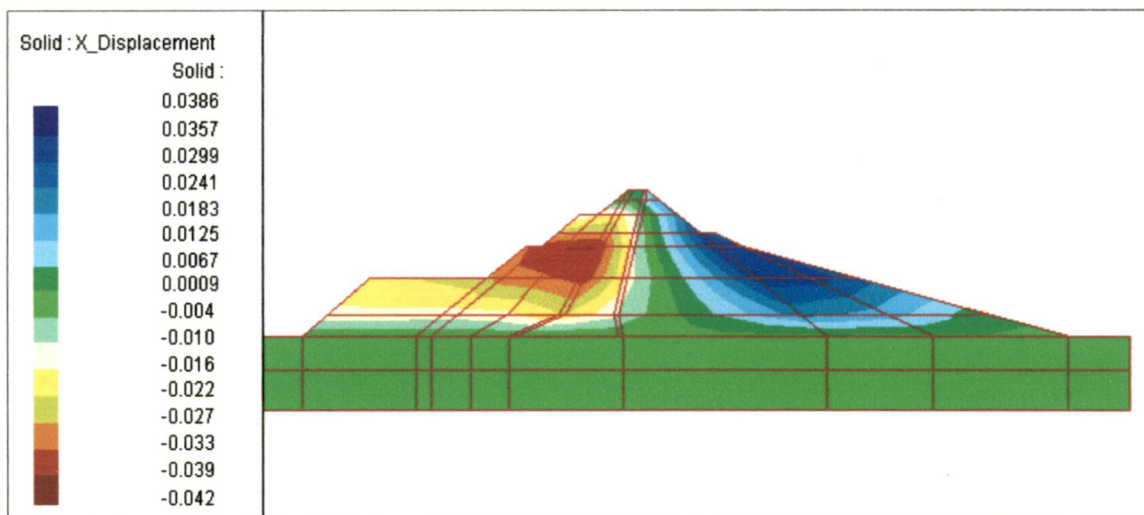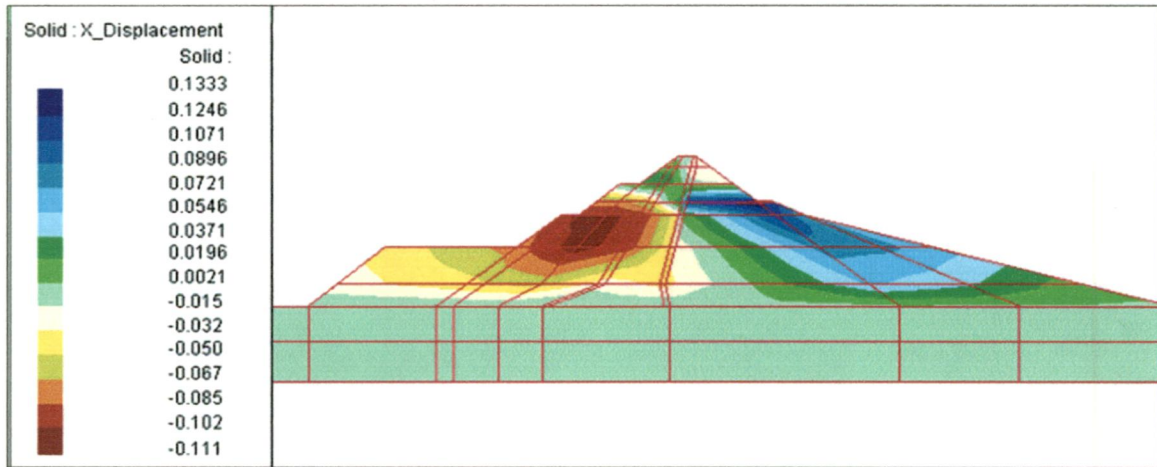
Figure 5.17. Contours of Model-3 horizontal deformations at the end of construction

3. Figure 5.18 shows the contour of the Model-3 settlements at the end of first reservoir filling period. The maximum settlement that occurs at two-third of the dam height within the downstream filter zone at 698 mm.
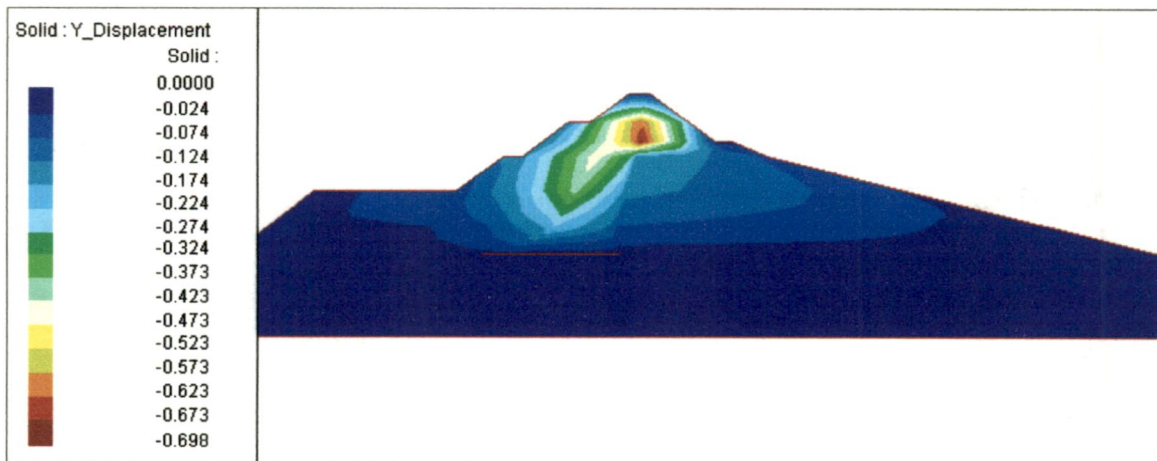
Figure 5.18. Contours of Model-3 settlements at the end of reservoir filling

It should be noticed that the contour shows the internal maximum settlements occurs in the downstream filter zone, whereas generally in case of inclined core, the maximum settlements is observed within either core zone or upstream shell as the submerged zones. Comparing with the

contour at the end of construction, settlements at the end of reservoir filling within the upstream shell and core zone are generally more and also caused by the same effects and phenomena of the presence of reservoir water. Magnitudes of maximum internal settlements of Model-3 during first reservoir filling are also the highest among the Models.

4. Figure 5.19 shows the contour of the Model-3 horizontal deformation at the end of reservoir filling. The movements are in the downstream direction throughout most of the dam, with exception of the toe of the upstream slope that 38 mm moved towards upstream. The maximum magnitude is observed at two-third height of the dam within downstream shell with the deformation at 328 mm. Therefore, it can be predicted that the reservoir water imposed a significantly loading on inclined core resulting considerable deformation towards downstream direction in the downstream shell of the dam. However, this maximum deformation still lesser than the deformation of Model-1, confirmed that Model-3 is more stable to retain effects of reservoir water than Model-1.
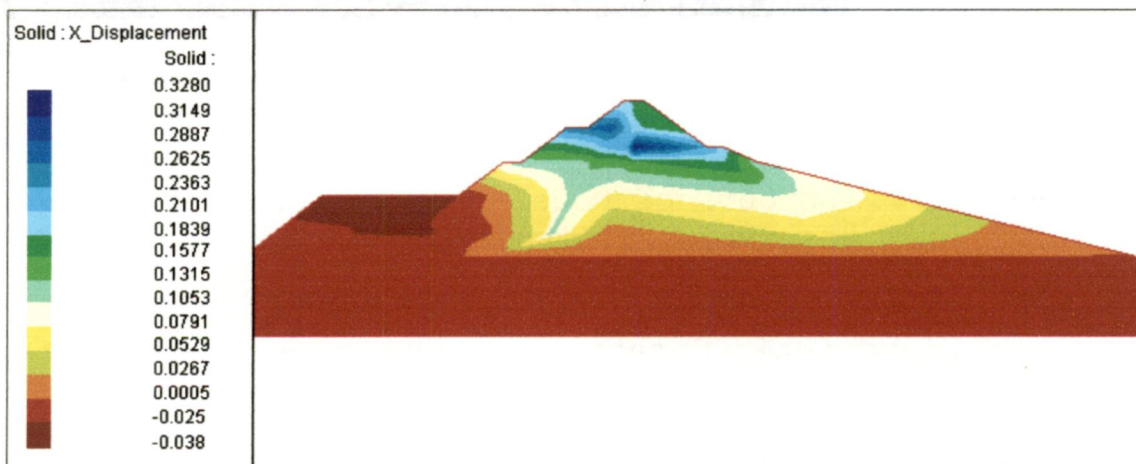
Figure 5.19. Contours of Model-3 horizontal deformations at the end of reservoir filling

5.4. DISCUSSION ON COMPARISSON BETWEEN OBSERVED AND CALCULATED SLOPES BEHAVIORS

5.4.1. Comparison During Construction Period

1. Figure 5.20 shows comparison of upstream slope settlements among the observed data, and analytical values with Model-1, Model-2 and model-3. The settlements are plotted along the heights of the dam along the upstream slope where markers are installed. Table 5.2 tabulates the comparative magnitudes.

Figure 5.20

Comparison of upstream slope settlements along the height of the dam

Marker No.	Level (+ m)	Height (m)	Observed Settlements (mm)	Model-1 Settlements (mm)	Model-2 Settlements (mm)	Model-3 Settlements (mm)
2	114.5	81.5	-44	-89	-32	-90
4	100	67	-267	-276	-75	-191
6	82	49	-33.2	-96	-32	-87

Table 5.2. Comparative magnitudes of upstream slope settlements

It is seen from the figure for all the cases maximum settlements on the upstream slope surface occurred at the three-forth of the dam height. Magnitudes of settlements of Model-1 (Modification) are the maximum and it can be concluded that material properties adopted in Model-1

resulted in comparable deformation of the dam.

2. Figure 5.21 shows comparison of downstream slope settlements among the observed data and analytical values with Model-1, Model-2 and model-3. The settlements are plotted along height of the dam along the downstream slope where markers are installed. Table 5.3 tabulates the comparative magnitudes.

Figure 5.21

Comparison of downstream slope settlements along the height of the dam

Marker No.	Level (+ m)	Height (m)	Observed Settlements (mm)	Model-1 Settlements (mm)	Model-2 Settlements (mm)	Model-3 Settlements (mm)
1	114.5	81.5	-44	-89	-39	-95
3	100	67	-238	-268	-64	-249
5	82	49	-110	-96	-28	-63
7	65	32	-33.2	-56	-10	-32

Table 5.3. Comparative magnitudes of downstream slope settlements

The figure shows the maximum settlements on the downstream slope also occurs at three-forth of the dam height, indicated by marker no.3. And still magnitudes of settlements of Model-1 are the maximum whereas settlements of Model-2 are found smallest. However, Model-1 has good similarity as compared with the observed values.

3. Figure 5.22 shows comparison of downstream slope horizontal deformations among the observed data, and analytical values with Model-1, Model-2 and model-3. The deformations are plotted along the height of the dam along the downstream slope where markers are installed. Table 5.4 tabulates the comparative magnitudes.
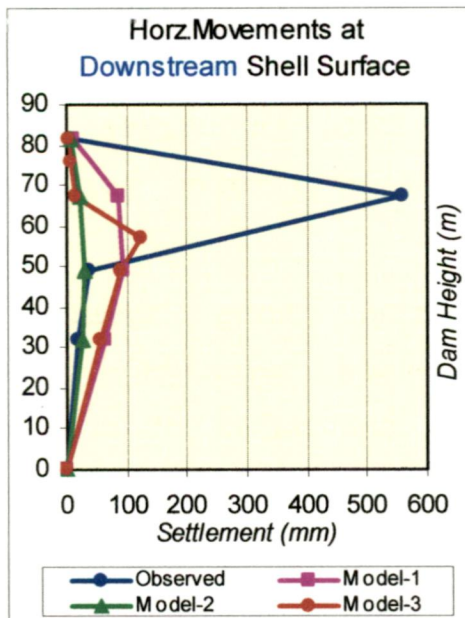
Figure 5.22

Comparison of downstream slope horizontal deformations along the height of the dam

Marker No.	Level (+ m)	Height (m)	Observed Horizontal deformation (mm)	Model-1 Horizontal deformation (mm)	Model-2 Horizontal deformation (mm)	Model-3 Horizontal deformation (mm)
1	114.5	81.5	12	13	7	5
3	100	67	559	88	21	16
5	82	49	37	93	30	91
7	65	32	18	65	27	58

Table 5.4. Comparative magnitudes of downstream slope horizontal deformations

Unusually large horizontal movement is observed at the downstream edge of the dam with 559 mm of deformation recorded at three-forth of the dam height by marker no.3. In normal cases the horizontal movement is generally less than the vertical settlement as shown by the values of three Models as well.

In case of Djatiluhur Dam horizontal movements are about three times larger than the settlement values. This is an indication of the structural stability problem of the dam especially for the core. No plausible explanation for larger horizontal movement at one elevation is possible. Hence, accuracy of the observed data in marker no.3 is suggested to be verified by fresh calibrated performance of the installed marker.

Although calculated results from those Models show significant differences when compared with the observed values, Model-1 can be chosen on the basis of comparison of vertical settlements in order to predict performance of the dam during construction period.

5.4.2. Comparison During Reservoir Filling

1. Figure 5.23 shows comparison of upstream slope settlements at the end of reservoir filling among the observed data and analytical values with Model-1, Model-2 and model-3. The settlements are plotted along the heights of the dam where the upstream slope markers installed. Table 5.5 tabulates the comparative magnitudes.
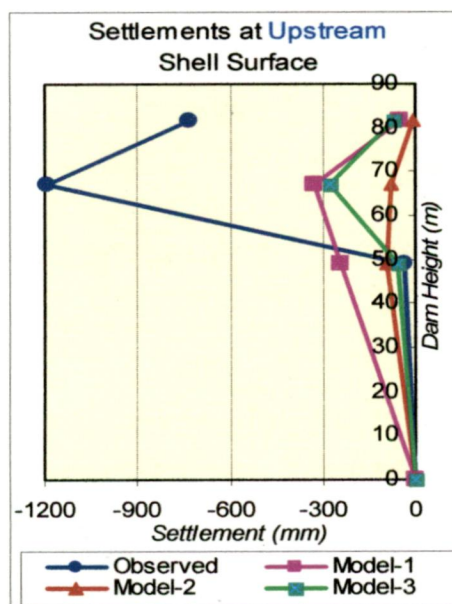
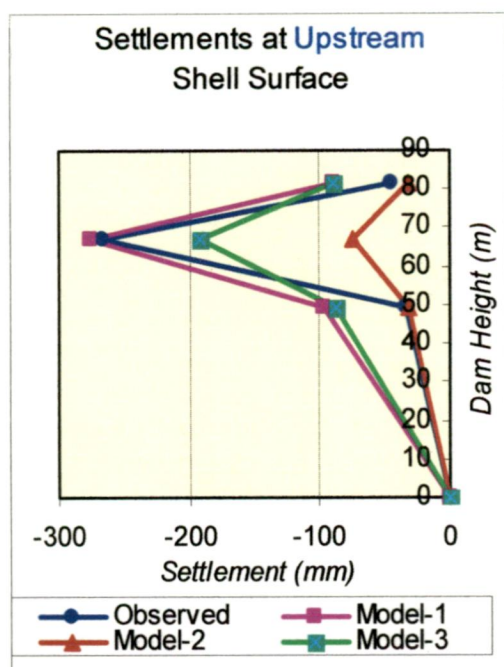**Figure 5.23**
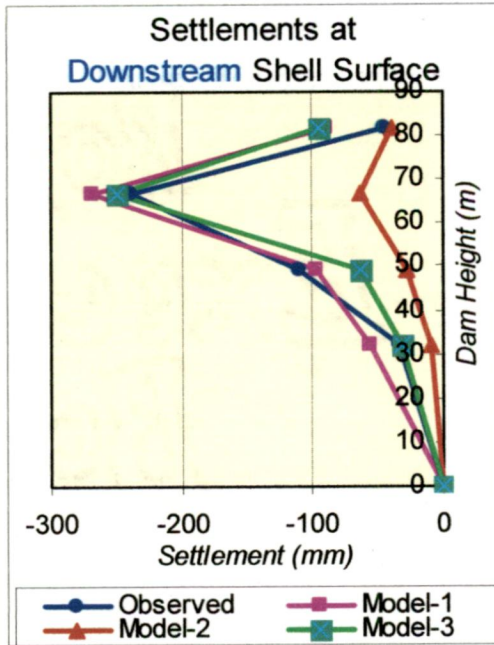Comparison of upstream slope settlements (EoRF) along heights of the dam

Marker No.	Level (+ m)	Height (m)	Observed Settlements (mm)	Model-1 Settlements (mm)	Model-2 Settlements (mm)	Model-3 Settlements (mm)
2	114.5	81.5	-728	-50	-10	-74
4	100	67	-1195	-328	-75	-274
6	82	49	-33.2	-238	-89	-54

Table 5.5. Comparative magnitudes of upstream slope settlements at the end of reservoir filling

The figure shows the observed maximum settlements on the upstream slope occurrs at three-forth of the dam height, recorded by marker no.4 with the magnitude at 1195 mm. It is found that observed settlement increments are much larger than the normally expected values. Settlements at the end of filling are about four times larger than the settlement values at the end of construction, an unusually high value.

Comparing with the calculated results, the observed data is extremely large. The largest calculated value is given by Model-1 with the settlement of 328 mm, which is 30% of the observed value. It can be primarily attributed to the softening effects of submerged zone which and decreases the material strength.

2. Figure 5.24 shows comparison of downstream slope settlements at the end of reservoir filling among the observed data and analytical values with Model-1, Model-2 and model-3. The settlements are plotted along the height of the dam where the downstream slope markers are installed. Table 5.6 tabulates the comparative magnitudes.

Settlements at Downstream Shell Surface

The figure shows the observed maximum settlements on the downstream slope also occurr at three-forth of the dam height, stated by marker no.3 with the magnitude of 773 mm.

Figure 5.24

Comparison of downstream slope settlements (EoRF) along height of the dam

Marker No.	Level (+ m)	Height (m)	Observed Settlements (mm)	Model-1 Settlements (mm)	Model-2 Settlements (mm)	Model-3 Settlements (mm)
1	114.5	81.5	-148	-28	-19	-49
3	100	67	-773	-340	-78	-224
5	82	49	-396	-112	-25	-74
7	65	32	-154	-74	-17	-24

Table 5.6. Comparative magnitudes of downstream slope settlements at the end of reservoir filling

It is also found that observed settlement increments are larger than the normal. Settlements at the end of reservoir filling are about three times larger than the settlement values at the end of construction. It could be confirmed that similar observable behaviours simultaneously occurred on both slopes of the dam at the same level.

Disagreement between observed and calculated magnitudes is also found. The largest calculated results is also given by Model-1 with the settlement is 340 mm, which is 50% of the observed value.

3. Figure 5.25 shows comparison of downstream slope horizontal deformations at the end of reservoir filling among the observed values, and the analytical values with Model-1, Model-2 and model-3. The deformations are plotted along the height of the dam where the downstream slope markers are installed. Table 5.7 tabulates the comparative magnitudes.
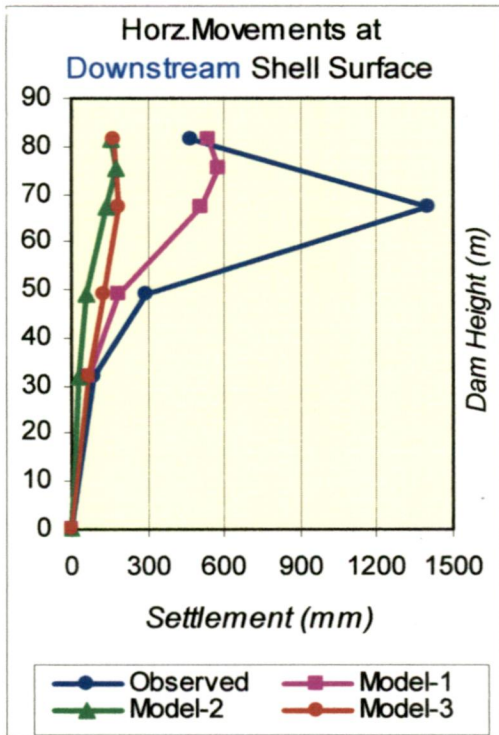
Figure 5.25

Comparison of downstream slope horizontal deformations (EoRF) along the height of the dam
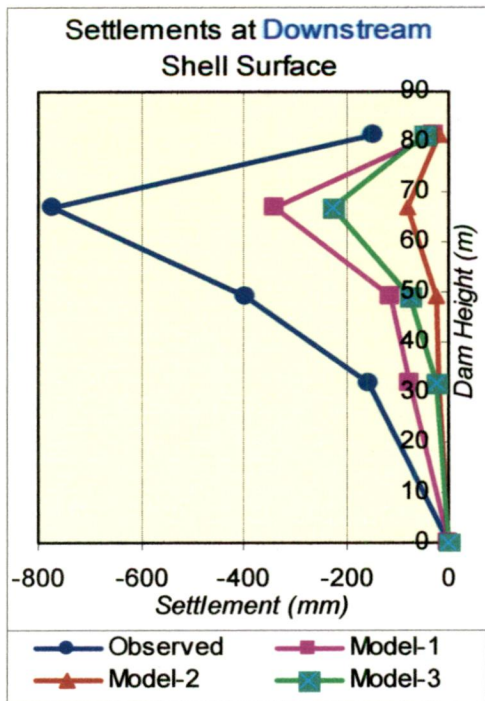
Marker No.	Level (+ m)	Height (m)	Observed Settlements (mm)	Model-1 Settlements (mm)	Model-2 Settlements (mm)	Model-3 Settlements (mm)
1	114.5	81.5	468	536	152	167
3	100	67	1400	576	172	183
5	82	49	298	189	57	125
7	65	32	87	73	30	71

Table 5.7. Comparative magnitudes of downstream slope horizontal deformations at the end of reservoir filling

The figure shows that the maximum observed horizontal deformation on the downstream slope also occurs at three-forth of the dam height, stated by marker no.3 with the magnitude of 1400 mm. The largest calculated results is also given by Model-1 with the settlement is 576 mm, which is 40% of the observed value.

The comparison of observed and calculated vertical settlements and horizontal settlements in both cases of loading with the three models reveal that:

a. Model-1 may be adopted for further studies in order to discuss and evaluate behaviours and performance of the Djatiluhur dam.

b. The observations of Marker-3 do not appear to be reliable and need field checking.

5.5. DISCUSSION OF ANALYTICAL ANALYSIS

After selecting of the Model-1, and after comparison of observed and computed values of vertical settlements and horizontal displacement, the results of analysis of Model-1 are further discussed for several factors such as load transfer, hydraulic fracturing susceptibility and potential cracks susceptibility will also be discussed based on the calculated deformations and stresses contours of Model-1.

5.5.1. Performance Prediction During Construction Period

1. When the embankment construction surface reached El. 103 m, about 11.5 meters below the crest, a longitudinal crack appeared along the joint between the core and the downstream fine filter (Monitoring Report, January 1965).

It first appeared near the midpoint of the dam axis and then extended rapidly in both directions, reaching a total length of more than 500 meters, or half length of the dam.

As mentioned in the beginning of this chapter that several conditions are found in Djatiluhur dam design and construction, which might result in unstable behaviour of the dam, including the occurrence of the cracks. These are as below:

- Susceptibility on the construction methodology and quality control during construction period, particularly in placing of rockfill materials, which resulted strength decrement of the constructed materials.

- The availability of undesired clay materials (high-plasticity clay) might be used without proper pre-constructed treatments for the materials, potentially initiated unstable behaviours of the dam.

- Incorrect assumed design parameters such as value of friction angle and design slope.

There is evidence that longitudinal cracks potentially appear at the dam crest probably due to developed tensile stress (*Sherard, 1963*).

From the contour of predicted minor principal stress (σ_x) at level 103 m, it can be seen from Figure 5.26.a below that the small tension zone (circled area, with tensile stress 3.9 T/m^2) appears within adjacent zones between core and the downstream fine filter only few meters below the top layer.

PENTAGON-3D Ver.2004

@Load_stage : 5

Solid : Stress_XX

Solid :
3.9696
0.1758
-7.411
-14.99
-22.58
-30.17
-37.76
-45.35
-52.93
-60.52
-68.11
-75.70
-83.28
-90.87
-98.46
-102.2

+103 m

(a) 2D-Plane

(b) 3D-Plane

Figure 5.26. Contour of minor principal stress at level 103 m
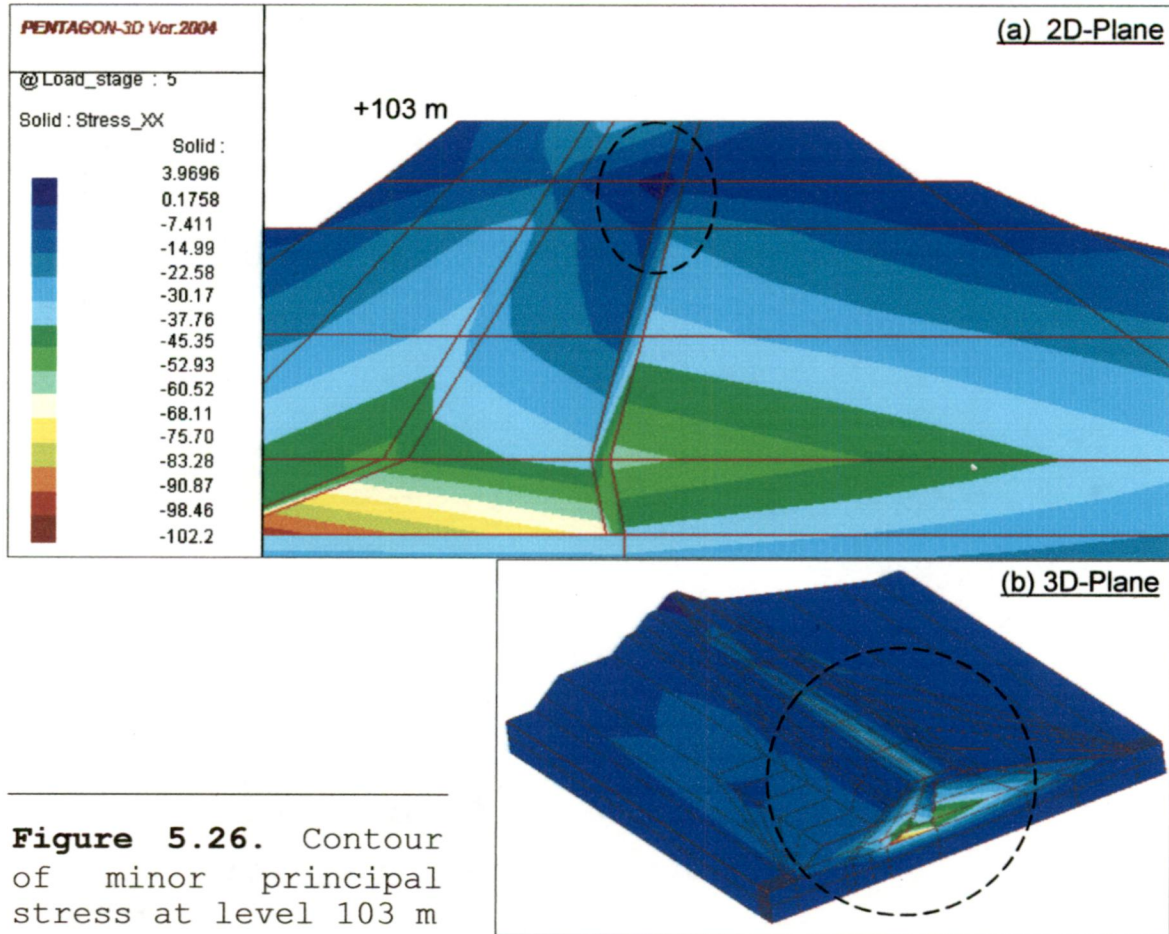
And from Figure 5.26.b, it can also be seen that tensile zone is present at the central section in about half the axis length on the same location where a cracks is observed.

2. Soon after construction was completed a longitudinal crack approximately 300 meters long appeared on the crest in the central portion of the dam *(Monitoring Report, August 1965)*.

Based on the same theoretical background mentioned in point 1 above, the contour of predicted minor principal stress (σ_x) at the end of construction is used in the

analysis. It can be seen from Figure 5.27 that the small tension zone continuously appears (circled area, with tensile stress 3.04 T/m^2) within adjacent zones between core and the downstream fine filter from level 90 m towards level 103 m or 10 meters below the crest level.
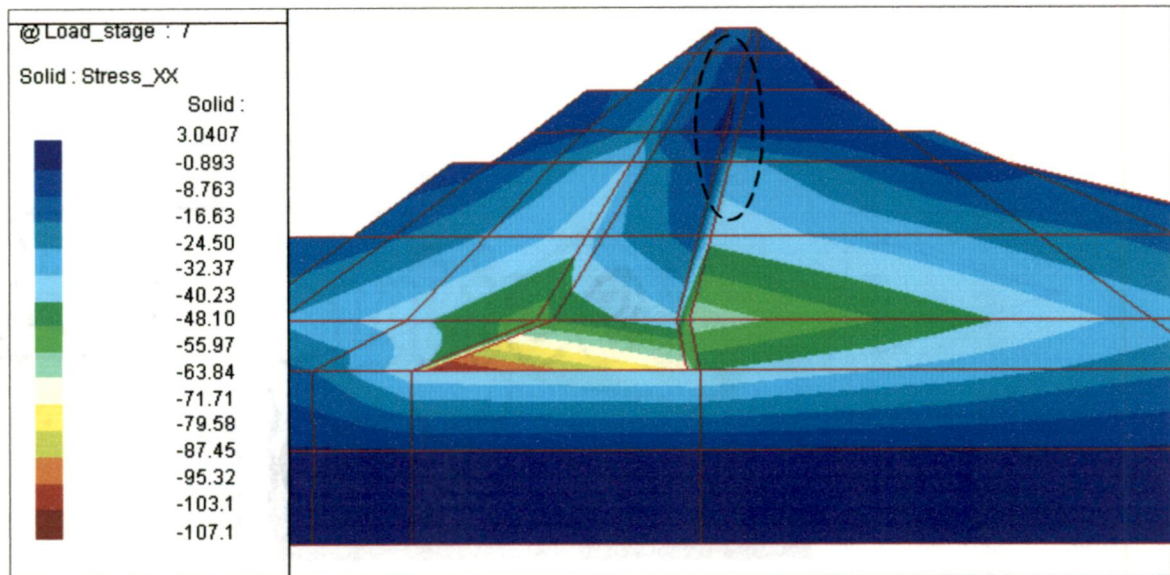
Figure 5.27. Contour of minor principle stresses at end of construction (level 114.5 m).

Even though the tensile stress magnitude slightly decreased, appearance of this zone potentially initiated the longitudinal crack on the crest of the dam.

It can be concluded that the computed results also illustrate a potential longitudinal crack, which appeared along the joint between the core and the downstream fine filter.

3. Figure 5.20 and 5.21 in Para 5.4.1 show that maximum settlements on upstream and downstream slopes are 267 mm and 238 mm respectively, and occur at the same level of the dam slope i.e. 100 – 103 m. Comparing with settlement

contour of Model-1 as selected model (Figure 5.8 in Para 5.3.1), it can be seen that the contour also illustrated the maximum upstream and downstream slopes settlements occur at the three-forth height of the dam (level 100 – 103 m) with magnitudes being 276 mm and 268 mm respectively. Figure 5.28 below superimposes Figure 5.20, 5.21 and 5.8 side by side.
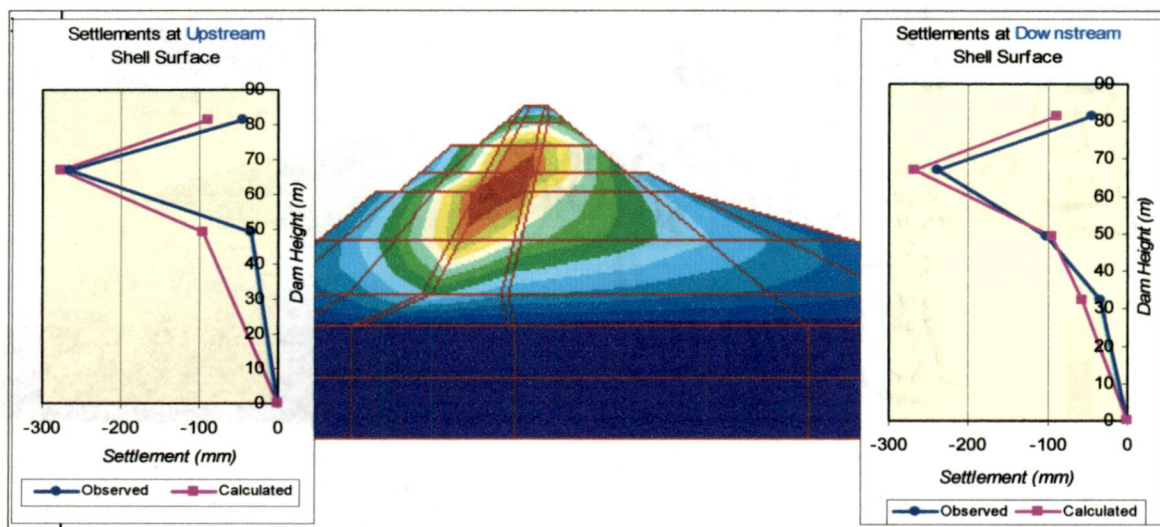
Figure 5.28. Slopes settlements and settlements contours at the end of construction period

The contour pattern shows that settlements within the upstream shell are little higher than those in the downstream and the maximum settlement appears at two-third of the dam height within the core zone with the value is 501 mm. It is known that the settlement of the upstream shell which is resting on inclined core portion will depend on settlement of the core. And normally, the settlement within core portion is higher than outer zones that could be due to high compressibility of the clay core *(Kuberran, et al., 1978)*. According to such general behaviours of inclined core, Figure 5.28 confirms good

agreement between the observable facts and the computed contour by the software.

4. Figure 5.22 in Para 5.4.1 shows that maximum horizontal deformation on downstream slope is 559 mm and occurs at the level 100 – 103 m. Comparing with horizontal deformations contour of Model-1 as selected model (Figure 5.9 in Para 5.3.1), it is seen that dam crest and downstream shell moves towards downstream and the maximum magnitude occurred at two-third of the dam height within the shell zone with the value around 130 mm. Meanwhile, maximum downstream slope horizontal deformation occurs at the same level (level 49 – 52 m) with magnitudes as 93 mm. Figure 5.29 below superimposes Figure 5.22 and 5.9 side by side.
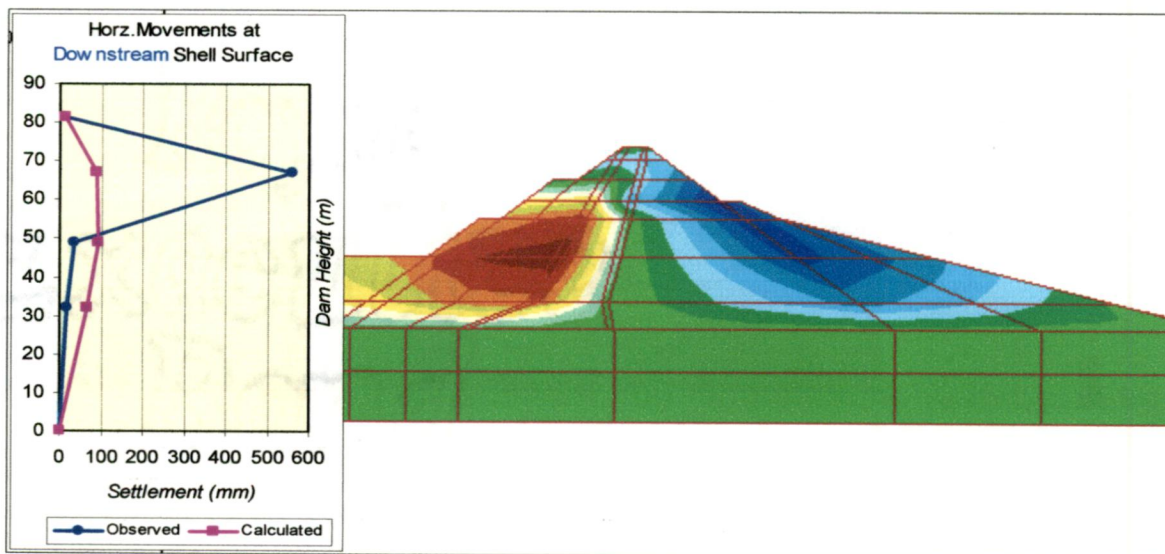
Figure 5.29. Slopes horizontal deformation and the contours at end of construction period

The unusual pattern of the observed horizontal deformation values may be due to:

a. Elasto-plastic behaviour of the soil at observed location. Where this behaviour is not modeled in the analysis and the large difference between the observed

and values at this location and the computed values may be because of this fact.

b. The observations may be erroneous and needs verification.

5. Figure 5.30 shows the major principal stress contours of Model-1 at the end of construction period, where the load transfer among the zone indicated. This load transfer can be evaluated by comparing the computed values of the major principle stress in the core and the core overburden pressure at any given depth below the crest. The ratio less than one indicates load transfer from core to shell, while the ratio greater than 1.0 indicates load transfer from the shell to the core.
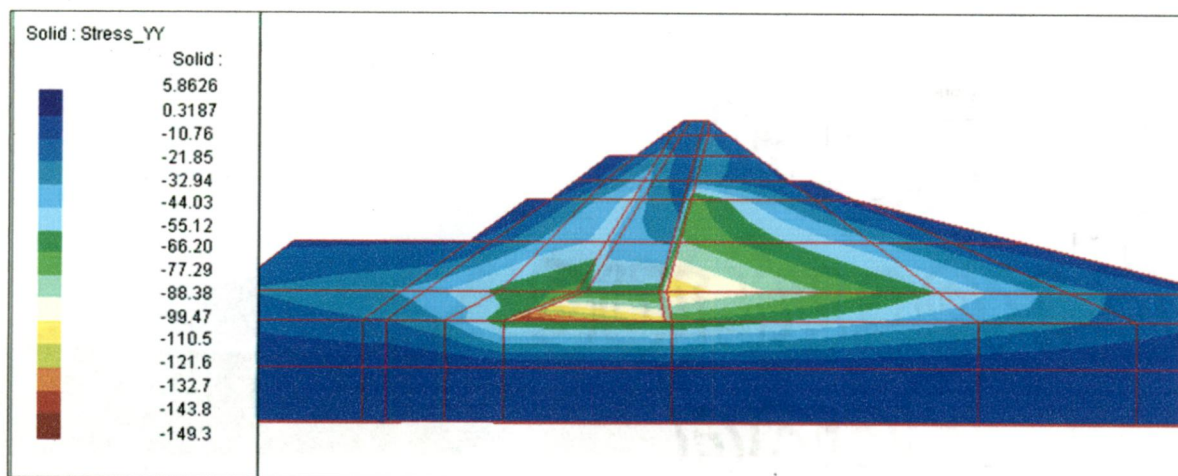
Figure 5.30. Major Principal Stress contours at end of construction period

The principal stresses in the core are lower as compared to the shell material particularly the downstream shell at all the levels except near crest of the dam and in upstream toe of the core. This generally happens due to load transfer from core to the both shells, as the stiffness of the core is less than that of the shell. In case of inclined core, it is known that vertical stress

are observed higher in downstream shell. It indicates that load transfer particularly occurs from core to the downstream shell. The maximum stresses are observed at the base of the dam in upstream toe of core enlargement portion and downstream face of downstream filter and the magnitudes are 143.8 T/m^2 and 110.5 T/m^2 respectively. In case of inclined core, normally, the maximum stresses are seen in adjacent zone between shells and filters (Raghuram, 2005). It can be assumed that core enlargement at base of the dam affects the shift of stress location.

Figure 5.31 shows load transfer ratio $(\sigma_y/\gamma.h)$ with respect to height of the dam at the end of construction period and the adjacent table lists the magnitudes. It is seen that the ratio is less than one for about 70 m height along the core height thus indicating load transferred from core to shell, particularly to the downstream shell. Except near crest of the dam, the ratio is greater than one and indicating load transferred from shell to core.

Dam Height (m)	σ_y (T/m^2)	$\gamma.h$ (T/m^2)	$\sigma_y/\gamma.h$
81	13.75	2.05	6.71
75	15.67	13.3	1.18
67	21.6	29.7	0.73
57	25.53	50.2	0.51
49	31.4	66.6	0.47
32	44.1	101.47	0.43
12	66.2	142.4	0.46
0	121.6	167.1	0.73
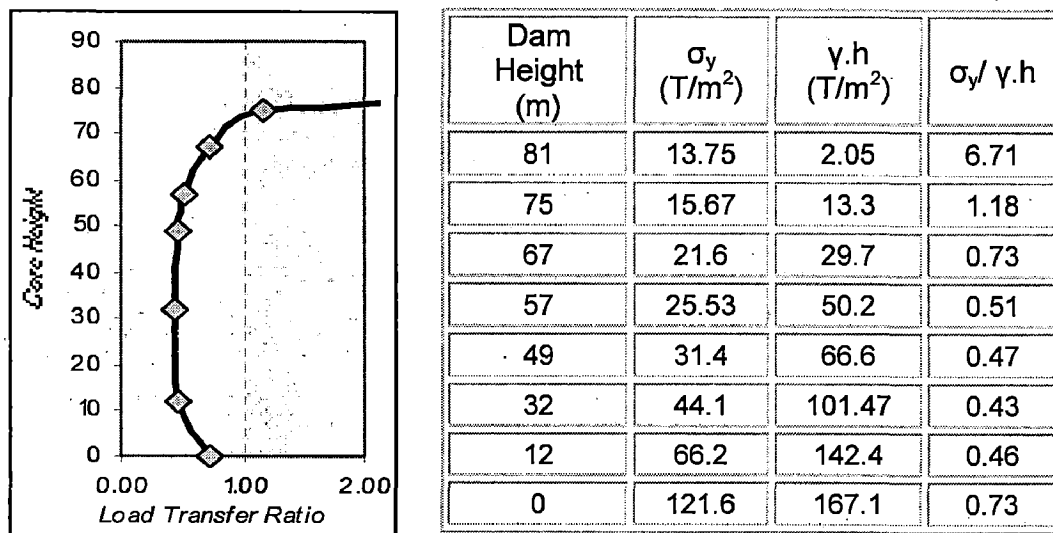
Figure 5.31. Load transfer ratio along the various core heights

It is seen also that the ratio at the base of the core is close to one. It denotes lesser load transfer from core to

shell and indicates good effects of core enlargement. It can be concluded that this behaviour shows satisfactory agreements with general condition which known that the stress transfer is of the order of about 70% near the base for the zoned dam, and at higher elevations where the geometric effects would be minimal, the stress transfer was constant at about 40% *(Eisenstein and Simmons, 1975)* at Mica dam.

5.5.2. Performance Prediction During Reservoir Filling

1. When impounding reached level 80-82 m, numerous horizontal cracks were observed in the upper portion of the core between 0 and 10 meter depths *(Monitoring Report, February 1966)*.

   Presence of differential construction settlements that could initiate the cracks can be observed in Figure 5.32.
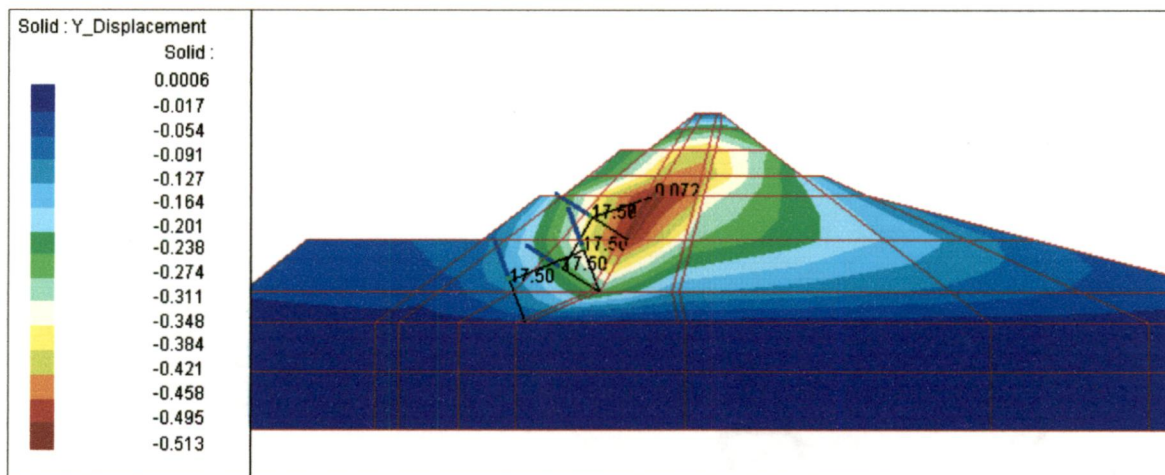
Figure 5.32. Settlement contour of reservoir filling at level 82 m

The Figure shows the settlement contour with reservoir filling up to level 82 m, when the water load is seen to have forced the core to move upstream. The 513 mm maximum

settlement appears at the mid height of upstream filter zone as part of submerged zone and reduces gradually towards the crest of the dam. Compared with the maximum settlement at the end of construction i.e. 501 mm, this settlement slightly increases and indicates the softening effects over the buoyant uplift forces. The contour also shows uniform and general settlements occurring within the dam, hence, this analysis indicates no differential settlements.

In order to observe the presence of tensile zone in the zone where the cracks occurred, contour of major principal stress of the dam at the level 82 m of reservoir filling is presented in Figure 5.33 below.
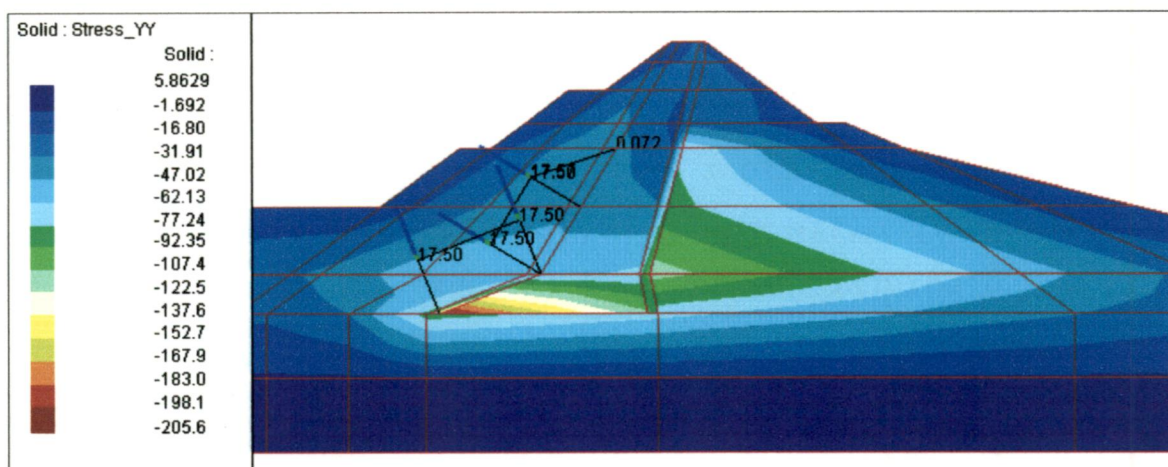
Figure 5.33. Major Principal stresses contour of reservoir filling at level 82 m

It is observed that the vertical normal compressive stresses reduced in most part of submerged upstream shell due to buoyant uplift and increased in base portion of the core due to water load on core. The contour also illustrates uniform distribution of stresses in top zone of the dam. Hence, prediction on horizontal cracks due to developed tensile zone also disagreed.

Therefore, to predict the dam performance based on the observed horizontal cracks, theory of secondary settlements may well be able to apply. Secondary settlement occurred due to consolidation during the period between completion of embankment and start of reservoir filling when no additional loads are applied and only the dissipation of pore water pressure developed in the core *(Inoue, et.al, 2000, at Tahamara Dam)*. This condition that could not be modeled by numerical analysis probably occurred within the top zone of the dam and initiated occurrence of the cracks.

2. When impounding reached level 100-103 m, the upstream edge of the crest settled about 50 cm with respect to the downstream edge *(Monitoring Report, June 1966)*.

Figure 5.34 shows the settlements contour of reservoir filling at level 103 m. This contour verifies that unseen internal cracks might have developed in the core due to presence of differential movements. These internal cracks were predictably developed and could initiate the settlements of the upstream crest.
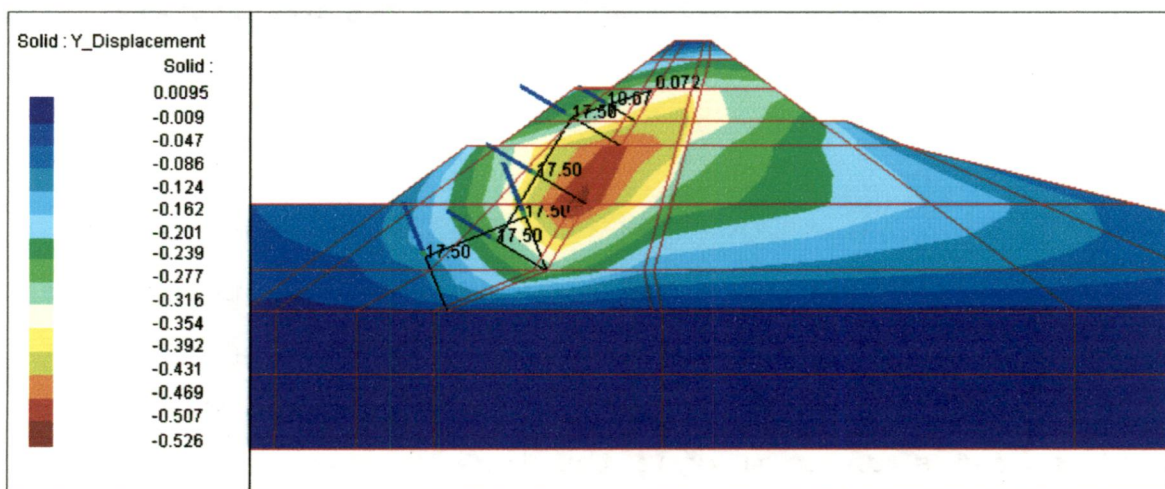
Figure 5.34. Settlements contour of reservoir filling at level 103 m

It can be seen that the crest is settling in downward direction and there are no differential settlements occurring in the top zone. Uniform settlements appear in top zone up to 20 meter below the crest, with magnitudes gradually increasing from 9 mm on crest to around 300 mm at 20 m depth. It is known that marker no.3 and 4 were installed on this level and there were no reports from these markers that informed the occurrence of the differential settlements. Internal settlements are shown with the 526 mm maximum settlement occurring in the mid height of the upstream filter zone. This maximum value is more compared with pervious water level stage (point 1) analysis. It is indicates the effect of softening and water load on core.

Figure 5.35 shows the horizontal deformation contour of reservoir filling at level 103 m. There were no differential deformations seen within the dam, especially in the top zone. Most of the dam body is moving towards downstream with the maximum magnitude being 420 mm occurring at the one-third height of the upstream filter.
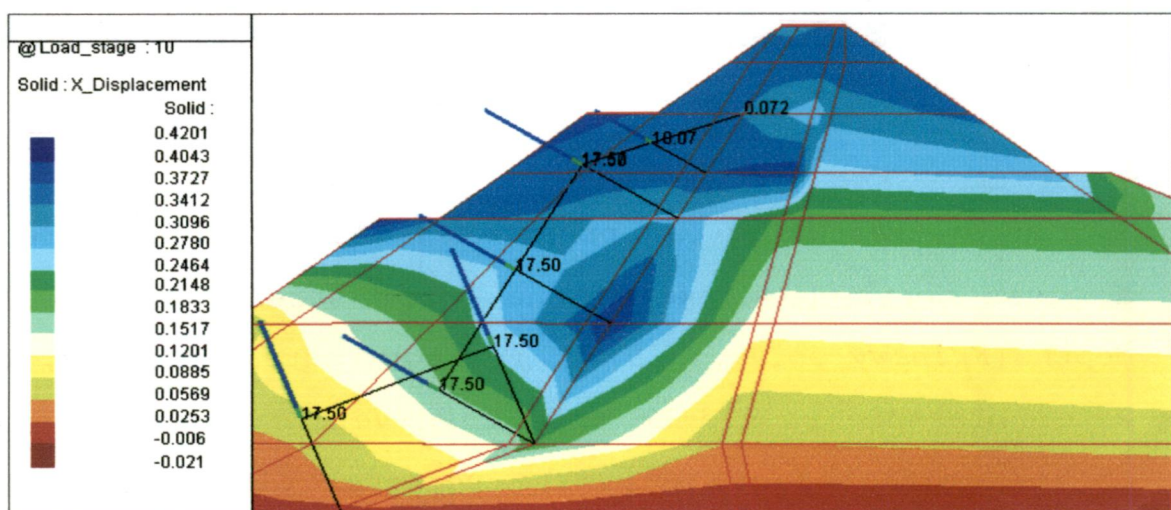
Figure 5.35. Horizontal deformation contour of reservoir filling at level 103 m

The contour of major and minor principal stresses of the dam at the level 103 m of reservoir filling could verify the presence of tensile zone and hydraulic fracturing within the top zone. Tensile zone could initiate the occurrence of unseen-internal cracks and gradually initiated settlements on the dam crest.

Figure 5.36 shows the minor principal stresses contour for reservoir filling at level 103 m. It shows a small tension zone, which was already there at the end of construction. It now continuously appears (circled area, with tensile stress 3.04 T/m^2) within adjacent zones between core and the downstream fine filter from level 90 m towards level 103 m or 10 meters below the crest level.
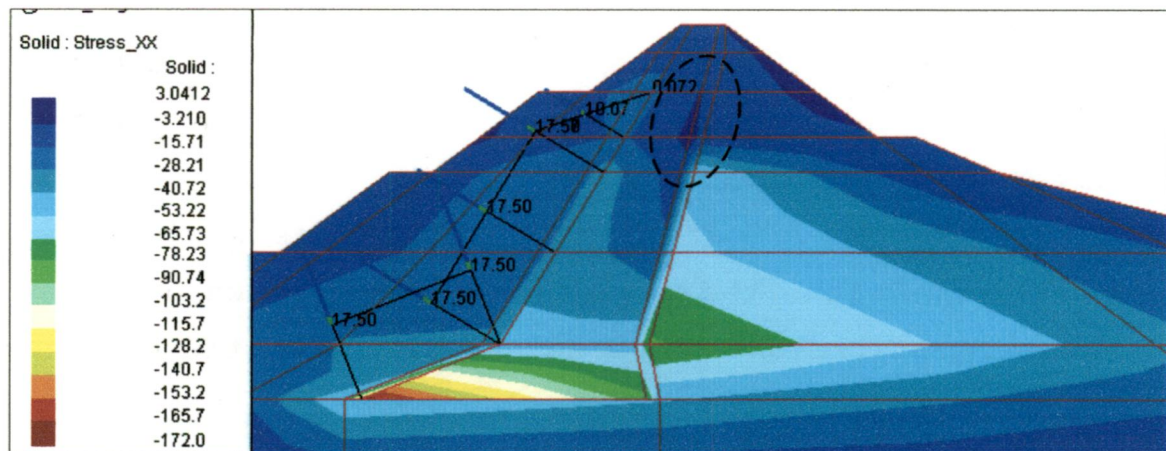
Figure 5.36. Minor Principal Stresses contour of reservoir filling at level 103 m

Hydraulic fracturing can occur when the water pressure at a given depth (σ_3) exceed the total stress at the same depth (*Kulhawy et al., 1976*). For horizontal cracking, the water pressure should be more than vertical stress (σ_y). If the initiated crack is the vertical plane, the water pressure would have to exceed the minor principal stress (σ_z, the stress in the core which is parallel to the face of the core).

Contour of major principal stress (σ_y) of the dam at the level 103 m of reservoir filling is presented in Figure 5.37 (a). It is observed that the stresses reduced in most part of submerged upstream shell due to buoyant uplift and increased in base portion of the core due to water load on core. Uniform distribution of stresses is also indicated on top zone of the dam and no tensile zone developed.
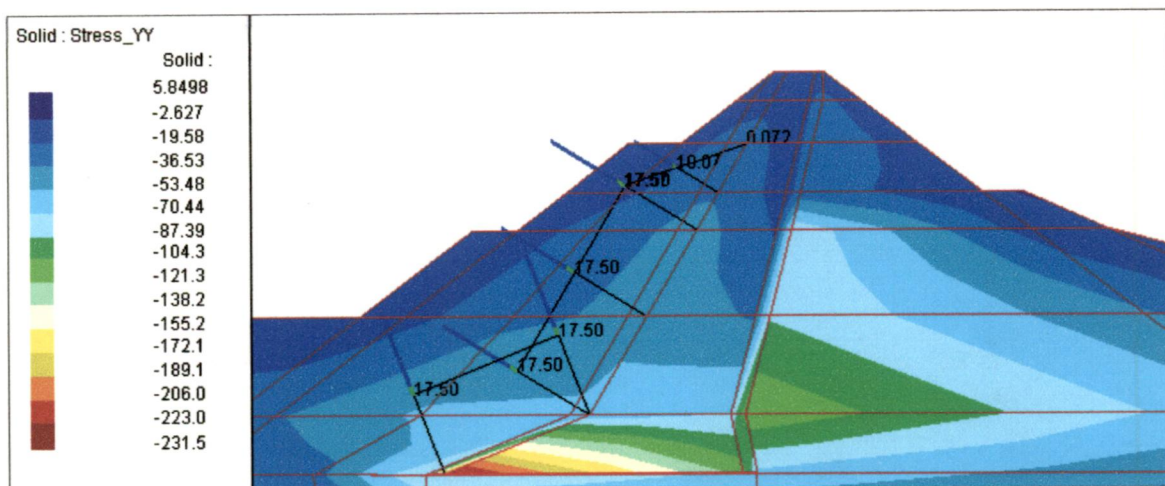
Figure 5.37 (a). Major Principal Stresses (σ_y) contour of reservoir filling at level 103 m
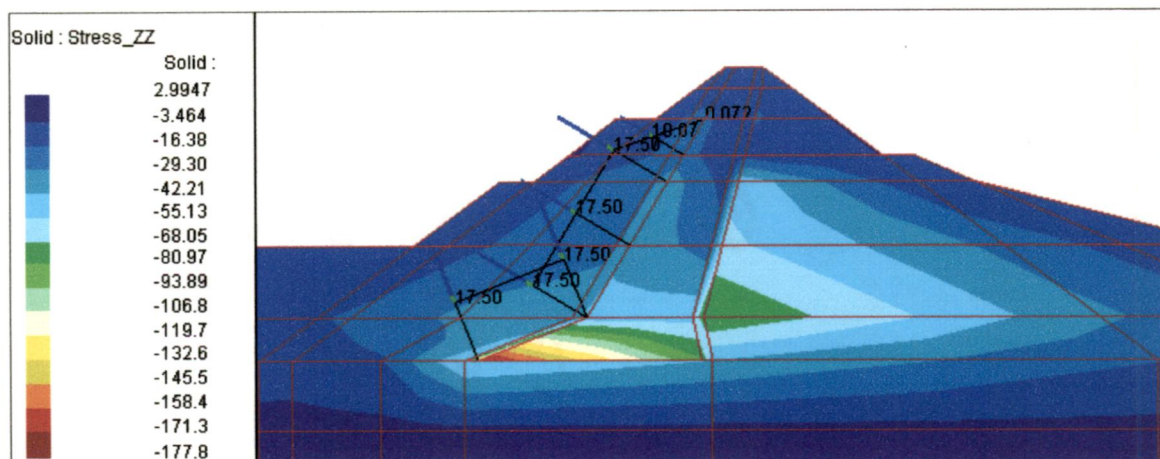
Figure 5.37 (b). Minor Principal Stresses (σ_z) contour of reservoir filling at level 103 m

Based on Figure 5.37(a) and 5.37(b), we can obtain the *Hydraulic Fracture Potential Ratio ($\sigma_y/\gamma_w.h$, $\sigma_z/\gamma_w.h$)* to

analyze hydraulic fracturing susceptibility within the dam.

Figure 5.38 shows variation of the Hydraulic Fracture Potential Ratio with height of the dam at the level 103 m of reservoir filling period, when in (a) and (b), major and minor stresses will be considered respectively.
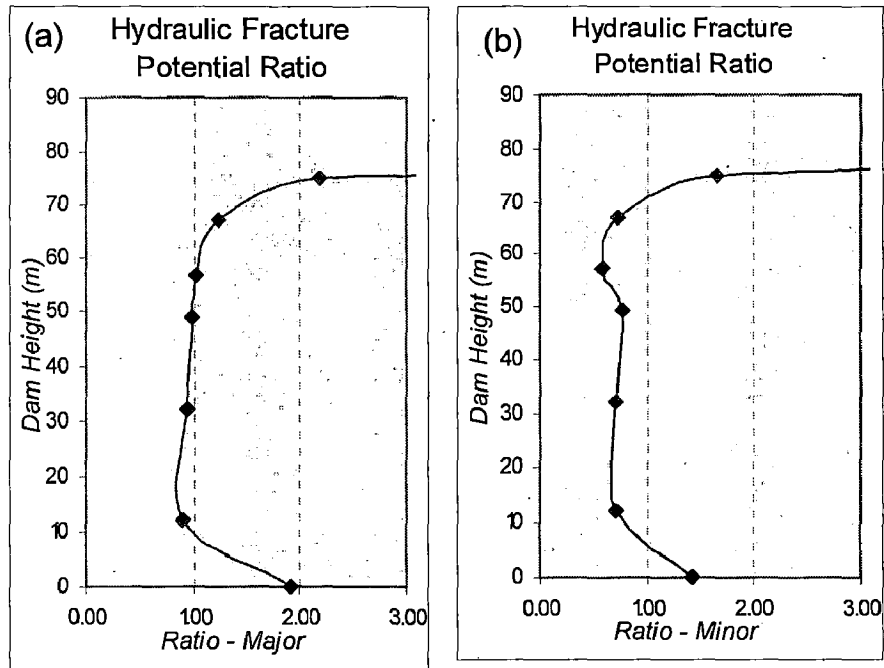
Figure 5.38. Hydraulic Fracture Potential Ratio along the various core heights

It is seen in figure 5.38(a) that the ratio is mostly greater than one along the core height except in one-third the core height where the ratio shown is smaller than one but not to any significant extent. It is indicating that the core zone is generally safe against occurrence of the horizontal cracks due to hydraulic fracturing. Figure 5.38(b) shows that the ratios are mostly less than one along the core height, except at the top and base of core zone. It denotes the susceptibility of hydraulic fracturing that induces cracks along the vertical plane. If it is combined with discussion on Figure 5.36 that

tensile zone take place in two-thirds of the core height, it corroborates the earlier finding to indicate the occurrence of internal longitudinal cracks at that particular level.

Therefore, it can be concluded from above discussions that crest settlements did not occur due to presence of the differential movements within the dam body. But, it confirms the occurrence of longitudinal cracks due to tensile zone and hydraulic fracturing in two-thirds of the core height to potentially induce the crest settlements.

3. Figure 5.23 and 5.24 in Para 5.4.2 show that maximum settlements on upstream and downstream slopes are 1195 mm and 773 mm respectively, and occurred at the same level of the dam slope i.e. 100 – 103 m. Comparing with settlement contour of Model-1 as selected model (Figure 5.10 in Para 5.3.1), it is seen that the contour show the upstream and downstream slopes settlements occurred at the three-forth height of the dam (level 100 – 103 m) with magnitudes are 328 mm and 340 mm respectively. Figure 5.39 below superimposes Figure 5.23, 5.24 and 5.10 side by side.
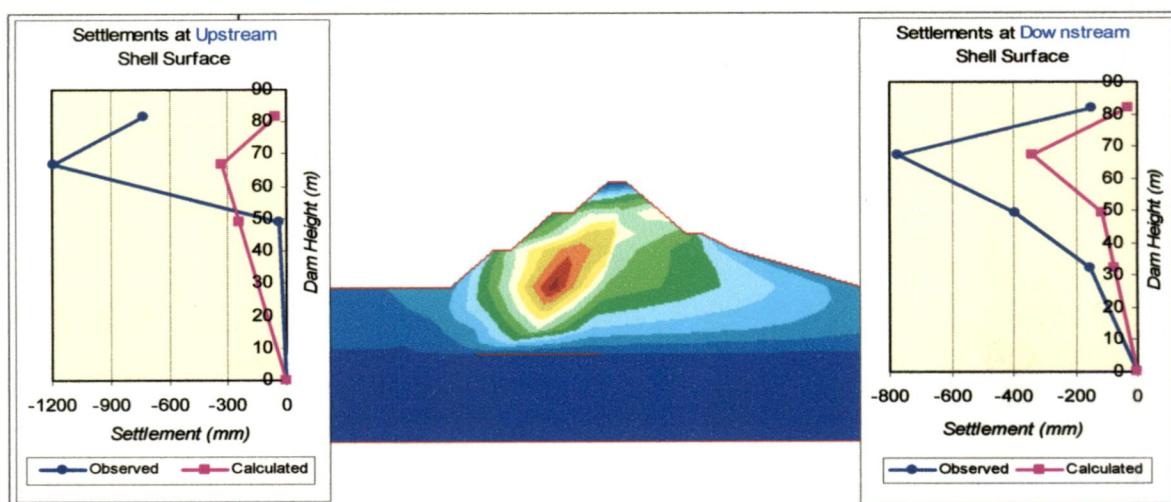
Figure 5.39. Slopes settlements and settlements contours at the end of reservoir filling period

The contour pattern shows settlements within the upstream shell (submerged zone) are slightly higher than those in the downstream. The maximum settlement appears at mid-height of the dam on the upstream core surface with the value at 539 mm. Comparing with the maximum calculated settlement at the end of construction, this slight increment also indicates effect of softening and water load over the buoyant uplift.

As mentioned before, no satisfactory agreement is found in comparison between calculated and the observed values. Comparing with the calculated results, the observed values are extremely large. It can be predicted that effects of softening caused excessive strength loss in submerged shell while the water load was acting on core surface, hence, additional settlements significantly occurred in shell zone pushing the inclined core and resulting in large settlements of the core zone that has high compressibility *(Nobari and Duncan, 1971, and Dibiagio et al., 1982)*. Gradually, this behaviour initiated plastification of the materials in the zone indicated.

Otherwise, good rigidity at the mid-height of upstream slope was stated by marker no.6. It could be affected by construction of the concrete tower.

4. Figure 5.25 in Para 5.4.2 shows that maximum observed horizontal deformation on downstream slope is 1400 mm and at the level 100 - 103 m. Comparing with horizontal deformations contour of Model-1 as selected model (Figure 5.11 in Para 5.3.1), it is seen the movements are in the downstream direction throughout most of the dam and the maximum magnitude stated at two-third of the dam height

with the deformation at 629 mm. Maximum predicted horizontal deformation of downstream slope stated at the same level (level 49 - 52 m) with magnitudes at 576 mm. Figure 5.29 below superimposes Figure 5.25 and 5.11 side by side.

As discussed in point 3 of Para 5.4.2, deformation at the end of reservoir filling is three times larger than the settlement values at the end of construction is normal, but the deformation at the end of construction it self is extraordinary high.
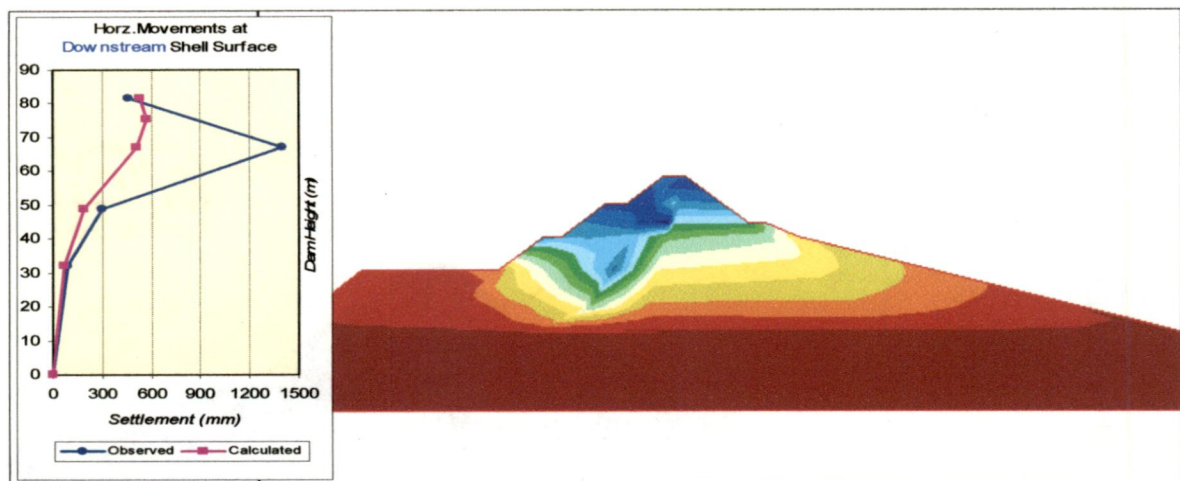
Figure 5.40. Slopes horizontal deformation curve and contours at the end of reservoir filling period

First presumption was that Marker no.3 did not perform properly, however, if we assume that the observed horizontal deformation data are accurate, this significant deformation results from secondary consolidation and plastification occurrences as mentioned at point 3 above. It was known that a deformation of horizontal extension in a direction parallel to the river causes a reduction in the horizontal confining stress, to a degree that the material plastifies.

5. Observations of contours of major and minor principal stresses at end of reservoir filling identify the hydraulic fracturing susceptibility of the dam. Excess load transfer from core to the shell may lead to hydraulic fracturing as discussed in chapter 3.

Figure 5.41 shows the contour of major principal stress at end of reservoir filling. The principal stresses in the upstream shell zone are in general same comparing with the stresses at the end of construction. However, the principal stresses in the upstream shell zone are lower than those in core and downstream shell zones. This happens due to effects of the softening and buoyant uplift of submerged zone.
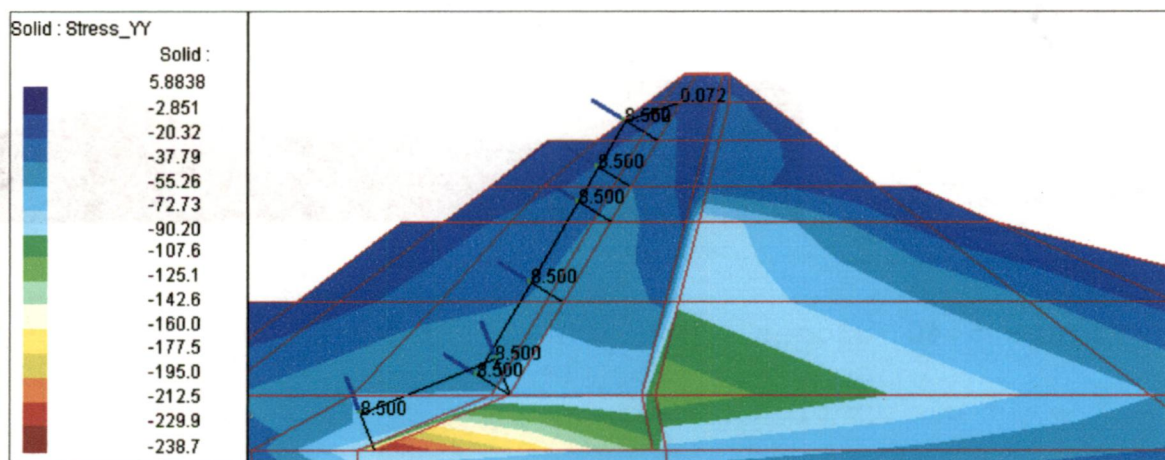
Figure 5.41. Major Principal Stress (σ_y) contours at the end of reservoir filling period

The maximum stresses that continuously observed at the base of the dam in upstream toe of core enlargement portion are 238.7 T/m^2. Comparing with the value at end of constructions, it is found significantly increased and could be predicted due to water load acting on the inclined core. There is no tensile zone in the dam body.
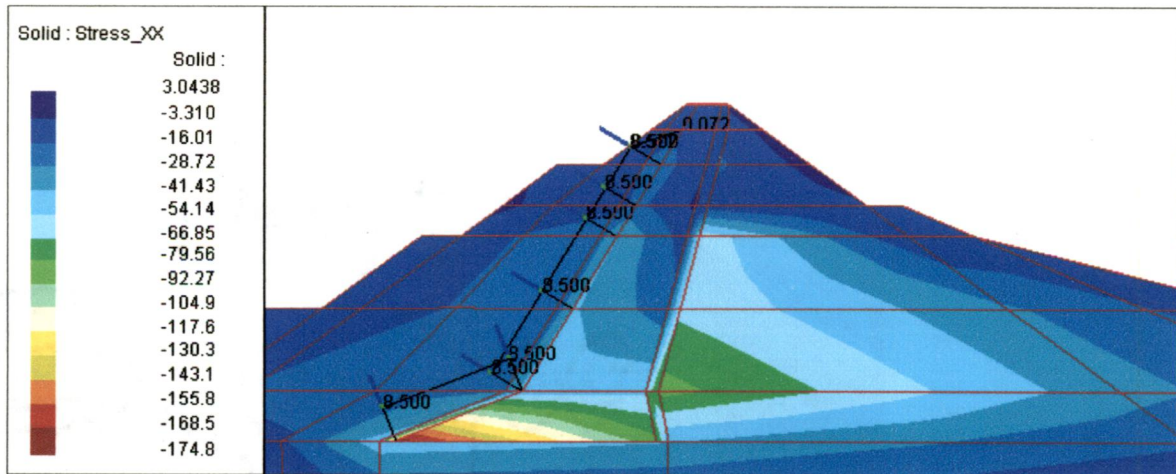
Figure 5.42. Minor Principal Stress (σ_x) contours at the end of reservoir filling period

Figure 5.42 shows the contour of minor principal stress (σ_x) at end of reservoir filling. The principal stresses in the upstream shell zone are lower as compared to the core and downstream shell zones and it happens also due to effects of the softening and buoyant uplift of submerged zone. However, effects of water load acting on the core surface caused the stresses in the core zone become higher. The maximum stresses that continuously predicted at the base of the dam in upstream toe of core enlargement portion at 174.8 T/m^2.

It is found that the small tension zone, which was present at the end of construction within adjacent between core zone and the downstream fine filter zone at level around 10 m, is disappeared. It could be predicted that, water load on core caused uniform horizontal deformation towards downstream and decreased tensile zone in the top zone.

6. Figure 5.43 shows the contour of minor principal stress (σ_z) at end of reservoir filling, which the maximum stresses is observed at the base of the dam in upstream toe of core enlargement portion at 183 T/m^2.
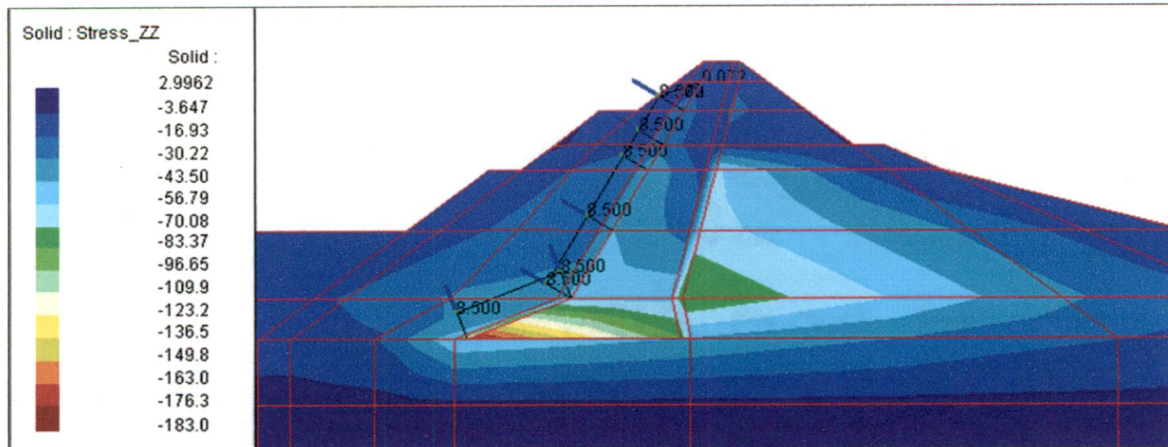
Figure 5.43. Minor Principal Stress (σ_z) contours at the end of reservoir filling period

Based on Figure 5.41 and 5.43, we can obtain the *Hydraulic Fracture Potential Ratio ($\sigma_y/\gamma_w.h$, $\sigma_z/\gamma_w.h$)* to analyze hydraulic fracturing susceptibility within the dam at the end of reservoir

Figure 5.44 shows variation of the Hydraulic Fracture Potential Ratio with respect to height of the dam at the end reservoir filling period, when in (a) and (b), major principal (σ_y) and minor principal stresses (σ_z) will be considered respectively.

It is seen in figure 5.44(a) that the ratio is mostly greater than one along the core height except at one-third the core height when the ratio is smaller than one but not too significant. It indicates that the core zone is generally safe against occurrence of the horizontal cracks due to hydraulic fracturing. It is known that the hydraulic fracturing phenomena generally occur along the upstream surface of the core zone for both horizontal cracks and vertical cracks occurrences.
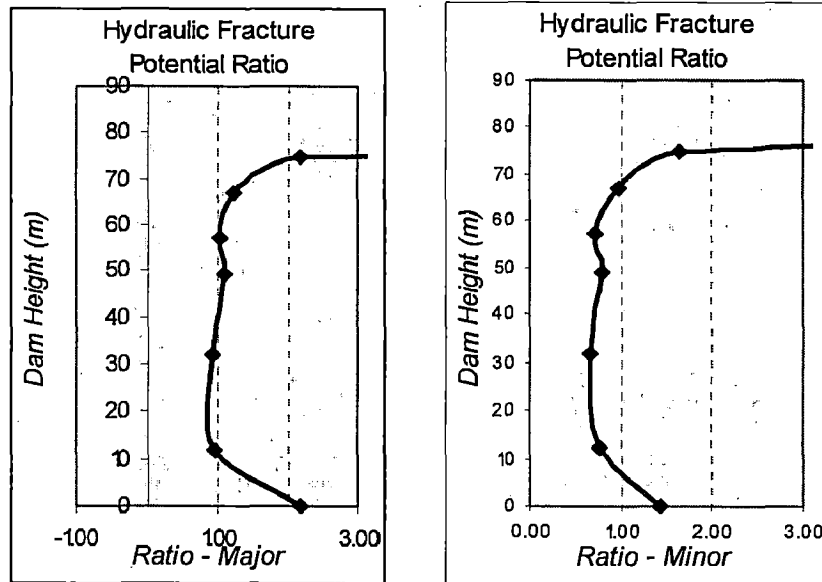
Figure 5.43. Hydraulic Fracture Potential Ratio at the end of reservoir filling along the various core heights

Figure 5.44(b) shows that the ratios are mostly less than one along the core height, except at the top and base of core zone. It denotes the susceptibility of hydraulic fracturing that induces cracks along the vertical plane.

This prediction has good concurrence if combined with discussion on point 3 above, in which the observed slopes settlements are extremely large. Hence plastification, which is initiated by the effects of softening and water load on upstream shell and core, occurred and was simultaneously followed by vertical cracks either within the core zone or the upstream filter zone.

Finally, this prediction could be the reason to explain the extraordinary occurrence of observed settlements. Even though, this behavior analysis could not be modeled into the package. As per literature review, the saturation of unsaturated soil generally leads to the loss of surface tension at contacts between soil particles due to water

entry into pores and to the movement of soil particles due to decrease of shear resistance between particle contacts, and, this actual behaviour is calculated based on the results of existing laboratory infiltration tests *(Inoue, et.al, 2000, at Tahamara dam).*

7. Regarding to extraordinary observed values, comparative incremental deformations among related dams in the world have already studied in order to investigate accuracy and ordinariness of those observable facts.

Table 5.8 below tabulates observed increments of dam deformation from seven dams in the world and one dissertation model. Incremental deformation obtained by comparing the deformation at the end of construction and deformation at the end of reservoir filling.

No.	Observed Dam (Author, Year)	Type of The Dam	Max Settlements (Location)			Max Horz.Defm (Location)		
			EoC (m)	EoRF (m)	Incr (%)	EoC (m)	EoRF (m)	Incr (%)
1	Fukuda Dam, Japan (Yasunaka et.al, 1985)	55 m Height Earthfill dam with Central Core	0.35	0.5	40	0.05	0.35	700
			Mid-height D/S Surface of Core			Mid-height D/S Core Surface		
2	Yequas Dam, France (Justro et.al, 2000)	87 m Height Eatrhfill Dam with Central Core	1.4	2	40	No data		
			Core Zone					
3	Tahamara Dam, Japan (Inoue et.al, 2000)	116 m Height Rockfill Dam with Central Core	0.21	0.29	38	No data		
			Dam Crest (Linear Analysis)					
4	Oroville Dam, USA (Nobari & Duncan, 1972)	770 ft Height Rickfill Dam with Inclined Core	-	0.5 (ft)	-	0.5 (ft)	0.72 (ft)	50
			Mid-height D/S Side of Core			(Not Maximum Value) Recorded at D/S Shell		

5	Alicura Dam, Argentina (Botta et.al, 1985)	130 m Height Earthfill Dam with Central Core	0.87	1.13	30	-	0.12	-
			At Mid-height of the Core			-		
6	El Infiernillo Dam, USA (Marsal & Ramirez, 1967)	148 Height Rockfill Dam with Central Core	No data			-	0.20	-
						-		
7	Svartevann Dam, Norway (Dibiagio et.al, 1982)	129 m Height Rockfill Dam with Inclined Core	1.2	1.75	45	-	1.2	-
			(Not Maximum Value) at 2/3 height of D/S Shell Surface			at 2/3 height of D/S Shell Surface		
8	Raghuram's Model (wrt Tehri, 2005)	150 m Height Rockfill Dam with Inclined Core	0.78	0.86	10	0.05	0.43	800
			At mid-Height of U/S Shell			At mid-Height of U/S Shell		

Table 5.8. Comparative magnitude of deformation increment

Based on the tabulated data above, it can be concluded that; 1) Maximum settlement increments stated from 10 up to 40%, 2) Maximum horizontal deformation increments stated from 50 up to 800%. However, the observed deformation increments of Djatiluhur dam recorded maximum settlements increment around 350% and horizontal deformation increment around 300%. It is confirmed that observed settlement increments occurred beyond the normal and horizontal deformation increments were found significant but not beyond the normal. However, extraordinary deformations were already stated at the end of construction period still have to be considered.

According to comparison discussed above, indication on potential plastification zone (elasto-plastic behaviours) and indication on unstable behavior due to excessive reservoir water effects still should be kept in mind. Secondly, accuracy of the observed data in marker no.3 is

suggested to be verified by calibrate performance of the installed marker.

8. Regarding to quality control applied during constructions, the evidence of cracks and settlements predictably may also be caused by:

- Susceptibility on the quality control during construction period, particularly in placing of rockfill materials, which resulted strength decrement of the constructed materials.

- The availability of undesired clay materials (high-plasticity clay) might be used without proper pre-constructed treatments for the materials, potentially initiated unstable behaviours of the dam.

- Incorrect assumed design parameters such as value of friction angle and design slope.

9. Generally, some difference between observed and predicted behaviour would appear to be unavoidable. As per review of literatures, except the unsatisfactory performance of the instruments used, the differences are probably caused by:

✓ Unsatisfied performance of the instruments used

✓ Possible sources of error may be found in the approximations in forming the constitutive law, the use of tri-axial data in a plane strain problem and in the inadequate representation of real variations in material properties, including anisotropy due to rolling and variations in placement moisture content *(Parkin et.al, 1982 in Dartmouth dam)*.

✓ It was impossible to obtain good correlation at embankment dam when the construction sequences were not

reproduced in the model properly *(Botta et.al, 1985 in Alicura dam).*

✓ It was believed that process of creep very well might explain the analytical under-prediction experienced for the settlements, which was not included in the analysis model *(Dibiago et.al, 1982 in Svartevann Dam, Norwegia).*

✓ Susceptibility on the quality control during placing of rockfill materials, where was not comparable with the design criterion.

The tangent modulus of material properties which reproduce the layer placement can be used with accurate results only if the fill placement is uniform and the rate of placements is in the normal range. Otherwise, a viscous-plastic model is required to reproduce the behaviours. *(Priscu, R et.al., 1985 in Riusor Dam, Romania).*

✓ Undesired method of constructions and quality control applied resulting in decrement of strength properties of used materials.

According to the analysis and discussions that have been given in previous chapters, the following conclusions are drawn from this study. The study is divided into three parts viz. (1) literature review, (2) selection of non-linear material properties model by comparison of observed data, and (3) the 3D FEM analysis of dam and interpretation of results. It is done for two stages i.e. end of construction and end of first reservoir filling.

The literature review has revealed several points as below:

✓ 3D-FEM is one of the best numerical methods for problem involving complex material properties and boundary conditions.

✓ Seven stages of construction could be sufficient to analyze the incremental embankment construction.

✓ Non-linear hyperbolic stress strain model is widely used.

✓ The sloping core results in increase of the vertical displacements than those for central core dams, though the effects of horizontal displacements are small.

✓ The maximum settlement occurs with range values between 0.2% up to 3.4% of the dam height, which below 1% is mostly recorded. It mostly occurred in the core zone of the dam.

✓ Deformation increments due to reservoir filling are 10-40% and 50-800% for settlements and horizontal deformations respectively.

✓ There is no significant change in the stresses and displacements in the dam with straight and curved axis under both construction and reservoir full conditions.

✓ The presence of a plastified zone in the part of the core and of the filters and transitions potentially initiate the large deformations of the dam.

✓ The movements observed during reservoir filling were first in upstream direction and later in downstream direction.

Since the material properties were not available for the analysis, 3D FEM analysis was done with 3 sets of values. Model-1 was selected by comparing observed slopes settlements with the computed values.

The interpretation of observations and results of analysis with Model-1 values reveals in the following paras.

6.1. PERFORMANCE OF THE DAM DURING CONSTRUCTION PERIOD

1. The observed longitudinal surface cracks and settlements that appeared in the dam at the end of construction period were predictably caused by aspects such as:

   a. Presence of tensile zone in the top zone.

   b. Susceptibility on the construction methodology and quality control during construction period.

   c. The availability of undesired clay materials (high-plasticity clay).

2. The maximum settlements on upstream and downstream slopes are 267 mm and 238 mm respectively, and occur at the same level of the dam slope i.e. 100 – 103 m.

3. Internal settlements within the upstream shell are higher than those in the downstream.

4. The maximum internal settlement appears at two-third of the dam height in the core zone with the value is 501 mm.

5. Large movements of observed horizontal deformation values on downstream slope at level 100-103 m, may be due to:

   a. Elasto-plastic behaviour of the soil, where this behaviour is not modeled in the analysis.

   b. The instrument is giving unreliable values and needs recalibration.

   c. The same aspects as mentioned in point 1.b and 1.c above.

6. The principal stresses in the core are lower as compared to the shell material at all the levels except near crest of the dam and in upstream toe of the core.

7. The maximum stresses are observed at the base of the dam in upstream toe of core enlargement portion at 143.8 T/m^2 and 107.1 T/m^2 for major and minor principal stresses respectively.

8. The load transfer ratio is less than one for about 70 m height along the core height thus indicating load transferred from core to shell, particularly to downstream shell of the dam.

9. Except near crest of the dam, the load transfer ratio shown greater than one and indicating load transferred from shell to core.

6.2. PERFORMANCE OF THE DAM DURING FIRST RESERVOIR FILLING

1. The numerous horizontal cracks were observed in the upper portion of the core at RWL 80-82 m, predictably caused by aspects such as:

   a. Presence of differential settlements and tensile zone are not confirmed by the analytical results.

   b. Unstable behaviours due to aspects as mentioned in point 1.b and 1.c Para 6.1 above.

   c. Unseen deformation in the top zone where is caused by occurrence of second consolidation, which could not be modeled by numerical analysis.

2. Occurrence of differential settlements on crest at RWL 100-103 m, may be due to:

   a. Presences of differential movements are not confirmed by the analytical results.

   b. Presence of tensile zone in the top zone (3.04 T/m^2) where is confirmed by the analytical results.

   c. Hydraulic fracturing potential ratio analysis confirms the susceptibility of hydraulic fracturing that induces cracks along the vertical plane in the upstream core. However no evidence is there for their existences.

   d. Unstable behaviours due to aspects as mentioned in point 1.b and 1.c Para 6.1 above.

3. Unsatisfactory agreement is found in comparison between calculated and the observed values of upstream-downstream slope settlements and horizontal deformations. These large movements may be due to:

   a. Effects of softening caused excessive strength loss in submerged shell and core and gradually, it initiate

plastification of the materials.

b. Similar causes as mentioned in Para 6.1 points 5.

4. The principal stresses in the upstream shell zone are lower than those in core and downstream shell zones.

5. The maximum principal stresses continuously observed at the base of the dam in upstream toe of core enlargement portion at 238.7 T/m^2 and 174.8 T/m^2 for major and minor principal stresses respectively.

6. There is no tensile zone within the dam at end of filling.

7. The small tension zone, which already appeared at the end of construction, has disappeared due to water load and uniform horizontal deformation towards downstream.

8. The core zone is generally safe against occurrence of the horizontal cracks due to hydraulic fracturing.

6.3. SUGGESTIONS FOR FURTHER STUDY

1. The study has been done by using limited data of material properties. The analysis should be carried out again with actual and sufficient material properties data.

2. The study may be extended with the elasto-plastic behaviours model analysis to accommodate the plastification analysis of the dam.

3. The study may be extended with behaviours analysis due to the reservoir drawdown effects, including the seepage analysis.

REFERENCES

Adikari, G.S.N., Donald, LB. and Parkin, A.K. (1982), "Analysis of the Construction Behavior of Dartmouth Dam", Proc. of the Fourth International Conference on Numerical Methods in Geomechanics, Edmonton, Canada, Vol. 2, pp. 645 654

Botta, L.P.I., Yarde, O.A., Paitovi, O. and Andersson, C.A. (1985), "Comparison between Predicted and Observed Behaviour of Alicura Dam, Argentina", Proc. ICOLD 15th Congress, Lausanne, Q.56, R.43, pp. 813 - 838

Clough, R.W. and Woodward, R.J. (1967), "Analysis of Embankment Stresses and Deformations", Journal of the Soil Mechanics and Foundations Division, ASCE, Vol. 93, No. SM4, pp. 529 - 549

Cole, B.R. and Cummins, P.J. (1981), "Behavour of Dartmouth Dam during Construction", Proc. 10th International Conference of Soil Mechanics and Foundation Engineering, Stockholm, Vol. 1, pp. 81 - 85

Desai, C.S. and Abel, J.F. (1987), "Introduction to The Finite Element Method: A Numerical Method for Engineering Analysis", First Edition, CBS Publisher & Distributors, New Delhi, India

Dibiagio, E., Myrvoll, F., Valstad T. and Hansteen, H. (1982), "Field Instrumentation, Observations and Performance Evaluations for The Svartevann Dam", Proc. ICOLD 14th Congress, Rio de Janeiro, Q.52, R.49, pp. 789 - 826

Domaschuk, L. and Valliappan, P. (1975), "Non-linear Settlement Analysis by Finite Element", Journal of the Geotechnical Engineering Division, ASCE, Vol. 101, No. GT7, pp.601 - 614

Duncan, J.M. and Chang, C.Y. (1970), "Non-linear Analysis of Stresses and Strain in Soils", Journal of the Soil Mechanics and Foundations Division, ASCE, Vol. 96, No. SM5, pp. 1629 - 1653

Duncan, J.M., Idriss, I.M. and Seed, H.B. (1975), "Criteria and Methods for Static and Dynamic Analysis of Earth Dam"

Eisenstein, Z., Krishnayya, A.V.G. and Morgenstern, N.R. (1972), "An Analysis of the Cracking at Duncan Dam", Proc. of ASCE Specialty Conference on Performance of Earth and Earth Supported Structures, Purdue University, Lafayette, Indiana, Vol. 1, pp. 765 - 778

Eisenstein, Z. and Simmons, J.V. (1975), "Three Dimensional Analysis of Mica Dam", Proc. of Symposium on Criteria and Assumption for Numerical Analysis of Dams, Swansea, pp. 1052 - 1069

Hosseini, M. and Tarkeshdooz, N. (2000), "A Comparison between Predicted and Instrumented Deformations of Karkheh Embankment Dam", Proc. ICOLD Congress, Beijing, Q.78, R.19, pp. 275 - 289

Justo, J.L. and Saura, J. (1983), "Three Dimensional Analysis of Infiernillo Dam during Construction and Filling of the Reservoir", International Journal of Numerical and Analytical Method in Geomechanics, Vol. 7, pp. 225 - 243

Justo, J.L., et al. (2000), "The Settlement of Yequas Dam During and After Construction", Proc. ICOLD Congress, Beijing, Q.78, R.49, pp. 759 - 769

Hosseini, M. and Tarkeshdooz, N. (2000), "A Comparison between Predicted and Instrumented Deformations of Karkheh Embankment Dam", Proc. ICOLD Congress, Beijing, Q.78, R.19, pp. 275 - 289

Kulhawy, F.H. and Duncan, J.M. (1976), "Stresses and Movements in Oroville Dam", Journal of the Soil Mechanics and Foundation Division, ASCE, No.SM4, pp. 1629 - 1653

Moreno, E. and Alberro, J. (1982), "Behaviour of Chicoasen Dam: Construction and First Filling", Proc. ICOLD 14th Congress, Rio de Janeiro, Q.52, R.9, pp. 155 - 182

Mori, Y., et al. (2000), "Analysis of Zoned Rockfill Dam with Centre Core during Construction and First Filling", Proc. ICOLD Congress, Beijing, Q.78, R.79, pp. 1309 - 1336

Naylor, D.J. and Mattar, D. Jr. (1988), "Layered Analysis of Embankment Dams", Proc. 6th International Conference on Numerical Methods in Geomechanics, Innsbruck, Rotterdam, Vol.2, pp. 1199 - 1205

Nobari, E.S. and Duncan, J.M. (1972), "Movements in Dams due to Reservoir Filling", Proc. of ASCE Specialty Conference on Performance of Earth and Earth Supported Structures, Perdue University, Lafayete, Indiana, Vol.1, pp.797 - 815

Nayak, G.C., et al., "Non-linear Analysis of High Rockfill Dam with Vertical and Inclined Cores",Analysis of Dam, Editor Naylor et al.

Ozawa,Y. and Duncan, J.M. (1976), "Elasto-plastic Finite Element Analysis of Sand~ Deformation", Int. Conference of Numerical Methods in Geomcchanics, ~ ASCE, pp. 243 - 263

Paul, D.K., (2002), "Seismic Testing of Tehri Dam", Proc. of 12th Symposium on Earthquake Engineering held at IIT Roorkee, Vol.2

Penman, A.D.M. and Charles, J.A. (1976), "The Quality and Suitability of Rockfill Used in Dam Construction", Proc. ICOLD 12nd Congress, Mexico, Q.44, R.26, pp. 533 - 556

Prasetyadhi, (2004), "3D FEM Study for Effect of Valley Shape on Behaviour of Earth and Rockfill Dam", M.Tech Dissertation, WRD&M Department, IIT Roorkee-India.

Priscu, R., Stematiu, D. and Dobrescu, D. (1985), "Capabilities of Mathematical Models to Predict Dam Behaviour during Erection of Riusor Rockfill Dam", Proc. ICOLD 15th Congress, Lausanne, Q.56, R.34, pp. 667 - 677

Raghuram, M., (2005), "Analysis of High Embankment Dam Using FEM", M.Tech Dissertation, WRD&M Department, IIT Roorkee, India.

Sherard, J.L., et al. (1963), "Earth and Earth Rock Dams", John Willey and Sons Inc., New York

Singh, R.P., Gupta, S.K. and Saini, S.S. (1985), "Three Dimensional Stress Analysis of Tehri Dam", Proc. Indian Geotechnical Conference, Roorkee, India, Vol. I, pp.481 - 486

Singh, R.P. (1991), "Three Dimensional Analysis of Rockfill Dams under Gravity Loading", Ph. D. Thesis, Water Resources Development Training Centre, University of Roorkee, India

Singh, B., and Varshney, R.S. (1995), "Engineering for Embankment Dams", Oxford & IBH Publishing Co. PVT. Ltd., India

Smith, G.N. (1971), "An introduction to Matrix and Finite Element Methods in Civil Engineering", Applied Science Publisher LTD, England

Yasunaka, M., Tanaka, T. and Nakano, R. (1985), "The Behaviour of Fukuda Rockfill Dam during Construction and Impounding of the Reservoir", Proc. ICOLD 15th Congress, Lausanne, Q.56, R.24, pp. 499 - 519